



UNIVERSITY OF PISA

School of Graduate Studies
"Scienza del Farmaco e delle Sostanze Bioattive"

PhD THESIS
2008–2010

**"Design and Development of Functionalized Ionic Liquids:
Synthesis, Temperature-dependent Properties and
Applications"**

Supervisor
Cinzia Chiappe

Author
Sunita Rajamani

DIRECTOR OF THE SCHOOL
Prof. Claudia Martini

2011

Dedicated to my amma and appa

Your blessings have always been my support.

Acknowledgements

First and foremost, I would like to thank the person without whom this PhD thesis would not have been possible. She is my Professor Cinzia Chiappe whose sincerity and encouragement I will never forget. She has been my inspiration during all the obstacles in the completion of this research work. She has never let me down and have always encouraged me with her beautiful smile and made me feel a never die attitude. Thanks to her for her full time availability towards me at any time and any day I needed her. I shall never forget her in my life because without her kindness, my life in Pisa would have been difficult. I can just say she is the answer to my prayers.

I cannot forget to thank the first attachments of my life, my parents. Though they have not participated during this thesis but without their blessings I would not have stood so stay far away from my home country. Thanks to my amma and appa for always trusting me. I am thanking my sisters Nirmala and Vidya who have been my all time encouragers. I thank my brother-in-law Mr. Sessa Sai, my nephews Abhishek and Avinash who have been my strength always. I would also thank my cousins Anand and Reshma to be my full-time support every time. Lastly, I would also thank Rahul to be my blind-supporter all the time.

Time to thank my labmates. I would thank Dr. Bernardo Melai who has always helped me without saying a single no whenever I needed him in my lab times. I am also thankful to my colleague Angelo Sanzone who has been my friend during my lab times and had funny and useful experiences with him. I deeply thank Tiziana for her kind and unconditional help during my thesis and experiments. Also I extend my thanks to Dario who had performed few experiments for me in the start of my final year. Atlast thanks to Carlotta, Giulia and Marco Malvaldi.

Time to thank few most important people of my life who have silently played many roles in my life. Its my immense pleasure to thank Dr. Sangram Keshari Samal who has played one of the most important role in my life by encouraging me in all my tough times and without him I would not have been a bold girl to stand in this competitive world. I also thank my friends Dr Mamoni Dash and Dr Sanghamitra Pradhan who have always been supportive, cooperative and caring for me. I again thank these friends to for their unfailing attempts for encouraging me and helping me in many ways. I am also happy to thank my best friend Dr. Amit Kumar Tevtia who has pulled me up when I was about to lose all my hopes. He has made himself available in a number of ways, has helped during my thesis in some way or the other without any demands and conditions. Thanks to all these friends for making my life in Pisa beautiful.

Last but not the least thanks to , Dr. Felicia Andrea to have helped me with some instruments during my thesis. I will not forget to thank Professoressa Braca who was my contact person during the times I was in India (before coming to Pisa). Lastly, thanks to Professoressa Claudia Martini and the school committee who made me a team of Univeristà di Pisa.

Table of Contents

| | |
|------------------------------------|-----|
| List of Schemes..... | i |
| List of Figures..... | iii |
| List of Tables..... | v |
| List of Abbreviations..... | vii |
| Scope and Outline of the Work..... | xii |

Contents

| | |
|---|-----------|
| 1. Introduction..... | 1 |
| 1.1 Definition of Ionic Liquids..... | 4 |
| 1.2 Acidic Ionic liquids..... | 5 |
| 1.2.1 Lewis acidic ionic liquids..... | 7 |
| 1.2.1.1 Lewis Acid ILs..... | 10 |
| 1.2.1.2 Applications of Lewis acids in synthesis..... | 15 |
| 1.2.2 Brønsted acidic ILs..... | 19 |
| 1.2.2.1 ILs containing COOH or SO ₃ H on the cation...20 | |
| 1.2.2.2 Protic Ionic Liquids..... | 25 |
| 1.2.2.3 Applications of Brønsted acidic ILs..... | 33 |
| 1.2.3 Dual-functionalized acidic Ionic Liquids..... | 43 |
| 1.2.3.1 Applications of dual-functionalized Lewis acidic ILs..... | 47 |
| | |
| 2. Physicochemical and Solvent Properties of Morpholinium Dicyanamide ILs and their Toxicity and Biodegradability Studies..... | 55 |
| 2.1 Introduction..... | 55 |
| 2.2 Experimental Section..... | 56 |
| 2.2.1 Synthesis..... | 56 |
| 2.2.1.1 Synthesis of <i>N</i> -alkyl- <i>N</i> -methylmorpholinium bromides ([Mor _{1,n}][Br]..... | 56 |
| 2.2.1.2 Synthesis of <i>N</i> -alkyl- <i>N</i> -methyl morpholinium | |

| | | |
|-----------|---|------------|
| | dicyanamides $[\text{Mor}_{1,n}[\text{N}(\text{CN})_2]]$ | 58 |
| 2.3 | Results and Discussion..... | 60 |
| 2.3.1 | Physico-chemical Properties..... | 61 |
| 2.3.2 | Density..... | 61 |
| 2.3.3 | Viscosity..... | 62 |
| 2.3.4 | Conductivity..... | 64 |
| 2.3.5 | Ionicity and Association..... | 65 |
| 2.3.6 | Solvent Properties and Polarity..... | 67 |
| 2.3.7 | Toxicity and Biodegradability..... | 69 |
| 2.3.7.1 | Toxicity..... | 70 |
| 2.3.7.2 | Biodegradability..... | 71 |
| 2.3.8 | Discussion on Toxicity and Biodegradability..... | 72 |
| 2.3.9 | Conclusion..... | 74 |
| 3. | Design and Development of Glyceryl-Substituted Ionic Liquids: Synthesis, Characterization and Temperature-Dependent Properties..... | 77 |
| 3.1 | Introduction..... | 77 |
| 3.2 | Materials and Methods..... | 80 |
| 3.3 | Determination of some Physico-Chemical Parameters..... | 92 |
| 3.4 | Determination of $E_T(30)$ and Kamlet-Taft Parameters..... | 93 |
| 3.5 | Results and Discussions..... | 94 |
| 3.5.1 | Physico-Chemical Properties..... | 94 |
| 3.5.2 | Solvatochromic Measurements and Polarity..... | 102 |
| 3.6 | Conclusion..... | 110 |
| 4. | New class of ionic liquids containing seven-membered rings: their synthesis and properties and comparing them with other six-membered rings..... | 155 |
| 4.1 | Introduction..... | 155 |
| 4.2 | Experimental section..... | 155 |
| 4.2.1 | Synthesis of all bromide and chloride salts..... | 156 |
| 4.2.2 | Synthesis of dicyanamide salts..... | 160 |

| | |
|--|------------|
| 4.3 Results and Discussion..... | 165 |
| 4.3.1 Physico-chemical properties..... | 165 |
| 4.3.2 Solvent properties..... | 170 |
| 4.4 Conclusions..... | 172 |
| | |
| 5. Applications of Brønsted acidic ILs in esterifications and transesterifications..... | 209 |
| 5.1 Introduction..... | 209 |
| 5.2 Materials and Methods..... | 210 |
| 5.3 Experimental Section..... | 214 |
| 5.3.1 Procedure for esterification of acetic acid with octanol..... | 214 |
| 5.3.2 Procedure for esterification of acetic acid with 1,2-propanediol..... | 214 |
| 5.3.3 Procedure for esterification of acetic acid with β -methyl-D-glucopyranoside..... | 214 |
| 5.3.4 Procedure for transesterification of trans-ethyl cinnamate..... | 215 |
| 5.3.4.1 Transesterification using methanol.. | 215 |
| 5.3.4.2 Transesterification using octanol.. | 215 |
| 5.4 Results and Discussions..... | 215 |
| 5.4.1. Esterification between octanol and acetic acid..... | 216 |
| 5.4.2. Esterification between 1,2-propanediol and acetic acid..... | 221 |
| 5.4.3 Esterification between β -methyl-D-glucopyranoside with acetic acid..... | 223 |
| 5.4.4 Transesterification of trans-ethyl cinnamate using methanol..... | 225 |
| 5.5 Conclusions..... | 229 |

| | |
|--|-----|
| 6. Preparation and Characterization of Glycerol Carbonate using Basic ILs | 231 |
| 6.1. Introduction..... | 231 |
| 6.2 Results and Discussions..... | 236 |
| 6.3 Experimental Section..... | 242 |
| 6.3.1 Materials and Methods..... | 242 |
| 6.3.2 Synthesis of glycerol carbonate..... | 242 |
| 6.4 Conclusions..... | 243 |

List of Schemes

- Scheme 1.1:** Preparation of a mono-functionalized Lewis acidic ILs
- Scheme 1.2:** Friedel-Crafts reactions of benzene and its derivatives with benzyl chloride
- Scheme 1.3:** Friedel-Crafts acylation reaction of benzene derivatives and acyl chloride
- Scheme 1.4:** Friedel-Crafts sulfonylation of aromatic compounds
- Scheme 1.5:** Friedel-Crafts acylation of acenaphthene to 3,6-dibenzoylacenaphthene
- Scheme 1.6:** Friedel-Crafts alkylation of anthracene with 2-chloropropane
- Scheme 1.7:** Formation of acetals
- Scheme 1.8:** Synthesis of long chain wax esters
- Scheme 1.9:** Fischer esterification of acetic acid and ethanol in presence of PILs
- Scheme 1.10:** Alcohol dehydrodimerization using PILs
- Scheme 1.11:** Pinacole rearrangement using PILs
- Scheme 1.12:** Ritter reaction of alcohols with nitriles in ILs
- Scheme 1.13:** 1-Allylimidazolium containing acidic ILs. Showing 1st four steps of Kun et al.
- Scheme 1.14:** Immobilized ILs (step 5 according to Kun Qiao et al.)
- Scheme 1.15:** Preparation of the IL supported polystyrene
- Scheme 1.16:** Diels-Alder reaction
- Scheme 1.17:** Mannich reaction
- Scheme 1.18:** Nitration of phenol and anisole in ILs
- Scheme 1.19:** Formation of aryl halides starting from sterically hindered aromatic compounds using [Hmim][NO₃]
- Scheme 1.20:** Catalytic effect of *N*-methyl pyrrolidinium dihydrogen phosphate
- Scheme 1.21:** Esterification of 1-octanol and acetic acid using triethylammonium ILs
- Scheme 1.22:** Acetylation using propanesulfonic acid on morpholinium as catalyst
- Scheme 1.23:** [C₄SC_nim][Cl]/AlCl₃
- Scheme 2:** ILs based on trichlorozincate anions
- Scheme 1.25:** Doubly-charged thionyl cations and chloroaluminate anions
- Scheme 36:** Benzene and 1-dodecene
- Scheme 1.27:** Dimerization of rosin using [HSO₃-(CH₂)₃-NEt₃]Cl-ZnCl₂
- Scheme 2.1:** Synthetic route to prepare *N*-alkyl-*N*-methylmorpholinium dicyanamide ILs
- Scheme 4.1:** Synthesis of bromide and chloride derivatives of hexamethylenimine
- Scheme 4.2:** Removal of the hydrogen chloride/bromide under basic condition
- Scheme 4.3:** Synthesis of the respective iodide derivatives of azepane
- Scheme 4.4:** Synthesis of dicyanamide derivatives of azepane

- Scheme 4.4:** Synthesis of functionalized piperidinium and morpholinium ILs
- Scheme 5.1:** Esterification of octanol with acetic acid using Bronsted acidic ILs
- Scheme 5.2:** Esterification of 1,2-propanediol using acetic acid in Brønsted acidic ILs
- Scheme 5.3:** Esterification between β -methyl-D-glucopyranoside with acetic acid
- Scheme 5.4:** Esterification of ethyl-trans cinnamate
- Scheme 5.5:** Esterification of octanol and ethyl-trans cinnamate
- Scheme 6.1:** Various products obtainable from glycerol
- Scheme 6.2:** Synthesis of glycerol carbonate byphosgenation (upper), direct carboxylation (middle part) or transesterification of glycerol (lower part)
- Scheme 6.3:** Synthesis of glycerol carbonate by glycerolysis of urea
- Scheme 6.4:** Formation of glycerol carbonate using ILs
- Scheme 6.5:** Mechanism for the formation of glycerol carbonate
- Scheme 6.6:** Various products formed on varying the amounts of DMC (Rokicki et al.)

List of Figures

- Figure 1.1:** Subsets of acidic ILs
- Figure 1.2a:** Cations most commonly used in Brønsted acidic ILs
- Figure 1.2b:** Imidazolium cations bearing functionalized alkyl chain
- Figure 1.3:** Imidazolium cation functionalized with boronic acid (Lewis acid)
- Figure 1.4:** FT-IR spectra of [bmim][Cl] with various metal halides
- Figure 1.5:** FT-IR spectra of ILs using ethanenitrile as a probe
- Figure 1.6:** FT-IR spectra of mixtures of acetonitrile and [bmim][Cl]-ZnCl₂ IL
- Figure 1.7:** Gutmann Acceptor Number of several chlorometallate ILs and molecular solvents
- Figure 1.8: Brønsted acidic ILs and the precursor zwitterions
- Figure 1.9:** Various combinations of cations and anions representing protic ILs
- Figure 1.10:** Superbases used to prepare hydrophobic PILs
- Figure 1.11:** ϵ -caprolactam or ϵ -butirolactam
- Figure 1.12:** Some protic pyridinium ILs
- Figure 1.13:** Some protic imidazolium ILs
- Figure 1.14: Determination of acidity of [C_nSC₄im]Cl₂/AlCl₃
- Figure 1.15:** FT-IR spectra of [HSO₃-(CH₂)₃-NEt₃]Cl-ZnCl₂ IL by using acetonitrile and pyridine as probe
- Figure 2.1:** Viscosity behavior of [Mor_{1,3}][N(CN)₂]
- Figure 2.2:** Behavior of viscosity of [Mor_{1,n}][N(CN)₂] with temperature
- Figure 2.3:** Walden plot for [Mor_{1,n}][N(CN)₂] from the conductivity and viscosity measured at 25°C (left) and 65°C (right). The ideal line is given by the line for KCl.
- Figure 2.4:** Relative percentages of the more relevant peaks observed in the positive and negative ESI-MS spectra of [Mor_{1,n}][N(CN)₂].
- Figure 2.5:** Acute toxicity (*V. fischeri*) values (EC₅₀) for DABCO- and morpholinium-based ILs
- Figure 2.6:** Percentage of biodegradability calculated for morpholinium ILs
- Figure 2.7:** Percentage of total dissolved organic carbon (TDC) calculated for morpholinium ILs with different lateral chain length (C2-C10).
- Figure 3.1:** Structures of glyceryl-substituted chloride derivatives
- Figure 3.2:** Structures of glyceryl-substituted N(CN)₂ derivatives
- Figure 3.3:** Structures of glyceryl-substituted Tf₂N derivatives
- Figure 3.4:** Separating funnel showing three different layers
- Figure 3.5:** This figure represents various washings of AgNO₃ test from 1st to 4th

Figure 3.6: Viscosity behavior of glyceryl $N(CN)_2$ compounds

Figure 3.7: Arrhenius plots of viscosity for dicyanamide-based glyceryl ILs

Figure 3.8: Behavior of viscosity with temperature for bistriflimide salts

Figure 3.9: Arrhenius plot of viscosity for five bistriflimide-based glyceryl ILs

Figure 3.10: Behavior of conductivity of dicyanamide (left) and bistriflimides (right) salts with temperature

Figure 3.11: Arrhenius plots of conductivity for dicyanamides

Figure 3.12: Reichardt's dye

Figure 3.13: Different solvation of ground and excited states

Figure 3.14: Illustration of interaction between the Reichardt's dye and the IL

Figure 3.15: Cartoon illustrating a plausible mechanism between Reichardt's dye and non-hydroxyl ILs

Figure 3.16: Variations of solvatochromic parameters with temperature.

Figure 4.1: Conductivity behavior with temperature

Figure 5.1: Brønsted acidic ILs used in this chapter

Figure 5.2: Figures showing stage after the reaction

Figure 5.3: C-NMR showing comparison between various acidic ILs used

Figure 5.4: C-NMR comparing between fresh, 1st, 2nd and 3rd recycle of [HPyrr][HSO₄]

Figure 5.5: H-NMR and C-NMR for esterification of glycerol with acetic acid using [HMIM][HSO₄]

Figure 5.6: C-NMR evidencing the acetylation at C6-position of sugar

Figure 5.7: C-NMR at 1st, 2nd and 4th hour showing reversibility reactions in case of [HMIM][NO₃]

Figure 5.8: H-NMR showing methyl-trans cinnamate product using [HMIM][HSO₄]

Figure 5.9: HNMR showing transesterification of ethyl trans cinnamate using octanol

Figure 6.1: A plot showing conversion yields at various temperatures

Figure 6.2: C-NMR of glycerol carbonate at 7.5, 10, 13 and 24 h when [Mor_{1,4}][N(CN)₂] is catalyst.

Figure 6.3: Comparison of various ILs in the product formation. (*) is byproduct at 74 and (#) is unreacted glycerol

Figure 6.4: CNMR suggested by Arresta et al.

Figure 6.5: C-NMR is shown for various recycles of [Mor_{1,4}][N(CN)₂] in the glycerol carbonate formation.

Figure 6.6: FT-IR spectrum of glycerol carbonate

List of Tables

- Table 1.1:** Nitration of various substituted phenol derivatives using [BHIM][HSO₄]
- Table 1.2:** Esterification of acetic acid with benzyl alcohol with various Brønsted ILs
- Table 1.3:** Esterification of acetic acid and 1-octanol using triethylammonium ILs
- Table 2.2:** VTF equation parameters for viscosity
- Table 2.3:** VTF equation parameters for conductivity
- Table 2.4:** Solvatochromic parameters of the [C_nMor_{1,n}][N(CN)₂]
- Table 3.1a:** Melting points of various glycerol chlorides
- Table 3.1b:** Physical Properties of ILs
- Table 3.2:** Viscosity values for six dicyanamide salts
- Table 3.3:** Arrhenius Fitting parameters and Vogel-Tamman-Fulcher (VTF) parameters for viscosity behavior as a function of temperature (N(CN)₂)
- Table 3.4:** Viscosity values for six bistriflimide salts
- Table 3.5:** Arrhenius Fitting parameters and VTF parameters for viscosity behavior as a function of temperature for Tf₂N ILs
- Table 3.6:** Conductivity values for all dicyanamide and bistriflimide salts from 293 to 363 K in mS cm⁻¹
- Table 3.7:** Arrhenius Fitting parameters and VTF parameters for viscosity behavior as a function of temperature
- Table 3.8:** Comparison of conductivities between three different ILs having various anions and common cation from 293 to 353 K
- Table 3.9:** Solvatochromic parameters of ILs and molecular solvents
- Table 3A1:** Changes in α , π^* , β and E_T^N , $E_{T(30)}$ at 25, 45, 65, 45 and 25°C ([Pip_{1,g}][N(CN)₂])
- Table 3A2:** DMI_{1,g} N(CN)₂ changes with temperature
- Table 3A3:** DMI_{1,g} Tf₂N:- changes with temperature
- Table 3A4:** Pyr_{1,g} Tf₂N:- changes with temperature
- Table 4.1:** Temperature-dependent physico-chemical properties
- Table 4.2a:** Viscosity values from 20–80°C for six N(CN)₂ ILs
- Table 4.2b:** Viscosity values from 20–80°C for five N(CN)₂ and one Tf₂N ILs
- Table 4.3a:** Arrhenius Fitting parameters for viscosity behavior as a function of temperature
- Table 4.3b:** VTF parameters for viscosity behavior as a function of temperature
- Table 4.4a:** Conductivity values from 20 to 80° C for six N(CN)₂ ILs
- Table 4.4b:** Conductivity values from 20 to 80° C for five N(CN)₂ and one Tf₂N ILs

- Table 4.5:** Arrhenius Fitting parameters and Vogel-Tamman-Fulcher (VTF) parameters for conductivity behavior as a function of temperature
- Table 4.6:** Polarity parameters of ILs and organic solvents at 25 °C
- Table 5.1:** Esterification of acetic acid with octanol (T=110 °C), time =4 h
- Table 5.2:** Recycling of [HPyrr][HSO₄]
- Table 5.3:** Product recovered using four Brønsted acidic ILs
- Table 5.4:** Product conversion using four Bronsted acidic ILs
- Table 5.5:** Showing yields of the recovered products
- Table 5.6:** Transesterification of ethyl *trans*-cinnamate in [HPip][HSO₄] using CH₃OH
- Table 5.7:** Transesterification of ethyl *trans* cinnamate using CH₃OH in various ILs
- Table 5.8:** Transesterification of *trans*-ethyl cinnamate and octanol in various Brønsted acidic ILs
- Table 6.1:** Different conditions using [Mor_{1,4}][N(CN)₂] at 120°C for 13h
- Table 6.2:** Different reaction temperature
- Table 6.3:** Different time of reaction with the same IL: [Mor_{1,4}][N(CN)₂] at 120°C
- Table 6.4:** Various catalysts showing their respective conversions at 120°C
- Table 6.5:** Recycle of IL [Mor_{1,4}][N(CN)₂] at 120°C for 13h

List of Abbreviations

| | |
|--|---|
| AlCl ₃ | Aluminium chloride |
| AgNO ₃ | Silver nitrate |
| AN | Gutmann Acceptor Number |
| Bet.HCl | Betaine hydrogen chloride |
| [BF ₄] ⁻ | Tetrafluoroborate |
| [bmim] | <i>N</i> -butyl- <i>N</i> '-methyl imidazolium |
| [bmim][H ₂ PO ₄] | <i>l</i> -Butyl-3-methylimidazolium dihydrogen phosphate |
| [(C ₂ H ₅) ₃ NH] | Triethylamine |
| [C ₅ dabco] | <i>N</i> -pentyl(dabco) |
| [C ₁₀ mim][FeCl ₄] | <i>N</i> -decyl- <i>N</i> -methyl-imidazolium iron(IV) chloride |
| CF ₃ COOH | Trifluoroacetic acid |
| CH ₂ Cl ₂ | Dichloromethane |
| CHCl ₃ | Chloroform |
| [CH ₃ SO ₃] | 2-Methylpyridinium methylsulfate |
| CuCl | Copper chloride |
| CT | Charge-transfer |
| [C ₄ SCnim] | 3-Alkyl- <i>l</i> -(butyl-4-sulfonyl) imidazolium chloride |
| [1,2-DiMIMPs] | 1,2-dimethyl imidazolium-3-yl propane-1/sulfonic acid |
| DMC | Dimethylcarbonate |
| DMF | Dimethylformamide |
| [DMI _{1,g}] | <i>l</i> -Glyceryl-2,3-dimethylimidazolium |
| DMSO | Dimethylsulfoxide |
| DPC | Diphenyl carbonate |
| DSC | Differential scanning calorimetry |

| | |
|---|--|
| [emim] | <i>N</i> -ethyl- <i>N'</i> -methyl imidazolium |
| [emPyr] | Methyl-ethylpyrrolidinium |
| [EtNH ₃][NO ₃] or EAN | Ethylammonium nitrate |
| EPA | Electron pair acceptor |
| EPD | Electron pair donor |
| ESI-MS | Electrospray mass spectrometry |
| FeCl ₂ | Iron(II) chloride |
| FeCl ₃ | Iron (III) chloride |
| [FHMPip _{1,g}] | <i>l</i> -Glyceryl- <i>l</i> -methyl-4-hydroxypiperidinium |
| FPFSI ⁻ or [(FSO ₂)(C ₂ F ₅ SO ₂)N] ⁻ | Pentafluoroethanesulfonyl)imide |
| FT-IR | Fourier Transformation Infra Red |
| GC | Gas chromatogram |
| [HSO ₄] | Hydrogen sulfate |
| HCl | Hydrochloric acid |
| HNO ₃ | Nitric acid |
| H ₂ SO ₄ | Sulfuric acid |
| [H ₂ PO ₄] | Dihydrogen phosphate |
| [Hbbim] | <i>l</i> -Butylbenzimidazolium |
| [HMIM][HSO ₄] | <i>N</i> -methylimidazolium hydrogen sulfate |
| H ₃ PO ₄ | Phosphoric acid |
| [HMIM][Cl] | <i>N</i> -methylimidazolium chloride |
| [HMIM][CF ₃ COO] | <i>N</i> -methylimidazolium trifluoroacetate |
| [HMIM][NO ₃] | <i>N</i> -methylimidazolium nitrate |
| [HMIM] ₂ [SO ₄] ²⁻ | <i>N</i> -methylimidazolium sulfate |
| [HMIM][H ₂ PO ₄] | <i>N</i> -methylimidazolium dihydrogen phosphate |

| | |
|--|---|
| [HMor][Cl] | <i>N</i> -methyl morpholinium chloride |
| [HMor][HSO ₄] | <i>N</i> -methylmorpholinium hydrogen sulphate |
| [HMor] ₂ [SO ₄] ²⁻ | <i>N</i> -methylmorpholinium sulfate |
| [HMor][NO ₃] | <i>N</i> -methyl morpholinium nitrate |
| [HPyrr][Cl] | <i>N</i> -methylpyrrolidinium chloride |
| [HPyrr][HSO ₄] | <i>N</i> -methylpyrrolidinium hydrogen sulfate |
| [HME _{H,4}][I] | <i>N</i> -butyl hexamethyleniminium bromide |
| [HME ₄][Br] | <i>N</i> -butyl hexamethylenimine |
| [Hbim][Tf ₂ N] | <i>I</i> -Butylimidazolium bistriflimide |
| HF | Hydrofluoric acid |
| [HME _{1,e}][I] | <i>N</i> -ethanol- <i>N</i> -methyl hexamethyleniminium iodide |
| [HME _{H,e}][Cl] | <i>N</i> -butyl hexamethyleniminium chloride |
| [HME _g] | <i>N</i> -glyceryl hexamethylenimine |
| [HPip] ₂ [SO ₄] ²⁻ | <i>N</i> -methylpiperidinium sulfate |
| [HPip][HSO ₄] | <i>N</i> -methylpiperidinium hydrogen sulfate |
| [HOEMIm] | <i>I</i> -Methyl-3-hydroxyethylimidazolium bistriflimide |
| [HPip][NO ₃] | <i>N</i> -methylpiperidinium nitrate |
| [HPyrr][HSO ₄] | <i>N</i> -methylpyrrolidinium hydrogen sulfate |
| [HME _{1,4}][I] | <i>N</i> -butyl- <i>N</i> -methyl hexamethyleniminium iodide |
| HBD | Hydrogen-bond donor |
| HBA | Hydrogen-bond acceptor |
| [HME _{1,g}][I] | <i>N</i> -glyceryl- <i>N</i> -methyl hexamethyleniminium iodide |
| [HME _{H,g}][Cl] | <i>N</i> -glyceryl hexamethyleniminium chloride |
| [HME _e][Cl] | <i>N</i> -ethanol hexamethylenimine |
| [HME _{1,e}][I] | <i>N</i> -ethanol- <i>N</i> -methyl hexamethyleniminium iodide |

| | |
|---|--|
| ILs | Ionic liquids |
| LiTf ₂ N | Lithium bistriflimide |
| LSER | Linear solvation energy relationships |
| [mim][BF ₄] | <i>1</i> -Methylimidazole tetrafluoroborate |
| [Mor _{1,g}] | <i>N</i> -glyceryl- <i>N</i> -methylmorpholinium chloride |
| [MIM _{1,g}] | <i>N</i> -glyceryl- <i>N</i> -methylimidazolium chloride |
| [MIM _{1,2}][FPFSI] | <i>1</i> -Methyl-3-ethylimidazolium fluorosulfonylamide |
| [Mor _{1,e}] | <i>N</i> -ethanol- <i>N</i> -methyl morpholinium chloride |
| [Mor _{2,e}] | <i>N</i> -ethanol- <i>N</i> -ethyl morpholinium chloride |
| [Mor _{1,n}][Br] | <i>N</i> -alkyl- <i>N</i> -methylmorpholinium bromides |
| [mim _{1,e}] | <i>N</i> -ethanol- <i>N</i> -methylimidazolium dicyanamide |
| [MIMPs] | 3-(1-methylimidazolium-3yl) propane-1 sulfonic acid |
| [2-MPyH][OTf] | 2-methylpyridinium triflate |
| [PF ₆] | Hexafluorophosphate |
| [N(CN) ₂] | Dicyanamide |
| Na ₂ CO ₃ | Sodium carbonate |
| NaN(CN) ₂ | Sodium dicyanamide |
| NMR | Nuclear magnetic resonance |
| [N(SO ₂ CF ₂ CF ₃) ₂] ⁻ or [beti] ⁻ | Bis(perfluoroethylsulfonyl)imide |
| [NH(Et) ₃] | Triethylammonium |
| [Omim] | <i>1</i> -Octyl-3-methylimidazolium hexafluorophosphate |
| PILs | Protic ILs |
| PS-IL | Polystyrene-IL |
| [Pyr][NO ₃] | Pyrrolidinium nitrate |
| pTSA | <i>p</i> -Toluenesulfonic acid |
| x | |

| | |
|---|---|
| [Pyrr _{1,g}] | <i>N</i> -glyceryl- <i>N</i> -methylpyrrolidinium |
| [Pip _{1,g}] | <i>N</i> -glyceryl- <i>N</i> -methylpiperidinium |
| [Pip _{1,e}] | <i>N</i> -ethanol- <i>N</i> -methyl piperidinium |
| [Pip _{2,e}] | <i>N</i> -ethanol- <i>N</i> -ethyl piperidinium |
| [PF ₆] ⁻ | Hexafluorophosphate |
| PAN | Propylammonium nitrate |
| [Pyrr _{1,3}][FPFSI] | <i>N</i> -propyl- <i>N</i> -methyl pyrrolidinium fluorosulfonyl |
| [Pyrr _{1,a}][Tf ₂ N] | <i>l</i> -Allyl-1-methylpyrrolidinium bistriflimide |
| [PyPs][TsO] | Pyridinium-1-propane sulfonic acid tosylate |
| SAXS | Small-angle X-ray scattering |
| SANS | Small-angle neutron scattering |
| SCFs | Supercritical fluids |
| [Tf ₂ N] ⁻ | Bistriflimide |
| [tbaim]Cl ₂ | 3,3'-Thionyl-bis-1,1'-alkylimidazolium |
| T _g | Glass transition temperature |
| THF | Tetrahydrofuran |
| [Tf ₂ N] | Bistriflimide |
| TDC | Total dissolve CO ₂ |
| UV | Ultraviolet |
| VOCs | Volatile organic compounds |
| VTF | Vogel-Tamman-Fulcher |
| WAXS | Wide-angle X-ray scattering |
| α | Hydrogen-bond donor acidity |
| β | Hydrogen-bond basicity |
| π^* | Dipolarity/polarizability |

Scope and Outline of the Work

Ionic liquids (ILs) are promising new media (also called as green solvents) which can be helpful in a variety of applications. They have high polarity values, many have good conductivity values and low viscosity values as well. But, it is always important to choose the best combination of cation and anion in order to meet the requirements of that particular application. Nevertheless, these ILs cannot be easily named as green solvents without testing their toxicity values. The cations and as well as the anions are both individually responsible for the toxicity value of that particular IL. Literature data present a variety of work which suggest that the aromatic cations (such as pyridinium and imidazolium, this latter representing the most investigated and applied class of ILs) are more toxic than aliphatic ones.

The main challenge in the chemistry world is, to reduce the process wastes, but the possibility of separation of the catalyst or solvent recovery, in other words recyclability, is difficult. The formation of large amounts of wastes on the other hand increases the cost of the reaction and overall production. To overcome these problems we have worked out few steps in this PhD work. Thus, this PhD work comprises of nontoxic ILs based on aliphatic amines, and we have studied their temperature-dependent physico-chemical properties such as density, conductivity, viscosity and solvent properties. The solvent properties helped us to decide the polarity values of various tested ILs. Both acidic ILs as well as basic ILs were prepared during this thesis. The acidic ILs were Brønsted acids and the anionic part were more responsible for their behavior. These acidic ILs were used in four reactions, three esterification reactions and one transesterification reaction. Few of these reactions were solvent-free and the solvent/catalyst (IL) was easily separable just by decantation.

An actual approach to achieve a high polarity of various ILs was by incorporating functional groups which were able to give high polarity values mainly when single or double hydroxyl groups were attached to the alkyl chain which were protonated to the nitrogen atom of the nitrogen base.

Overall this thesis is a combination of synthesis of neutral, acidic and basic ILs; temperature-dependent properties like density, conductivity, viscosity and solvent properties; toxicity and biodegradability; and applications of acidic ILs in order to replace Brønsted acidic ILs in various esterifications and transesterification reactions; and applications of basic ILs in transesterification of dimethyl carbonate.

The synthesis, temperature-dependent properties like density, conductivity, viscosity and solvent properties of morpholinium dicyanamides were reported; and toxicity and biodegradability values of morpholinium bromides were also reported in Chapter 2.

Then ILs were functionalized using “renewable” compounds, such as 1,3-chloropropanediol, which arises from glycerol (a natural product, which is obtained as byproduct during the production of glycerol). To prepare these functionalized ILs, we have used several nitrogen bases; *N*-methylimidazole, *N*-methylpyrrolidine, *N*-methylmorpholine, dimethyl imidazole, 4-hydroxy-*N*-methyl piperidine and *N*-methylpiperidine. The synthesis of these ILs were carried out. Then their temperature-dependent properties such as density, conductivity, viscosity and solvent properties were studied, data are reported in Chapter 3. Also in this chapter, the analysis of the behavior of some properties (viscosity and conductivity) in terms of the Arrhenius and VTF equations have been reported for all the synthesized ILs. Finally, for four ILs also the thermosolvatochromism was investigated.

An introduction to a new series of ILs starting from a seven-membered ring amine, namely azepane (hexamethylenimine), has been reported in Chapter 4. The structural effect on the physico-chemical properties of this class of ILs having dicyanamide as counteranion was studied by changing the alkyl chains to butyl, ethanol and glyceryl groups. The properties of this new class of ILs were compared with those of analogously morpholinium (a functionalized ring) and piperidinium (a non-functionalized ring) salts. The temperature-dependent behavior of viscosity and conductivity of these ILs were compared. The polarity values were also compared and the seven-membered ring having a non-functionalized alkyl chain gave high polarity values.

Acidic ILs were prepared starting from nitrogen bases and inorganic acids. These acidic ILs were tried to replace few Brønsted acids in three esterification reactions and one transesterification reaction. These Brønsted acidic ILs were used both as solvent and catalyst in the esterification of octanol and acetic acid in which the product recovery was very simple, by just decanting the product, as the product and the IL formed two separate phases. The IL was also recycled easily by just drying in rotary to remove the water formed during the esterification process. Few of these Brønsted acidic ILs were used in esterification of 1,2-propanediol and acetic acid in which multiple product formation was observed and also yields were not so very high. Some Brønsted acidic ILs were also used to study the selectivity of primary hydroxyl group on the C6 position of β -methyl-D-glucopyranoside. Lastly, these Bronsted acidic ILs were used

to study the transesterification of ethyl-trans cinnamate using methanol as well as octanol. All these studies are explained in Chapter 5.

Some of the ILs studied in this PhD thesis can be classified also as basic ILs by taking into consideration their anionic part. In particular, the dicyanamide-based IL can be included in this category. These basic ILs were used as solvent as well as catalyst to prepare an important compound, namely glycerol carbonate, starting from two cheap compounds i.e. glycerol and dimethyl carbonate. The conversion yields were very high though the product separation was not possible without distillation at reduced pressures. This application is explained in Chapter 6.

Chapter 1

Introduction

Green chemistry represents a trend in chemically related research, aiming at waste minimization and cost effectiveness.¹ Recently, there has been a gradual but steadfast rise of general interest in environmental science, technology and practice, which aims at improving health, aesthetics and in many cases, the economics of individual chemical operations.² In the chemical world, this can be achieved via designing new reactions or modifying existing chemical processes. To reduce the environmental impact of chemical processes, different strategies can be followed: i) it is important to select raw materials and chemical reaction to avoid or reduce the handling and storage of hazardous and toxic chemicals; ii) it is necessary (when possible) to use raw materials arising from renewable feedstocks, for competing reactions; iii) it is necessary to adjust the temperature, pressure and catalyst to obtain high yields of desired products; iv) it is necessary to avoid solvent having an high environmental impact. Many of these strategies are resumed in the 12 principles of green chemistry³ that can be conceptually summarized as the following:

- 1) Waste prevention instead of remediation
- 2) Atom efficiency
- 3) Less hazardous/toxic chemicals
- 4) Safer products by design
- 5) Innocuous solvents and auxiliaries
- 6) Energy efficient use by design
- 7) Renewable raw materials and solvents should be used
- 8) Shorter synthesis (reducing protection–deprotection steps)
- 9) Biocatalytic or catalytic rather than thermal processes
- 10) Design the products for degradation without pollutant problems
- 11) Efficient analytical methodologies for pollution detection and prevention
- 12) Inherently safer processes

As we can deduce from principle 5, chemical processes should be performed in innocuous solvents. Most problems with conventional organic solvents are concerned with their toxicity, flammability, and volatility; conventional organic solvents, like dichloromethane, methanol or acetonitrile, tend to evaporate easily, making the reactions difficult to work with. Moreover, they have an important environmental impact. They have been implicated as one of the sources of ozone depletion, global climatic change and smog formation. Nevertheless, they are applied in large amounts in a wide range of industrial applications (synthesis, extractions and purification processes).⁴ Today, in the fine-chemical or pharmaceutical industries the solvent/product ratio

Chapter 1

varies between 100 and 1000 and, consequently, solvents are considered as the major cause of the environmental damage attributed to an industrial process.

Although in many green chemistry books and monographs one can find that “the greenest solvent is no solvent at all” there are definitely clear advantages in using solvents as part of chemical processes. We can highlight the fact that reactions proceed faster and more smoothly when the reactants are dissolved, because mass transfer restrictions are reduced. In addition, solvents may have a positive effect on the rate and/or selectivity of the reaction, due to the differential solvation of reagents, intermediates or transition states. Solvents act as heat transfer media, removing heat liberated in an exothermic reaction, reducing thermal gradients in a reaction vessel and allowing a smooth and safe reaction. Finally, solvents often facilitate separation and purification of reaction products.⁵

The qualitative and quantitative importance of solvents in chemical processes, together with the increasing legal restrictions concerning the use of organic solvents derived from petrol (recent environmental legislation is aimed at strict control of volatile organic compounds (VOCs) emissions and the eventual phasing out of greenhouse gases and ozone-depleting compounds) has resulted in a remarkable growth in interest for green solvents for industry. Traditionally, green solvents are classified in five main categories, although there is still controversy concerning the labeling of some of these categories as truly “green”: 1) water, 2) ionic liquids (ILs), 3) fluoruous solvents, 4) supercritical fluids (SCFs) and 5) organic solvents from renewable sources.

ILs constitute probably the largest group of those solvents, often defined as neoteric solvents, that include all chemical compounds constituted exclusively by ions which are liquid at/or near room temperature, by definition below 100°C. Although the use of ILs shows several advantages, we must also mention that they show some inconveniences, such as high cost, difficulties in purification and toxicity issues. There is already enough evidence to conclude that some ILs are potentially as harmful as the conventional organic solvents, therefore, careful design in the synthesis of ILs is required to reduce their toxicity and improve physico-chemical properties. Anyway, the main feature of ILs is the fact that all the properties (physical, chemical and biological) can be modified or modulated selecting the opportune anion–cation combination, or introducing on cation or anion specific functional groups; therefore, the possibility to design a nontoxic IL having the ability to act as suitable solvent and eventually as catalyst is not so fantastic.^{6,7,8,9,10,11}

It is noteworthy that functionalization of IL can be used not only to improve the solvent properties of these media but also to confer new specific functions. Functionalized ILs can act as

catalysts offering the advantage to have a homogeneous liquid system in which the catalyst is anchored to the solvent and leaching problems are reduced or by-passed.

Many organic reactions are performed in the presence of a catalyst and catalytic processes are involved in the manufacture of the majority of chemicals. Among the most frequently used catalysts are the acidic ones, which are generally applied in a homogeneous phase. The use of homogeneous acidic catalysts may have the following intrinsic drawbacks: *i*) a neutralization or washing step is usually required and, depending on the amount of homogeneous catalyst to be used, this can determine the formation of large amounts of waste salts. Disposal of these salts is usually expensive or entirely prohibited; *ii*) separation of homogeneous catalysts from the reaction mixture is generally a difficult step; *iii*) the use of Brønsted acids is often accompanied by corrosion of the process equipments; *iv*) some of the applied catalysts are toxic or otherwise difficult to handle (air or water sensitive). The aforementioned problems together with the increasing environmental concerns and restrictive legislation have prompted research to find new effective catalysts, which avoid these drawbacks. Consequently, during the last decades solid acids are receiving increasing attention as catalysts in organic synthesis on laboratory and fine chemicals manufacturing scale. Though the solid acids are nonvolatile and can represent a solution to some of the above-mentioned intrinsic drawback of homogeneous acidic catalysts (they can readily be separated from the reaction mixture, they are easier to handle, solid acids are less corrosive, many solid acids can be regenerated and reused and they may be adapted for use in a continuous flow reactors) they present other disadvantages including the restricted accessibility of the matrix-bound acidic sites (transport of reactants is generally not difficult in homogeneous catalysis), the high molecular weight/active-site ratios, and the rapid deactivation.^{12,13} Nevertheless, the desire to improve or alter the selectivity of a chemical process may be a further reason for selecting a solid catalyst. The structural and electronic properties of the solid catalyst can put constraints on the diffusion of molecules to and from active sites and on the geometric configuration of the transition state. These constraints may lead to kinetic control over reaction pathways, resulting in non-thermodynamic product compositions. However, the products formed from the primary reaction may also react in a secondary reaction, depending on the contact time and the strength of the interaction with the active site. It is therefore desirable that the products of the primary reaction de-absorb readily into the bulk of the surrounding medium. The contact time between catalysts and reactants and products may have a strong influence on the product selectivity.

Hence, taking into account both the advantages and disadvantages of solid acids, it is evident that a new field of research may be represented by immobilized liquid acidic catalysts which covered

both the nonvolatility as well greater effective surface area and continued potential activity of a liquid phase. Acidic ILs, combining all the above factors, in an ionic structure can be considered as one of the most promising new reaction media.¹⁴

1.1 Definition of Ionic Liquids

'Ionic liquids' (ILs), a term which is now very well-known to the chemists, was less than 20 years ago very remote in the chemical literature. This is because their existence and consequently their potential as solvents was not recognized before. But, the ILs are not very new as it seems, some of them have been known for a century. For instance ethylammonium nitrate ($[\text{EtNH}_3][\text{NO}_3]$), which has a melting point of 12°C , was first described in the year 1914.¹⁵ However, one of the important development recorded in the chemical literature about these ILs and their existence was in 1940. The two US scientists, Tom Weir and Frank Hurley working in the Rice Institute were looking for a cheaper and easier way to electroplate aluminium when they mixed and gently warmed powdered pyridinium halides with AlCl_3 , the powders reacted, obtaining a clear, colorless liquid.¹⁶ Hence, they accidentally prepared liquid electrolytes, namely chloroaluminate ILs, which belongs to a class of ILs now known as the first generation ILs. However, the chemists of those times hardly noticed the potential of these astonishingly important liquids. In the late 1980s, the scientists working in the US Air Force Academy were instrumental in initiating the preliminary research in the realm of ILs. The eminent scientists such as King and Wilkes and associates can be regarded as the beginners of seminal activity on ILs which involved the synthesis of structurally diverse ILs, their characterization, investigation of physical properties and so on.¹⁷ The pioneering work of Seddon and his associates introduced the ILs to the modern day's chemists.¹⁸ Starting from these works, ILs have been considered as alternative environmentally friendly solvents, recyclable media for synthetic organic chemistry, separation sciences and other chemical sciences and engineering. It was evidenced that in contrast to the conventional organic solvents that are composed of molecular entities, such as DMSO, DMF, CH_2Cl_2 , CHCl_3 and THF, ILs have no significant vapor pressure, thus allow chemical processes to be carried out with essentially zero emission of toxic species into the environment. In some cases, products can be obtained through distillation from these nonvolatile reaction media whereas in the other cases the products and the ILs form two separate phases and hence they can be separated easily without any use of energy (such as distillation) and without any toxic solvents such as ether, ethylacetate etc. (products may be soluble). ILs possess high ionic conductivity, high ion concentration and good electrochemical stability. Applications benefiting from these materials may include electrical energy storage devices (such as electrolytic capacitors, batteries

and fuel cells), as well as supporting media for catalysts. They have also been found to be efficient in standard separating processes, eliminating the need of noxious organic solvents.¹⁹ Therefore, such systems are becoming increasingly technologically important. More recently, it has been shown that the beauty of ILs is the fact that combining different cations and anions produces wholly new ILs with their own unique structures and properties. Several million possible combinations of cations and anions able to give salts liquid at room temperature have been hypothesized, presenting an immense opportunity to engineer solvents or media with specific properties for different applications. But it also presents an unusual problem – synthesizing, characterizing and testing the seemingly limitless possibilities, is a near impossible task.²⁰

1.2 Acidic Ionic liquids

Research on IL is growing at a very fast rate, new ILs and new applications in different sectors, not necessarily directly related to chemistry, appear daily. Although many investigated ILs can be defined as practically neutral salts, an important subset of ILs is represented by acidic ILs. The acidic nature can be related to the anion or to the cation or both. Moreover, they can be defined as Lewis acidic ILs due to their ability to act as electron pair acceptors, the anion is generally responsible for this kind of acidity, or Brønsted acidic ILs whose ability to act as proton donor may be due to the cation or anion. Figure 1.1 shows the subsets of acidic ILs. ILs having dual properties (Lewis and Brønsted acidity) have been also prepared.

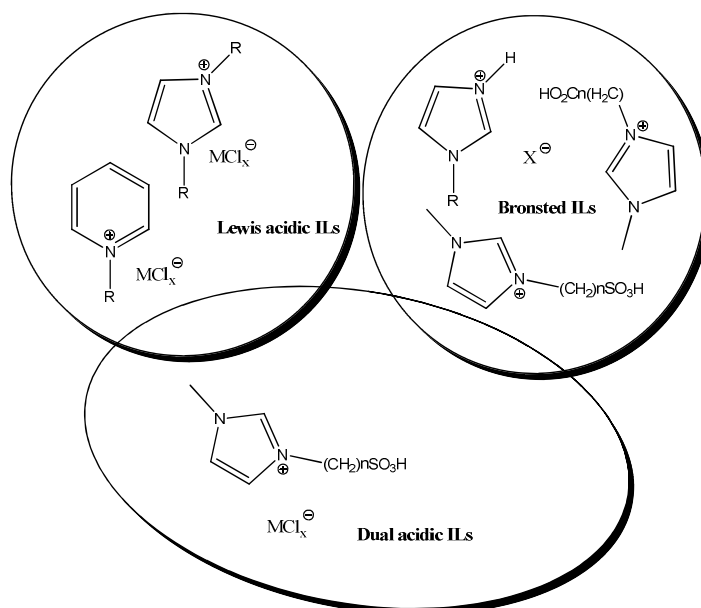


Figure 1.1: Subsets of acidic ILs

The cations most commonly used in Brønsted acidic ILs are represented in Figure 1.2a, including primary, secondary and tertiary ammonium ions, imidazolium and pyridinium salts, protonated lactams and guanidinium ions.

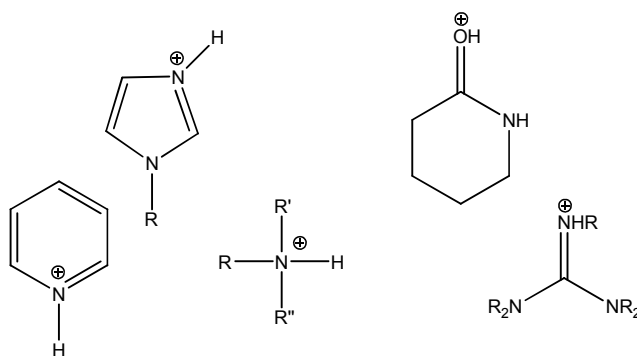


Figure 1.2a: Cations most commonly used in Brønsted acidic ILs

Imidazolium and other cations bearing a properly functionalized alkyl chain with a SO_3H or COOH group can also be included in this class (Figure 1.2b).

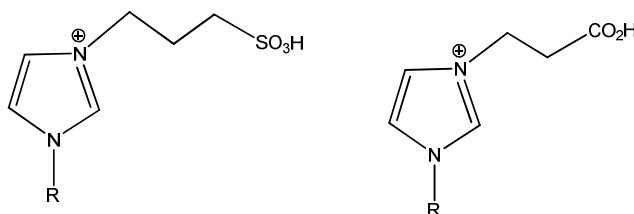
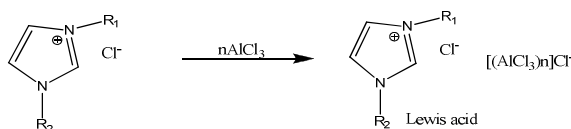


Figure 1.2b: Imidazolium cations bearing functionalized alkyl chain

On the other hand, Brønsted acidic ILs can also be obtained by introducing proton donor anions such as HSO_4^- , H_2PO_4^- and conjugate bases of dicarboxylic acids. At variance, with few exceptions Lewis acidic ILs contain an acidic anion. These latter are prepared by addition of the proper amount of a Lewis acid to a neutral IL.

1.2.1. Lewis acidic ILs

Until 2001, the chloroaluminate ILs by far have been the most widely explored class of ILs. Hurley and Wier²¹ first disclosed the room temperature melts, composed of *N*-alkylpyridinium halides and AlCl_3 , in a series of US patents. The room temperature ILs composed of varying portions of AlCl_3 and 1-ethyl-3-methylimidazolium chloride ([emim]Cl) were discovered in the year 1982.²² Chloroaluminate ILs, or the first generation ILs, are prepared by mixing the appropriate quaternary ammonium salt, such as 1-butyl-3-methylimidazolium chloride ([bmim]Cl), with AlCl_3 .²²



Scheme 1.1: Preparation of a mono-functionalized Lewis acidic ILs

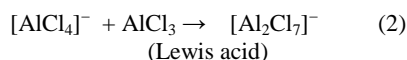
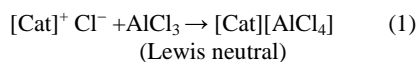
Preparation of [bmim]Cl: Equimolar amounts of chlorobutane and 1-methylimidazole were added to a round-bottomed flask fitted with a reflux condenser for 24–72 h at 70°C with stirring until two phases were formed. The top phase, containing unreacted starting material, was decanted and ethyl acetate (a volume approximately equal to half that of the bottom phase) was

Chapter 1

added with thorough mixing. The ethyl acetate was decanted followed by the addition of fresh ethyl acetate and this step was repeated twice. Washing with ethyl acetate should suffice to remove any unreacted material from the bottom phase. After the third decanting of ethyl acetate, any remaining ethyl acetate was removed by heating the bottom phase to 70°C and stirring while on a vacuum line. The product, [bmim]Cl, is slightly yellow and may be crystalline at room temperature, depending on the amount of water present in that phase. This method was given by Jonathan G. Huddleston et al.,²³ in the year 2001.

Preparation of [bmim]Cl/AlCl₃ :- Commercial AlCl₃ was mixed with Al turnings and 1 wt% NaCl and sublimed under 50 mmHg nitrogen, at least twice, until no ash-like residue was left. [bmim]Cl/AlCl₃ was prepared by slowly mixing weighed amounts of [bmim]Cl with re-sublimed AlCl₃ in a glove bag under nitrogen using dry ice for cooling. In Scheme 1.1, we can say R₁=C₄H₉ and R₂=CH₃.

Equations (1) and (2) show the acid–base reactions that occur when organic chloride salts ([Cat]Cl) and AlCl₃ are mixed. The Lewis acid, AlCl₃, forms AlCl₄⁻, a Lewis neutral species and Al₂Cl₇⁻, a Lewis acid, when mixed with the organic chloride salt, as shown below in Equations (1) and (2).



The molar fraction of the Lewis acid determines therefore the acidic, basic or neutral properties of the resulting salts²⁴ as well as their physico-chemical and thermal properties.

The liquid range (the range of temperatures in which the compound exists in the liquid state) of these salts depends on the structure of the cation and the mole fraction of AlCl₃, this latter determining the anion structure. The anion composition affects also viscosity; in the case of [emim]Cl + AlCl₃ it has been shown²⁵ that when [emim]Cl is below 50 mol% the viscosity is practically constant (changing from 14 cP to 18 cP, at 303 K). However, when [emim]Cl exceeds 50 mol%, the absolute viscosity begins to increase rising to over 190 cP at 67 mol% [emim]Cl. This dramatic increases is correlated to the corresponding growth in chloride ion concentration and it has been attributed to the ability of this anion to give hydrogen bonding to the hydrogen atoms of imidazolium cation. Contemporaneously, molar conductivity decreases on going from ILs having as counteranion [Al₂Cl₇]⁻ (for 34–66 mol% [emim]Cl–AlCl₃ λ = 4.46 S cm² mol⁻¹, at 298 K) or [AlCl₄]⁻ (for 50–50 mol% [emim]Cl–AlCl₃ λ = 4.98 S cm² mol⁻¹, at 298 K) to system

containing an excess of chloride ions (for 66–34 mol% [emim]Cl–AlCl₃ $\lambda = 1.22 \text{ S cm}^2 \text{ mol}^{-1}$, at 298 K).

It is to note that cations and anions diffusion values correlate well with ionic conductivity in the case of acidic imidazolium chloroaluminates; as expected, both cation and anion diffusion coefficients increases with increase in the conductivity. Nevertheless, the decline in cation diffusion coefficients under “basic” composition (i.e., in the presence of an excess of [emim]Cl) is consistent with the presence of an hydrogen bonding between chloride anion and the imidazolium cation.

But, one of the most important property of these systems is surely the fact that they may provide a distinctly homogenous Lewis acidic medium in contrast to the conventional Lewis acid, AlCl₃ when used in molecular solvents. Unfortunately, for practical applications, these chloroaluminate ILs suffer from their poor stability to moisture which can lead to undesired side reactions and causing considerable potential for corrosion (due to the release of HCl).

More recently, however, water stable chlorometallate ILs have been prepared and characterized. The appropriate molar combination of an organic chloride salt (e.g., [bmim]Cl) with indium trichloride, or niobipentachloride affords the corresponding ILs. For example, [bmim][InCl₄] (mp -6°C) is a air stable IL characterized²⁶ by physico-chemical properties (density, viscosity, electrical conductivity and electrochemical window) complementary to the classical tetrafluoroborate or hexafluorophosphate analogues possessing, at the same time, a Lewis acidity similar to organoaluminate melts. Zinc or iron-containing ILs are other moisture-stable alternatives to chloroaluminate ILs²⁷ whose acidic property can be easily modified by adjusting the composition of cations and metal halide, in analogy to chloroaluminates. In this sub-class of moisture-stable Lewis acidic ILs, we have to include a series of inexpensive and more sustainable Lewis acidic ILs prepared from choline chloride and ZnCl₂,²⁸ both these reagents are indeed accessible, easy to handle, relatively cheap and moisture stable, hence these match several of the principles of green chemistry.

But, surely a peculiar class of chlorometallate ILs is that arising by combination of chloride-based ILs and FeCl₃. Iron-containing ILs, such as [bmim][FeCl₄], are not only catalytically active and moisture-stable Lewis acids but they are also magnetic,²⁹ they play an important role for the formation of ionogels³⁰ and their mixtures with water show a peculiar thermomorphism (i.e., a thermally induced demixing)³¹. Related to the magnetic properties, although iron-based ILs are simply paramagnetic, they still respond to an applied magnetic field. It has been shown³² that droplets of the [C₁₀mim][FeCl₄] and [PR₄][FeCl₄] salts can be added to water, with which they are initially immiscible and they can then be quite easily manipulated with the application of an

Chapter 1

external strong magnetic field. Nevertheless, although the droplets of $[\text{C}_{10}\text{mim}][\text{FeCl}_4]$ dissolve themselves in the aqueous phase after several hours, $[\text{PR}_4][\text{FeCl}_4]$ droplets remain intact almost indefinitely (over several months) showing the potential of this latter ILs for magnetic transport through aqueous systems.

Finally, it is to mention that although a significant Lewis acidity is generally a property related to the anion, and to the presence of halometallates, in 2009 an example of an IL bearing a functionalized imidazolium cation with an efficient Lewis acid, boronic acid, has been reported.³³

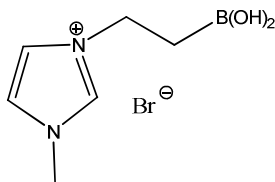
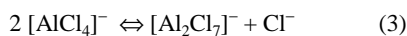


Figure 1.3: Imidazolium cation functionalized with boronic acid (Lewis acid)

The boronic acid is a weak Brønsted acid but a very efficient Lewis acid. The activity coefficients of various solutes determined in 1-propyl boronic acid-3-alkylimidazolium bromide showed that this IL can play an important role for the separation of aromatics, chloroalkanes, and alcohols from alkanes. Recently, 1-propyl boronic acid-3-alkylimidazolium bromide has been used³⁴ as dispersant of petroleum asphaltenes: the presence of the boronic moiety enhances interactions between asphaltenes and ILs and limits considerable asphaltenes aggregation.

1.2.1.1. Lewis Acid ILs

As reported above, the most common Lewis acidic ILs are composed of metal halides and quaternary nitrogen or phosphorus-containing halide salts, with the apparent mole fraction of metal halides (MCl_X), X , greater than the stoichiometric neutral point. Consequently, the Lewis acidity of these melts is referred (at least, in the first papers published on these systems) not to Lewis acidity as it is frequently assumed, but to the acidity of an anionotropic solvent system, in which a base is a substance that liberates a characteristic anion (e.g., chloride), whereas an acid consumes it.^{35,36,37} Consequently, it has been determined in the case of chloroaluminates by chloride activity, according to the equation (3):



and has been defined in terms of $-\log_{10}[\text{Cl}^-]$. For example, an equilibrium constant of 2×10^{-19} for equation (3) was determined from potenziometric titration data for $[\text{emim}]\text{Cl}-\text{AlCl}_3$.²²

Nevertheless, nuclear magnetic resonance (NMR) spectroscopy (^{27}Al , ^{31}P and ^1H) has been used to determine the form and the fraction of the anionic species,^{37,38} whereas other techniques, e.g., UV and IR spectroscopy and electrochemical methods, have been used to monitor the interaction between donors and anionic species.^{36,37,39,40} Unfortunately, all of these techniques suffer from disadvantages such as strong medium-specificity, little available reference information and/or difficulties in manipulation.

More recently, Ya-li Yang and Yuan Kou have determined⁴¹ the Lewis acidity (as electron pair acceptor ability) of several chloroaluminate ILs based on the 1-butyl-3-methylimidazolium ($[\text{bmim}]^+$) cation by means of an IR spectroscopic method using pyridine and ethanenitrile, a weaker base than pyridine, as molecular probes. Both these probes present band shifts as a consequence of the coordination at the Lewis acid sites, moreover, pyridine giving a band near 1540 cm^{-1} as a consequence of the formation of pyridinium ion can be used also a probe molecule for Brønsted acidic sites. After pyridine (py:IL = 1:5 by volume) was added to ILs of the type $[\text{bmim}]\text{Cl}/\text{MCl}_x$ under acidic conditions the wavenumber of the band corresponding to the coordination at Lewis acid sites increases from 1444 cm^{-1} for $[\text{bmim}]\text{Cl}/\text{CuCl}$ to 1446 cm^{-1} for $[\text{bmim}]\text{Cl}/\text{FeCl}_3$, 1450 cm^{-1} for $[\text{bmim}]\text{Cl}/\text{ZnCl}_2$ and 1454 cm^{-1} for $[\text{bmim}]\text{Cl}/\text{AlCl}_3$, indicating that the Lewis acidity increases in the following order $\text{CuCl} < \text{FeCl}_3 < \text{ZnCl}_2 < \text{AlCl}_3$ at the point at which ILs have strong Lewis acidities. At variance, under neutral conditions (when $X = 0.5$ for $[\text{bmim}]\text{Cl}/\text{MCl}_x$ ($M \neq \text{Zn}$) and $X = 0.33$ for $[\text{bmim}]\text{Cl}/\text{ZnCl}_2$) only free pyridine band at 1437 cm^{-1} was observed for each sample.

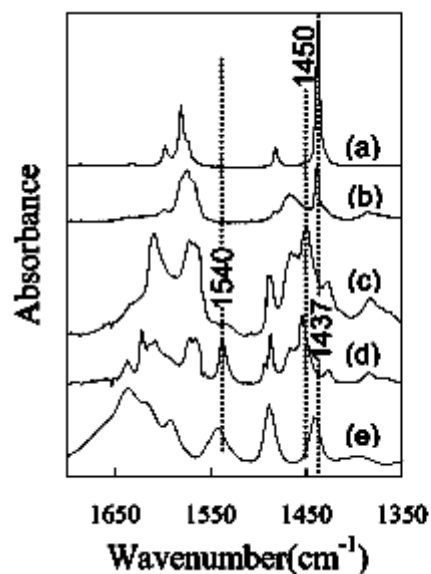


Figure 1.4 A

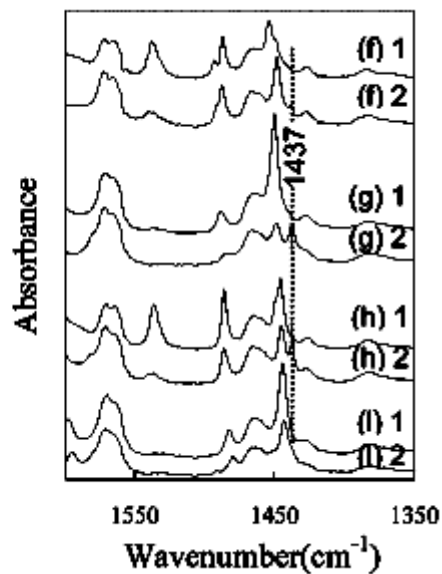


Figure 1.4 B

Figure 1.4: FT-IR spectra of [bmim]Cl with various metal halides. (A) FT-IR spectra of (a) pure pyridine; (b) pyridine + [bmim][BF₄] (1:5 by vol.); (c) pyridine + [bmim]Cl/ZnCl₂ ($x = 0.67$) (1:5 by vol.); (d) pyridine + [bmim]Cl/AlCl₃ ($x = 0.67$) (1:5 by vol.); (e) pyridine + HCl solution (36 wt%). Bands at 1437 cm⁻¹ in (a) and the neutral IL (b) arise from free pyridine whereas bands near 1450 cm⁻¹ in (c) and (d) result from pyridine coordinated at Lewis acid sites. Bands near 1540 cm⁻¹ in (d) and (e) indicate the presence of pyridinium cations formed by protonation at Brønsted acid sites. (B) FT-IR spectra of mixtures (1:5 by vol.) of pyridine + [bmim]Cl/MCl_x. (f) [bmim]Cl/AlCl₃, 1 $X = 0.67$, 2 $X = 0.5$; (g) [bmim]Cl/ZnCl₂, 1 $X = 0.67$, 2 $X = 0.33$; (h) [bmim]Cl/FeCl₃, 1 $X = 0.67$, 2 $X = 0.5$; (i) [bmim]Cl/CuCl, 1 $X = 0.67$, 2 $X = 0.5$.

An analogous trend ($\text{CuCl} < \text{FeCl}_3 < \text{ZnCl}_2 < \text{AlCl}_3$) was observed using ethanenitrile that shows two characteristic bands at 2292 and 2252 cm⁻¹, originating from its CN stretching vibrations, as pure compound and when added to either HCl or [bmim][BF₄], which have no Lewis acidity. However, the addition of ethanenitrile to [bmim]Cl/MCl_x ($X = 0.67$) (Figures 1.4 A (d)–(g)) results in the appearance of a new band at higher wavenumber (at 2292 cm⁻¹ for [bmim]Cl/CuCl, 2310 cm⁻¹ for [bmim]Cl/FeCl₃, 2318 cm⁻¹ for [bmim]Cl/ZnCl₂, and 2338 cm⁻¹ for [bmim]Cl/AlCl₃) showing that the Lewis acidity increases in the order. The behavior of ethanenitrile with various Lewis acidic ILs are shown in Figures 1.5 (a)–(g), below.

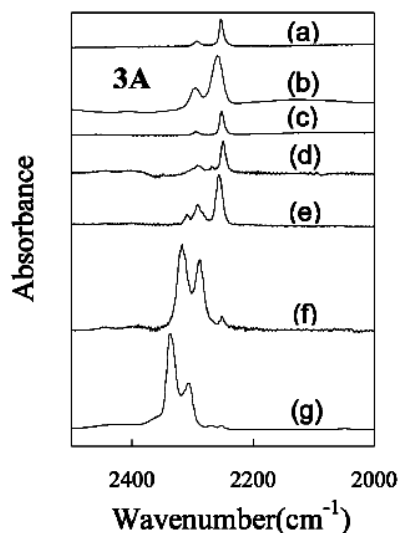


Figure 1.5 FT-IR spectra of ILs using ethanenitrile as a probe. (a) pure ethanenitrile; (b) ethanenitrile + HCl solution (36 wt%); (c) ethanenitrile + [bmim][BF₄] (1:5 by vol.); (d) ethanenitrile + [bmim]Cl/CuCl ($X = 0.67$) (1:5 by vol.); (e) ethanenitrile + [bmim]Cl/FeCl₃ ($X = 0.67$) (1:5 by vol.); (f) ethanenitrile + [bmim]Cl/ZnCl₂ ($X = 0.67$) (1:5 by vol.); (g) ethanenitrile + [bmim]Cl/AlCl₃ ($X = 0.67$) (1:5 by vol.).

The same approach has been applied⁴² more recently using acetonitrile as the basic probe molecule to determine the acidity of the ILs which contain metal halide ZnCl₂, FeCl₃ or FeCl₂. Also in this case modifications in the CN stretching frequencies were observed on going from neutral ILs to acidic media. Only two characteristic ν_{CN} stretching vibration bands of acetonitrile, at 2250 and 2287 cm⁻¹, were observed when acetonitrile was mixed with the IL with a ZnCl₂/[bmim]Cl molar ratio of 0.9 (X), indicating that there is no interaction between the IL and acetonitrile. However, when X was higher than 1.0, an additional band appeared at around 2312 cm⁻¹ and a monotonic blue shift of all these bands were observed with an increase of the molar ratio of ZnCl₂ to [bmim]Cl (X). The band around 2312 cm⁻¹ was considered indicative of Lewis acid–base interaction between the IL and acetonitrile. Moreover, the intensity of IR band around 2312 cm⁻¹ become stronger with the increase of the fraction of ZnCl₂, implying that the increased amount of ZnCl₂ leads to a stronger Lewis acid–base interaction between the IL and acetonitrile. Using acetonitrile as a probe molecule, Lewis acidity of the ILs containing FeCl₃ or FeCl₂ showed the similar results.

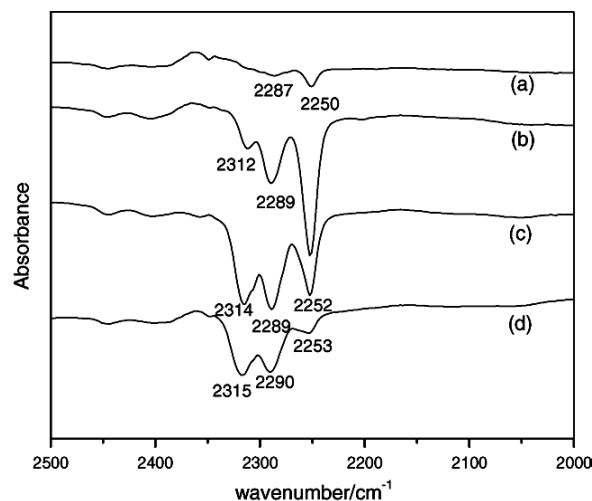


Figure 1.6: FT-IR spectra of mixtures of acetonitrile and [bmim]Cl–ZnCl₂ IL: (a) molar ratio of ZnCl₂ to [bmim]Cl = 0.9; (b) molar ratio of ZnCl₂ to [bmim]Cl = 1.0; (c) molar ratio of ZnCl₂ to [bmim]Cl = 1.5; (d) molar ratio of ZnCl₂ to [bmim]Cl = 2.0.

Finally, pyridine was used by Duan et al. to determine the acidity of choline chloride–ZnCl₂ and benzyltrimethylammonium chloride–ZnCl₂. A similar Lewis acid strength of the four ILs, which caused practically the same band shift of pyridine molecule, was evaluated from these experiments showing that cation structure practically does not affect chlorometallate Lewis acidity.

Recently, the Gutmann Acceptor Number (AN) has been used to evaluate the acceptor ability of some chlorometallate(III) ILs. This parameter has been estimated⁴³ using the ³¹P-NMR chemical shift of a probe molecule, triethylphosphine oxide, for a range of chlorometallate(III) ILs, based aluminium(III), gallium(III) and indium(III) and the 1-octyl-3-methylimidazolium cation, at different compositions. The results are shown in the next page.

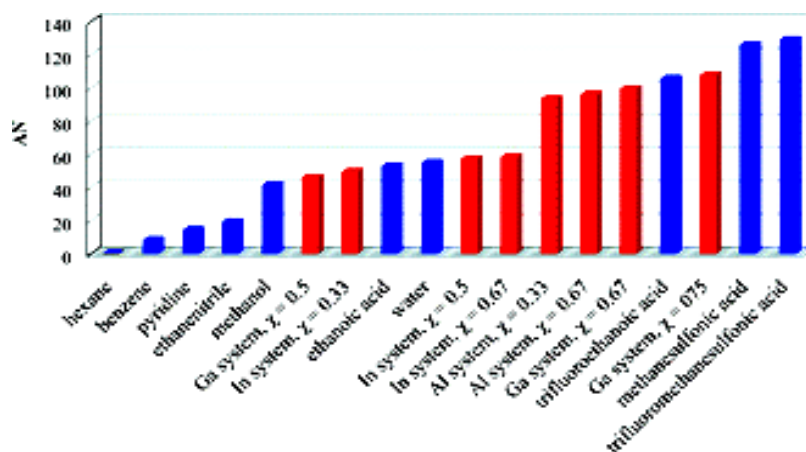


Figure1.7: Gutmann Acceptor Number of several chlorometallate ILs and molecular solvents

1.2.1.2. Applications of Lewis acids in synthesis

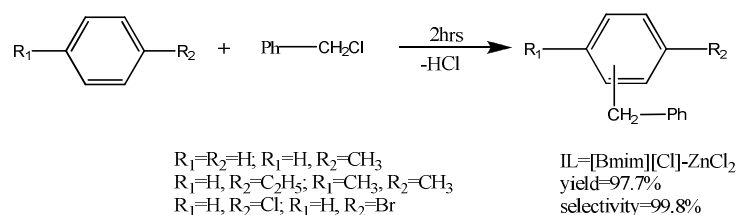
A. Friedel Crafts reactions using imidazolium chlorides along with metal halides

Acidic chloroaluminate(III) ILs, $X(\text{AlCl}_3) = 0.67$, have been widely applied in reactions conventionally catalyzed by Lewis acids. Several important compounds have been prepared with high yields and selectivities through Friedel-Craft acylation,⁴⁴ sulfonylation⁴⁵ or alkylation processes.⁴⁶ However, the very high sensitivity of these ILs to moisture, that determines the necessity to work during synthesis and use under inert atmosphere, has contributed to promote research towards other more stable catalytic systems.

In 2006, D. Yin et al.⁴⁷ reported synthesis of diphenylmethane and its derivatives via Friedel-Crafts benzylation reaction of benzylchloride with benzene and the corresponding derivatives using Lewis acidic ILs for the first time as solvents and catalysts. The used ILs were moisture stable [bmim]Cl–ZnCl₂, [bmim]Cl–FeCl₃ and [bmim]Cl–FeCl₂ systems. Easy separation of the reaction products, increased reaction rates with respect to conventional molecular solvents and high selectivity towards mono-alkylated products were obtained, showing that these ILs were not only more moisture stable, and therefore less problematic to use, but their acidic property could be easily modified by adjusting the composition of cations and metal halides in order to increase reactivity or selectivity; hence, they might be suitable candidates for Friedel-Crafts reactions.

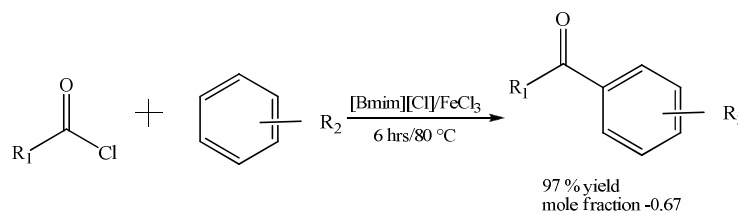
Chapter 1

Nevertheless, all these ILs could be reused, especially [bmim]Cl–ZnCl₂, which could be recycled for eight times without any noticeable drop in its activity.



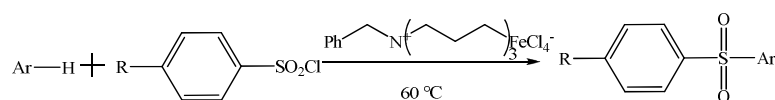
Scheme 1.2: Friedel-Crafts reactions of benzene and its derivatives with benzyl chloride

Subsequently, Li et al.⁴⁸ tested the efficiency of the same moisture stable Lewis acidic ILs (i.e. [bmim]Cl/FeCl₃ and [bmim]Cl/ZnCl₂), with respect to conventional molecular solvents and the classical Lewis acidic [bmim]Cl/AlCl₃, in the synthesis of benzophenone and its derivatives via Friedel-Crafts reaction. Among the investigated Lewis acidic IL, [bmim]Cl/FeCl₃ showed the higher catalytic activity; good to excellent yields (up to 97%) of acylation products were obtained in short reaction time.



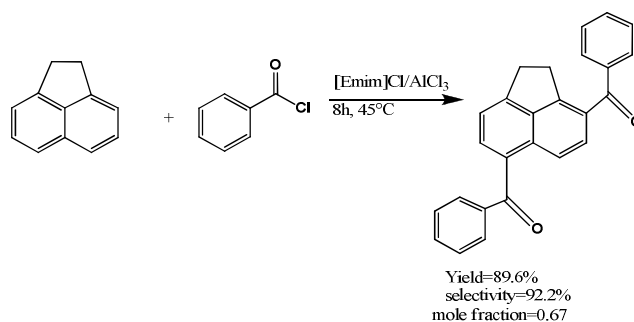
Scheme 1.3: Friedel-Crafts acylation reaction of benzene derivatives and acyl chloride

On the other hand, FeCl₃-based ILs have been used with success also in the selective Friedel-Crafts sulfonylation of aromatic compounds.⁴⁹ Deactivated arenes, such as chlorobenzene and bromobenzene, underwent sulfonylation in excellent yields. Further, an improvement in the regioselectivity was observed in the sulfonylation of naphthalene with benzenesulfonyl chloride and 4-methylbenzenesulfonyl chloride. The evidenced advantages arising from the use of FeCl₃-based IL were; mild reaction conditions, excellent yields, short reaction times, simple work-up procedure, low cost and easy preparation and handling of the catalyst.



Scheme 1.4: Friedel-Crafts sulfonylation of aromatic compounds

However, not all data from literature are in agreement with the fact that moisture-stable chlorometallates can always substitute chloroaluminate-based ILs; their lower Lewis acidity can be an important detrimental factor in some reactions. Studies performed on the preparation of 3,6-dibenzoylacenaphthene by acylation of acenaphthene in Lewis acidic ILs ([emim]Cl/AlCl₃, [emim]Cl/FeCl₃ and [emim]Cl/ZnCl₂) showed that [emim]Cl/AlCl₃ gave the best yield, whereas practically no product was obtained in [emim]Cl/ZnCl₂.⁵⁰ Experiments performed on methyl imidazolium salts bearing longer alkyl chains on nitrogen (butyl and octyl) were also carried out; however, [emim]Cl/AlCl₃ was found to be the best IL for this kind of reaction. Thus, taking this into consideration the mole fractions of [emim]Cl/AlCl₃ was varied from 0.33 to 0.75 and the best mole fraction was found to be 0.67; under these conditions the yield increased to 89.6% with a selectivity of 92.2%.

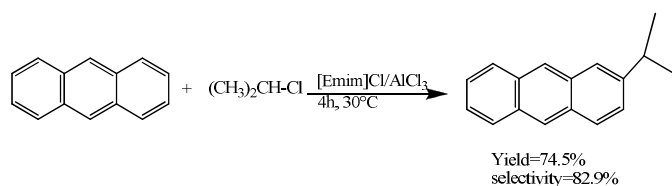


Scheme 1.5: Friedel-Crafts acylation of acenaphthene to 3,6-dibenzoylacenaphthene

Finally, also recycling experiments were performed to confirm the high efficiency of this catalytic system. After five recycles, only a small reduction in yield (4% approximately, from 89.6% in the cycle to 85.5% in the fifth cycle) and selectivity (2% approximately, from 92.2% in the first cycle to 90.6% in the fifth cycle) was observed.

The higher catalytic activity of [emim]Cl/AlCl₃ was also confirmed by the same authors in another work related to the alkylation of anthracene with 2-chloropropane where the same Lewis acidic ILs were used. In agreement with the previously discussed results, Chen et al.⁵¹ found that [emim]Cl/AlCl₃ gave best results in terms of yield (74.5%) and selectivity (82.9%). On increasing the alkyl chain length on the imidazolium ring to butyl and octyl the percentage of

yield decreased just as same as in the previous work and again zero performance was obtained when ZnCl_2 was used as metal halide.



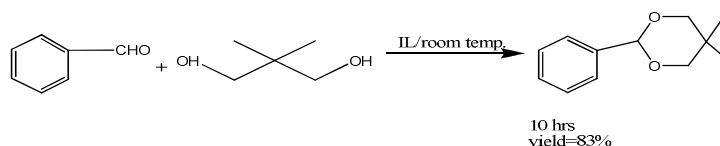
Scheme 1.6: Friedel-Crafts alkylation of anthracene with 2-chloropropane

On the other hand, when the alkylation of benzene was performed in several 1-alkyl-3-methylimidazolium halide- AlCl_3 ILs comprising various alkyl group (butyl, octyl and dodecyl) and various halogens (Cl, Br and I) the best catalytic performance was found in the case of $[\text{bmim}]\text{Al}_2\text{Cl}_6\text{Br}$ and this ability was attributed to the Lewis acidity strength and polarizability of this salt; the presence of a bromide instead of a chloride increases the Lewis acidity of the anion, as determined in the same work by FT-IR measurements.⁵²

B. Lewis acidic ILs as catalysts for carbonyl protection reactions

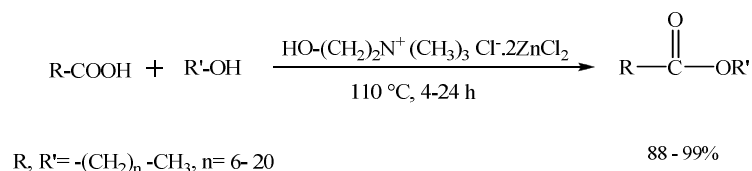
Despite their extensive investigation in Friedel-Crafts reactions, Lewis acidic ILs have also been applied in many other processes. 1-Ethyl-3-methylimidazolium iodide- AlCl_3 (AlCl_3 : $[\text{emim}]\text{I}$ ratio > 1:1) has been used with success in acylative cleavage of ethers,⁵³ whereas other imidazolium or pyridinium chloraluminates has been applied in coumarine synthesis via Pechmann condensation of phenols with ethyl acetoacetate,⁵⁴ Knoevenagel condensation,⁵⁵ oligomerization⁵⁶ or dimerization⁵⁷ of olefins, or as alternative media for the synthesis of 4-chloropyrans via Prins reactions.⁵⁸

Nevertheless, also moisture stable Lewis acidic ILs have been employed as alternative media in other Lewis-catalyzed reactions. For example, onium ILs based on choline- $x\text{ZnCl}_2$ ($x = 1-3$) or benzyltrimethylammonium chloride- 2ZnCl_2 , have been applied⁵⁹ as efficient and recyclable catalysts for the protection of carbonyls to 1,3-dioxolanes and 1,3-dioxanes at room temperature under solvent-free conditions. The catalytic system choline- 2ZnCl_2 could be reused upto five times without any appreciable loss of activity.



Scheme 1.7: Formation of acetals

The same IL (choline-2ZnCl₂) has been used⁶⁰ with success also in the synthesis of long chain wax esters. The reported reaction system has the advantages of both homogeneous and heterogeneous catalysis with high product yield (>88–99%) and the ease of product as well as catalyst separation, without the use of an organic solvent (Scheme 1.8). The authors evidenced that the applied system, which can be recycled up to six times without any significant loss of activity, present the following advantages over existing methods for wax ester synthesis: (a) choline chloride.2ZnCl₂ shows superior catalytic activity than all reported systems; (b) this IL is cheap and easy to prepare compared to imidazolium-based ILs; (c) as the IL is moisture insensitive, there is no need to remove water produced during the reactions and the IL can be reused for at least six cycles without any pretreatment or significant loss of activity; and (d) liquid esters (as a separate phase) can be conveniently decanted above their melting point avoiding the use of volatile organic solvents.



Scheme 1.8: Synthesis of long chain wax esters

Relevant results have been reported recently also related to the use of the water-tolerant Lewis acidic [bmim][FeCl₄], which has been found to be an efficient and recyclable catalyst in the synthesis of 4-aryl-dihydropyrimidinones through Biginelli condensation⁶¹ and in the synthesis of coumarin derivatives via Pechmann reaction.⁶²

1.2.2. Brønsted acidic ILs

The term Brønsted acidic ILs defines a large class of ionic compounds having as common property the ability to donate a proton. This class generally includes ILs bearing an acidic group on the cation (such as -SO₃H and -CO₂H), ILs arising from the reaction of a Brønsted acid with a Brønsted base (generally defined also as protic ILs, PILs) and ILs having an available proton

Chapter 1

on anion (HSO_4^- , H_2PO_4^-). In this latter class, we can include also ILs arising by the addition of a protic acid to an aprotic IL, eg., $[\text{bmim}]\text{Cl}/\text{HCl}$.

1.2.2.1. ILs containing COOH or SO_3H on the cation

In 2002, J.H. Davis and coworkers⁶³ reported for the first time the synthesis and the application of two ILs designed to be strong Brønsted acids;

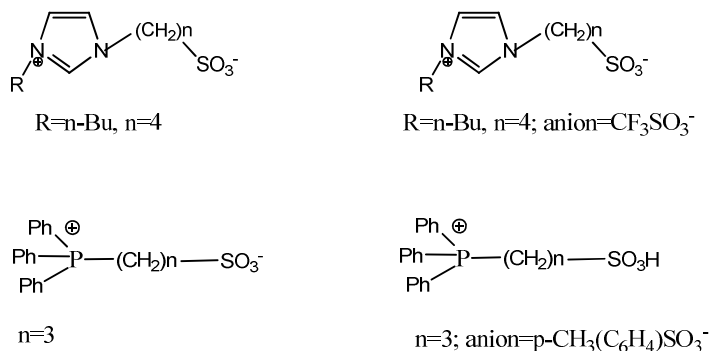


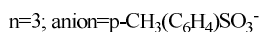
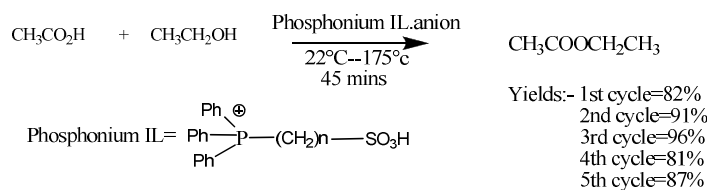
Figure 1.8: Brønsted acidic ILs and the precursor zwitterions

Really, the synthetic approach used to assemble the zwitterionic precursors was already reported by H. Ohno⁶⁴ by reaction of neutral nucleophiles, such as *N*-butyl imidazole or triphenylphosphine with 1,4-butane or 1,3-propane sulfone, respectively, it is possible to isolate in excellent yields the corresponding zwitterions. However, it is the second step that through the addition of an equivalent of acid allows the simultaneous realization of the latent acidity of the zwitterions and their conversion into acidic ILs. The chemical yields for both the zwitterion formation and acidification step are essentially quantitative. Moreover, since neither reaction produces byproducts, the IL syntheses are 100% atom efficient. To realize the quantitative conversion of the zwitterion into an IL cation bearing an appended sulfonic acid group is however necessary the addition of an equimolar amount of an acid possessing a $\text{p}K_a$ sufficiently low to convert the pendant sulfonate group into an alkane sulfonic acid, the $\text{p}K_a$ of the latter being expected to be -2 . The donor acids used by J.H. Davis and coworkers were trifluoromethanesulfonic acid and *p*-toluenesulfonic acid hydrate, $\text{pTSA}\cdot\text{H}_2\text{O}$. These acids were chosen because of the resistance of their anions toward hydrolytic decomposition, a common problem with some strong acid anions (e.g., PF_6^-). Each acidification was performed by stirring together the neat reagents and warming gently for almost 24 h. The new imidazolium-based IL was somewhat a viscous liquid at room temperature, whereas the IL with phosphonium core was a stiff glass that liquefied around 80°C . Similarly with the behavior of other ILs, neither any

fumes of new species or any observable degree of vapor pressure was observed. Furthermore, treatment of imidazole-based new IL under vacuum (10 Torr) at 150°C resulted in no observed loss of triflic acid ($\text{CF}_3\text{-SO}_3\text{H}$; bp=162°C at 760 Torr) from the IL. Conversely, washing of the phosphonium IL with toluene or diethyl ether resulted in no extraction of free pTSA (soluble in either liquid). All of these behaviors were considered as an evidence of the fact that these acidic ILs are not simply mixtures of added strong acids with dissolved zwitterions, a possibility this latter which cannot be excluded *at priori*, but the used donor acids are fully incorporated into the ILs.

Recently, the Hammett acidity functions of a series of Brønsted acidic ILs (including two protic acidic ILs) has been determined⁶⁵ spectrophotometrically determining the protonation of an uncharged indicator (various aniline) in acetonitrile, in terms of the measurable ratio of $[\text{I}]/[\text{IH}^+]$. Although determined in a molecular solvent, these measurements show that the relative acidity of the SO_3H -functionalized ILs is stronger than that of protic ILs, bearing an available proton both on cation and anion (methylimidazolium hydrogen sulfate, $[\text{mim}][\text{HSO}_4]$, and methylimidazolium dihydrogenphosphate, $[\text{mim}][\text{H}_2\text{PO}_4]$). Moreover, the acidity depends on the nature of the anion, with the triflate anion being the most acidic.

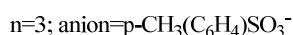
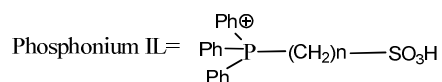
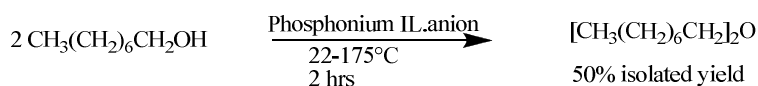
Brønsted acidic ILs, with a SO_3H group covalently linked through an alkyl chain to the cation have been widely applied as solvents and/or catalysts for several classical acid-promoted organic reactions. In his pioneeristic work, Davis and coworkers emphasized⁶³ in particular showed the use of phosphonium ILs, which were screened in Fischer esterification, alcohol dehydrodimerization and the pinacole/benzopinacole rearrangement. Phosphonium ILs with counter anion as $\text{p-CH}_3(\text{C}_6\text{H}_4)\text{SO}_3^-$ are indeed solids at room temperature and melt at 80°C. Therefore, they provide a direct access to a convenient mode of separation, by decantation, which parallels the manner in which solid acids are removed from reaction media. Related to the Fisher esterification, the formation of an important commodity ester, ethyl acetate, from ethanol and acetic acid using the phosphonium IL as the solvent/catalyst in a batch-type process was examined. In this reaction, the IL was recycled five times; the yield of ester increased from cycles 1 to 3, only to drop off again in cycle 4. During these cycles, the mass of the solvent/catalyst medium also increased, consistent with the entrapment of materials by the cooled catalyst phase. Post-cycling analysis of the IL by GC and NMR showed appreciable quantities of water and acetic acid. When heated under vacuum to remove these volatile materials, the catalytic activity of this phosphonium IL was found to increase, in line with the degree to which water was removed from the system. For an equilibrium reaction in which water is a product, the initial increase in ester yield accompanying the retention of water in cycles 1–3 was unexpected.



Sche

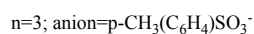
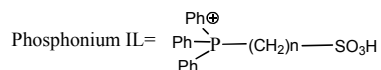
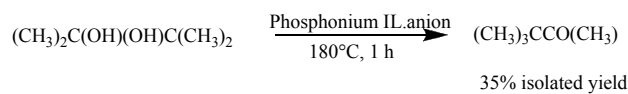
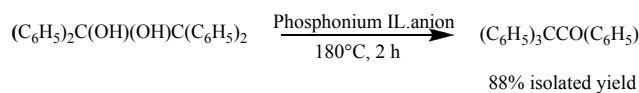
me 1.9: Fischer esterification of acetic acid and ethanol in presence of phosphonium ILs

But these ILs have been used also in other important processes. In particular, it has been observed that depending upon the substrate or the phosphonium IL stoichiometry, 1-octanol was selectively converted to octyl ether in 16–56% isolated yield with minimal byproduct formation. In a control experiment, pTSA-H₂O gave a better yield of octyl ether; however, more byproducts were formed, and the separation of the pTSA from the reaction mixture was considerably more difficult whereas using Nafion-117 the catalyst/product separation was straightforward and byproduct formation was minimized, but the yield of octyl ether was quite poor (3%).



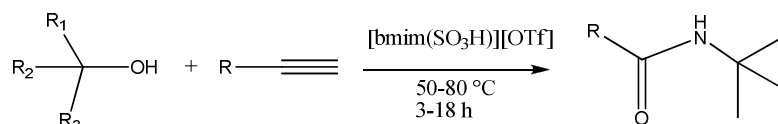
Scheme 1.10: Alcohol dehydrodimerization using phosphonium ILs

Phosphonium ILs have been used also in the rearrangement of pinacol to pinacolone, a process of considerable industrial importance, for which using various solid acid catalysts reported yields of pinacolone ranging from 2 to 71%, but long reaction periods are necessary, and the use of a VOC is required, which complicates the isolation.⁶⁶ Using phosphonium ILs as catalyst/solvent, an unoptimized yield of pinacolone of 35% was obtained during a 1-h reaction period which increased to 88% over a 2-h period. Moreover, the pinacolone was readily distilled as a pure compound straight from the reaction mixture whereas the unreacted pinacol was retained by the solvent/catalyst phase. Ultimately, it is to note the ease with which these ILs were recycled.



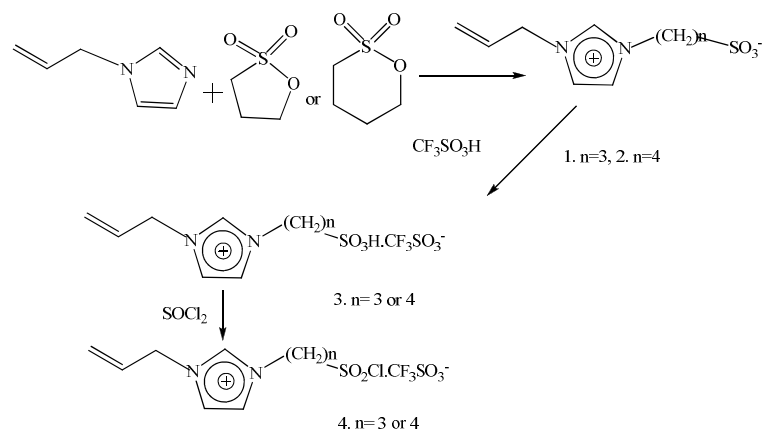
Scheme 1.11: Pinacole rearrangement using PILs

The utility of Brønsted acidic imidazolium ILs, in particular [bmim(SO₃H)][OTf], as catalysts has been recently tested⁶⁷ in synthesis of amides via the Ritter reaction of alcohols with nitriles; a wide variety amides in high yields were obtained under mild conditions. The recovery of the IL for reuse was not tried since in these reactions the ILs were used only in catalytic amounts; however, the authors state that the IL could be conveniently recovered and reused.

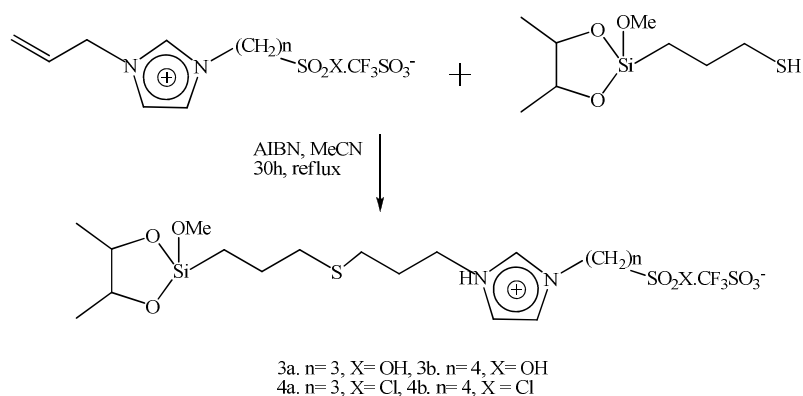


Scheme 1.12: Ritter reaction of alcohols with nitriles in ILs

Although the potentiality of functionalized ILs is largely related to the possibility to have a liquid catalyst, acidic ILs bearing a SO₃H moiety has been investigated also by using supported systems. Kun Qiao et al.⁶⁸ in the year 2006 presented a work in which an acidic IL immobilized on silica gel was used as a novel solid catalyst for esterification and nitration reactions. The catalytic systems characterized by covalently-bonded ILs were prepared in 5 steps via radical chain transfer reaction of 1-allylimidazolium-based ILs.



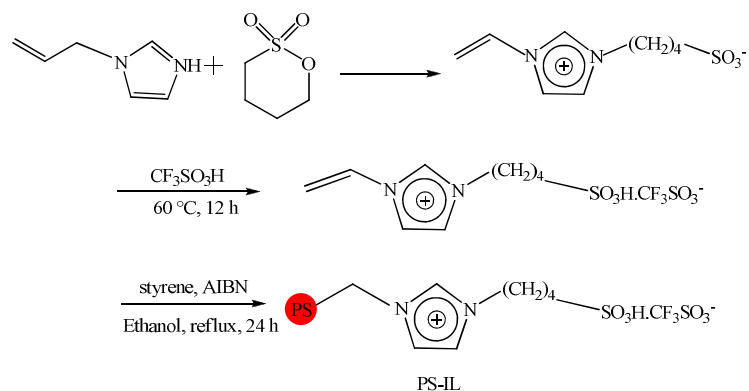
Scheme 1.13: 1-Allylimidazolium containing acidic ILs. Showing 1st four steps of Kun Qiao et al.⁶⁸



Scheme 1.14: Immobilized ILs (step 5 according to Kun Qiao et al.⁶⁸)

These ILs have been applied in the nitration reaction of aromatic compounds.

Subsequently, Sugimura et al.⁶⁹ reported the immobilization, practically of the same acidic ILs, by copolymerization with styrene (Scheme 1.15).



Scheme 1.15: Preparation of the IL supported polystyrene

These ILs were used as catalyst for acetal formation. It was noted that although polystyrene-IL (PS-IL) could be readily prepared with the initial IL/styrene ratio (in mol) below 10%, it was a little viscous when the initial IL/styrene ratio was too high. The initial ratio below 5% could offer PS-IL in very well physical form as a white powder.

The question arises now why immobilization is required. The immobilization of homogeneous catalysts on polymeric supports could offer some practical benefits including easy separation of the catalyst from reagents and reaction products, and simplification of the methods of recycling the catalysts. For example, conventionally the acetylation reaction is carried out in a homogeneous system in the presence of corrosive acids such as pTSA, triflic acid or dry HCl, which inevitably leads to tedious work-up procedures.⁷⁰ Moreover, neutralization of the strong acidic media will produce undesired wastes. Therefore, there had been great deals of efforts to overcome these drawbacks by employing solid acid catalysts.

1.2.2.2. Protic Ionic Liquids

Protic ionic liquids (PILs), formed by a stoichiometric reaction of a Brønsted acid with a Brønsted base are an important subclass of ILs having peculiar properties and potential applications.^{71,72}

Surely, there are many combinations of acids and bases which can give a stable salt, however, to obtain a true IL it is necessary to have a complete transfer of the proton from the acid to the base (conventionally, > 99.9%). The aqueous pK_a values for the precursors acids and bases are considered as being predictive of the behavior of the formed protic ILs; more in particular, ΔpK_a greater than 8–10 ($\Delta pK_a = pK_a(\text{base}) - pK_a(\text{acid})$), are reported to produce protic ILs of ideal ionicity starting from this assumption, considering that pK_a values of amine bases have little

variations, at least in comparison with acids, these latter surely are able to play the most important role in protic ILs' ionicity; inorganic acids such HNO_3 and H_2SO_4 have sufficiently low $\text{p}K_a$ values to give ILs with practically all organic amines. Related to the validity to use aqueous $\Delta\text{p}K_a$ values of the Brønsted acid–Brønsted base pair to estimate the ionicity of the formed IL, although it has been the object of discussion, it is noteworthy that specific $\Delta\text{p}K_a$ values recently extracted⁷³ directly from electrochemical experiments performed on ten protic ILs show an excellent correlation with the aqueous values, demonstrating that aqueous $\text{p}K_a$ data provide a good approximation to proton activity in PILs.

In the last 3–4 years, PILs containing primary, secondary and tertiary ammonium cations have been extensively investigated by Drummond et al.;⁷⁴ several important papers have been published showing the effect of increasing substitution on ammonium cation, alkyl chains structure, presence of oxygenated functionalities (OH, CH_3O) and anionic structure. Although the authors were particularly interested in the behavior of PILs as amphiphile self-assembly solvents, fundamental physico-chemical data (density, viscosity and conductivity) have been reported showing that the investigated class of PILs present ionic conductivities up to 51.7 mS/cm, viscosities down to 5.4 mPas, surface tension between 38.3 and 82.1 nN/m and densities ranging from 0.99 to 1.558. The presence of hydroxyl groups on PILs led to higher surface tensions and therefore higher Gordon values. The Gordon parameter is considered to give a measure of the cohesiveness of the liquids and consequently an indication of the driving force for self-assembly of amphiphiles. It has been therefore suggested that PILs possess a degree of solvent–solvent interaction that is stronger than the solvent–hydrocarbons (amphiphile) interaction and the entropy contribution to the free energy of association play a role analogous to the hydrophobic effect of water.

Recently, also cyclic secondary amines (pyrrolidine and morpholine) have been used to synthesize PILs.^{64,75} In particular, the association of pyrrolidinium cation with anions such as nitrate, hydrogensulfate, formate, acetate, trifluoroacetate and octanoate give to a series of ionic compounds liquid at room temperature characterized by high conductivities (up to 56 mS cm^{-1} at 25°C). The nature of anion strongly affects the physico-chemical properties of these compounds. In particular, pyrrolidinium nitrate, $[\text{Pyr}][\text{NO}_3]$, and pyrrolidinium hydrogen sulfate, $[\text{Pyr}][\text{HSO}_4]$, are superior conductors (superionic liquids): for these ILs it has been hypothesized that the Grothus mechanism for proton transfer becomes predominant. At variance, formate and acetate give “poor ionic liquids”. Nevertheless, all these ILs show extreme fragility. An extreme fragility characterizes also morpholinium formates, including the unsubstituted morpholinium, *N*-methylmorpholinium and *N*-ethylmorpholinium cation,⁷⁶ whose conductivities are however

lower than those of pyrrolidinium-based PILs. Transport properties measurements show that viscosity increases with the number of hydrogen bonds between ions and the size of cation; consequently, conductivity decreases in relation to the same parameters. At low temperatures, these PILs form glasses (T_g ranging from -84 to -86°C) which are able to give cold crystallization when reheated to the ambient temperature. Finally, these ILs present Newtonian behavior and a temperature dependence which can be described by the Vogel-Tamman-Fulcher (VTF) equation.

In good agreement with these results are also the recently published⁷⁷ data on electrochemical and physico-chemical properties of cyclic amine-based (pyrrolidinium, piperidinium and azepanium) Brønsted acidic ILs containing formate, trifluoroacetate or hydrogen sulfate as anions. ILs having formate anion have lower viscosity, lower density and higher conductivity compared to those having trifluoroacetate and hydrogen sulfate anions but they present also a relatively low anodic potential ($+ 0.7$ V). It is however noteworthy that pyrrolidinium-, piperidinium- and azepanium-based ILs exhibit large electrochemical windows (3.22–3.99 V) as compared to other protic ILs.

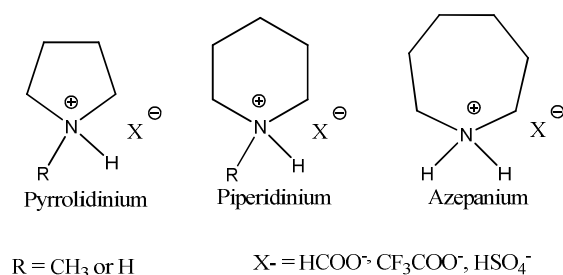


Figure 1.9: Various combinations of cations and anions representing protic ILs

Cation–anion combination affects indeed the electrochemical properties of PILs. Anions (formate, carboxylate, hydrogensulfate, etc.) are oxidized at relatively low potential whereas reduction of cation proceeds through a two-step mechanism; deprotonation followed by proton reduction. The proton availability of these salt is considered as the main factor responsible for their smaller potential windows (normally, lower than 3 V) with respect to aprotic ILs and higher sensitivity to the nature of electrode materials.^{60–78}

During the last 5 years also other bases have been employed to prepare PILs and protonated pyridinium- and imidazolium-based ILs have been prepared and applied in synthesis (see below). It is noteworthy that another important feature that distinguishes PILs from aprotic ILs is their

lower thermal stability. PILs present an intrinsic vapor pressure that results from the retro-proton transfer between the constituting ions, generating the parent Brønsted acid and base species which determine a marked vaporization at elevated temperatures lacking of strong Coulombic interactions.⁷⁹ The vapor pressure is largely determined by the equilibrium concentrations of the neutral acid and base forms from which the IL is prepared and consequently it is strongly correlated to the above discussed ΔpK_a , $\Delta pK_a = pK_a(\text{base}) - pK_a(\text{acid})$. Since for some applications high thermal stability is a fundamental requirement, recently a novel family of hydrophobic PILs derived from pairing between diverse superbases (phosphazanes, bicyclic guanidines and 1,1,3,3-tetramethylguanidine) and the super-acid derived anions, bistriflimide ($[\text{Tf}_2\text{N}]^-$) and bis(perfluoroethylsulfonyl)imide ($[\text{N}(\text{SO}_2\text{CF}_2\text{CF}_3)_2]^-$ generally reported as $[\text{beti}]^-$) have been prepared.⁸⁰

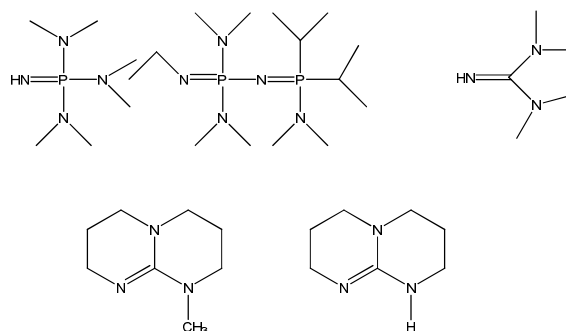


Figure 1.10: Superbases used to prepare hydrophobic PILs

These PILs exhibit the highest thermal stability yet observed for any PIL, suggesting potential for application in PEM-type fuel cells working at 150°C and beyond.

But PILs have also been synthesized using relatively weaker bases than amines and more or less strong acids. Surely, high ionicity and elevated thermal stability are not the main features of these salts which, however, can have other important properties. In this class, we have to mention the lactam-based protic ILs that arise from neutralization reactions of a lactam, generally ϵ -caprolactam or γ -butyrolactam (i.e., 2-pyrrolidone), with a strong acid. In 2005, Deng et al. have prepared⁸¹ twelve new PILs by reacting ϵ -caprolactam or γ -butyrolactam with six different Brønsted acids (Figure 1.11).

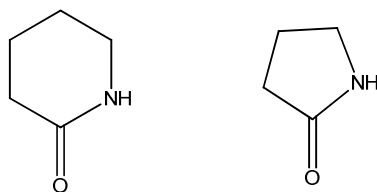


Figure 1.11: ϵ -caprolactam or γ -butyrolactam

Although the researchers proposed that the resulting cations are protonated on the amide nitrogen atoms, it is more probable that the protonation occurs on the more acidic carbonyl oxygen atom. The density, viscosity, electrochemical window, ionic conductivity and thermal properties of these PILs were measured and investigated in detail showing that caprolactam trifluoroacetate and pyrrolidonium trifluoroacetate ILs have very low viscosities, 28 and 11 cP, respectively, although their conductivities remain less than 0.144 S/m (25°C).

Acidity Measurements

Although acidity is the peculiarity of this class of ILs the acidity level was evaluated only for a limited number of PILs. The Brønsted acidity of protons is mainly determined by their solvation state, and consequently, the properties of protons depend on both the nature of the solvent and the nature and concentration of the acid. The Brønsted superacidity of HCl in a liquid chloroaluminate or the Brønsted acidity of HNTf₂ in [bmim][Tf₂N] has been evaluated from the determination of the Hammett acidity functions using UV–vis spectroscopy (Hammett method), wherein a basic indicator was used to trap the dissociative proton. The H_0 value was calculated using equation (4)

$$H_0 = \text{p}K_{\text{a},\text{aq}} + \log\left(\frac{[\text{I}]}{[\text{IH}^+]}\right) \quad (4)$$

where $\text{p}K_{\text{a},\text{aq}}$ is the $\text{p}K_{\text{a}}$ value of the indicator referred to an aqueous solution, and [I] and [IH⁺] are the molar concentrations of the unprotonated and protonated forms of the indicator in a solvent, respectively. Since this method suffers from some limitations, at first, the fact that the solvent is assumed to be totally dissociating, and consequently the known $\text{p}K_{\text{a}}$ values of the indicators are also assumed as valid (indications arising from literature induce some doubts about this assumption), this problem is generally overcome by defining the Hammett function as an “apparent” acidity function. Although the measured acidity level in a given solvent different

from water might be lowered as a result of the association process, the order of the relative acidities is maintained if the solvent properties of the solvent are not too different from water.⁸² Unfortunately, the acidity determination of a pure acidic IL applying this method and using the acidic IL as solvent is impossible because the initial absorbance of the total unprotonated form of the indicator (blank value) cannot be obtained. Therefore, the acidity of several PILs have been determined in molecular solvents (CH_2Cl_2 , ethanol and acetonitrile). In dichloromethane, the acidity order of three pyridinium⁸³ ($[\text{2-MPyH}][\text{OTf}]$, $[\text{2-MPyH}][\text{CH}_3\text{SO}_3]$, $[\text{2-MPyH}][\text{Tfa}]$) ILs:

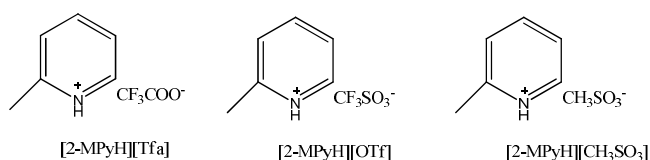


Figure 1.12: Some protic pyridinium ILs

was the following: $[\text{2-MPyH}][\text{OTf}] > [\text{2-MPyH}][\text{CH}_3\text{SO}_3] > [\text{2-MPyH}][\text{Tfa}]$.

Whereas the acidity order of some protic imidazolium salts ($[\text{MIMPs}][\text{HSO}_4]$, $[\text{MIMPs}][\text{BF}_4]$, $[\text{PyPs}][\text{TsO}]$, $[\text{MIMPs}][\text{TsO}]$, $[\text{1,2-DiMIMPs}][\text{TsO}]$, $[\text{MIMPs}][\text{H}_2\text{PO}_4]$, $[\text{MIM}][\text{TsO}]$).

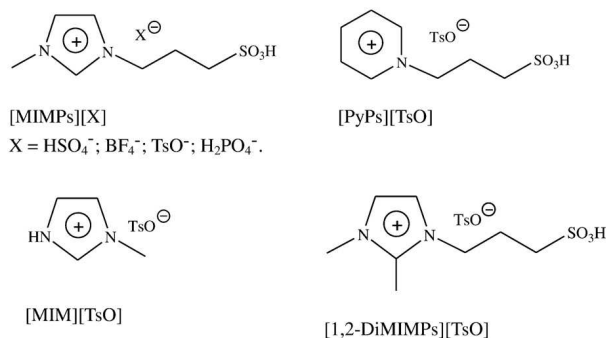


Figure 1.13: Some protic imidazolium ILs

determined⁸⁴ in ethanol was the following: $[\text{MIMPs}][\text{HSO}_4] > [\text{MIMPs}][\text{BF}_4] > [\text{PyPs}][\text{TsO}] > [\text{MIMPs}][\text{TsO}] > [\text{1,2-DiMIMPs}][\text{TsO}] > [\text{MIMPs}][\text{H}_2\text{PO}_4] > [\text{MIM}][\text{TsO}]$.

But, what are the other main structural features characterizing protic ILs and, in particular, the widely investigated ammonium PILs?

With few exceptions, ammonium PILs present a “poor” ionic behavior: in the Walden plots, reporting $\log(\Lambda)$ against $\log(1/\eta)$, they exhibit conductivities significantly lower than the ideal

line obtained considering that: i) ions have mobilities that are determined only by viscosity of the medium, ii) the number of ions present in the equivalent volume is that indicated by salt composition. Ionicity of PILs is a complex property due to the peculiarity of these salts which are practically always in equilibrium with the corresponding molecular species (precursors acid and base), consequently, it depends by the degree of proton transfer from acid to base. Moreover, in analogy with the situation characterizing aprotic ILs, it depends by aggregation phenomena, i.e., by the presence of neutral complexes, or more extensive solvent structuring. Many ILs are nanostructured, they possess populations of cations and anions that are ordered on specific length scales; these nanostructures typically are due to aggregation of the ILs in polar and apolar regions. The small-angle neutron scattering (SANS) patterns of ethylammonium nitrate (EAN) and propylammonium nitrate (PAN), the most frequently studied PILs, show that both these salts present a structural organization;⁸⁵ the solvophobic interaction between alkyl groups is the main factor for the generation of nanostructures, but electrostatic and hydrogen bonding attractions between the amine nitrogen and the nitrate anion will also play an important role. In particular, using far-IR spectroscopy it has been suggested⁸⁶ that EAN form a three-dimensional hydrogen-bonded network similar to that of water, although the tetrahedral structure is only present for water; probably, the Coulombic forces present in EAN impose a very different type of solvent ordering. Nevertheless, the investigation of alkylammonium, dialkylammonium, trialkylammonium and cyclic ammonium cations, combined with organic and inorganic acids, using small- and wide-angle X-ray scattering (SAXS and WAXS) has confirmed⁸⁷ that many of the investigated PILs present a nanostructure that result from segregation of polar and nonpolar components of the IL. This segregation is enhanced by long alkyl chains, whereas the presence of methoxyl or (much more) hydroxyl groups on alkyl chains led to much less ordered liquids. It is to note that formate anion appears to disrupt the long range order. Nevertheless, aggregates have been evidenced also through electrospray mass spectrometry (ESI-MS) experiments. ESI-MS gives information about the segregation ability in the gas-phase, however, these data can be considered a qualitative or semi-quantitative evaluation of the cluster ability in the net liquid although it is highly probable that inherent differences between the aggregates observed in gas-phase by ESI-MS and in the bulk-liquid-phase (SWAXS) exist. However, the ESI-MS measurements performed⁸⁸ on monoalkylammonium nitrates, showing aggregates of eight cations and seven anions ($C_8A_7^+$) as the dominant species in positive mode, are consistent with the strong peak present in the SWAXS, representative of intermediate range order. Analogously, the presence of other aggregates having a lower mass/charge (m/e) value in the ESI-MS spectra of PILs bearing other alkyl chains (two or three alkyl chains on nitrogen) is in agreement with

the structures observed for the same PILs by SAXS that show a reduction of aggregate size. On the other hand, the ESI-MS measurements show also that the formation and size of aggregates is dependent on the nature of anion: the nitrate anion, small, tripodal, and highly charged, is suitable of forming a network of hydrogen bonds with the available protons of ammonium cations, whereas the larger formate and lactate anions, with lower charge density, did not support the formation of aggregates.

The formation of aggregates strongly affect ionic diffusion in the solid and liquid state and self diffusion coefficients obtained from NMR measurements can be useful for detecting dimers and ion pairs or nanoaggregates in the liquid state. However, due to dynamic exchange between dissociated ions and hypothetical ion pairs, it is practically impossible to distinguish between ion states: the spectroscopically determined self diffusion coefficients sum the contribution of both the associated IL and the dissociated ions. Recently, an NMR relaxation and diffusion characterization has been performed⁸⁹ on several PILs at high (500 MHz) and low (18.3 MHz) magnetic fields. The dynamic of cations and anions were similar at both the frequencies, with similar trends and magnitudes for each cation–anion couple. The diffusion of ions were strongly correlated to the IL components and Arrhenius plots of diffusions indicated that these liquids are highly associated. Dynamics are restricted by the interactions with the surrounding ions; longer range motions can involve ion pairs and ion aggregates. At high magnetic field, diffusion was dominated by mobile species that follow the Stokes-Einstein behavior; whereas diffusion at low field evidenced relatively immobile species that displayed fractional Stokes-Einstein behavior. It is noteworthy that no evidence was found to indicate the influence of the magnetic field on structural and dynamic of the investigated ILs, although variation between diffusion coefficients at different magnetic fields indicates dynamic heterogeneities (or temporal aggregates) within the IL. Nevertheless, diffusion NMR studies performed on six ILs that incorporate the *N*-methyl-2-hydroxyethylammonium cation with various carboxylic acid anions (from formate to pentanoate) suggest the presence of an ordered lamellar/micellar liquid crystal phase for those ILs that contain an alkyl chain in the anionic species.⁹⁰ The size and type of alkyl chain determine also the effect of temperature on some physico-chemical properties; local structure models should be applied to explain the macroscopic behavior in terms of the molecular arrangement.

It is to note that the three-dimensional structure of PILs strongly affects also their solvation ability.⁹¹ It is noteworthy that the mechanism of solvation in ILs is completely different from that characterizing molecular polar solvents. In polar solvents the solvation process is extremely rapid; in a polar solvent, solvent molecules re-oriented themselves around the solute molecules, whereas in ILs, the motions of cations and anions around the solute are responsible for solvation.

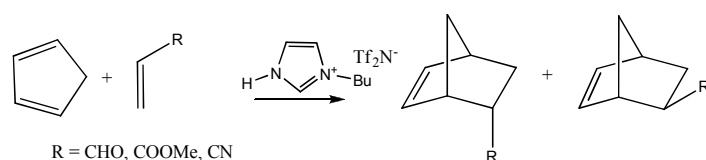
The solvation times in molecular solvents falls in the range of 1–10 ps, in ILs the range is 0.1–10 ns⁹² and strongly depends on the dynamic properties of IL. The solvent relaxation and orientation dynamics of cumarin 153 with a variation of temperature have been recently investigated in *N,N*-dimethylethanolammonium formate. This PIL, whose optimized structure has been obtained by quantum mechanical calculations using density functional theory methods, is characterized by a hydrogen bond between the hydrogen atom attached on nitrogen of the cation and the oxygen atom of the anion. The hydrogen bonding determines a high bulk viscosity; solvent relaxation and orientation dynamics of cumarin 153 are linearly well-correlated with the bulk-viscosity of the medium and consequently they are dependent on the entity of cation–anion interactions, i.e., on the IL three-dimensional structure.

1.2.2.3. Applications of Brønsted acidic ILs

There are *n*-number of cited papers almost since the last 10 years which imply the use of Brønsted acidic ILs as catalysts in many named reactions such as Knoevenagel condensation, Diels Alder reaction, Fisher esterification, Mannich reaction, Pechmann reaction etc. Almost in all laboratories to chemical manufacturing plants, the use of strong Brønsted acids is common.⁹³ Since many of these reactions have been recently reviewed⁹⁴ we will focus only on a few examples.

EAN has been used with success in Knoevenagel condensation reaction of Muldrum' acid with aromatic aldehydes and of active methylene compounds with aromatic aldehydes.⁹⁵ The yields and reaction times (80–97% in 0.2–12h) show the excellent ability of EAN when used as solvent and catalyst in this kind of reactions. For comparison, also aprotic ILs having BF₄⁻ and PF₆⁻ as anions have been used by obtaining the expected products in lower yields (54–77 %) with longer reaction times (24 h).

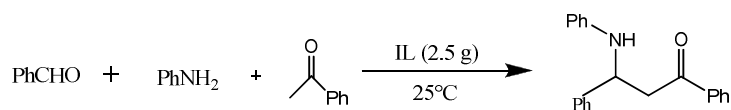
In 1989, EAN was used⁹⁶ with success in Diels-Alder reaction of cyclopentadiene with a series of dienophiles obtaining a selectivity towards the endo product of 6.4/7.4 that, although lower than that characterizing the same process in water (7.4/9.3), represented practically one of the best values reported in literature. More recently, this reaction has been widely investigated in several ILs, including protic imidazolium ILs.⁹⁷ Kinetic measurements and product distribution studies have shown that 1-butylimidazolium bistriflimide, [Hbim][Tf₂N], gives the highest endo selectivity and reaction rate, at least when acrolein or methyl acrylate are used as dienophile.



Scheme 1.16: Diels-Alder reaction by using [Hbim][Tf₂N] as catalyst

Nevertheless, both the multiparameter linear solvation energy relationships (LSER) and theoretical calculation suggest⁹⁸ the primary role exerted by the cationic component of the IL on selectivity which is attributed, respectively, directly to the hydrogen bond ability (α) and dipolarity/polarizability (π^*) of a single cation, or to a more coordinated effect of the solvation shell. The first solvation shell, which may be described by three cations (one of which coordinated with the carbonyl and two stacked respectively above and below the cyclopentadiene-dienophile in their transition state) and three anions, enhances the π - π dispersion interaction between the reactants, in particular in the endo approach, blocking dienophile and consequently diene as a molecular “clamp”. On the other hand, the effect of ILs on reactivity, which is described in a less efficient way by the LSER approach, has been rationalized by theoretical calculations on the basis of a “solvophobic” effect which arises from the fact that the solvation free energy of a neutral solute in an IL is dominated by the unfavorable process of creating a cavity of suitable size to accommodate the solute. This latter process is determined by the interactions between the ILs components; as previously reported, these interactions are particularly strong and important in PILs.

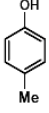
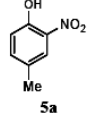
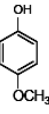
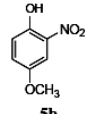
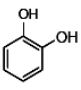
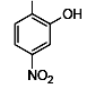
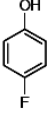
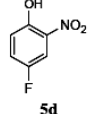
In 2004, G. Zhao et al.⁹⁹ synthesized several Brønsted acidic ILs and successfully used them as solvents and catalysts for the three-components Mannich reaction of aldehydes, amines and ketones at 25°C. The used Brønsted acidic ILs include 1-butyl-3-methylimidazolium hydrogen sulfate ([bmim][HSO₄]), 1-butyl-3-methylimidazolium dihydrogen phosphate ([bmim][H₂PO₄]), 1-methylimidazolium *p*-toluenesulfonic acid ([Hmim][Tsa]) and 1-methylimidazolium trifluoroacetic acid ([Hmim][Tfa]). Higher yields (83%) were obtained in the presence of [Hmim][Tfa] in comparison with other Brønsted acidic ILs. The [Hmim][Tfa] was reused four times without any considerable loss in activity.

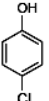
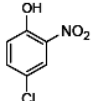
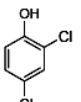
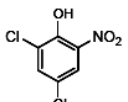
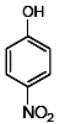
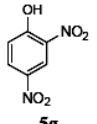
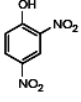
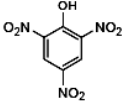
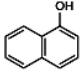
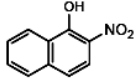
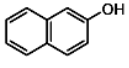
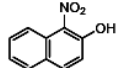
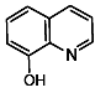
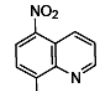


Scheme 1.17: Mannich reaction

At variance, [bmim][HSO₄] reacted readily with amine due to its strong acidity and no Mannich base was produced. The efficiency of the system was dependent on the starting compounds; several aliphatic amines and carbonyl compounds in [Hmim][Tfa] at 25°C gave, unfortunately, a mixture of products and MS analysis indicated that the main products were not Mannich bases. Subsequently, Tajik et al.¹⁰⁰ used an IL bearing an acidic anion, [bmim][HSO₄], in selective nitration of phenols under mild conditions (acetonitrile at room temperature). Selective nitration of phenols with sodium nitrate was carried out in the presence of the above Brønsted IL at room temperature, obtaining the expected product(s) in good to high yields in short reaction times.

Table 1.1: Nitration of various substituted phenol derivatives using [BHIM][HSO₄]

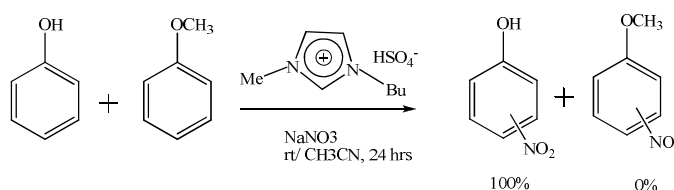
| Entry | Substrate | Product | Time (min) | Yield (%) ^b |
|-------|---|--|------------|------------------------|
| 1 |  |  5a | 5 | 91 |
| 2 |  |  5b | 10 | 92 |
| 3 |  |  5c | 20 | 90 |
| 4 |  |  5d | 30 | 80 |

| | | | | |
|----|---|---|-----|----------|
| 5 |  |  5e | 20 | 85 |
| 6 |  |  5f | 30 | 75 |
| 7 |  |  5g | 30 | 76 |
| 8 |  |  5h | 180 | No Reac. |
| 9 |  |  | 60 | 92 |
| 10 |  |  | 10 | 80 |
| 11 |  |  | 5 | 90 |

^aThe ratio of the substrate, NaNO₃ and the IL are 1:1:1. ^bIsolated yield.

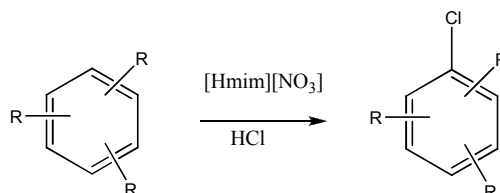
From the data collected in Table 1.1, Tajik et al. concluded that the introduction of an electron withdrawing group (e.g., nitro group) on the aromatic ring (entries 7 and 8) decreases the rates of the reactions and yields of the products. On the other hand, the introduction of an electron donating group (e.g., CH₃ or -OCH₃) enhances the rate and the yields of the products (entries 1 and 2). Naphthols and hydroxyl quinolines reacted in short reaction times by this method (entries

9–11). It is noteworthy that when the competitive reaction between phenol and anisole was carried out under identical conditions, it was observed that the nitration of phenol proceeded exclusively whereas anisole remained intact in the reaction mixtures even after 24 h.



Scheme 1.18: Nitration of phenol and anisole in ILs

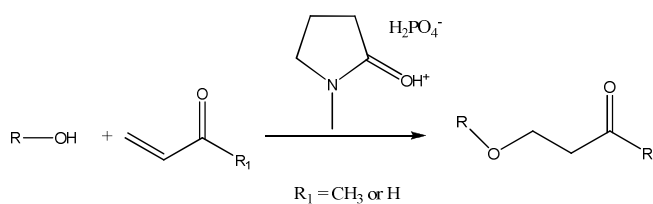
On the other hand, the Brønsted acidic [Hmim][NO₃] has been used as a cosolvent and ‘‘promoter’’ for oxidative halogenation of aromatic compounds with aqueous halohydric acids.¹⁰¹ [Hmim][NO₃] is air stable, easy to prepare and handle and is able to oxidize hydrohalic acids, being at the same time re-oxidized by oxygen. Aryl halides have been therefore obtained starting from non-activated or sterically hindered arenes.



Scheme 1.19: Formation of aryl halides starting from sterically hindered aromatic compounds using [Hmim][NO₃]

It is noteworthy that under the reaction conditions, arylmethylketones are α -halogenated on the methyl group whereas aromatic aldehydes are transformed into the corresponding acids.

Although imidazolium- and ammonium-based Brønsted acidic ILs represent the most investigated classes of protic ILs, recently the improved catalytic effect of *N*-methylpyrrolidonium dihydrogen phosphate with respect to the traditional neutral and acidic imidazolium ILs has been evidenced in synthesis of β -alkoxyketones by the oxa-Michael addition reactions.¹⁰² The higher activity of this IL, when used as solvent and catalyst, has been attributed to its dual ability to interact with substrate and transition state: it is able to activate the ketone or aldehyde by carbonyl protonation, as all the other protic ILs, but at the same time the unprotonated form of the pyrrolidone is able to interact with the hydroxyl group of alcohol, via hydrogen bonding, increasing oxygen nucleophilicity.



Scheme 1.20: Catalytic effect of *N*-methyl pyrrolidinium dihydrogen phosphate

Unfortunately, no mechanistic study has been performed to establish if the unprotonated pyrrolidone exerting a catalytic effect is that formed after hydrogen transfer from IL to reagent or is present in solution due to the relatively low basicity of the lactam system.

One of the most widely investigated reaction in PILs is however the esterification reaction. Esterification of carboxylic acids with alcohols is a reaction which has a lot of industrial importance. Compounds are prepared in bulks in this manner in various industries like chemical, petrochemical and pharmaceutical industries.

In the year 2003, Hua-Ping Zhu et al.¹⁰³ claimed that a “green method” for esterification of aliphatic and aromatic acids (acetic acid, *n*-decanoic acid, stearic acid, undecanoic acid, lactic acid, crotonic acid, oxalic acid, benzoic acid and 3-hydroxybenzoic acid) with simple alcohols (methanol, ethanol, butanol and octanol) may be represented by the use of 1-methylimidazole tetrafluoroborate ([mim][BF₄]). Over other ILs, such as 1-hexyl-3-methylimidazolium hydrogen sulphate and 1-[2-(2-hydroxyethoxy)ethyl]-3-methylimidazolium hydrogen sulphate,¹⁰⁴ whose synthesis require a multistep process, [mim][BF₄] is obtained by addition of HBF₄ to methylimidazole. Nevertheless, since all the obtained esters are insoluble in [mim][BF₄], they could be easily separated. The low solubility moreover helped driving the equilibrium towards the product side and very high yields were achieved using this IL. Finally, the IL could be recycled and reused. On the other hand, in 2006 Duan et al.¹⁰⁵ suggested that not only acidic ILs but also a neutral IL, like [bmim][BF₄], promotes highly selective esterification of tertiary alcohols by acetic anhydride; the role exerted by the eventual formation of HF, under the reaction conditions, was not discussed being at the moment not so clear the fact that the stability of these ILs may be limited in the presence of water.

About this latter possibility, it is however to note that in 2005, Joseph et al.¹⁰⁶ reported some data about the use of a series of ILs based on 1-methyl imidazolium (Brønsted acidic cation) and 1-butyl-3-methylimidazolium (a neutral cation), and three anions (BF₄⁻, PF₆⁻ and PTSA⁻) in the

Fischer esterification. All these ILs afforded good alcohol conversion and excellent ester selectivity. In particular, [bmim][PTSA] as a catalyst showed 100% substrate conversion and 100% product selectivity over a period of 2 h. At variance with ILs bearing fluorinated anions, this IL should be stable in the presence of water; the catalytic effect cannot be attributed to the formation of strong acids under the reaction conditions. Nevertheless, data reported in the same paper related to the determination of acidity of the investigated ILs using pyridine as a probe molecule by monitoring the IR bands in the range of 1350–1600 cm^{-1} , showed that only in the case of [mim][BF₄] an additional band near 1540 cm^{-1} , indicating the presence of Brønsted acid sites due to the formation of pyridinium ions, was present. However, all the investigated ILs presented a band near 1450 cm^{-1} , suggesting the coordination of pyridine to the Lewis acid sites (!!).

Table 1.2: Esterification of acetic acid with benzyl alcohol with various Brønsted ILs

| IL | Ratio ^a | Time (h) | C % | S% |
|--------------------------|--------------------|----------|------|-----------------|
| [mim][BF ₄] | 1 : 1 | 4 | 91 | 100 |
| [mim][BF ₄] | 1 : 0.4 | 4 | 70.2 | 100 |
| [bmim][PF ₆] | 1:1 | 2 | 100 | 90 ^b |
| [bmim][PTSA] | 1:1 | 2 | 100 | 100 |
| [bmim][BF ₄] | 1:1 | 4 | 80 | 100 |

Reaction conditions: acetic acid : benzyl alcohol (2 : 1); IL = 1 g; Temperature = 110°C.

^aRatio of imidazole to anion source.

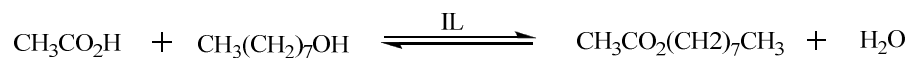
^b[Bmim][PF₆] gave 90% ester selectivity and 10% dibenzyl ether was formed.

C% and S% represent conversion and selectivity percentages, respectively.

But also other classes of PILs have been investigated in esterification reaction. In 2007,¹⁰⁷ Pralhad and his group suggested that PILs can be used as an acid catalyst in Fischer esterification reactions. Brønsted acidic ILs used in this case for esterification of carboxylic acids with primary alcohols were: triethylammonium sulfate ([NH(Et)₃][HSO₄]), triethylammonium dihydrogen phosphate ([NH(Et)₃][H₂PO₄]) and triethylammonium tetrafluoroborate ([NH(Et)₃][BF₄]), conveniently prepared using inexpensive and available materials. Since the esterification reaction is a reversible process to push the equilibrium towards the product side it is necessary the continuous removal of the excess water produced during the esterification process or addition of an excess of the reactants. All the investigated ILs are very water absorbing in nature, hence,

Chapter 1

they can help to make the reaction proceed further. Moreover, the IL and the ester formed two separate phases in all the experiments. The scheme is shown below and the results are shown in Table 1.3.



Scheme 1.21: Esterification of 1-octanol and acetic acid using triethylammonium ILs

Table 1.3: Esterification of acetic acid and 1-octanol using triethylammonium ILs

| Entry ^a | Acetic acid (mmol) | 1-Octanol (mmol) | Ionic Liquid ^b | Temp (°C) | Time (h) | Yield ^c of <i>n</i> -octyl acetate (%) |
|--------------------|--------------------|------------------|---------------------------|-----------|----------|---|
| 1 | 20 | 20 | 1 | 90 | 4 | 77 |
| 2 | 20 | 24 | 1 | 90 | 4 | 81 |
| 3 | 20 | 24 | 1 | 90 | 6 | 80 |
| 4 | 20 | 24 | 1 | 110 | 4 | 84 |
| 5 | 20 | 24 | 1^d | 90 | 4 | 84 |
| 6 | 24 | 20 | 1 | 90 | 4 | 85 |
| 7 | 10 | 20 | 1 | 90 | 4 | 98 |
| 8 | 20 | 24 | 2 | 90 | 4 | 26 |
| 9 | 20 | 24 | 3 | 90 | 4 | 18 |
| 10 ^e | 20 | 24 | 3 | 90 | 4 | 90 |

^a Reactions were performed under nitrogen atmosphere. ^b 1 g of ionic liquid was used. ^c Based on acetic acid taken. ^d 2 g of ionic liquid was used. ^e *p*-Toluenesulfonic acid (100 mg) was added.

[NH(Et)₃][HSO₄] was used two times without much change in the conversion rates. Because of possibility of reusability of [NH(Et)₃][HSO₄], this IL was used also for esterification of various acids with primary alcohols. The results are shown in Table 1.4 below.

Table 1.4: Esterification of various acids with primary alcohols using [NH(Et)₃][HSO₄]

| Entry ^a | Acid | Alcohol | Yield ^b of ester (%) |
|--------------------|---|---|---------------------------------|
| 1 | CH ₃ CO ₂ H | CH ₃ (CH ₂) ₃ OH | 97 |
| 2 | CH ₃ CO ₂ H | CH ₃ (CH ₂) ₇ OH | 98 |
| 3 | CH ₃ CO ₂ H | CH ₃ (CH ₂) ₁₁ OH | 99 |
| 4 | CH ₃ CO ₂ H | PhCH ₂ OH | 96 |
| 5 | CH ₃ (CH ₂) ₂ CO ₂ H | CH ₃ (CH ₂) ₃ OH | 99 |
| 6 | CH ₃ (CH ₂) ₇ CO ₂ H | CH ₃ (CH ₂) ₃ OH | 94 |
| 7 ^c | CH ₂ =CH-CO ₂ H | CH ₃ (CH ₂) ₃ OH | 91 |
| 8 | C ₆ H ₁₁ CO ₂ H | CH ₃ (CH ₂) ₃ OH | 56 |
| 9 | PhCO ₂ H | CH ₃ (CH ₂) ₃ OH | 56 |
| 10 | <i>p</i> -HO-C ₆ H ₄ -CO ₂ H | CH ₃ (CH ₂) ₃ OH | 63 |

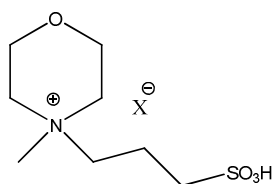
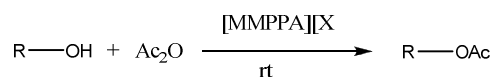
^a Conditions: acid (10 mmol), alcohol (20 mmol), [NH(Et)₃][HSO₄] = 1 g, 90°C, 4 h, under nitrogen. ^b Based on acid taken. ^c Acrylic acid (20 mmol) and 1-butanol (24 mmol) were taken. Hydroquinone (15 mg) was added as a polymerization inhibitor.

The various primary alcohols used were 1-butanol (97%), 1-octanol (98%), 1-dodecanol (99%) and benzyl alcohol (96%) (entries 1–4). The percentages denoted within the brackets are the ester yields, respectively. Then 1-butanol was taken as a constant, the acids were changed to butyric acid (99%), nonanoic acid (94%), acrylic acid (91%), cyclohexane carboxylic acid (56%), benzoic acid (56%) and *p*-hydroxybenzoic acid (63%). The percentages denoted within the brackets are the ester yields, respectively. From the above results of yields Pralhad et al.¹⁰⁷ concluded that aliphatic carboxylic acids showed much higher reactivity comparatively to the aromatic ones. In case of aromatic substrates no separate phases were formed.

Subsequently, Shuan-Hu Chen et al.¹⁰⁸ reported the preparation and characterization of a novel benzimidazolium Brønsted acidic IL and its application in esterifications.

Thermal gravimetric analysis of the Brønsted acidic 1-butylbenzimidazolium tetrafluoroborate [Hbbim][BF₄] indicated that although the new IL began to decompose at slightly lower temperature than that of imidazole series, it displayed high thermal stability. The sample was stable till the temperature reached 210°C and showed a weight loss of 90% between 220 and 270°C. When used as solvent and catalyst in the Fisher esterification of acetic acid with a series of aliphatic alcohols (ethanol, 1-butanol, iso-butyl alcohol, sec-butyl alcohol and tert-butyl alcohol) products, whose yields ranged from 96 to 98% with primary alcohols and 58% with the tertiary alcohol, were easily separated due to their insolubility in this medium.

But research in this field is a continuous. Recently, a rapid and efficient acetylation of alcohols and phenols with acetic anhydride has been performed in the presence of economical Brønsted acidic ILs bearing a propanesulfonic acid group on the morpholinium cation as catalysts under solvent-free conditions.¹⁰⁹



Scheme 1.22: Acetylation using propanesulfonic acid on morpholinium as catalyst

In particular, *N*-methylmorpholinium propanesulfonic acid hydrogen sulfate [MMPPA][HSO₄], having two catalytic groups, was found to be the most efficient catalyst able to give when employed in 0.1 mol% a complete acetylation of primary and secondary alcohols in few minutes working at room temperature under solvent-free conditions. Tertiary alcohols such as tert-butyl alcohols can also be acetylated in 64% yield and there was no elimination. It is to note that product recovery was performed by addition of water that allowed the separation of the formed product from the catalyst. The upper organic phase was washed with an aqueous solution of sodium bicarbonate, dried and purified by column chromatography, whereas the IL was recovered by concentrating the (bottom) water phase and was reused.

Although one of the main advantage offered by the use of acidic ILs is that to have an acid catalyst in homogeneous phase, the possibility to support acidic ILs to favor product separation has been explored. In the year 2010, Kelkar et al. reported¹¹⁰ the dehydration of glycerol over several silica-supported Brønsted acidic ILs showing that, although all the catalysts prepared were active for the synthesis of acrolein (conversion of glycerol was observed in the range of 35–90% with selectivity to acrolein in the range 29–58%), triphenyl(3-sulfopropyl)phosphonium tosylate gave the best results.

Considering the industrial role played by diphenyl carbonate (DPC) as intermediate, it is to mention the recent use of Brønsted (*N*-methylpyrrolidonium hydrogen sulfate and *N*-methylimidazolium hydrogen sulfate and tosylate) and Lewis acidic (choline–ZnCl₂) ILs as promoter of the transesterification of dimethyl carbonate with phenol to methylphenyl carbonate and DPC, using dibutyltin oxide as catalyst; a significant increase in yield was observed in the presence of acidic ILs.¹¹¹

Finally, it is to mention the application of PILs in cellulose field. The ability of some ILs to dissolve cellulose have attracted in the last 3–4 years an increasing interest. Recently, an exhaustive commentary having the objective to analyze literature data to provide new perspectives for the understanding of the dissolution process of cellulose has been published.¹¹²

Although, generally non-functionalized ILs have been used to solubilize cellulose, in the year 2009 Amarasekara and Owereth reported¹¹³ the possibility to use some Brønsted acidic ILs, 1-(1-propylsulfonic)-3-methylimidazolium chloride and 1-(1-butylsulfonic)-3-methylimidazolium chloride, for dissolution and hydrolysis of cellulose under mild reaction temperatures (70°C): the hydrolysis of Sigmacell cellulose (DP *ca.* 450) in 1-(1-propylsulfonic)-3-methylimidazolium chloride produced the highest total reducing sugar (62%) and glucose (14%) yields. In contrast, poor yields were obtained in *N*-1-propylsulfonic-*N,N,N*-triethanolammonium chloride. The inability of onium ILs to dissolve cellulose has been evidenced¹¹⁴ also in a more recent

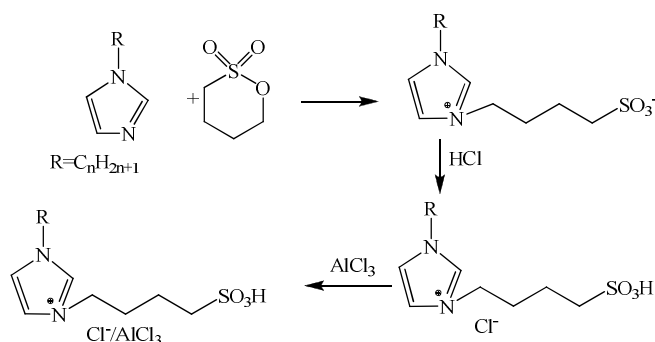
investigation about protic ILs arising from combination of four organic acids (formic acid, acetic acid, malonic acid and citric acid) and five amines (ethanolamine, diethanolamine and triethanolamine, propan-1-olamine and diallylamine); none of the resulting ILs was able to dissolve crystalline cellulose even if the presence of hydroxyl groups on cation favored the formation of a fine dispersion. All these data have considered a confirmation of the higher performance of aromatic cations in cellulose processing.

Last but not the least, one should mention the use of acidic ILs ([bmim][HSO₄])¹¹⁵ and a series of acidic ILs containing COOH group on cations,¹¹⁶ whose catalytic properties have been found to be closely related to behave, as extractants and catalysts in the oxidative desulfurization of dibenzothiophenes in the presence of H₂O₂ in model oil.

1.2.3 Dual-functionalized acidic Ionic Liquids

To increase the catalytic properties of acidic ILs also dual- and multi-functionalized ILs have been synthesized. Generally, dual-functionalized acidic ILs are characterized by a cation bearing a Brønsted acidic group (–SO₃H or –COOH on the alkyl chain), or having an acidic proton on the nitrogen atom associated with a Lewis acidic anion. The dual-functionalized ILs bearing a Brønsted acidic cation associated to a Brønsted acidic anion ([HSO₄][–] or [H₂PO₄][–]) have been described in the previous section being characterized by a unique kind of acidity.

In 2005, Wang et al.¹¹⁷ synthesized and characterized one of the first example of IL of this class.



Scheme 1.23: [C₄SC_n'im][Cl]/AlCl₃

The zwitterionic-type precursors of these ILs were obtained, as previously reported, by direct sulfonation reaction of the nitrogen base (1-methyl imidazole in this case) and 1,4-butane

sulfone. The subsequent acidification by mixing of the zwitterion with HCl (1:1 mol) converts the pendant sulfonic group into an alkane sulfonic acid. Finally, reaction of 3-alkyl-1-(butyl-4-sulfonyl) imidazolium chloride ($[\text{C}_4\text{SC}_n\text{im}][\text{Cl}]$) with AlCl_3 gives the dual acidic ILs, $[\text{C}_4\text{SC}_n\text{im}][\text{Cl}]/\text{AlCl}_3$. It is however noteworthy that the production of $[\text{C}_4\text{SC}_n\text{im}][\text{Cl}]/\text{AlCl}_3$ requires an initiator or promoter. In this case, $[\text{bmim}]\text{Cl}/\text{AlCl}_3$ (this is prepared as described previously) was used as promoter. These ILs are characterized by high decomposition temperatures, ranging around 320°C . Their acidity was determined⁹⁰ by FT-IR using pyridine (Py) as probe (Figure 1.14); considering that, as previously reported, the presence of a band near 1450 cm^{-1} can be assumed as an indication of the presence of pyridine coordinated to Lewis acidic sites, whereas a band near 1540 cm^{-1} an indication of the formation of pyridinium ions resulting from the presence of Brønsted acidic sites. When pyridine was added to $[\text{C}_4\text{SC}_4\text{im}][\text{Cl}]$ (Figure 1.14C) a band at 1540 cm^{-1} , indicating Brønsted acidity for $[\text{C}_4\text{SC}_4\text{im}][\text{Cl}]$, was observed. On the other hand, in the mixture of $[\text{C}_4\text{SC}_4\text{im}][\text{Cl}]/\text{AlCl}_3$ and $[\text{C}_4\text{mim}][\text{Cl}]/\text{AlCl}_3$ ($X(\text{AlCl}_3)=0.60$) (Figure 1.14E), both the band at 1540 cm^{-1} and at 1450 cm^{-1} , indicating respectively Brønsted and Lewis acidity, were present. Moreover, taking into account the band at 1454 cm^{-1} of $[\text{C}_4\text{mim}][\text{Cl}]/\text{AlCl}_3$ ($X(\text{AlCl}_3)=0.67$) (Figure 1.14D), it was observed that the quantitative addition of $[\text{C}_4\text{SC}_4\text{im}][\text{Cl}]$ produce a band shift to 1450 cm^{-1} ; the Al_2Cl_7^- anion in $[\text{C}_4\text{SC}_4\text{im}][\text{Cl}]/\text{AlCl}_3$ reacting with Cl^- form AlCl_4^- anion.

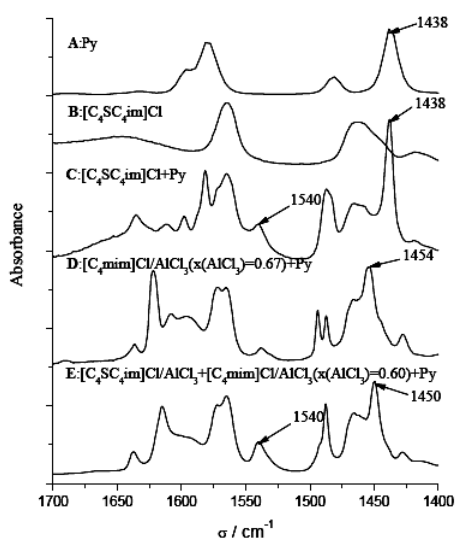
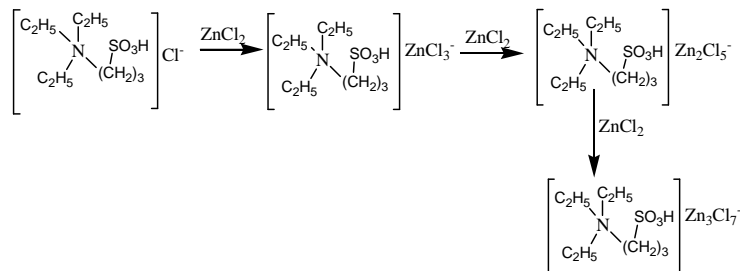


Figure 1.14: Determination of acidity of $[\text{C}_n\text{SC}_4\text{im}]\text{Cl}_2/\text{AlCl}_3$

Subsequently, Liu et al.¹¹⁸ proposed another dual-functionalized IL having both Lewis and Brønsted acidic character; $[\text{HSO}_3-(\text{CH}_2)_3-\text{NEt}_3]\text{Cl}-\text{ZnCl}_2$. This IL was prepared according to the procedure explained below in Scheme 1.24. The Lewis acidity of IL, as well as other important properties (including viscosity) depended on the ZnCl_2 mass: on increasing the ZnCl_2 mass the viscosity of the obtained IL increases.

**Scheme 2:** ILs based on trichlorozincate anions

Related to the Lewis and Brønsted acidic character of this dual-functionalized IL, also in this case it was determined by FT-IR using acetonitrile (ACN) and pyridine (Py) as a probe. As shown in Figure 1.15A, after reacting with Py, $[\text{HSO}_3-(\text{CH}_2)_3-\text{NEt}_3]\text{Cl}-\text{ZnCl}_2$ ($X=0.64$) had two new characteristic absorption peaks of 1540 and 1448 cm^{-1} in the FT-IR spectra indicating that $[\text{HSO}_3-(\text{CH}_2)_3-\text{NEt}_3]\text{Cl}-\text{ZnCl}_2$ ($X=0.64$) had both Brønsted and Lewis acidic characteristics. However, when ACN, a weaker base, was used as probe the positions of peaks of $\text{ACN}/[\text{HSO}_3-(\text{CH}_2)_3-\text{NEt}_3]\text{Cl}-\text{ZnCl}_2$ ($X=0.5$) were entirely the same as those of ACN, indicating that $[\text{HSO}_3-(\text{CH}_2)_3-\text{NEt}_3]\text{Cl}-\text{ZnCl}_2$ ($X=0.5$) was not Lewis acidic. At variance, in the spectra of $\text{ACN}/[\text{HSO}_3-(\text{CH}_2)_3-\text{NEt}_3]\text{Cl}-\text{ZnCl}_2$ ($X=0.6$) and $\text{ACN}/[\text{HSO}_3-(\text{CH}_2)_3-\text{NEt}_3]\text{Cl}-\text{ZnCl}_2$ ($X=0.64$), a new absorption peak at 2318 and 2326 cm^{-1} , respectively, appeared indicating that both $[\text{HSO}_3-(\text{CH}_2)_3-\text{NEt}_3]\text{Cl}-\text{ZnCl}_2$ ($X=0.6$) and $[\text{HSO}_3-(\text{CH}_2)_3-\text{NEt}_3]\text{Cl}-\text{ZnCl}_2$ ($X=0.64$) were Lewis acidic. Moreover, the wavenumber of $[\text{HSO}_3-(\text{CH}_2)_3-\text{NEt}_3]\text{Cl}-\text{ZnCl}_2$ ($X=0.64$) was higher than that of the IL $[\text{HSO}_3-(\text{CH}_2)_3-\text{NEt}_3]\text{Cl}-\text{ZnCl}_2$ ($X=0.6$), which indicated that the Lewis acidity of $[\text{HSO}_3-(\text{CH}_2)_3-\text{NEt}_3]\text{Cl}-\text{ZnCl}_2$ ($X=0.64$) was stronger than that of $[\text{HSO}_3-(\text{CH}_2)_3-\text{NEt}_3]\text{Cl}-\text{ZnCl}_2$ ($X=0.6$).

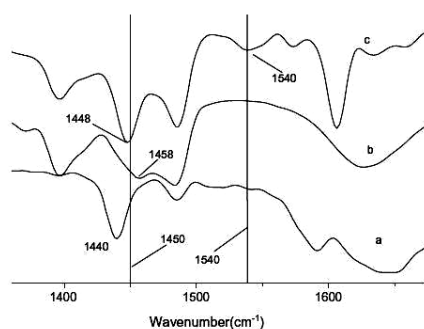


Figure 1.15 A

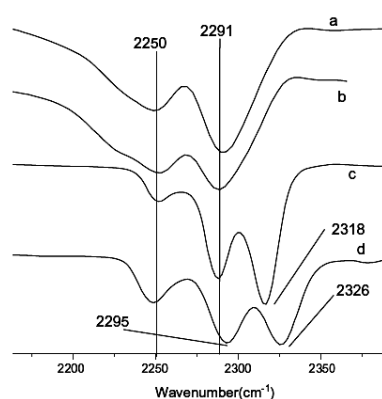
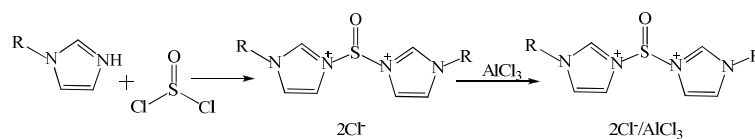


Figure 1.15 B

Figure 1.15: FT-IR spectra of $[\text{HSO}_3-(\text{CH}_2)_3-\text{NEt}_3]\text{Cl}-\text{ZnCl}_2$ IL by using acetonitrile and pyridine as probe. **(A)** FT-IR spectra of samples using pyridine as probe. **(a)** Pure pyridine, **(b)** IL $[\text{HSO}_3-(\text{CH}_2)_3-\text{NEt}_3]\text{Cl}-\text{ZnCl}_2$ ($X=0.64$), **(c)** Pyridine/ $[\text{HSO}_3-(\text{CH}_2)_3-\text{NEt}_3]\text{Cl}-\text{ZnCl}_2$ ($X=0.64$), $V(\text{pyridine}):V(\text{IL}) = 1:2$. **(B)** FT-IR spectra of ILs using acetonitrile as probe. **(a)** Pure acetonitrile, **(b)** acetonitrile/ $[\text{HSO}_3-(\text{CH}_2)_3-\text{NEt}_3]\text{Cl}-\text{ZnCl}_2$ ($X=0.5$), **(c)** acetonitrile/ $[\text{HSO}_3-(\text{CH}_2)_3-\text{NEt}_3]\text{Cl}-\text{ZnCl}_2$ ($X=0.6$), **(d)** acetonitrile/ $[\text{HSO}_3-(\text{CH}_2)_3-\text{NEt}_3]\text{Cl}-\text{ZnCl}_2$ ($X=0.64$), $V(\text{acetonitrile}):V(\text{IL}) = 1:2$ in the samples of **b-d**.

Among the dual-functionalized acidic ILs one more class of Lewis acidic ILs, 3,3'-thionyl-bis-1,1'-alkylimidazolium chloroaluminate ($[\text{tbaim}]\text{Cl}_2/\text{AlCl}_3$) can be mentioned, synthesized by He et al.¹¹⁹ characterized by doubly-charged thionyl cations and chloroaluminate anions.



1a: $[\text{tbim}]\text{Cl}_2/\text{AlCl}_3$, $R = \text{CH}_3$; 1b: $[\text{tbeim}]\text{Cl}_2/\text{AlCl}_3$, $R = \text{C}_2\text{H}_5$; 1c: 1a: $[\text{tbbim}]\text{Cl}_2/\text{AlCl}_3$, $R = \text{C}_4\text{H}_9$

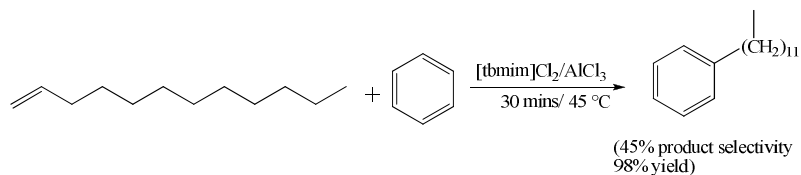
Scheme 1.25: Doubly-charged thionyl cations and chloroaluminate anions

1.2.3.1 Applications of dual-functionalized Lewis acidic ILs

Friedel Crafts reactions using dual-functionalized acidic ILs

a.) The dual-functionalized 3,3'-thionyl-bis-1,1'-alkylimidazolium chloroaluminate, $[\text{tbaim}]\text{Cl}_2/\text{AlCl}_3$, has been applied in the Friedel-Crafts alkylation of benzene with 1-dodecene. The reaction almost instantaneously completed after 1-dodecene was dropped into the

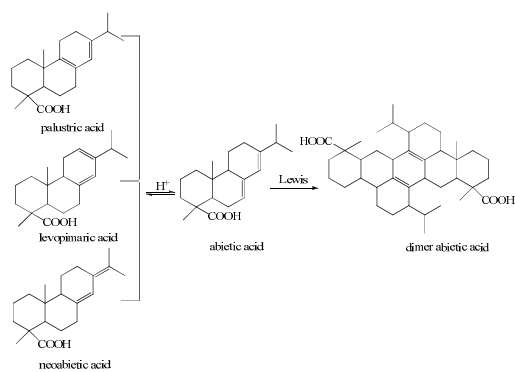
benzene/ILs mixture; the turnovers of 1-dodecene were higher than 99%. By varying reaction time, no obvious promotion was observed. When the mole fraction of AlCl_3 ($X(\text{AlCl}_3)$) was 0.50, which means that there was no Al_2Cl_7^- in the ILs, the alkylation could not occur. The effects of the molar ratio of benzene to 1-dodecene were also explored. On increasing the molar ratio of benzene to 1-dodecene, the yield of the target product was enhanced. Furthermore, use of $[\text{tbaim}]\text{Cl}_2/\text{AlCl}_3$ led to a significant simplification in product isolation. The maximum yield of the monododecylbenzene was about 98%, whereas the product selectivity was about 45%. The molar ratios of IL was varied from 0.33 to 0.55 to 0.67; 0.67 gave the best results. Also the molar ratio of benzene to 1-dodecene was increased from 2:1 to 10:1. And 10:1 gave the best yield. Increase in time did not play much important role in the reaction.



Scheme 36: Benzene and 1-dodecene

It is however noteworthy that the comparative study of the IL $[\text{tbaim}]\text{Cl}_2/\text{AlCl}_3$ as catalytic system with the traditional AlCl_3 or $[\text{bmim}]\text{Cl}/\text{AlCl}_3$ system (DeCastro et al.¹²⁰ in the year 2000, used $[\text{bmim}]\text{Cl}/\text{AlCl}_3$ as catalyst and solvent in the Friedel-Crafts alkylation of benzene with 1-dodecene) evidenced that similarly to $[\text{bmim}]\text{Cl}/\text{AlCl}_3$ ($X(\text{AlCl}_3) = 0.67$), $[\text{tbaim}]\text{Cl}_2/\text{AlCl}_3$ ($X(\text{AlCl}_3) = 0.67$) has better catalytic efficiency than AlCl_3 . In both the IL systems moreover when the mole fraction of AlCl_3 ($X(\text{AlCl}_3)$) was 0.50 the alkylation did not occur due to the absence of Al_2Cl_7^- : $[\text{bmim}][\text{AlCl}_4]$ had no Lewis acidity.¹²¹

In 2008, Liu et al.⁹⁸ applied the dual acidic $[\text{HSO}_3-(\text{CH}_2)_3-\text{NEt}_3]\text{Cl}-\text{ZnCl}_2$ for the dimerization of rosin.



Scheme 1.27: Dimerization of rosin using $[HSO_3-(CH_2)_3-NEt_3]Cl-ZnCl_2$

The reaction was carried out using various mole fractions of IL Lewis acid; considering all the ratios investigated, was concluded that $[HSO_3-(CH_2)_3-NEt_3]Cl-ZnCl_2$ ($X = 0.64$) was an effective catalyst for this reaction, and with the increase of the Lewis acid, the catalytic performance of IL was also increased for the dimerization. However, the softening point of polymerized rosin was decreased when the mole fraction of $ZnCl_2$ was more than 0.64. This behavior was attributed to the increased IL viscosity on increasing the $ZnCl_2$ mass. When the mole fraction of $ZnCl_2$ was more than 0.64, the IL dispersivity was very bad in the mixture of reaction. Therefore, it was concluded that the Brønsted–Lewis acidic IL had a good catalytic performance in this process. Moreover, the recycle tests showed that softening point of polymerized rosin was almost unchanged after $[HSO_3-(CH_2)_3-NEt_3]Cl-ZnCl_2$ ($X = 0.64$) was used repeatedly for five times. This good reusability result was explained by the following two points. Firstly, in the structure of $[HSO_3-(CH_2)_3-NEt_3]Cl-ZnCl_2$ ($X = 0.64$), the alkyl sulfonic acid group is covalently tethered in the IL cation; therefore, it is not easily lost. Secondly, the anion $[Zn_2Cl_5]^-$ of IL is inert and stable to water or Brønsted acid.

References

-
- ¹ Anastas, P. T.; Warner, J. C. *Green Chem.*; Oxford: New York, **1998**.
- ² Meyers, R. A., Editor-in-Chief. The Wiley Encyclopedia of Environmental Pollution and Clean Up; Wiley: New York, **1999**; Vol. 1–2.
- ³ Anastas, P. T.; Warner J. C. *Green Chem.: Theory and Practice*. Oxford University Press, **1998**.
- ⁴ (a) Lide, D. R. *Handbook of Organic Solvents*; CRC: Baton Rouge, **1995**.
(b) Wypych, G.; Ed. *Handbook of Solvents*; ChemTec Publishing: New York, **2000**.
- ⁵ Anderson, N. G. *Practical Process Research and Development*; Academic Press: San Diego, **2000**.
- ⁶ Bates, E. D.; Mayton, R. D.; Ntai, I.; Davis, J. H., Jr. *J. Am. Chem. Soc.* **2002**, *124*, 926–927.
- ⁷ Visser, A. E.; Holbrey, J. D.; Rogers, R. D. *Chem. Commun.* **2001**, 2484–2485.
- ⁸ Visser, A. E.; Swatloski, R. P.; Reichert, W. M.; Mayton, R.; Sheff, S.; Wierzbicki, A.; Davis, J. H., Jr.; Rogers, R. D. *Chem. Commun.* **2001**, 135–136.
- ⁹ Merrigan, T. L.; Bates, E. D.; Dorman, S. C.; Davis, J. H., Jr. *Chem. Commun.* **2000**, 2051–2052.
- ¹⁰ Forrester, K. J.; Davis, J. H., Jr. *Tetrahedron Lett.* **1999**, *40*, 1621–1622.
- ¹¹ Morrison, D. W.; Forbes D. C.; Davis, J. H., Jr. *Tetrahedron Lett.* **2001**, *42*, 6053–6057.
- ¹² Ishihara, K.; Hasegama, A. and Yamamoto, H. *Angew. Chem., Int. Ed.* **2001**, *40*, 4077–4079.
- ¹³ Harmer, M. A.; Sun, Q. *Appl. Catal., A* **2001**, *221*, 45–62.
- ¹⁴ Seddon, K. R. *J. Chem. Technol. Biotechnol.* **1997**, *68*, 351–356.
- ¹⁵ Welton, T. *Chem. Rev.* **1999**, *99*, 2071.
- ¹⁶ Hurley, F. H. US patent 4446331, **1948**.
- ¹⁷ Wilkes, J. S. *Green Chem.* **2002**, *4*, 73.
- ¹⁸ Earle, M. J.; Seddon, K. R. *Pure Appl. Chem.* **2000**, *72*, 1391.
- ¹⁹ Visser, A. E.; Swatloski, R. P.; Reichert, W. M.; Davis, J. H., Jr.; Rogers, R. D.; Mayton, R.; Sheff, S.; Wierzbicki, A. *Chem. Comm.* **2001**, 135.
- ²⁰ Nicola Wood and Gill Stephens. Accelerating the discovery of biocompatible ionic liquids. *Phys. Chem. Chem. Phys.*, **2010**, *12*, 1670 (DOI: [10.1039/b923429b](https://doi.org/10.1039/b923429b)).
- ²¹ (a) Hurley, F. H. *U.S. Patent*. 2446331, **1948**. (b) Wier, T. P., Jr.; Hurley, F.H. *U.S. Patent* 2446349, **1948**.
- ²² Wilkes, J. S.; Levisky, J. A.; Wilson, R. A.; Hussey, C. L. *Inorg. Chem.* **1982**, *21*, 1263.

- ²³ Huddleston, J. G.; Visser, A. E.; Reichert, W. M.; Willauer, H. D.; Broker, G. A. and Rogers, R. D. *Green Chem.*, **2001**, 3, 156–164.
- ²⁴ Piao, L.Y.; Fu, X.; Yang, Y.L.; Tao, G.H.; Kou, Y. *Catal. Today*, **2004**, 301, 93–95.
- ²⁵ Wasserscheid, P. and Welton, T. *Ionic liquids in Synthesis*, 2nd ED. Wiley-VCH, Weinheim, **2008**.
- ²⁶ Neto, B. A. S.; Ebeling, G.; Gonçalves, R. S.; Gozzo, F. C.; Eberlin, M. N.; Dupont, J. *Synthesis* **2004**, 8,1155.
- ²⁷ (a) Abbott, A.P.; Capper, G.; Davies, D.L.; Rasheed, R.K.; Tambyrajah, V. *Green Chem.*, **2002**, 4, 24.
- (b) Yin, D.H.; Li, C.; Li, B.; Tao, L.; Yin, D. *Adv. Synth. Catal.* **2005**, 347, 137.
- ²⁸ Abbott, A.P.; Capper, G.; Davies, D.L.; Munro, H.L.; Rasheed, R.K.; Tambyrajah, V. *Chem. Commun.*, **2001**, 2010.
- ²⁹ (a) Lee, S. H.; Ha, S. H.; Ha, S. S.; Jin, H. B.; You, C. Y.; Koo, Y. M. *J. Appl. Phys.*, **2007**, 101, 09j102.
- (b) Hayashi, S. and Hamagushi, H. O. *Chem. Lett.* **2004**, 33, 1590.
- ³⁰ (a) Xie, Z. L.; Jelicic, A.; Wang, P. F.; Rabu, P.; Friedrich, A.; Beurmann, S.; Taubert, A. *J. Mater. Chem.* **2010**, 20, 9543.
- (b) Vioux, A.; Viau, L.; Volland, S.; Le Bideau, J. *C. R. Chim.* **2010**, 13, 242.
- ³¹ Xie, Z. L.; Taubert, A. *Chem. Phys. Chem.*, **2011**, 12, 364.
- ³² Brian, L. S.; Wilkes, J. S. McCleskey, T. M.; Burrell, A.K.; Baker, G. A.; Thompson, J. D. *Chem. Comm.* **2008**, 447.
- ³³ Mutelet, F.; Jaubert, J.-N.; Rogalski, M.; Boukherissa, M.; Dicko, A. *J. Chem. Eng. Data* **2006**, 51, 1274.
- ³⁴ Boukherissa, M.; Mutelet, F.; Modarressi, A.; Dicko, A.; Drafi, D.; Rogalski, M. *Energy Fuels* **2009**, 23, 2557.
- ³⁵ Seddon, K. R. *J. Chem. Technol. Biotechnol.*, **1997**, 68, 351.
- ³⁶ Woodcock, C. and Shriver, D. F. *Inorg. Chem.*, **1986**, 25, 2137.
- ³⁷ Zawodzinski, T. A. Jr.; and Osteryoung, R. A. *Inorg. Chem.*, **1989**, 28, 1710.
- ³⁸ (a) Gray, J. L. and Maciel, G. E. *J. Am. Chem. Soc.*, **1981**, 103, 7147.
- (b) Carlin, R. T. *J. Mol. Catal.*, **1990**, 63, 125.
- (c) Fannin, A. A. Jr.; King, L. A.; Levisky, J. A. and Wilkes, J. S. *J. Phys. Chem.*, **1984**, 88, 2609.

- (d) Chauvin, Y.; Tiggelen, F. D. M.-V. and Olivier, H. *J. Chem. Soc., Dalton Trans.*, **1993**, 1009.
- ³⁹ Angell, C. A. and Bennett, P. D. *J. Am. Chem. Soc.*, **1982**, *104*, 6304.
- ⁴⁰ Hsiu, S. I.; Huang, J. F.; Sun, I. W.; Yuan, C. H. and Shiea, J. *Electrochim. Acta*, **2002**, *47*, 4367.
- ⁴¹ Yang, Y.; Kou, Y. *Chem. Commun.* **2004**, 226.
- ⁴² Yin, D.; Li, C.; Tao, L.; Yu, N.; Yin, D. *J. Mol. Catal. A: Chemical*, **2006**, *245*, 260.
- ⁴³ Estager, J.; Oliferenko, A. A.; Seddon, K. R.; Swadzba-Kwaśny, M. *Dalton Trans.*, **2010**, *39*, 11375.
- ⁴⁴ (a) Adams, C. J.; Earle, M. J.; Roberts, G.; Seddon, K. R. *Chem. Commun.*, **1998**, 2097.
(b) Rebeiro, G. L.; Kadilkar, B.M. *Syn. Commun.*, **2000**, *30*, 1605.
- ⁴⁵ Nara, S. J.; Harjani, J. R.; Salunkhe, M. M. *J. Org. Chem.*, **2001**, *66*, 8616.
- ⁴⁶ Kim, S. D.; Ahn, W. S. *Korean J. Chem. Eng.*, **2003**, *20*, 39.
- ⁴⁷ Yin, D.; Li, C.; Tao, L.; Yu, N.; Hu, S.; Yin, D. *J. Mol. Catal. A: Chemical*, **2006**, *245*, 260–265.
- ⁴⁸ Li, C.; Liu, W.; Zhao, Z. *Cat. Commun.* **2007**, *8*, 1834–1837.
- ⁴⁹ Bahrami, K.; Khodei, M. M.; Shahbazi, F. *Tetrahedron Lett.* **2008**, *49*, 3931.
- ⁵⁰ Chen, M.; Huang, L.; Luo, Y.; He, M.; Xie, J.; Yuan, X. *React. Kinet. Catal. Lett.*, **2009**, *98*, 355–363.
- ⁵¹ Chen, M.; Luo, Y.; Li, G.; He, M.; Xie, J.; Li, H.; Yuan, X. *Korea J. Chem. Eng.* **2009**, *26*, 1563.
- ⁵² Xin, H.; Wu, Q.; Han, M.; Wang, D.; Jin, Y. *Appl. Catal. A: General*. **2005**, *292*, 354.
- ⁵³ Green, L.; Hemeon, I.; Singer, R. D. *Tetrahedron*. **2000**, *41*, 1343.
- ⁵⁴ Potdar, M. K.; Mohile, S. S.; Salunkhe, M. M. *Tetrahedron Lett.* **2001**, *42*, 9285.
- ⁵⁵ Harjani, J. R.; Nara, S. J.; Salunkhe, M. M. *Tetrahedron Lett.* **2002**, *43*, 1127.
- ⁵⁶ Stenzel, O.; Brull, R.; Wahner, U.; Sanderson, R. D.; Raubenheimer, H. G. *J. Mol. Catal. A: Chemical*. **2003**, *192*, 217.
- ⁵⁷ Kumar, A.; Pawar, S. S. *J. Mol. Catal. A: Chemical*. **2004**, *208*, 33.
- ⁵⁸ Yadav, Y. S.; Reddy, B. V. S.; Reddy, M. S.; Niranjana, N.; Prasad, A. R. *Eur. J. Org. Chem.* **2003**, *9*, 1779.
- ⁵⁹ Duan, Z.; Gu, Y.; Deng, Y. *Cat. Commun.* **2006**, *7*, 651.
- ⁶⁰ Sadula, S.; Kanjilal, S.; Reddy, P. S.; Prasad, R. B. N. *Tetrahedron Lett.* **2007**, *48*, 6962.
- ⁶¹ Chen, X.; Peng, Y. *Catalysis Lett.* **2008**, *122*, 310.

- ⁶² Kumar, V.; Tomar, S.; Patel, R.; Yousaf, A.; Parmar, V. S.; Malhotra, S. V. *Synth. Commun.* **2008**, *38*, 2646.
- ⁶³ Cole, A. C.; Jensen, J. L.; Kim, I. N.; Tran, L. T.; Weaver, K. J.; Forbes, D. C. and Davis, J. H. Jr *J. Am. Chem. Soc.*, **2002**, *124*, 5962.
- ⁶⁴ Yoshizawa, M.; Hirao, M.; Ito-Akita, K.; Ohno, H. *J. Mater. Chem.* **2001**, *11*, 1057–1062.
- ⁶⁵ Yan, N.; Yuan, Y.; Dykeman, R.; Kou, Y.; Dyson, P. J. *Angew. Chem. Int. Ed.* **2010**, *49*, 5549.
- ⁶⁶ Hsien, M.; Sheu, H.-T.; Lee, T.; Cheng, S.; Lee, J.-F. *J. Mol. Catal. A: Chem.* **2002**, *181*, 189–200 and references therein.
- ⁶⁷ Kalkhambkar, R.; Waters, S. N.; Laali, K. K. *Tetrahedron Lett.* **2011**, *52*, 867.
- ⁶⁸ Qiao, K.; Hagiwara, H.; Yokoyama, C. *J. Mol. Cat A: Chemical.* **2006**, *246*, 65–69.
- ⁶⁹ Sugimura, R.; Qiao, K.; Tomida, D.; Yokoyama, C. *Cat. Commun.* **2007**, *8*, 770–772.
- ⁷⁰ (a) Wenkert, E.; Goodwin, T.E. *Synth. Commun.* **1977**, *7*, 409.
(b) Yang, H.; Li, B.; Cui, Y. *Synth. Commun.* **1993**, *28*, 1233, and references cited therein.
- ⁷¹ Johnson K. E.; Pagni, R. M.; Bartmess *J. Monatshefte fur Chemie.* **2007**, *138*, 1077.
- ⁷² Greves, T- L- and Drummond C. *J. Chem. Rev.* **2008**, *108*, 206.
- ⁷³ Bautista-Martinez, J. A; Tang, L.; Belieres, J. P.; Zeller, R.; Angell, C.A.; Friesen, C. *J. Phys. Chem. C.* **2009**, *113*, 12586.
- ⁷⁴ (a) Greaves, T. L.; Weerawardena, A.; Fong, C.; Drummond, C. J. *J. Phys. Chem. B.* **2007**, *111*, 4082.
(b) Greaves, T. L.; Weerawardena, A.; Fong, C.; Krodkiewska, I.; Drummond, C. J. *J. Phys. Chem. B.* **2006**, *110*, 22479.
(c) Greaves, T. L.; Weerawardena, A.; Krodkiewska, I.; Drummond, C. J. *J. Phys. Chem. B.* **2008**, *112*, 896.
- ⁷⁵ Anouti, M.; Caillon-Caravanier, M.; Dridi, Y.; Galiano, H.; Lemordant, D. *J. Phys. Chem. B.* **2008**, *112*, 13335.
- ⁷⁶ Brigouleix, C.; Anouti, M.; Jacquemin, J.; Caillon-Caravanier, M.; Dridi, Y.; Galiano, H.; Lemordant, D. *J. Phys. Chem. B* **2010**, *114*, 1757.
- ⁷⁷ Wu, T-Y; Su, S.-G.; Lin Y-C.; Wang, H. P.; Lin, M. W; Gung, S. T.; Sun, I. W *Electrochim. Acta.* **2010**, *56*, 853.
- ⁷⁸ Zhao, C.; Burrell, G.; Torriero, A. A. J.; Separovic, F.; Dulop, N. F.; MacFarlane, D. R.; Bond, A. M. *J. Phys. Chem. B.* **2008**, *112*, 6923.
- ⁷⁹ Rebelo, L. P. N; Lopes, J. N. C.; Esperanca, J.; Lachwa, H.; Najdanovic-Visak, V.; Visak, Z. *P. Acc. Chem. Res.* **2007**, *40*, 1114.

- ⁸⁰ Luo, H.; Gary, G. A.; Lee, J. S.; Pagni, R. M.; Dai, S. *J. Phys. Chem. B* **2009**, *113*, 4181.
- ⁸¹ Du, Z.; Li, Z.; Guo, S.; Zhang, J.; Zhu, L.; Deng, Y. *J. Phys. Chem. B* **2005**, *109*, 19542.
- ⁸² Magna, L.; Bildé, J.; Olivier-Bourbigou, H.; Robert, T.; Gilbert, B. *Oil & Gas Sci. Technol.* **2009**, *64*, 669.
- ⁸³ Duan, Z.; Gu, Y.; Zhang, J.; Zhu, L.; Deng, Y. *J. Mol. Cat. A: Chemical* **2006**, *250*, 163.
- ⁸⁴ Yang, J.; Zhou, H.; Lu, X.; Yuan, Y. *Catal. Commun.* **2010**, *11*, 1200.
- ⁸⁵ Atkin, R.; Warr, G. G. *J. Phys. Chem. B* **2008**, *112*, 4164.
- ⁸⁶ Fumino, K.; Wulf, A.; Ludwig R. *Angew. Chem. Int. Ed.* **2009**, *48*, 3184.
- ⁸⁷ Greaves, T. L.; Kennedy, D. F.; Mudie, S. T.; Drummond, C. J. *J. Phys. Chem. B* **2010**, *114*, 10022.
- ⁸⁸ Kennedy, D. F. and Drummond, C. J. *J. Phys. Chem. B* **2009**, *113*, 5693.
- ⁸⁹ Burrell, I. M.; Burgar, Q.; Gong, N. F.; Dunlop, F. *J. Phys. Chem. B* **2010**, *114*, 11436.
- ⁹⁰ Alvarez, V. H.; Dosil, N.; Gonzalez-Cabaleiro, R.; Mattedi, S.; Martinez-Pastor, M.; Iglesias, M.; Navaza, J. M. *J. Chem. Eng. Data* **2010**, *55*, 625.
- ⁹¹ Malvaldi, M.; Bruzzone, S.; Chiappe, C. *Phys. Chem. Chem. Phys.* **2007**, 5576.
- ⁹² Jin, H.; Baker, G. A.; Arzhantsev, S.; Ding, J.; Maroncelli, M. *J. Phys. Chem. B* **2007**, *111*, 7291.
- ⁹³ Smith, M. B.; March, J. *March's Advanced Organic Chemistry*; Wiley-Interscience: New York, **2001**; Chapter 8.
- ⁹⁴ Greaves, T. L.; Drummond, C. J. *Chem. Rev.* **2008**, *108*, 206.
- ⁹⁵ (a) Narvatkar, N. B.; Deorikhar, A. R.; Bhilare, S. V.; Salunke, M. M. *Synth. Commun.* **2006**, *36*, 3043.
- (b) Hu, Y.; Chen, J.; Le, Z. G.; Zheng, Q. G. *Synth. Commun.* **2005**, *35*, 739.
- ⁹⁶ Jaeger, D. A.; Tucker, C. E. *Tetrahedron Lett.* **1989**, *30*, 1785.
- ⁹⁷ Bini, R.; Chiappe, C.; Mestre, V.L.; Pomelli, C. S.; Welton, T. *Org. Biomol. Chem.* **2008**, *6*, 2522.
- ⁹⁸ (a) Bini, R.; Chiappe, C.; Mestre, V. L.; Pomelli, C. S.; Welton, T. *Theor. Chem. Acc.* **2009**, *123*, 347.
- (b) Chiappe, C.; Malvaldi, M.; Pomelli, C. S. *J. Chem. Theory Comput.* **2010**, *6*, 176.
- (c) Chiappe, C.; Malvaldi, M.; Pomelli, C. S. *Green Chem.* **2010**, *12*, 1330.
- ⁹⁹ Zhao, G.; Jiang, T.; Gao, H.; Han, B.; Huang, J. and Sun, D. *Green Chem.*, **2004**, *6*, 75–77.
- ¹⁰⁰ Tajik, H.; Niknam, K. and Parsa, F. *J. Iran. Chem. Soc.* **2009**, *6(1)*, 159–164.
- ¹⁰¹ Chiappe, C.; Leandri, E.; Tebano, M. *Green Chem.* **2006**, *8*, 742.

- ¹⁰² Gou, H.; Li, X.; Wang, J. L.; Jin, X. H.; Lin, X. F. *Tetrahedron*. **2010**, *66*, 8300.
- ¹⁰³ Zhu, H.-P. et al. *Green Chem.* **2003**, *5*, 38–39.
- ¹⁰⁴ Fraga-Dubreuil, J.; Bourahla, K. and Rahmouni, M. *Catal. Commun.* **2002**, *3*, 185.
- ¹⁰⁵ Duan, Z.; Gu, Y.; Deng, Y. *J. Mol. Cat. A Chemical*. **2006**, *24*, 670–675.
- ¹⁰⁶ Joseph, T.; Sahoo, S.; Halligudi, S.B. *J. Mol. Cat A: Chemical*. **2005**, *234*, 107–110.
- ¹⁰⁷ Ganeshpure, P. A.; George, G. and Das, J. Application of triethylammonium salts as ionic liquid catalyst and medium for Fischer esterification. *ARKIVOC*. **2007**, 273–278.
- ¹⁰⁸ Chen, S.-H.; Zhao, Q. and Xu, X.-W. *J. Chem. Sci.*, **2008**, *120(5)*, 481–483.
- ¹⁰⁹ Yue, C.; Liu, Q.; Yi, T.; Chen, Y. *Monatsh Chem.* **2010**, *141*, 975.
- ¹¹⁰ Munshi, M. K.; Lomate, S. T.; Deshpande, R. M.; Rane, V. H.; Kelkar, A. A. *J. Chem. Biotechnol.* **2010**, *85*, 1319.
- ¹¹¹ Deshmikh K. M.; Qureshi, Z. S. Q.; Dhake, K. P.; Bhanage, B. M. *Cat. Commun.* **2010**, *12*, 207.
- ¹¹² Pinkert, A.; Marsh, K. N.; Pang, S. *Ind. Eng. Chem. Res.* **2010**, *49*, 11121.
- ¹¹³ Amarasekara, A. S.; Owereh, O. S. *Ind. Eng. Chem. Res.* **2009**, *48*, 10152.
- ¹¹⁴ Pinkert, A.; Marsh, K. N.; Pang, S. *Ind. Eng. Chem. Res.* **2010**, *49*, 11809.
- ¹¹⁵ Zhang, W.; Xu, K.; Zhang, Q.; Liu, D.; Wu, S.; Verpoort, F.; Song X.-M. *Ind. Eng. Chem. Res.* **2010**, *49*, 11760.
- ¹¹⁶ Gui, J.; Liu, D.; Sun, Z.; Liu, D.; Min, D.; Song, B.; Peng, X. *J. Mol. Cat. A*. **2010**, *331*, 64.
- ¹¹⁷ Wang, X. H.; Tao, G. H.; Zhang, Z. Y.; Kou, Y. *Chinese Chem. Lett.* **2005**, *16(12)*, 1563–1565.
- ¹¹⁸ Liu S. et al. *Cat. Commun.* **2008**, *9*, 2030–2034.
- ¹¹⁹ He, L.; Tao, G. H.; Liu, W. S.; Xiong, W.; Wang, T.; Kou, Y. *Chinese Chem. Lett.* **2006**, *17(3)*, 321–324.
- ¹²⁰ DeCastro, C.; Sauvage, E.; Valkenberg, M. H.; Holderich, W. F. *J. Catal.*, **2000**, *196*, 86.
- ¹²¹ Piao, L. Y.; Fu, X.; Yang, Y. L.; Tao, G. H.; Kou, Y. *Catal. Today*, **2004**, *301*, 93–95.

Chapter 2

Physicochemical and Solvent Properties of Morpholinium Dicyanamide ILs and their Toxicity and Biodegradability Studies

Abstract

The role of the length of the alkyl chain on some physico-chemical properties was evaluated for a series of *N*-alkyl-*N*-methylmorpholinium dicyanamide-based ionic liquids (ILs); the alkyl chain ranging from 2 to 9 carbon atoms ($n = 2, 3, 4, 5, 6, 7, 8$ and 9). The temperature-dependent properties like viscosity, ionic conductivity and solvent properties have been determined. The results allow us to classify these ILs according to a classical Walden diagram. In addition, their ability to give clusters was determined by electron spray ionization-mass spectrometry (ESI-MS) measurements. The toxicity and biodegradability studies were reported for *N*-alkyl-*N*-morpholinium bromide (where alkyl=C2 to C9). These toxicity and biodegradability measurements were compared with other nitrogen bases like dabco and imidazolium. The IL having lowest alkyl chain i.e. [Mor_{1,2}][Br] showed the least toxicity and highest biodegradability.

2.1 Introduction

The most commonly studied ILs are based on imidazolium cations, combined with different anions such as hexafluorophosphate [PF₆]⁻, tetrafluoroborate [BF₄]⁻ or bistriflimide [Tf₂N]⁻. Very recently, morpholinium-based ILs have received attention because of their structural properties especially for the design of IL crystals.¹ Nevertheless, they have been considered also of interest as catalysts for organic synthesis,² heat stabilizers, or antioxidants for lubricating oils³ and for electrochemical applications.⁴ Toxicity tests recently performed⁵ on morpholinium bromides evidence a significant lower environmental impact with respect to other commonly used ILs. However, the association of the morpholinium cations to common anions, such as [BF₄]⁻, [Tf₂N]⁻, [PF₆]⁻ or Br⁻, gives ILs characterized by higher viscosities and lower conductivities than the analogous pyrrolidinium- or piperidinium-based ILs. Dicyanamide anion is known to give highly conductive ILs.⁶ Therefore, with the aim of increasing the understandings of the unusual characteristics of ILs and continuing part of our program aimed at developing new ILs having low melting, low viscosity and high chemical stability associated with a low toxicity, we conducted a systematic study on the synthesis and characterization of a series of *N*-alkyl-*N*-methylmorpholinium dicyanamide-based ILs. Their physical properties such as density, viscosity, conductivity and absorption spectra of selected solvatochromic dyes in the liquids were measured to estimate quantitatively the ion association, polarity and hydrogen-bonding interactions. Ion association was evaluated also by examining the electrospray mass

spectra of pure ILs dissolved in acetonitrile. The melting points and DSC measurements were compared with the corresponding anions BF_4 , Tf_2N , PF_6 . The toxicity and biodegradability studies were reported for *N*-alkyl-*N*-morpholinium bromide (where alkyl=C2 to C9). The IL having lowest alkyl chain i.e. $[\text{Mor}_{1,2}][\text{Br}]$ showed the least toxicity and highest biodegradability. These measurements of toxicity and biodegradability were compared with imidazolium and DABCO respectively.

2.2 Experimental Section

2.2.1 Synthesis

Solvents were distilled before use. Morpholinium-based bromides and chlorides were synthesized by Menshutkin reaction of *N*-methylmorpholine with respective alkyl bromides (whose alkyl chain length varies from 2 to 9). The general procedure is reported below. It was observed that the higher alkyl chain compounds i.e. $[\text{Mor}_{1,8}][\text{Br}]$ to $[\text{Mor}_{1,10}][\text{Br}]$ formed some bubbles when dissolved in water.

2.2.1.1 Synthesis of *N*-alkyl-*N*-methylmorpholinium bromides ($[\text{Mor}_{1,n}][\text{Br}]$): The respective bromoalkane ($n=1, 2, 3, 4, 5, 6, 7, 8, 9$ and 3-chloropropanediol) was added dropwise over 1 h to an equimolar solution of 4-methylmorpholine in acetonitrile (ca. 0.5 mmol in 200 ml) while stirring vigorously, and N_2 was bubbled through the solution. In the case of bromoethane, as the boiling point of bromoethane is very low, 2% excess was taken in the reflux. The mixture was refluxed for 8 h at 70°C . The molten salt was decanted, washed three times with 100 ml of CH_2Cl_2 , and dried for 1 h at 45°C under low pressure. If the product was found to have traces of brown or yellowish color, then it was washed with acetone and recrystallized in acetone. They were characterized using H-NMR and C-NMR.

$[\text{Mor}_{1,2}][\text{Br}]$: Crystalline white solid (yield 95%). $T_m=188\pm 2^\circ\text{C}$. ^1H NMR (250 MHz, D_2O) δ : 1.34 (tt, 3H, $J=7.3, 1.80$ Hz, 3H, $\text{CH}_3\text{CH}_2\text{N}^+\text{CH}_3$); 3.12 (s, 3H, $\text{CH}_3\text{N}^+\text{CH}_3$); 3.38–3.56 (m, 6H, $\text{CH}_3\text{CH}_2\text{N}^+(\text{CH}_2)_2$); 4.01 (m, $J=4.8$ Hz, 4H, $-\text{CH}_2\text{OCH}_2-$). ^{13}C NMR (63 MHz, D_2O) δ : 6.40 ($\text{CH}_3\text{CH}_2\text{N}^+\text{CH}_3$), 45.93 ($\text{CH}_3\text{N}^+\text{CH}_2\text{CH}_3$), 58.95 ($\text{CH}_2\text{N}^+\text{CH}_2$), 60.29 ($-\text{CH}_2\text{OCH}_2-$), 60.81 ($\text{CH}_3\text{CH}_2\text{N}^+$).

$[\text{Mor}_{1,3}][\text{Br}]$: Crystalline white solid (yield 94%). $T_m=178\pm 2^\circ\text{C}$. ^1H NMR (250 MHz, D_2O) δ : 0.95 (t, $J=7.3$ Hz, 3H, $\text{CH}_3\text{CH}_2\text{CH}_2\text{N}^+-\text{CH}_3$); 1.78 (m, 2H, $\text{CH}_3\text{CH}_2\text{CH}_2\text{N}^+\text{CH}_3$); 3.15 (s, 3H, $\text{CH}_3\text{N}^+\text{CH}_2\text{CH}_2\text{CH}_3$); 3.35–3.54 (m, 6H, $(\text{CH}_2)_2\text{N}^+\text{CH}_2$); 4.01 (t, $J=4.8$, 4H, $-\text{CH}_2\text{OCH}_2-$). ^{13}C

NMR (63 MHz, D₂O) δ : 9.66 (CH₃CH₂CH₂N⁺CH₃), 14.57 (CH₃CH₂CH₂N⁺CH₃), 46.74 (CH₃N⁺CH₂CH₂CH₃), 59.42 (CH₂N⁺CH₂), 60.28 (-CH₂OCH₂-), 66.41 (CH₃CH₂CH₂N⁺CH₃).

[Mor_{1,4}][Br]: Crystalline white solid (yield 90%). $T_m=215\pm 2$ °C. ¹H NMR (250 MHz, D₂O) δ : 0.93 (t, $J=7.3$ Hz, 3H, CH₃(CH₂)₂CH₂N⁺CH₃); 1.31–1.45 (m, 2H, CH₃CH₂CH₂CH₂N⁺CH₃); 1.69–1.81 (m, 2H, CH₃CH₂CH₂CH₂N⁺CH₃); 3.16 (s, 3H, CH₃N⁺(CH₂)₃CH₃); 3.40–3.55 (m, 6H, (CH₂)₂N⁺CH₂); 4.02 (t, $J=4.85$, 4H, -CH₂OCH₂-). ¹³C NMR (63 MHz, D₂O) δ : 12.77 (CH₃CH₂CH₂CH₂N⁺CH₃), 19.06 (CH₃CH₂CH₂CH₂N⁺CH₃), 22.89 (CH₃CH₂CH₂CH₂N⁺CH₃), 46.82 (CH₃N⁺CH₂CH₂CH₂CH₃), 59.53 (CH₂N⁺CH₂), 60.41 (-CH₂OCH₂-), 65.04 (CH₃CH₂CH₂CH₂N⁺CH₃).

[Mor_{1,5}][Br]: Crystalline white solid (yield 90%). $T_m=150\pm 2$ °C. ¹H NMR (250 MHz, D₂O) δ : 0.87 (t, $J=6.5$ Hz, 3H, CH₃(CH₂)₃CH₂-N⁺-CH₃); 1.30–1.36 (m, 4H, CH₃(CH₂)₂CH₂CH₂N⁺CH₃); 1.77 (m, 2H, CH₃CH₂CH₂CH₂CH₂N⁺CH₃); 3.15 (s, 3H, CH₃N⁺CH₂(CH₂)₃CH₃); 3.38–3.55 (m, 6H, (CH₂)₂N⁺CH₂); 4.01 (t, $J=5.4$, 4H, -CH₂OCH₂-). ¹³C NMR (63 MHz, D₂O) δ : 13.01 (CH₃(CH₂)₃CH₂N⁺CH₃), 20.52 (CH₃CH₂CH₂CH₂CH₂N⁺CH₃), 21.44 (CH₃CH₂CH₂CH₂CH₂N⁺CH₃), 27.67 (CH₃CH₂CH₂CH₂CH₂N⁺CH₃), 46.90 (CH₃N⁺CH₂(CH₂)₃CH₃), 60.29 (CH₂N⁺CH₂), 63.76 (-CH₂OCH₂-), 65.41 (CH₃(CH₂)₃CH₂N⁺CH₃).

[Mor_{1,6}][Br]: Crystalline white solid (yield 93%). $T_m=155\pm 2$ °C. ¹H NMR (250 MHz, D₂O) δ : 0.86 (t, $J=6.8$ Hz, 3H, CH₃(CH₂)₄CH₂N⁺CH₃); 1.33 (m, 6H, CH₃(CH₂)₃CH₂CH₂N⁺CH₃); 1.78 (m, 2H, CH₃(CH₂)₃CH₂CH₂N⁺CH₃); 3.16 (s, 3H, CH₃N⁺-CH₂(CH₂)₄CH₃); 3.48 (m, 6H, (CH₂)₂N⁺CH₂); 4.02 (t, $J=4.9$, 4H, -CH₂OCH₂-). ¹³C NMR (63 MHz, D₂O) δ : 13.01 (CH₃(CH₂)₄CH₂N⁺CH₃), 21.07 (CH₃CH₂(CH₂)₃CH₂N⁺CH₃), 21.80 (CH₃CH₂CH₂(CH₂)₂CH₂N⁺CH₃), 25.10 (CH₃CH₂CH₂CH₂CH₂N⁺CH₃), 30.41 (CH₃(CH₂)₃CH₂CH₂N⁺CH₃), 46.69 (CH₃N⁺CH₂(CH₂)₄CH₃), 59.55 (CH₂N⁺CH₂), 60.65 (-CH₂OCH₂-), 64.92 (CH₃CH₂CH₂CH₂CH₂CH₂N⁺CH₃).

[Mor_{1,7}][Br]: Crystalline white solid (yield 97%) $T_m=102\pm 2$ °C. ¹H NMR (250 MHz, D₂O) δ : 0.84 (t, $J=6.2$ Hz, 3H, CH₃(CH₂)₅CH₂N⁺CH₃); 1.28 (m, 8H, CH₃(CH₂)₄CH₂CH₂N⁺CH₃); 1.77 (m, 2H, CH₃(CH₂)₅CH₂CH₂N⁺CH₃); 3.15 (s, 3H, CH₃-N⁺CH₂(CH₂)₅CH₃); 3.49 (m, 6H, (CH₂)₂N⁺CH₂); 4.02 (t, $J=4.9$, 4H, -CH₂OCH₂-). ¹³C NMR (63 MHz, D₂O) δ : 13.19 (CH₃(CH₂)₅CH₂N⁺CH₃), 20.70 (CH₃CH₂(CH₂)₄CH₂N⁺CH₃), 21.80 (CH₃CH₂CH₂(CH₂)₄N⁺CH₃), 25.65 (CH₃CH₂CH₂CH₂(CH₂)₃-N⁺CH₃), 27.85 (CH₃(CH₂)₃CH₂CH₂-N⁺CH₃).

$\text{CH}_2\text{N}^+\text{CH}_3$), 30.78 ($\text{CH}_3(\text{CH}_2)_4\text{CH}_2\text{CH}_2\text{N}^+\text{CH}_3$), 46.72 ($\text{CH}_3\text{N}^+\text{CH}_2(\text{CH}_2)_5\text{CH}_3$), 59.55 ($\text{CH}_2\text{N}^+\text{CH}_2$), 60.46 ($-\text{CH}_2\text{OCH}_2-$), 65.23 ($\text{CH}_3(\text{CH}_2)_5\text{CH}_2\text{N}^+\text{CH}_3$).

[Mor_{1,8}][Br]: Crystalline white solid (yield 90%). $T_m = 152 \pm 2^\circ\text{C}$. ^1H NMR (250 MHz, D_2O) δ : 0.83 (t, $J=6.4$ Hz, 3H, $\text{CH}_3(\text{CH}_2)_6\text{CH}_2\text{N}^+\text{CH}_3$); 1.24–1.34 (m, 10H, $\text{CH}_3(\text{CH}_2)_5\text{CH}_2\text{CH}_2\text{N}^+\text{CH}_3$); 1.76 (m, 2H, $\text{CH}_3(\text{CH}_2)_5\text{CH}_2\text{CH}_2\text{N}^+\text{CH}_3$); 3.14 (s, 3H, $\text{CH}_3\text{N}^+\text{CH}_2\text{CH}_2(\text{CH}_2)_5\text{CH}_3$); 3.46 (m, 6H, $(\text{CH}_2)_2\text{N}^+\text{CH}_2$); 4.01 (t, $J=4.50$, 4H, $-\text{CH}_2\text{OCH}_2$). ^{13}C NMR (63 MHz, D_2O) δ : 13.31 ($\text{CH}_3(\text{CH}_2)_6\text{CH}_2\text{N}^+\text{CH}_3$), 20.75 ($\text{CH}_3\text{CH}_2(\text{CH}_2)_5\text{CH}_2\text{N}^+\text{CH}_3$), 21.90 ($\text{CH}_3\text{CH}_2\text{CH}_2(\text{CH}_2)_5\text{N}^+\text{CH}_3$), 25.41 ($\text{CH}_3\text{CH}_2\text{CH}_2\text{CH}_2(\text{CH}_2)_4\text{N}^+\text{CH}_3$), 28.07 ($\text{CH}_3(\text{CH}_2)_3\text{CH}_2\text{CH}_2(\text{CH}_2)_2\text{N}^+\text{CH}_3$), 30.91 ($\text{CH}_3(\text{CH}_2)_5\text{CH}_2\text{CH}_2\text{N}^+\text{CH}_3$), 46.70 ($\text{CH}_3\text{N}^+\text{CH}_2(\text{CH}_2)_6\text{CH}_3$), 59.41 ($\text{CH}_2\text{N}^+\text{CH}_2$), 60.31 ($-\text{CH}_2\text{OCH}_2-$), 65.27 ($\text{CH}_3(\text{CH}_2)_6\text{CH}_2\text{N}^+\text{CH}_3$).

[Mor_{1,9}][Br]: Crystalline white solid (yield 95%). $T_m = 122 \pm 2$. ^1H NMR (250 MHz, D_2O) δ : 0.83 (t, $J=6.6$ Hz, 3H, $\text{CH}_3(\text{CH}_2)_7\text{CH}_2\text{N}^+\text{CH}_3$); 1.33 (m, 12H, $\text{CH}_3(\text{CH}_2)_6\text{CH}_2\text{CH}_2\text{N}^+\text{CH}_3$); 1.76 (m, 2H, $\text{CH}_3(\text{CH}_2)_6\text{CH}_2\text{CH}_2\text{N}^+\text{CH}_3$); 3.15 (s, 3H, $\text{CH}_3\text{N}^+\text{CH}_2(\text{CH}_2)_7\text{CH}_3$); 3.45 (m, 6H, $(\text{CH}_2)_2\text{N}^+\text{CH}_2$); 4.02 (t, $J=4.8$, 4H, $-\text{CH}_2\text{OCH}_2-$). ^{13}C NMR (63 MHz, D_2O) δ : 13.31 ($\text{CH}_3(\text{CH}_2)_7\text{CH}_2\text{N}^+\text{CH}_3$), 20.74 ($\text{CH}_3\text{CH}_2(\text{CH}_2)_6\text{CH}_2\text{N}^+\text{CH}_3$), 21.93 ($\text{CH}_3\text{CH}_2\text{CH}_2(\text{CH}_2)_5\text{CH}_2\text{N}^+\text{CH}_3$), 25.32 ($\text{CH}_3\text{CH}_2\text{CH}_2\text{CH}_2(\text{CH}_2)_4\text{CH}_2\text{N}^+\text{CH}_3$), 28.21 ($\text{CH}_3\text{CH}_2\text{CH}_2\text{CH}_2(\text{CH}_2)_3\text{CH}_2\text{CH}_2\text{N}^+\text{CH}_3$), 31.07 ($\text{CH}_3(\text{CH}_2)_6\text{CH}_2\text{CH}_2\text{N}^+\text{CH}_3$), 46.75 ($\text{CH}_3\text{N}^+\text{CH}_2(\text{CH}_2)_7\text{CH}_3$), 59.40 ($\text{CH}_2\text{N}^+\text{CH}_2$), 60.30 ($-\text{CH}_2\text{OCH}_2-$), 65.15 ($\text{CH}_3(\text{CH}_2)_7\text{CH}_2\text{N}^+\text{CH}_3$).

2.2.1.2 Synthesis of *N*-alkyl-*N*-methyl morpholinium dicyanamides ([Mor_{1,n}][N(CN)₂])

To a colorless solution of [Mor_{1,n}][Br] (70–100 mmol) in water (100 ml) an equimolar amount of silver dicyanamide (white solid, freshly prepared from AgNO_3 and $\text{NaN}(\text{CN})_2$ in water) was added. The mixture was stirred for 3 h at 40°C . After cooling at room temperature the precipitate was filtered off, washed with water (2×10 ml) and the resulting colorless aqueous solution (approximately 200 ml) was heated to 70°C under vacuum for 1 h to remove the water. The colorless liquid was dissolved in anhydrous acetone and the solution was cooled at -20°C for 48 h. After filtration on glass septa (porosity 4) containing two different powdered layers of 1 cm each of celite (lower layer) and decolorizing carbon (upper layer), the solvent was removed under vacuum (2×10^{-3} mm Hg, 80°C , 6 h) to give the pure IL. All the ILs were colorless.

[Mor_{1,2}][N(CN)₂]: Yield 80%. ^1H NMR (250 MHz, D_2O) δ : 1.46 (tt, $J=7.40$, 2.16 Hz, 3H, $\text{CH}_3\text{CH}_2\text{N}^+\text{CH}_3$); 3.23 (s, 3H, $\text{CH}_3\text{N}^+\text{CH}_2\text{CH}_3$); 3.47–3.66 (m, 6H, $\text{CH}_3\text{CH}_2\text{N}^+(\text{CH}_2)_2$); 4.12 (t, $J=5.2$ Hz, 4H, $-\text{CH}_2\text{OCH}_2-$). ^{13}C NMR (63 MHz, D_2O) δ : 6.59 ($\text{CH}_3\text{CH}_2\text{N}^+\text{CH}_3$), 46.02

($\text{CH}_3\text{N}^+\text{CH}_2\text{CH}_3$), 59.12 ($\text{CH}_2\text{N}^+\text{CH}_2$), 60.43 ($-\text{CH}_2\text{OCH}_2-$), 60.89 ($\text{CH}_3\text{CH}_2\text{N}^+$), 119.91 ($\text{N}(\text{CN})_2$).

[Mor_{1,3}][N(CN)₂]: Yield 80%. ¹H NMR (250 MHz, D₂O) δ : 1.04 (t, $J=7.35$ Hz, 3H, $\text{CH}_3\text{CH}_2\text{CH}_2\text{N}^+\text{CH}_3$); 1.86 (m, 2H, $\text{CH}_3\text{CH}_2\text{CH}_2\text{N}^+\text{CH}_3$); 3.2 (s, 3H, $\text{CH}_3\text{N}^+\text{CH}_2\text{CH}_2\text{CH}_3$); 3.41–3.61 (m, 6H, $(\text{CH}_2)_2\text{N}^+\text{CH}_2$); 4.08 (t, $J=5.2$, 4H, $-\text{CH}_2\text{OCH}_2-$). ¹³C NMR (63 MHz, D₂O) δ : 9.89 ($\text{CH}_3\text{CH}_2\text{CH}_2\text{N}^+\text{CH}_3$), 14.84 ($\text{CH}_3\text{CH}_2\text{CH}_2\text{N}^+\text{CH}_3$), 46.90 ($\text{CH}_3\text{N}^+\text{CH}_2\text{CH}_2\text{CH}_3$), 59.55 ($\text{CH}_2\text{N}^+\text{CH}_2$), 60.65 ($-\text{CH}_2\text{OCH}_2-$), 66.51 ($\text{CH}_3\text{CH}_2\text{CH}_2\text{N}^+$), 120.01 ($\text{N}(\text{CN})_2$).

[Mor_{1,4}][N(CN)₂]: Yield 75%. ¹H NMR (250 MHz, D₂O) δ : (t, $J=7.30$ Hz, 3H, $\text{CH}_3(\text{CH}_2)_3\text{N}^+\text{CH}_3$); 1.34–1.48 (m, 2H, $\text{CH}_3\text{CH}_2\text{CH}_2\text{CH}_2\text{N}^+\text{CH}_3$); 1.72–1.84 (m, 2H, $\text{CH}_3\text{CH}_2\text{CH}_2\text{CH}_2\text{N}^+\text{CH}_3$); 3.18 (s, 3H, $\text{CH}_3\text{N}^+\text{CH}_2\text{CH}_2\text{CH}_2\text{CH}_3$); 3.42–3.52 (m, 6H, $(\text{CH}_2)_2\text{N}^+\text{CH}_2$); 4.04 (t, $J=5.10$, 4H, $-\text{CH}_2\text{OCH}_2-$). ¹³C NMR (63 MHz, D₂O) δ : 13.01 ($\text{CH}_3(\text{CH}_2)_3\text{N}^+\text{CH}_3$), 19.42 ($\text{CH}_3\text{CH}_2\text{CH}_2\text{CH}_2\text{N}^+\text{CH}_3$), 23.09 ($\text{CH}_3\text{CH}_2\text{CH}_2\text{CH}_2\text{N}^+\text{CH}_3$), 46.90 ($\text{CH}_3\text{N}^+(\text{CH}_2)_3\text{CH}_3$), 59.55 ($\text{CH}_2\text{N}^+\text{CH}_2$), 60.65 ($-\text{CH}_2\text{OCH}_2-$), 65.04 ($\text{CH}_3\text{CH}_2\text{CH}_2\text{CH}_2\text{N}^+$), 120.19 ($\text{N}(\text{CN})_2$).

[Mor_{1,5}][N(CN)₂]: Yield 85%. ¹H NMR (250 MHz, D₂O) δ : 0.99 (t, $J=6.8$ Hz, 3H, $\text{CH}_3(\text{CH}_2)_4\text{N}^+\text{CH}_3$); 1.42–1.48 (m, 4H, $\text{CH}_3\text{CH}_2\text{CH}_2\text{CH}_2\text{CH}_2\text{N}^+\text{CH}_3$); 1.81 (m, 2H, $\text{CH}_3\text{CH}_2\text{CH}_2\text{CH}_2\text{CH}_2\text{N}^+\text{CH}_3$); 3.25 (s, 3H, $\text{CH}_3\text{N}^+(\text{CH}_2)_4\text{CH}_3$); 3.48–3.63 (m, 6H, $(\text{CH}_2)_2\text{N}^+\text{CH}_2$); 4.10 (t, $J=4.85$ Hz, 4H, $-\text{CH}_2\text{OCH}_2-$). ¹³C NMR (63 MHz, D₂O) δ : 13.24 ($\text{CH}_3(\text{CH}_2)_4\text{N}^+\text{CH}_3$), 20.69 ($\text{CH}_3\text{CH}_2\text{CH}_2\text{CH}_2\text{CH}_2\text{N}^+\text{CH}_3$), 21.68 ($\text{CH}_3\text{CH}_2\text{CH}_2\text{CH}_2\text{CH}_2\text{N}^+\text{CH}_3$), 27.74 ($\text{CH}_3(\text{CH}_2)_2\text{CH}_2\text{CH}_2\text{N}^+\text{CH}_3$), 46.80 ($\text{CH}_3\text{N}^+(\text{CH}_2)_4\text{CH}_3$), 59.56 ($\text{CH}_2\text{N}^+\text{CH}_2$), 60.43 ($-\text{CH}_2\text{OCH}_2-$), 65.30 ($\text{CH}_3(\text{CH}_2)_3\text{CH}_2\text{N}^+$), 119.81 ($\text{N}(\text{CN})_2$).

[Mor_{1,6}][N(CN)₂]: Yield 78%. ¹H NMR (250 MHz, D₂O) δ : 0.87 (t, $J=7.0$ Hz, 3H, $\text{CH}_3(\text{CH}_2)_5\text{N}^+\text{CH}_3$); 1.34 (m, 6H, $\text{CH}_3(\text{CH}_2)_3\text{CH}_2\text{CH}_2\text{N}^+\text{CH}_3$); 1.79 (m, 2H, $\text{CH}_3(\text{CH}_2)_3\text{CH}_2\text{CH}_2\text{N}^+\text{CH}_3$); 3.16 (s, 3H, $\text{CH}_3\text{N}^+(\text{CH}_2)_5\text{CH}_3$); 3.40–3.56 (m, 6H, $(\text{CH}_2)_2\text{N}^+\text{CH}_2$); 4.03 (t, $J=4.8$, 4H, $-\text{CH}_2\text{OCH}_2-$). ¹³C NMR (63 MHz, D₂O) δ : 13.13 ($\text{CH}_3(\text{CH}_2)_5\text{N}^+\text{CH}_3$), 20.75 ($\text{CH}_3\text{CH}_2(\text{CH}_2)_4\text{N}^+\text{CH}_3$), 21.65 ($\text{CH}_3\text{CH}_2\text{CH}_2(\text{CH}_2)_3\text{N}^+\text{CH}_3$), 25.07 ($\text{CH}_3(\text{CH}_2)_2\text{CH}_2(\text{CH}_2)_2\text{N}^+\text{CH}_3$), 30.37 ($\text{CH}_3(\text{CH}_2)_2\text{CH}_2(\text{CH}_2)_2\text{N}^+\text{CH}_3$), 46.68 ($\text{CH}_3\text{N}^+(\text{CH}_2)_5\text{CH}_3$), 59.42 ($\text{CH}_2\text{N}^+\text{CH}_2$), 60.32 ($-\text{CH}_2\text{OCH}_2-$), 65.19 ($\text{CH}_3(\text{CH}_2)_4\text{CH}_2\text{N}^+\text{CH}_3$), 120.56 ($\text{N}(\text{CN})_2$).

[Mor_{1,7}][N(CN)₂]: Yield 85%. ¹H NMR (250 MHz, D₂O) δ : 0.97 (t, $J=6.0$ Hz, 3H, $\text{CH}_3(\text{CH}_2)_6\text{N}^+\text{CH}_3$); 1.40 (m, 8H, $\text{CH}_3(\text{CH}_2)_4\text{CH}_2\text{CH}_2\text{N}^+\text{CH}_3$); 1.87 (m, 2H, $\text{CH}_3(\text{CH}_2)_4\text{CH}_2\text{CH}_2\text{N}^+\text{CH}_3$); 3.24 (s, 3H, $\text{CH}_3\text{N}^+(\text{CH}_2)_6\text{CH}_3$); 3.48–3.63 (m, 6H, $(\text{CH}_2)_2\text{N}^+\text{CH}_2$); 4.10 (t, $J=4.8$ Hz, 4H, $-\text{CH}_2\text{OCH}_2-$). ¹³C NMR (63 MHz, D₂O) δ : 13.74 ($\text{CH}_3(\text{CH}_2)_6\text{N}^+\text{CH}_3$),

Chapter 2

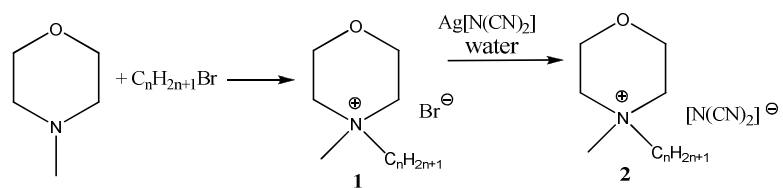
21.07 ($\text{CH}_3\text{CH}_2(\text{CH}_2)_5\text{N}^+\text{CH}_3$), 22.17 ($\text{CH}_3\text{CH}_2\text{CH}_2(\text{CH}_2)_4\text{N}^+\text{CH}_3$), 25.83 ($\text{CH}_3(\text{CH}_2)_2\text{CH}_2(\text{CH}_2)_3\text{N}^+\text{CH}_3$), 28.22 ($\text{CH}_3(\text{CH}_2)_3\text{CH}_2(\text{CH}_2)_2\text{N}^+\text{CH}_3$), 31.15 ($\text{CH}_3(\text{CH}_2)_4\text{CH}_2\text{CH}_2\text{N}^+\text{CH}_3$), 46.90 ($\text{CH}_3\text{N}^+(\text{CH}_2)_6\text{CH}_3$), 59.55 ($\text{CH}_2\text{N}^+\text{CH}_2$), 60.83 ($-\text{CH}_2\text{OCH}_2$), 65.59 ($\text{CH}_3(\text{CH}_2)_5\text{CH}_2\text{N}^+$), 120.01 ($\text{N}(\text{CN})_2$).

[Mor_{1,8}][N(CN)₂]: Yield 85%. ¹H NMR (250 MHz, D₂O) δ : 0.95 (t, $J=6.5$ Hz, 3H, $\text{CH}_3(\text{CH}_2)_7\text{N}^+\text{CH}_3$); 1.36 (m, 10H, $\text{CH}_3(\text{CH}_2)_5\text{CH}_2\text{CH}_2\text{N}^+\text{CH}_3$); 1.83 (m, 2H, $\text{CH}_3(\text{CH}_2)_5\text{CH}_2\text{CH}_2\text{N}^+\text{CH}_3$); 3.22 (s, 3H, $\text{CH}_3\text{N}^+(\text{CH}_2)_7\text{CH}_3$); 3.44–3.54 (m, 6H, $(\text{CH}_2)_2\text{N}^+\text{CH}_2$); 4.07 (t, $J=4.8$, 4H, $-\text{CH}_2\text{OCH}_2-$). ¹³C NMR (63 MHz, D₂O) δ : 13.79 ($\text{CH}_3(\text{CH}_2)_7\text{N}^+\text{CH}_3$), 21.15 ($\text{CH}_3\text{CH}_2(\text{CH}_2)_6\text{N}^+\text{CH}_3$), 22.39 ($\text{CH}_3\text{CH}_2\text{CH}_2(\text{CH}_2)_5\text{N}^+\text{CH}_3$), 25.84 ($\text{CH}_3(\text{CH}_2)_2\text{CH}_2(\text{CH}_2)_4\text{N}^+\text{CH}_3$), 28.63 ($\text{CH}_3(\text{CH}_2)_3\text{CH}_2(\text{CH}_2)_3\text{N}^+\text{CH}_3$), 28.68 ($\text{CH}_3(\text{CH}_2)_4\text{CH}_2(\text{CH}_2)_2\text{N}^+\text{CH}_3$), 31.42 ($\text{CH}_3(\text{CH}_2)_5\text{CH}_2\text{CH}_2\text{N}^+$), 46.80 ($\text{CH}_3\text{N}^+(\text{CH}_2)_7\text{CH}_3$), 59.57 ($\text{CH}_2\text{N}^+\text{CH}_2$), 60.39 ($-\text{CH}_2\text{OCH}_2-$), 65.25 ($\text{CH}_3(\text{CH}_2)_6\text{CH}_2\text{N}^+$), 119.74 ($\text{N}(\text{CN})_2$).

[Mor_{1,9}][N(CN)₂]. Yield 75%. ¹H NMR (250 MHz, D₂O) δ : 0.96 (t, $J=6.5$ Hz, 3H, $\text{CH}_3(\text{CH}_2)_8\text{N}^+\text{CH}_3$); 1.38–1.46 (m, 12H, $\text{CH}_3(\text{CH}_2)_6\text{CH}_2\text{CH}_2\text{N}^+\text{CH}_3$); 1.86 (m, 2H, $\text{CH}_3(\text{CH}_2)_6\text{CH}_2\text{CH}_2\text{N}^+\text{CH}_3$); 3.25 (s, 3H, $\text{CH}_3\text{N}^+(\text{CH}_2)_8\text{CH}_3$); 3.52–3.56 (m, 6H, $(\text{CH}_2)_2\text{N}^+\text{CH}_2$); 4.09 (t, $J=6.6$, 4H, $-\text{CH}_2\text{OCH}_2-$). ¹³C NMR (63 MHz, D₂O) δ : 13.89 ($\text{CH}_3(\text{CH}_2)_8\text{N}^+\text{CH}_3$), 21.30 ($\text{CH}_3\text{CH}_2(\text{CH}_2)_7\text{N}^+\text{CH}_3$), 22.60 ($\text{CH}_3\text{CH}_2\text{CH}_2(\text{CH}_2)_6\text{N}^+\text{CH}_3$), 26.02 ($\text{CH}_3(\text{CH}_2)_2\text{CH}_2(\text{CH}_2)_5\text{N}^+\text{CH}_3$), 28.92 ($\text{CH}_3(\text{CH}_2)_3\text{CH}_2(\text{CH}_2)_4\text{N}^+\text{CH}_3$), 29.10 ($\text{CH}_3(\text{CH}_2)_4\text{CH}_2(\text{CH}_2)_3\text{N}^+\text{CH}_3$), 29.26 ($\text{CH}_3(\text{CH}_2)_5\text{CH}_2(\text{CH}_2)_2\text{N}^+\text{CH}_3$), 31.78 ($\text{CH}_3(\text{CH}_2)_6\text{CH}_2\text{CH}_2\text{N}^+\text{CH}_3$), 46.81 ($\text{CH}_3\text{N}^+(\text{CH}_2)_8\text{CH}_3$), 59.60 ($\text{CH}_2\text{N}^+\text{CH}_2$), 60.40 ($-\text{CH}_2\text{OCH}_2-$), 65.26 ($\text{CH}_3(\text{CH}_2)_7\text{CH}_2\text{N}^+$), 119.77 ($\text{N}(\text{CN})_2$).

2.3 Results and Discussions

The synthetic route to prepare morpholinium-based salts herein is shown in Scheme 2.1. In the first step, the corresponding alkyl bromide and *N*-methylmorpholine were reacted in acetonitrile at temperatures ranging from 60 to 70°C to produce *N*-alkyl-*N*-methylmorpholinium bromides, [Mor_{1,n}]⁺Br⁻, **1**. Generally, an excess of the alkyl halide was used to prevent problems arising from evaporation (in particular, in the case of short chain halides) due to the reaction temperature. Subsequent metathesis of **1** with silver dicyanamide ($\text{Ag}[\text{N}(\text{CN})_2]$) in water ($\text{Ag}[\text{N}(\text{CN})_2]$ was freshly prepared by reacting AgNO_3 and $\text{Na}[\text{N}(\text{CN})_2]$ in equimolar quantities) resulted in the corresponding dicyanamide salts **2**, i.e. [Mor_{1,n}][N(CN)₂].



Scheme 2.1: Synthetic route to prepare *N*-alkyl-*N*-methylmorpholinium dicyanamide ILs

All the above salts were characterized using electrospray ionization–mass spectroscopy (ESI–MS), 1H and ^{13}C NMR spectroscopy. All synthesized *N*-alkyl-*N*-methylmorpholinium bromides are colorless solid at room temperatures whereas the corresponding dicyanamides are colorless liquids.

2.3.1 Physico-chemical Properties: Physico-chemical properties characterizing ILs **2** are shown in Table 2.1.

Table 2.1: Physical Properties of Dicyanamide ILs^a

| Salt | d $g\ cm^{-3}$ | PM | C mol | κ $S\ cm^{-1}$ | Λ S | η cP |
|------------------------------------|---------------------|-----|------------|--------------------------|------------------|--------------|
| [C2] | 1.17 | 196 | 0.0060 | 4.42×10^{-3} | 0.736 | 96 |
| [C3] | 1.16 | 210 | 0.0055 | 1.94×10^{-3} | 0.353 | 588.5 |
| [C4] | 1.12 | 224 | 0.0050 | 1.41×10^{-3} | 0.282 | 598 |
| [C5] | 1.12 | 238 | 0.0047 | 0.84×10^{-3} | 0.179 | 758.5 |
| [C6] | 1.07 | 252 | 0.0042 | 0.72×10^{-3} | 0.171 | 759.5 |
| [C7] | 1.06 | 266 | 0.0040 | 0.26×10^{-3} | 0.065 | 874 |
| [C8] | 1.03 | 280 | 0.0037 | 0.11×10^{-3} | 0.030 | 986 |
| [C9] | 1.03 | 294 | 0.0035 | 0.09×10^{-3} | 0.026 | 1076 |
| [emim] ^b | | | | 2.8×10^{-2} | | 16 |
| [Pyr _{1,2}] ^b | | | | 2.0×10^{-2} | | 27 |
| [Mor _{1,4}] ^c | | | | 0.4×10^{-3} | | 532 |

^aC, molar concentration at 25 °C for dicyanamide salts and at 35°C;

κ , ionic conductivity at 25 °C Λ , molar conductivity at 25°C, η , viscosity

at 20°C. ^bIt is [Pyr_{1,2}][N(CN)₂]. Ionic conductivity and viscosity at 25°C,

from referenc 6. ^cIt is [Mor_{1,2}][Tf₂N]. Ionic conductivity and viscosity at 25°C,

from reference 7.

2.3.2 Density

The density (d) of ILs falls typically in the range 1.1–1.7 g cm⁻³. It is affected by anion although the nature of the substituents on cation also plays an important role: normally, density decreases as the alkyl chain on cation elongates. This behavior has been observed also in the case of *N*-alkyl-*N*-methylmorpholinium dicyanamides; d decreases from 1.17 to 1.03 g cm⁻³ on going from C2 to C9.

2.3.3 Viscosity

The variation of alkyl chain length exerts a drastic effect also on viscosity (η). Viscosity of ILs typically ranges from 30 to 1000 cP at room temperature: it is determined by the identity of the cation and anion (size and shape) that compose the IL. The mobility of an IL is generally ruled by the slow ion-exchange mechanism, which is dependent on the interaction strength. The possibility of anions and cations to give more or less strong Coulombic interactions and the presence of van der Waals interactions in contraposition with the contribution of the conformational degrees of freedom (together with the capacity of anion and/or cation to form hydrogen bonds) are some of the factors that determine IL's viscosity. In the case of cyclic quaternary ammonium ILs, having common fluorinated anions and comparable alkyl chains, viscosity increases in the following order *N*-alkyl-*N*-methylpyrrolidinium < *N*-alkyl-*N*-methyloxazolidinium < *N*-alkyl-*N*-methylpiperidinium < *N*-alkyl-*N*-methylmorpholinium.⁸ As shown in the Table 2.1, *N*-alkyl-*N*-methylmorpholinium dicyanamide ILs are characterized by relatively low viscosity values, comparable to the analogous bistriflimide salts, and maintain the order pyrrolidinium < morpholinium observed for fluorinated anions. The reason can be that the anion Tf₂N is bigger than the N(CN)₂ anion. Nevertheless, viscosity increases when the alkyl chain in the cation elongates, probably as a consequence of the increased van der Waals interactions not completely counterbalanced by the increased mobility freedom degrees.

With the exception of [Mor_{1,2}][N(CN)₂] that exhibits a clear Newtonian behavior, all the other salts (at least at 25°C) could be defined either Newtonian or non-Newtonian (pseudoplastic) depending on the used regression. The rheological behavior shows only little better correlation coefficients (1 vs 0.9998) when the power law regression is used with respect to the linear regression. The pseudoplastic behavior in the interval of analysis, characterized by a decrease of viscosity with increasing rate of shear, became however more evident at high shear stresses. Moreover, as frequently happens with shear-thinning systems, in every case the down curve is slightly displaced with respect to the upper curve, showing that all the investigated ILs have a lower consistency at any one of the rate of shear on the down curve of the rheogram, in agreement with the presence of thixotropy. A thixotropic behavior might indicate a breakdown of structure that does not reform immediately when the stress is reduced (Figure 2.1).

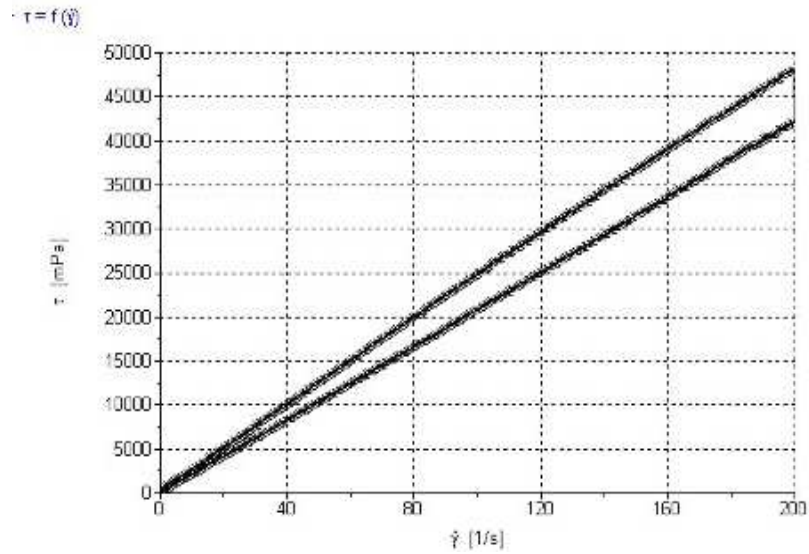


Figure 2.1: Viscosity behavior of $[\text{Mor}_{1,3}][\text{N}(\text{CN})_2]$

Furthermore, it is noteworthy that an odd/even alkyl chain length effect can be also evidenced, at least at the lower temperatures; the salts having odd alkyl chain lengths exhibit viscosity values significantly higher than those of adjacent salts having even alkyl chain lengths. This effect decreases on going from C3 to C7. On the other hand, for all investigated salts dynamic viscosity decreases significantly with temperature. At low temperatures until a gentle descent is achieved at the higher values: in particular salts having $n \geq 3$ present a distinct curvature at lower temperatures in the Arrhenius plots. Therefore, viscosity data have been fitted to the Vogel-Tamman-Fulcher (VTF) equation:

$$\eta = \eta_0 \exp[B/(T-T_0)] \quad (1)$$

where η_0 (cP), B (K) and T_0 (K) are fitting parameters. The best-fit parameters and the associated squared correlation coefficients R^2 are given in Table 2.2.

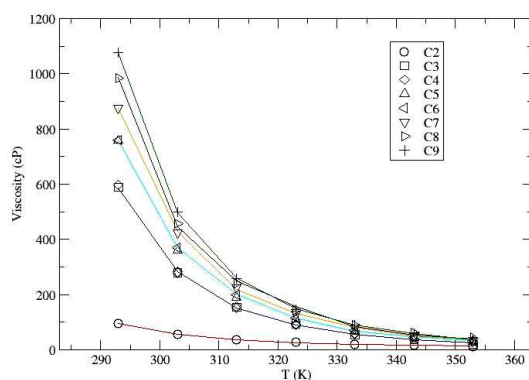


Figure 2.2: Behavior of viscosity of $[\text{Mor}_{1,n}][\text{N}(\text{CN})_2]$ with temperature

Table 2.2: VTF equation parameters for viscosity (η_0 , B and T_0) (equation 1)

| Salt | η_0 (cP) | B (K) ^a | T_0 (K) | R^{2b} |
|----------------------|---------------|--------------------|-----------|----------|
| $[\text{Mor}_{1,2}]$ | 1.49 (0.5) | 275.2 (60) | 227 (9) | 0.9996 |
| $[\text{Mor}_{1,3}]$ | 0.076 | 1006 (250) | 180 (15) | 0.9997 |
| $[\text{Mor}_{1,4}]$ | 0.282 (0.08) | 705 (120) | 201 (8) | 0.9998 |
| $[\text{Mor}_{1,5}]$ | 0.085 (0.01) | 1018 (32) | 181 (2) | 1 |
| $[\text{Mor}_{1,6}]$ | 0.038 (0.02) | 1259 (190) | 165 (10) | 0.9999 |
| $[\text{Mor}_{1,7}]$ | 0.028 (0.02) | 1378 (267) | 160 (14) | 0.9998 |
| $[\text{Mor}_{1,8}]$ | 0.34 (0.3) | 745 (264) | 199 (18) | 0.9992 |
| $[\text{Mor}_{1,9}]$ | 0.076 | 1089 (52) | 179 (3) | 0.9999 |

^aBR=activation energy (kJ mol^{-1}). ^b Squared correlation coefficient.

2.3.4 Conductivity

Present conductivity values are comparable to most values reported earlier for ILs, in particular for ILs based on cyclic onium cations. As expected, conductivities increase with temperature, up to 12.0 mS cm^{-1} at 85°C in the case of $[\text{Mor}_{1,2}][\text{N}(\text{CN})_2]$. Moreover, conductivities for $[\text{Mor}_{1,n}][\text{N}(\text{CN})_2]$ salts having $n \geq 3$ exhibit non-Arrhenius behavior, in agreement with the viscosity results.

Therefore, the Vogel-Tamman-Fulcher (VTF) equation 2 was used to represent temperature dependence of the conductivity:

$$\sigma = \sigma_0 \exp[-B / (T-T_0)] \quad (2)$$

The best-fit parameters and the associated squared correlation coefficients R^2 are given in Table 2.3.

Table 2.3: VTF equation parameters for conductivity (σ_0 , B and T_0) (equation 2)

| Salt | σ_0 (S cm ⁻¹) | B (K) ^a | T_0 (K) | R^{2b} |
|-----------------------|----------------------------------|--------------------|-----------|----------|
| [Mor _{1,3}] | 0.076 (0.003) | 351 (10) | 210 (8) | 0.9998 |
| [Mor _{1,4}] | 0.079 (0.015) | 353 (44) | 212 (8) | 0.9997 |
| [Mor _{1,5}] | 0.048 (0.009) | 313 (40) | 224 (7) | 0.9996 |
| [Mor _{1,6}] | 0.038 (0.004) | 254 (25) | 233 (5) | 0.9997 |
| [Mor _{1,7}] | 0.016 (0.002) | 310 (24) | 223 (4) | 0.9998 |
| [Mor _{1,8}] | 0.014 (0.004) | 291 (64) | 228 (11) | 0.9988 |
| [Mor _{1,9}] | 0.011 (0.008) | 267 (134) | 235 (23) | 0.9938 |

^aBR = activation energy (kJ mol⁻¹). ^b Squared correlation coefficient.

Since the behavior of all investigated ILs (except for [Mor_{1,2}][N(CN)₂]) can be fitted with a single VTF curve, all components can be characterized by a limited set of parameters; i.e. σ_0 , B and T_0 .

The linearity obtained in comparison to the curvature of the Arrhenius plots may be considered a consequence of the fact that the conductivity mechanism is affected by strong interactions between oppositely charged ions.⁹ This hypothesis finds a further support in the fact that the ideal glass transition temperatures T_0 obtained from equations 1 and 2 for viscosity and conductivity, respectively are significantly different. In contrast to viscosity, conductivity data contain another contribution arising from temperature-dependent ion association. Thus, the fact that T_0 values of our ILs calculated from viscosity and conductivity are significantly different can be tentatively explained assuming an increased association on going from C3 to C9.

2.3.5 Ionicity and Association:

One way of assessing ionicity of ILs is to use the classification diagram based on the classical Walden rule. This rule relates the ionic mobilities represented by the equivalent conductivity (Λ) to the fluidity of the medium through which the ions move. Figure 2.3 shows the equivalent

conductivity (Λ) versus the reciprocal viscosity ($1/\eta$) in logarithmic form for the morpholinium salts at 25 and 65 °C. The interpretation of ILs' plots with respect to their deviation from the so-called ideal KCl line, determined with 1 mol L⁻¹ aqueous KCl solutions,¹⁰ has been recently questioned.¹¹ It is however evident that morpholinium salts from C3 to C6 lies on or around the so-called "ideal" Walden product line, atleast at room temperature. The other morpholinium salts (C7–C9) are characterized by conductivities significantly lesser than the ideal and a peculiar trend can be observed on increasing alkyl chain from C3 to C9.

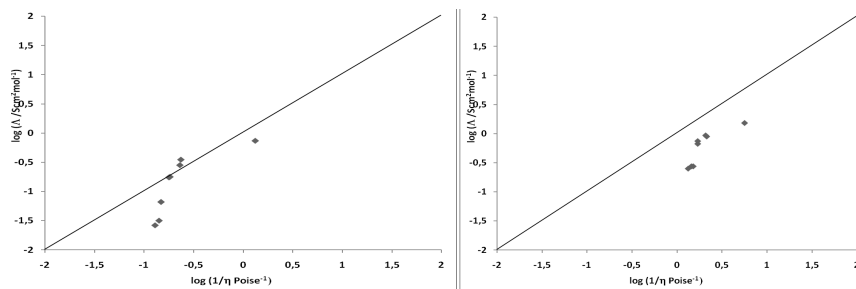


Figure 2.3: Walden plot for $[\text{Mor}_{1,n}][\text{N}(\text{CN})_2]$ from the conductivity and viscosity measured at 25 °C (left) and 65 °C (right). The ideal line is given by the line for KCl.

Thus, Walden plot suggest an increase in association degree on increasing the alkyl chain length which is slightly affected by temperature.

It is noteworthy that, in the case of 1-methyl-3-alkylimidazolium salts ESI–MS experiments have evidenced¹² that steric effects exerted by long alkyl chain lengths may contribute to a reduction of the anion–cation interactions although longer alkyl groups induce interionic van der Waals forces between the alkyl groups. In order to obtain further information about the association degree of *N*-alkyl-*N*-methylmorpholinium dicyanamides as function of the alkyl chain length ESI–MS experiments were performed. The positive ion ESI mass spectra of $[\text{Mor}_{1,n}][\text{N}(\text{CN})_2]$ ($n=2-9$) exhibit parent peaks respectively at m/z corresponding to the expected cations, whereas the anion parent peak was never been evidenced. On the other hand, aggregates based on small cation–anions clusters, which are reduced in intensity as the concentration of IL–acetonitrile solution is reduced, characterized the negative and positive spectra of all examined ILs (Figure 2.5). Since all the spectra were registered under identical conditions (solvent, concentration, ionization energy etc.) the comparison of the clusters' peaks distribution can give a semi-quantitative evaluation of the strength of anion–cation interaction. It is evident that $[\text{N}(\text{CN})_2]^-$ anion gives a significant number of clusters in ESI-MS (in vacuum), and probably in pure liquid. In contrast with the situation evidenced in imidazolium salts the increase in alkyl chain length does not reduce the ability to give clusters: in negative mode the sole anion was never detected

and larger clusters increase in percentages on going from $[\text{Mor}_{1,6}][\text{N}(\text{CN})_2]$ to $[\text{Mor}_{1,9}][\text{N}(\text{CN})_2]$. It is noteworthy that $[\text{Mor}_{1,5}][\text{N}(\text{CN})_2]$ and $[\text{Mor}_{1,7}][\text{N}(\text{CN})_2]$ show also strong peaks (not reported in figure) due to clusters bearing double negative charges, $\text{C}_3\text{A}_5^{-2}$ and $\text{C}_5\text{A}_7^{-2}$. Therefore, the ESI-MS measurements support the indication arising from Walden plots; even long alkyl chains substituted methylmorpholinium salts give association phenomena.

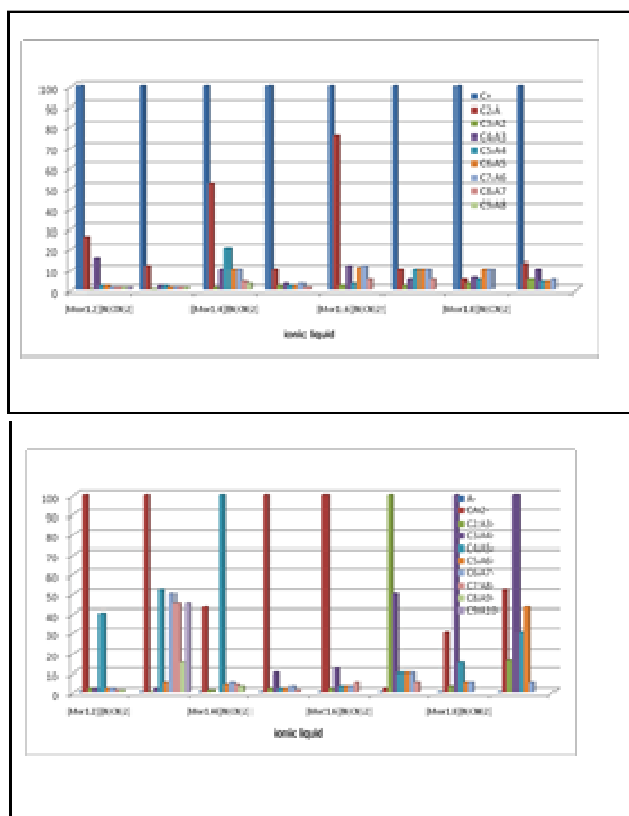


Figure 2.4: Relative percentages of the more relevant peaks observed in the positive and negative ESI-MS spectra of $[\text{Mor}_{1,n}][\text{N}(\text{CN})_2]$.

2.3.6 Solvent Properties and Polarity

Although a wide range of solvatochromic dyes has been used to estimate ILs' polarity by comparison to well-known polarity scales based on molecular solvents,¹³ E_T^N and Kamlet-Taft parameters are probably the most extensively employed to classify ILs and molecular solvents.¹⁴ Therefore, E_T^N and Kamlet-Taft parameters have been determined for ILs using Reichardt's

betaine dye, *N,N*-diethyl-4-nitroaniline and 4-nitroaniline.¹⁵ Table 2.3 presents the $E_{T(30)}$, dipolarity/polarizability (π^*), hydrogen-bond acidity (α) and hydrogen-bond basicity (β) values of the $[\text{Mor}_{1,n}][\text{N}(\text{CN})_2]$ salts. For comparison, the corresponding values of other three dicyanamide salts (1-butyl-3-methyl imidazolium dicyanamide, $[\text{bmim}][\text{N}(\text{CN})_2]$ and methyl-ethylpyrrolidinium dicyanamide, $[\text{emPyr}][\text{N}(\text{CN})_2]$), *N*-pentyl(dabco) dicyanamide, $[\text{C}_5\text{dabco}][\text{N}(\text{CN})_2]$, and some molecular solvents have been inserted. At 25°C the polarities of $[\text{Mor}_{1,n}][\text{N}(\text{CN})_2]$ ILs, as expressed by E_T^N values, are higher than those of acetone, acetonitrile and dimethylsulfoxide; however, they are slightly lower than those of the corresponding imidazolium salt ($[\text{bmim}][\text{N}(\text{CN})_2]$), water and methanol. On the other hand, π^* parameters evidence a high dipolarity–polarizability; the values reported for these salts are higher than those of methanol and acetone and are close to that for water. $[\text{Mor}_{1,n}][\text{N}(\text{CN})_2]$ ILs show moreover a hydrogen bond acidity, as expressed by α parameter, significantly lower than that of $[\text{bmim}][\text{N}(\text{CN})_2]$, but comparable to analogous pyrrolidinium- and *N*-alkyl dabco-based salts. Surely, the presence of an ether portion in the cationic core increases the polarity of the morpholinium salts with respect to the pyrrolidinium analogous; π^* parameters of $[\text{Mor}_{1,n}][\text{N}(\text{CN})_2]$ ILs are higher than those reported for all the other salts and they are practically unaffected by the alkyl chain length. At variance, this latter parameter affects both hydrogen bond acidity and basicity in an opposite way: α decreases and β increases. The β values for our ILs are close to those for methanol and acetone, evidencing a significant hydrogen bond basicity. Although β depends mainly on the nature of the anion a moderate cation effect can be envisaged. At 25 °C the β values for $[\text{C}_n\text{dabco}][\text{N}(\text{CN})_2]$ and $[\text{Mor}_{1,n}][\text{N}(\text{CN})_2]$ are lower than that of $[\text{bmim}][\text{N}(\text{CN})_2]$, suggesting a correlation with the cation polarity and hydrogen bond acidity. Therefore, considering the behavior of the solvatochromic parameters for $[\text{Mor}_{1,n}][\text{N}(\text{CN})_2]$ and for the other dicyanamide-based ILs reported in Table 2.4, we can state that these measurements support the viscosity and conductivity data being in agreement with an increase in the interactions inside the IL on going from $[\text{empyr}][\text{N}(\text{CN})_2]$ to $[\text{Mor}_{1,n}][\text{N}(\text{CN})_2]$, attributable at least partially to the effect of the oxygen on conformational rigid six-membered cation that increases the associated dipole. On the other hand, the elongation of the alkyl chain on morpholinium cation probably modifies the three-dimensional cation–anion network; thus, the anion basicity (β) increases as a consequence of the reduced interaction with the morpholinium cation(s). On the other hand, a reduced interaction among anions and cations on going from C2 to longer alkyl chains may be unable to increase hydrogen bond acidity due to the steric effects of the alkyl chain that inhibit the interaction of the positively charged cation with the solvatochromic dye. The limited ionic conductivity of the morpholinium salts bearing longer

alkyl chains, despite their lower Coloumbic interactions between oppositely charged species suggested by the solvatochromic parameters, may be therefore attributed to the increased van der Waals interactions among the alkyl chains. These latter interactions may be fundamental for the formation of organized three-dimensional networks of cations and anions separated by unpolar regions due to the alkyl chain in this class of ILs, as the π - π interactions that contribute to the association in imidazolium and pyridinium salts is absent in the morpholinium salts.

Table 2.4: Solvatochromic parameters of the $[C_n\text{Mor}_{1,n}][\text{N}(\text{CN})_2]$

| Salt | $E_{T(30)}$ | E_T^N | π^* | α | β |
|---|-----------------------|------------------|----------------|----------------|---------------------|
| $[bmim][\text{N}(\text{CN})_2]^{a,b}$ | 51.4 | 0.639 (0.629) | 1.05 (1.13) | 0.51 (0.46) | <i>Nd</i> (0.70) |
| $[emPyr][\text{N}(\text{CN})_2]^a$ | 48.7 | 0.556 | 1.03 | 0.37 | <i>Nd</i> |
| $[C_5dabco][\text{N}(\text{CN})_2]^c$ | 48.4 | 0.546 | 1.11 | 0.31 | 0.55 |
| $[\text{Mor}_{1,2}][\text{N}(\text{CN})_2]$ | 50.30 | 0.605 | 1.1193 | 0.4286 | 0.5065 |
| $[\text{Mor}_{1,3}][\text{N}(\text{CN})_2]$ | 50.23 | 0.6027 | 1.1230 | 0.4214 | 0.4944 |
| $[\text{Mor}_{1,4}][\text{N}(\text{CN})_2]$ | 49.48 | 0.5796 | 1.1161 | 0.3777 | 0.5308 |
| $[\text{Mor}_{1,5}][\text{N}(\text{CN})_2]$ | 49.54 | 0.5814 | 1.1147 | 0.3814 | 0.5384 |
| $[\text{Mor}_{1,6}][\text{N}(\text{CN})_2]$ | 49.59 | 0.5831 | 1.1158 | 0.3850 | 0.5461 |
| $[\text{Mor}_{1,7}][\text{N}(\text{CN})_2]$ | 49.23 | 0.5719 | 1.1129 | 0.3637 | 0.5435 |
| $[\text{Mor}_{1,8}][\text{N}(\text{CN})_2]$ | 49.11 | 0.5682 | 1.1144 | 0.3548 | 0.5449 |
| $[\text{Mor}_{1,9}][\text{N}(\text{CN})_2]$ | 49.17 | 0.5701 | 1.1136 | 0.3593 | 0.5444 |
| Water ^d | 53.7 ^{e,f} | 1.000 | 1.13 | 1.12 | 0.50 |
| Methanol ^d | 55.4 ^g | 0.760 | 0.73 | 1.05 | 0.61 |
| Acetone ^d | 42.2 ^{e,f} | 0.350 | 0.70 | 0.20 | 0.54 |
| Acetonitrile ^d | 45.6 ^g | 0.460 | 0.75 | 0.19 | 0.40 |
| DMSO ^d | 45.1 ^{e,f,g} | 0.444 | 1.00 | 0.00 | 0.76 |

^aFrom ref. 12. ^bFrom ref. 16. ^cFrom ref. 17. ^dFrom ref. 18. ^eFrom ref. 19.

^fFrom ref. 20. ^gFrom ref. 21.

2.3.7 Toxicity and Biodegradability

In this chapter, we are reporting experimental data on the aquatic toxicity and biodegradability of *N*-alkyl-*N*-methylmorpholinium(Morph)-based ILs as function of the alkyl chain length. Only few sporadic data of toxicity have been reported for

dialkylmorpholinium-based ILs.^{22,23,24} Recent studies have however shown that dicyanamide anion generally characterized by toxicity levels at least to aquatic species (algae and crustaceans) lower than analogous salts bearing other common anions, such as tetrafluoroborate and trifluoromethanesulfonate.²⁵

The hazard assessment on aquatic environment of the morpholinium series of ILs was estimated using the standard Microtox[®] Acute Toxicity test system, determining the effective concentration at 50% to the marine bacterium *Vibrio fischeri*. Ultimate biodegradability was evaluated by the CO₂ headspace test, using the test substances as the only source of carbon for the inoculated environmental microorganisms. CO₂ headspace test and Microtox[®] bioassay (*V. fischeri*) were carried out according to Pretti et al.²⁶

2.3.7.1 Toxicity

V. fischeri: acutotoxicity: The ecotoxicological test data are shown in Figure 2.5 (expressed as log₁₀ EC₅₀/mM). DABCO- and morpholinium-based bromides, bearing the same alkyl side-chains as substituents on nitrogen, were characterized by similar EC₅₀ values. In the Figure 2.5 shown below the morpholinium bromide salts bearing various alkyl chains are compared with DABCO salts with the same corresponding alkyl chains.

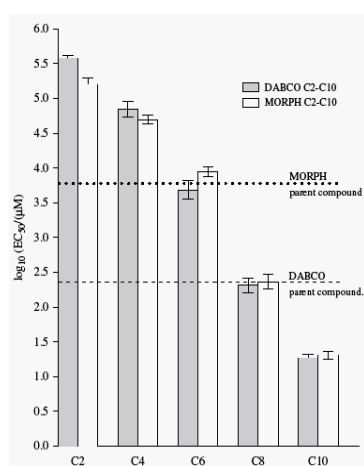


Figure 2.5: Acute toxicity (*V. fischeri*) values (EC₅₀) for DABCO- and morpholinium-based ILs with different lateral chain lengths (C2–C10) after 30 mins of incubation. Results are expressed as average log₁₀(EC₅₀/M)±standard deviation (*n*=3). Dotted lines represent the EC₅₀ values of parent compounds (DABCO and *N*-methylmorpholine). Results are expressed as average log₁₀(EC₅₀/M)±standard deviation (*n*=3). Significance, tested by oneway ANOVA, Tukey's multiple comparison test (*p*<0.05), evidenced that each DABCO-bar significantly differs from the other DABCO-bars and that each morpholinium-bar significantly differs from the other morpholinium-bars.

Nevertheless, in both the series a strong correlation between toxicity and the alkyl side-chain length was found; a monotonic decrease in EC_{50} values for the bioluminescence activity of *V. fischeri* with increasing chain length of ILs has been observed. The lowest EC_{50} values were 1.3 ± 0.1 for both DABCO C10 and *N*-methylmorpholinium C10, corresponding to an EC_{50} of app. 20 ± 4.5 expressed as mM. The highest EC_{50} values were 5.6 ± 0.1 and 5.2 ± 0.1 for DABCO C2 and *N*-methylmorpholinium C2, respectively. The corresponding values expressed as mM were 378.582 ± 71 and 161.90 ± 31 for DABCO C2 and *N*-methylmorpholinium C2, respectively. Parent compounds were also tested: the EC_{50} were 2.4 ± 0.4 and 3.8 ± 0.2 for DABCO and *N*-methylmorpholine, respectively. The C2 derivatives had higher EC_{50} comparatively to the parent compound.

2.3.7.2 Biodegradability

The biodegradability of morpholinium-based bromides was assessed by the CO_2 headspace test. Concerning the sodium benzoate (reference substance) curve, a difference in the efficiency of biodegradation of about 10% was observed between filtered and not filtered samples, probably related to the occurrence of adsorption phenomena. Under the experimental conditions, the reference substance reached the maximum level of biodegradation (90% in not filtered samples) between day 7 and day 14 and all biodegradation rates of tested ILs were referred as percentage of reference, as shown in Figure 2.6, below.

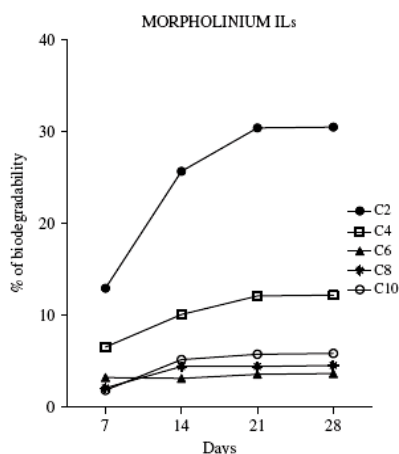


Figure 2.6: Percentage of biodegradability calculated for morpholinium ILs with different lateral chain length (C2–C10). Observations were performed after 7, 14, 21 and 28 days from the inoculums. Experiments were carried out in triplicate, levels were reported as average data ($n=3$).

All investigated ILs showed a low percentage of biodegradation (<60%). The biodegradation trend showed that the higher percentage of biodegradation is reached between day 15 and day 21 after sampling. Morpholinium ILs showed a biodegradation efficiency lower than those of DABCO ILs: the percentage of biodegradation varied from 30% (C2, day 28) to 3–5% (C6, C8 and C10, day 28). In this case, no significant differences were found as a function of the alkyl side chain on going from C6 to C10. Observed time trends related to the total dissolved organic carbon (TDC) measured in the experimental vials have been reported in Figure 2.7, below. Residual values higher than 30% (day 28) were observed for morpholinium molecules.

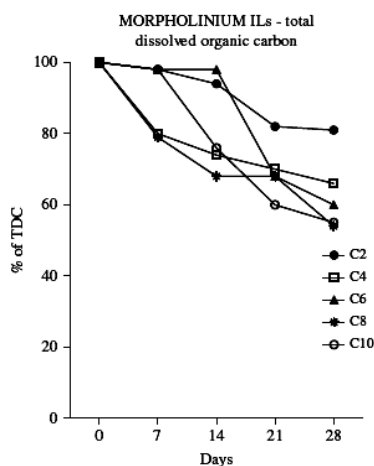


Figure 2.7: Percentage of total dissolved organic carbon (TDC) calculated for morpholinium ILs with different lateral chain length (C2–C10). Observations were performed at 0, 7, 14, 21 and 28 days from the inoculums. Experiments were carried out in triplicate, levels were reported as average data ($n=3$).

2.3.8 Discussion on Toxicity and Biodegradability

About the acute toxicity towards *V. fischeri*, for morpholinium-based ILs an EC_{50} value of 4.3 (expressed as $\log_{10} EC_{50}/mM$) was reported by Stolte et al.²⁴ in the year 2007 for *N*-methyl-*N*-butylmorpholinium bromide ($[Mor_{1,4}][Br]$). This value is in agreement with our results giving an EC_{50} (expressed as $\log_{10} EC_{50}/mM$) of 4.7 for the same IL, although Stolte et al.²⁴ in the year 2007 used a different detection method (LUMIS tox). On the basis of the data represented in Figure 2.5, it is evident that the transformation of both DABCO and *N*-methylmorpholine into the corresponding bromide salts bearing short alkyl chains reduces toxicity towards *V. Fischeri* except to C8 and C10. The comparison of the

EC₅₀ values characterizing starting amines and the corresponding salts also shows that small amounts of the unreacted starting substrate (DABCO or *N*-methylmorpholine) cannot significantly affect toxicity of the corresponding salts. On the other hand, in agreement with the behavior already evidenced with other ILs (imidazolium, pyridinium, ammonium, pyrrolidinium, piperidinium and so on), a correlation between toxicity to *V. fischeri* and lipophilicity can be envisaged: toxicity increases on increasing the alkyl chain length. However, when ILs bearing alkyl chains of comparable length are considered, morpholinium-based ILs show toxicity towards *V.fischeri* significantly lower than imidazolium and pyridinium salts also referred in Stolte et al.²⁴ in the year 2007). The investigated morpholinium-based ILs did not show high levels of ultimate biodegradability: mineralization in 28 days was for all examined ILs lower than 60%; consequently, none could be defined as “readily biodegradable”. However, the values characterizing the morpholinium salts bearing the shortest alkyl chain (ethyl) were significantly higher than those found for other widely used imidazolium-, phosphonium- and pyridinium-based ILs as referred in Pham et al.²⁷ in the year 2010. Percentages of biodegradation around 35% have been reported only for imidazolium-based ILs containing an ester side group as shown in Harjani et al.²⁸ 2008, which is known to increase significantly the biodegradability. In fact, compared to the other ones there is a strong increase in the ultimate biodegradability from day 21 onwards. However, all the degradation patterns are included in a narrow range of total biodegradation and the observed effect could be considered as a natural fluctuation of the density of the microbial population. Concerning morpholinium, observed TDC values remained close to 60% till the end of the incubation. This behavior could be both due to differences in the equilibrium processes and due to the different efficiency of microbial population in the degradation of the dissolved fraction of the tested molecules. Nevertheless, it is noteworthy that in morpholinium-based ILs, at variance with previously investigated imidazolium salts, biodegradability does not increase on increasing alkyl chain length on going from butyl to octyl (C4–C8); consequently, the more biodegradable ILs are also less toxic to *V. fischeri*. This suggests the presence of peculiar sites of biodegradation attack with respect to alkyl substituted imidazolium, pyridinium and ammonium salts. Moreover, considering that in the case of C2 and C4 substituted salts the percentage of biodegradation corresponds to the organic carbon content present in sites of the head group near to the oxygen (morpholinium), the hypothesis that this heteroatom may direct biodegradation favoring the attack by mono-oxygenases can be advanced. On the other hand, in the case of morpholinium ILs bearing longer alkyl chains, the reduced contribution of the headgroup

carbons to the total amount of carbon and the possible biocidal effects could explain the lower biodegradation.

2.3.9 Conclusion

A series of *N*-alkyl-*N*-methylmorpholinium dicyanamides (alkyl = C_nH_{n+1}, *n*=2, 3, 4, 5, 6, 7, 8 and 9) were synthesized starting from the corresponding bromides and characterized. All the dicyanamide salts were liquid at room temperature. Their physical properties such as density, viscosity and conductivity have been experimentally measured in a broad range of temperatures. Moreover, the absorption spectra of selected solvatochromic dyes in these ILs and electrospray mass spectra of these ILs in acetonitrile were measured to estimate the ion association, polarity and hydrogen-bonding interactions. The experimental results may contribute to a better understanding of the structure–property relationship of this type of fluid.

In particular, these data show that morpholinium dicyanamides are characterized by a significant ability to give clusters (ESI-MS measurements). ESI-MS, solvatochromic and conductivity–viscosity measurements suggest that in the case of morpholinium salts bearing long alkyl chains on cation, this cluster ability is determined by the interaction between nonpolar alkyl chains whereas in the case of [Mor_{1,2}][N(CN)₂] Coulombic interactions determine the supermolecular assembly. Although at the moment we do not have data about the structural features of the resulting three-dimensional networks as function of the alkyl chain length, we hypothesize that the absence of π – π interactions, strongly contributing to the ion association in imidazolium and pyridinium salts, the van der Waals interactions between alkyl chains may become determinant to the cluster ability of these ILs based on non-aromatic cations.

References

-
- ¹ (a) Szklarz, P.; Owczarek, M.; Bator, G.; Lis, T.; Gatner, K.; Jakubas, R. *J. Mol. Struct.* **2009**, 929, 48. (b) Lava, K.; Binnemans, K.; Cardinaels, T. *J. Phys. Chem. B.* **2009**, 113, 9506.
- ² Choudhary, A.; Agarwal, S.; Sharma, V. *Indian J. Chem., Sect. A: Inorg., Bio-inorg., Phys., Theor. Anal. Chem.* **2009**, 48A, 362.
- ³ Bodesheim, G.; Schmidt-Amelunxen, M.; Sohn, D.; Grundei, S. **2008**, WO 2008154998 A1 20081224.
- ⁴(a) Kim K. S.; Choi S.; Dembereinyamba D.; Lee H.; Oh, J.; Lee B. B.; Mun S. J. *Chem. Commun.*, **2004**, 828.

- (b) Kim J.; Singh R. P.; Shreeve J. M.; *Inorg. Chem.* **2004**, *43*, 2960.
- (c) Kim K. S.; Park S. Y.; Yeon S. H.; Lee H. *Electrochim Acta.* **2005**, *50*, 5673.
- (d) Kim K. S.; Park S. Y.; Choi S.; Lee H. *J. Power Sources.* **2006**, *155*, 385.
- ⁵ Pretti, C.; Chiappe, C.; Baldetti, I.; Brunini, S.; Monni, G.; Intorre, L. *Ecotoxicol. Environ. Saf.* **2009**, *72*, 1170.
- ⁶ Yoshida Y.; Baba O.; Saito G. *J. Phys. Chem. B.* **2007**, *111*, 4742.
- ⁷ Zhou, Z. B.; Matsumoto H.; Tatsumi K. *Chem. Eur. J.* **2006**, *12*, 2196.
- ⁸ Zhou, Z. B.; Matsumoto H.; Tatsumi K. *Chem. Eur. J.* **2006**, *12*, 2196.
- ⁹ Zhu, Q.; Song, Y.; Zhu, X.; Wang X. *J. Electroanal. Chem.* **2007**, *601*, 229.
- ¹⁰ Zu, W.; Cooper, E. I.; Angell C. A. *J. Phys. Chem. B.* **2003**, *107*, 6170.
- ¹¹ Schreiner C.; Zugmann S.; Hartl R.; Gores H. J. *J. Chem. Eng. Data*, **2010**, *55*, 1784.
- ¹² Bini, R.; Bortolini, O.; Chiappe, C.; Pieraccini, D.; Siciliano T. *J. Phys. Chem. B* **2007**, *111*, 598.
- ¹³ (a) Chiappe, C.; Pieraccini D. *J. Phys. Chem. A.* **2006**, *110*, 4937.
(b) Oehlke, A.; Hofmann, K.; Spange S. *New J. Chem.* **2006**, *30*, 533.
- ¹⁴ (a) Crowhurt, L.; Mawdsley, P. R.; Perez-Arlandis, J. M.; Salter, P.; Welton, T. *Phys. Chem. Chem. Phys.* **2003**, *5*, 2790.
(b) Reichardt C., *Green Chem.* **2005**, *7*, 339. Lee, J. M.; Ruckes, S.; Prausnitz J. M. *J. Phys. Chem. B*, **2008**, *112*, 1473.
- ¹⁵ (a) Kamlet, M. J.; Taft, W. R. *J. Am. Chem. Soc.* **1976**, *98*, 377.
(b) Taft, W. R.; Kamlet M. J. *J. Am. Chem. Soc.* **1976**, *98*, 2886.
(c) Kamlet, M. J.; Abboud, J. L.; Abraham, M. H.; Taft, W. R. *J. Org. Chem.* **1983**, *48*, 2877.
- ¹⁶ Chiappe, C.; Pieraccini, D.; Zhao, D.; Fei, Z.; Dyson P. J. *Adv. Synt. Cat.* **2006**, *348*, 68.
- ¹⁷ Persson, I. *Pure Appl. Chem.* **1986**, *58*, 1153.
- ¹⁸ Dahl, K.; Sando, G. M.; Fox, D. M.; Sutto, T. E.; Owrutsky, J. C. *J. Chem. Phys.* **2005**, *123*, 084504/1-11.
- ¹⁹ Reichardt, C.; Harbusch-Gornert, E. *Liebigs Ann. Chem.* **1983**, 721–743.
- ²⁰ Laurence, C.; Nicolet, P.; Reichardt, C. *Bull. Soc. Chim. Fr.* **1987**, 125–130.
- ²¹(a) Dimroth, K.; Reichardt, C.; Siepmann, T.; Bohlmann, F. *Liebigs Ann. Chem.* **1963**, *661*, 1–37.
(b) Dimroth, K.; Reichardt, C. *Liebigs. Ann. Chem.* **1969**, *727*, 93–105.
(c) Reichardt, C. *Liebigs Ann. Chem.* **1971**, *752*, 64–67.
- ²² Docherty, K. M.; Culpa, C. F. *Green Chem.* **2005**, *7*, 185.

²³ Pretti, C.; Chiappe, C.; Baldetti, I.; Brunini, S.; Monni, G.; Intorre, L. *Ecotoxicol. Environ. Saf.* **2009**, *72*, 1170.

²⁴ Stolte, S.; Matzke, M.; Arning, J.; Boschen, A.; Pittner, W.R.; Welz-Biermann, U.; Jastorff, B.; Ranke, J., *Green Chem.* **2007**, *9*, 1170–1179.

²⁵ Latała, A.; Nedzi, M.; Stepnowski, P. *Green Chem.* **2009**, *11*, 580.

²⁶ Pretti, C.; Renzi, M.; Focardi, S. E.; Giovani, A.; Monni, G.; Melai, B.; Rajamani, S.; Chiappe, C. **2010**, manuscript accepted in *Ecotox. Environ. Safe*.

²⁷ Pham, T.P.T., Cho, C., Yun, Y. *Water Res.* **2010**, *44*, 352–372.

²⁸ Harjani, J.R., Singer, R.D., Garcia, M.T., Scammells, P.J., *Green Chem.* **2008**, *10*, 436–438.

Chapter 3

Design and Development of Glyceryl-Substituted Ionic Liquids: Synthesis, Characterization and Temperature-Dependent Properties

Abstract

A series of new ionic liquids (ILs) has been prepared by introducing the 1,2-dihydroxypropyl (glyceryl) appendage in many quaternizable bases, including *N*-methylimidazole, *N*-methylmorpholine, 1,2-dimethyl imidazole, *N*-methylpyrrolidine, *N*-methylpiperidine and 4-hydroxy-1-methylpiperidine. The initially synthesized chloride salts were then converted to the corresponding dicyanamides as well as bistriflimides. Also the corresponding nitrate salt was prepared for pyrrolidinium-based IL. Density, viscosity, conductivity and polarity of these ILs were studied at different temperatures: *N*-methyl-*N*-glycerylpyrrolidinium dicyanamide, [Pyr_{1,g}][N(CN)₂], has the lowest viscosity and highest conductivity among all the studied glyceryl-substituted ILs, in the investigated temperature range. The polarity of these ILs covers a rather wide range and is strongly anion-dependent. Changes in Kamlet–Taft parameters (dipolarity/polarizability (π^*), hydrogen-bond donor acidity (α) and hydrogen-bond basicity (β)) with temperature show interesting trends.

3.1 Introduction

There are few doubts that in this moment ionic liquids (ILs) show enormous potential as reaction media characterized by unusual and improved properties with respect to many molecular solvents.¹ Surely, the fact that they are composed of ions alone and are still liquid at ambient conditions has been reason enough to evoke the initial curiosity among researchers. But, the option of fine-tuning the physico-chemical properties by an appropriate choice of cations and anions is the fact that has stimulated much of the current excitement with respect to these compounds, which are consequently defined as “designer solvents”.² However, for a rational application of ILs that arises from a careful selection of the optimal anion–cation combination for each application, it is fundamental to know the solvent properties of this extremely large class of compounds and how these properties change on changing IL structure. Most published work has focused on ILs containing imidazolium cations. For these ILs, for example, it is generally reported that polarity is close to that of short-chained alcohols. Some parameters characterizing ILs such as [emim][Tf₂N] and [bmim][Tf₂N] are comparable to those of 2-butanol but this

statement cannot be generalized; also for imidazolium salts polarity depends on anion and eventually on the substituents present on the cation.^{3,4,5} A careful selection of an appropriate solvent for a reaction under study requires however a good and quantitative classification of the solvent polarity. In a pioneeristic approach, Stobbe⁶ divided the solvents into two groups according to their ability to isomerize tautomeric compounds. To some extent, his classification reflects the modern division of solvents into hydrogen-bond donor (HBD, protic) solvents and non-hydrogen-bond donor (non-HBD, aprotic) solvents.

However, the ability of the medium to interact with dissolved species, i.e. the solvent polarity, is generally quantitatively evaluated using the so-called solvatochromic dyes or probes. It has long been known that UV/Vis/near-IR absorption spectra of chemical compounds may be influenced by the surrounding medium and that solvents can bring about a change in the position, intensity and shape of the absorption bands.^{7,8} Hantzschlater termed this phenomenon solvatochromism. A hypsochromic (or blue) shift of the UV/Vis/near-IR absorption band with increasing solvent polarity is usually called “negative solvatochromism”. The corresponding bathochromic (or red) shift with increasing solvent polarity is termed “positive solvatochromism”. Obviously, solvatochromism is caused by differential solvation of the ground and first excited state of the light-absorbing molecule (or its chromophore): if, with increasing solvent polarity, the ground-state molecule is better stabilized by solvation than the molecule in the excited state, negative solvatochromism will result. Or vice versa, better stabilization of the molecule in the first excited state relative to that in the ground state, with increasing solvent polarity, will lead to positive solvatochromism. In this context, “first excited state” means the so-called Franck-Condon excited state with the solvation pattern present practically in the same position of the ground state. Since the time required for a molecule to get electronically excited is much shorter than that required to execute vibrations or rotations, the nuclei of the absorbing entity (i.e., absorbing molecule + solvation shell) do not appreciably alter their positions during an electronic transition (Franck-Condon principle).⁹ In this context, the solvatochromism observed depends on the chemical structure and physical properties of the chromophore and the solvent molecules, which, for their part, determine the strength of the intermolecular solute–solvent interactions in the equilibrium ground state and the Franck-Condon excited state. Surely, depending on the solute–solvent interaction(s), a solubilizing medium may exert a profound effect on the electronic transition of a solute. In solvatochromic absorbance and fluorescence probes, such changes in electronic transitions are systematic with respect to some property of the medium. Many of such properties, e.g., dipolarity/polarizability, dipolarity, static dielectric constant, hydrogen-bond donating (HBD) acidity, hydrogen-bond accepting (HBA) basicity, etc., are

readily manifested through molecular absorbance or fluorescence spectra of a variety of solvatochromic probes.^{10,11,12,13}

Although the changes in absorbance and/or fluorescence of a solvatochromic probe with solvent structure can be considered a direct consequence of the changes in nonspecific and specific solute–solvent interactions, also modifications in the properties of the milieu, as a result of changing conditions, for e.g. change in temperature and/or pressure, can affect the spectroscopic property of a solvatochromic dye. Surely, temperature has a profound effect on the physico-chemical properties of a liquid and these latter affect the ability of the solvent to interact with a dye.¹⁴

The temperature dependence of polarity parameters or “thermosolvatochromism” is a property reported both in molecular solvents and ILs, however, the temperature effect on the solvatochromic shift in ILs is generally much more pronounced and therefore it is more easily evaluable. Recently, El Seoud et al.¹⁵ have investigated the thermosolvatochromism in binary mixtures of water and ILs (1-allyl-3-alkylimidazolium chlorides) to assess the relative importance of solute–solvent solvophobic interactions. Previously, the same group had reported thermosolvatochromic behavior of certain dyes in aqueous [bmim][BF₄] and compared it with behaviors of aqueous alcohols in the temperature range 10–60°C.¹⁶ An earlier report on thermosolvatochromic behavior of chloro-nickel complexes in 1-hydroxyalkyl-3-methylimidazolium cation based ILs suggested changes in the structure of the complex as the temperature was changed.¹⁷ Interesting results were found also by Kumar et al.¹⁴ by contrasting thermosolvatochromic trends in three series of ILs in the temperature range 298–353 K. The temperature-dependent polarity of [bmim][PF₆] was studied by Baker et al.^{1k} emphasizing that HBD strength of imidazolium cation was strongly temperature-dependent but HBA abilities were weak functions of temperature and added water. Also Shruti Trivedi et al.¹⁸ in the year 2010, showed temperature-dependent behavior of solvatochromic probes within [bmim][PF₆], [bmim][BF₄], and aqueous mixtures of [bmim][BF₄] is found to depend on the identity of the probe.

At variance with dialkyl-substituted imidazolium salts, the solvents properties of functionalized ILs have been only marginally investigated. However, it has been shown that ILs bearing an hydroxyl group on cation (hereafter as hydroxyl ILs), which were first reported by Branco et al.,¹⁹ endow classical ILs with useful polarity/solvation properties, and could replace traditional alcohols in certain applications. Hydroxyl ILs was found to play an important role on the

reaction. For example, addition of less than 1% hydroxyl ILs was sufficient to enhance the enzyme activity by a factor of up to 4 and also to increase the enantioselectivity of the reaction.²⁰ Diels-Alder reactions sensitive to polarity processed in 1-methyl-3-hydroxyethylimidazolium bistriflimide, [HOEMIm][Tf₂N], produced a much higher endo/exo ratio as compared to other ILs.²¹ Hydroxyl ILs were also suggested as an excellent stabilizer for the synthesis of nanostructure material.²² For example, Rh nanoparticles can be readily synthesized and stabilized in hydroxyl containing ILs as compared to non-functionalized ILs, providing an effective and highly stable catalytic system for biphasic hydrogenation reactions. The hydroxyl group in ILs is more effective than those in water and alcohols to coordinate with the metal ion in the octahedral configuration.²³ However, despite their extensive application of hydroxyl ILs and the large number of studies published in the past few years, some of their unique properties remain poorly understood, and little has been conducted to explore the relationship between ILs structure and solvent polarity.²⁴

During the course of this PhD thesis, a series of new ILs has been prepared by introducing the 1,2-propanediol group in many quaternizable bases, including *N*-methylimidazole, *N*-methylmorpholine, 1,2-dimethylimidazole, *N*-methylpyrrolidine, *N*-methylpiperidine and 4-hydroxy-1-methylpiperidine. The physico-chemical and solvent properties for each of them by changing their counter anions to bistriflimide, [Tf₂N]⁻ and dicyanamide, [N(CN)₂]⁻ were studied.

3.2 Materials and Methods:

3.2.1 Preparation of *N*-glyceryl-*N*-methylpyrrolidinium chloride [Pyrr_{1,g}][Cl]

26.58 g of 3-chloro-1,2-propanediol (Acros-99%) was added dropwise over 1 h to a solution of 20.05 g of *N*-methylpyrrolidine (Acros-98%) in 100 ml of acetonitrile (J.T. Baker, Deventer, Holland) while stirring vigorously, and N₂ was bubbled through the solution. The mixture was refluxed for 4.5 days at 70°C. The molten salt was decanted, washed three times with 100 ml of acetone, and dried on a rotovapor for 1 h at 45°C under low pressure. The product was dried in vacuum. If the product was found to have traces of brown or yellowish color, then it was washed again with acetone and recrystallized in acetone. A crystalline white solid was obtained and the product yield was 75%. *T*_m=100±2°C.

^1H NMR (250 MHz, D_2O) δ in ppm=4.28 (p, $J=5.71$ Hz, 1H, $\text{CH}_3\text{-N}^+\text{-CH}_2\text{-CH(OH)-CH}_2\text{(OH)}$); 3.36-3.63 (m, 4H, $\text{CH}_2\text{-N}^+\text{-CH}_2$); 3.15 (s, 3H, $\text{CH}_3\text{-N}^+\text{-CH}_2\text{-CH(OH)-CH}_2\text{(OH)}$); 3.36-3.63 (m, 4H, $\text{CH}_3\text{-N}^+\text{-CH}_2\text{-CH(OH)-CH}_2\text{(OH)}$); 2.23 (m, 4H, $-\text{CH}_2\text{-CH}_2\text{-N}^+\text{-CH}_2\text{-CH}_2-$).

^{13}C NMR (63 MHz, D_2O): δ in ppm= 20.48 ($-\text{CH}_2\text{-CH}_2\text{-N}^+\text{-CH}_2\text{-CH}_2-$); 21.31 ($-\text{CH}_2\text{-CH}_2\text{-N}^+\text{-CH}_2\text{-CH}_2-$); 63.56 ($\text{CH}_2\text{-N}^+\text{-CH}_2$); 65.51, 65.79 ($\text{CH}_3\text{-N}^+\text{-CH}_2\text{-CH(OH)-CH}_2\text{(OH)}$); 48.46 ($\text{CH}_3\text{-N}^+\text{-CH}_2\text{-CH(OH)-CH}_2\text{(OH)}$); 66.68 ($-\text{CH}_2\text{-CH}_2\text{-N}^+\text{-CH}_2\text{-CH(OH)-CH}_2\text{(OH)}$).

3.2.2 Preparation of *l*-glyceryl-2,3-dimethylimidazolium chloride [$\text{DMI}_{1,g}$][Cl]

31.16 g of 3-chloro-1,2-propanediol (Acros-99%) was added dropwise over 1 h to a solution of 27.1 g of dimethylimidazole (Aldrich-98%) in 100 ml of acetonitrile (J.T. Baker, Deventer, Holland) while stirring vigorously, and N_2 was bubbled through the solution. The mixture was refluxed for 4.5 days at 70°C . The molten salt was decanted, washed three times with 100 ml of acetone, and dried on a rotovapor for 1 h at 45°C under low pressure. The product was dried in vacuum. If the product was found to have traces of brown or yellowish color, then it was washed again with acetone and recrystallized in acetone. A crystalline white solid was obtained and the product yield was 69%. $T_m = 115 \pm 2^\circ\text{C}$.

^1H NMR (250 MHz, D_2O) δ in ppm= 2.80 (s, 3H, $^+\text{N}=\text{C-CH}_3$); 3.84 (s, 2H, $\text{C-N-CH}_2\text{-CH(OH)-CH}_2\text{(OH)}$); 3.98 (s, 3H CH-N-CH_3); 4.29 (m, 1H, $\text{CH-N-CH}_2\text{-CH(OH)-CH-H(OH)}$); 4.35 (m, 1H, $\text{CH-N-CH}_2\text{-CH(OH)-CH-H(OH)}$); 4.46 (m, 1H, $\text{CH-N-CH}_2\text{-CH(OH)-CH}_2\text{(OH)}$); 7.55 (M, 2H, $\text{N-CH}=\text{CH-N}$).

^{13}C NMR (63 MHz, D_2O): δ in ppm= 6.79 ($\text{CH}_3\text{-N}^+\text{-C-CH}_3$); 32.34 ($=\text{C-N}^+\text{-CH}_2\text{-CH(OH)-CH}_2\text{(OH)}$); 47.97 ($\text{N}^+\text{-CH}_3$); 60.08 ($=\text{C-N}^+\text{-CH}_2\text{-CH(OH)-CH}_2\text{(OH)}$); 67.79 ($=\text{C-N}^+\text{-CH}_2\text{-CH(OH)-CH}_2\text{(OH)}$); 118.99, 119.92 ($\text{CH}=\text{CH}$).

3.2.3 Preparation of *N*-glyceryl-*N*-methylpiperidinium chloride [$\text{Pip}_{1,g}$][Cl]

22.74 g of 3-chloro-1,2-propanediol (Acros-99%) was added dropwise over 1 h to a solution of 20.4 g of *N*-methylpiperidine (Aldrich-99%) in 100 ml of acetonitrile (J.T. Baker, Deventer, Holland) while stirring vigorously, and N_2 was bubbled through the solution. The mixture was

refluxed for 4.5 days at 70°C. The molten salt was decanted, washed three times with 100 ml of acetone, and dried on a rotovapor for 1 h at 45°C under low pressure. The product was dried in vacuum. If the product was found to have traces of brown or yellowish color, then it was washed again with acetone and recrystallized in acetone. A crystalline white solid was obtained and the product yield was 95%. $T_m=115\pm 2^\circ\text{C}$.

^1H NMR (250 MHz, D_2O) δ in ppm=1.61-1.68 (m, 2H, $-\text{CH}_2-\text{CH}_2-\text{CH}_2-\text{N}^+-\text{CH}_2-\text{CH}(\text{OH})-\text{CH}_2(\text{OH})$); 1.85-1.87 (m, 4H, $\text{CH}_2-\text{CH}_2-\text{N}^+-\text{CH}_2-\text{CH}_2$); 3.13 (s, 3H, $\text{CH}_3-\text{N}^+-\text{CH}_2-\text{CH}(\text{OH})-\text{CH}_2(\text{OH})$); 3.41-3.56 (m, 4H, $\text{CH}_3-\text{N}^+-\text{CH}_2-\text{CH}(\text{OH})-\text{CH}_2(\text{OH})$); 3.41-3.56 (m, 4H, $-\text{CH}_2-\text{CH}_2-\text{N}^+-\text{CH}_2-\text{CH}_2$); 4.26 (p, $J=5.4$, 1H, $-\text{CH}_2-\text{CH}_2-\text{N}^+-\text{CH}_2-\text{CH}_2$).

^{13}C NMR (63 MHz, D_2O): δ in ppm= 48.91 ($-\text{CH}_2-\text{N}^+-\text{CH}_3$); 20.34 ($\text{CH}_3-\text{N}^+-\text{CH}_2-\text{CH}_2-\text{CH}_2-\text{CH}_2$); 63.63 ($\text{CH}_3-\text{N}^+-\text{CH}_2-\text{CH}_2-\text{CH}_2$); 64.91 ($\text{CH}_3-\text{N}^+-\text{CH}_2-\text{CH}_2-\text{CH}_2$); 65.63 ($\text{CH}_3-\text{N}^+-\text{CH}_2-\text{CH}(\text{OH})-\text{CH}_2(\text{OH})$); 19.50 ($\text{CH}_3-\text{N}^+-\text{CH}_2-\text{CH}_2-\text{CH}_2-\text{CH}_2-\text{CH}_2$); 62.02 ($\text{CH}_3-\text{N}^+-\text{CH}_2-\text{CH}(\text{OH})-\text{CH}_2(\text{OH})$).

3.2.4 Preparation of *l*-glyceryl-*l*-methyl-4-hydroxypiperidinium chloride [FHMPip_{1,g}][Cl]

23.47 g of 3-chloro-1,2-propanediol (Acros-99%) was added dropwise over 1 h to a solution of 24.43 g of *N*-methyl-4-hydroxy piperidinium chloride (Acros-98%) in 100 ml of acetonitrile (J.T. Baker, Deventer, Holland) while stirring vigorously, and N_2 was bubbled through the solution. The mixture was refluxed for 4.5 days at 70°C. The molten salt was decanted, washed three times with 100 ml of acetone, and dried on a rotovapour for 1 h at 45°C under low pressure. The product was dried in vacuum. The product was dissolved in ethanol to obtain the pure compound. The product obtained was a brown solid which is little sticky to the glass. The product yield was 85%. $T_m=110\pm 2^\circ\text{C}$.

^1H NMR (250 MHz, D_2O) δ in ppm=2.176 (m, 2H, $\text{OH}-\text{CH}-\text{CH}_2-\text{CH}_2-\text{N}^+-\text{CH}_3$); 2.37 (m, 2H, $\text{OH}-\text{CH}-\text{CH}_2-\text{CH}_2-\text{N}^+-\text{CH}_3$); 3.57 (s, 3H, $\text{CH}_3-\text{N}^+-\text{CH}_2-\text{CH}(\text{OH})-\text{CH}_2(\text{OH})$); 3.65-3.74 (m, 8H, $(\text{CH}_2)_2-\text{N}^+-\text{CH}_2-\text{CH}(\text{OH})-\text{CH}_2(\text{OH})$); 3.78 (m, 1H, $\text{CH}_3-\text{N}^+-\text{CH}_2-\text{CH}(\text{OH})-\text{CH}_2(\text{OH})$); 3.80 (m, 1H, $\text{CH}_2-\text{CH}(\text{OH})-\text{CH}_2-\text{CH}_2$).

^{13}C NMR (63 MHz, D_2O): δ in ppm=24.39, 24.55 ($-\text{CH}_2-\text{CH}(\text{OH})-\text{CH}_2$); 46.05 ($\text{CH}_3-\text{N}^+-\text{CH}_2-\text{CH}(\text{OH})-\text{CH}_2(\text{OH})$); 55.76, 56.10, 56.45 ($(\text{CH}_2)_2-\text{N}^+-\text{CH}_2-\text{CH}(\text{OH})-\text{CH}_2(\text{OH})$); 59.47 ($\text{CH}_3-\text{N}^+-\text{CH}_2-\text{CH}(\text{OH})-\text{CH}_2(\text{OH})$); 60.98 ($\text{CH}_3-\text{N}^+-\text{CH}_2-\text{CH}(\text{OH})-\text{CH}_2(\text{OH})$); 63.15 ($-\text{CH}_2-\text{CH}(\text{OH})-\text{CH}_2$).

3.2.5 Preparation of *N*-glyceryl-*N*-methylmorpholinium chloride [Mor_{1,g}][Cl]

33.05 g of 3-chloro-1,2-propanediol (Acros-99%) was added dropwise over 1 h to a solution of 30.24 g of *N*-methylmorpholine (Acros-99%) in 100 ml of acetonitrile (J.T. Baker, Deventer, Holland) while stirring vigorously, and N₂ was bubbled through the solution. The mixture was refluxed for 4.5 days at 70°C. The molten salt was decanted, washed three times with 100 ml of acetone, and dried on a rotovapor for 1 h at 45°C under low pressure. The product was dried in vacuum. If the product was found to have traces of brown or yellowish colour, then it was washed again with acetone and recrystallized in acetone. A crystalline white solid was obtained and the product yield was 75%. *T*_m=137±2°C.

¹H NMR (250 MHz, D₂O) δ in ppm=3.31 (s, 3H, CH₂-N⁺-CH₃); 4.34 (p, 1H, CH₃-N⁺-CH₂-CH(OH)-CH₂(OH)); 3.60 (m, 8H, (CH₂)₂-N⁺-CH₂-CH(OH)-CH₂(OH)); 4.05 (m, 4H, -CH₂-O-CH₂-).

¹³C NMR (63 MHz, D₂O): δ in ppm= 47.8 (-CH₂-N⁺-CH₃); 63.06 (-CH₂-O-CH₂-); 59.90 (CH₃-N⁺-CH₂-CH(OH)-CH₂(OH)); 60.11 (-CH₂-N⁺-CH₂-); 60.51 (CH₃-N⁺-CH₂-CH(OH)-CH₂(OH)); 65.83 (CH₃-N⁺-CH₂-CH(OH)-CH₂(OH)).

3.2.6 Preparation of *N*-glyceryl-*N*-methylimidazolium chloride [MIM_{1,g}][Cl]

34.67 g of 3-chloro-1,2-propanediol (Acros-99%) was added dropwise over 1 h to a solution of 25.75 g of *N*-methylimidazole in 100 ml of acetonitrile (J.T. Baker, Deventer, Holland) while stirring vigorously, and N₂ was bubbled through the solution. The mixture was refluxed for 4.5 days at 70°C. A colorless viscous liquid was formed which was decanted, washed three times with 100 ml of acetone, and dried on a rotovapor for 1 h at 45°C under low pressure. The product was dried in vacuum. The product yield was 75%.

¹H NMR (250 MHz, D₂O) δ in ppm= 3.3 (m, 1H, -N⁺-CH₂-CH(OH)-CH₂-OH); 3.68 (m, 2H, -N⁺-CH₂-CH(OH)-CH₂-OH); 3.88 (m, 2H, -N⁺-CH₂-CH(OH)-CH₂-OH); 3.63 (s, 3H, -N⁺-CH₃); 6.76 (s, 1H, N-CH=CH-N⁺-); 6.84 (s, 1H, N-CH=CH-N⁺-); 7.29 (s, 1H, -N⁺=CH-N-CH₃).

¹³C NMR (63 MHz, D₂O): δ in ppm= 53.9 (-N⁺-CH₂-CH(OH)-CH₂-OH); 68.1 (-N⁺-CH₂-CH(OH)-CH₂-OH); 74.4 (-N⁺-CH₂-CH(OH)-CH₂-OH); 46.8 (=HC-N-CH₃); 126.2 (CH₃-N-CH=CH-N⁺); 143.4 (N=CH-N-CH₃).

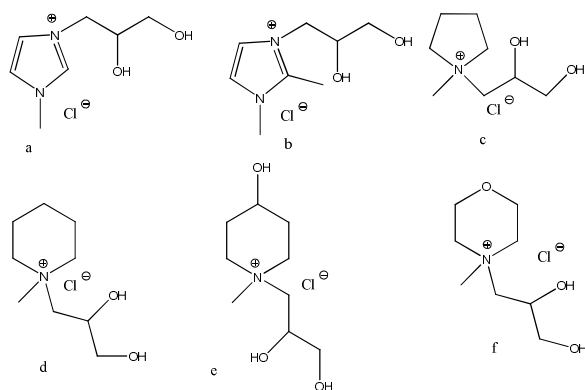


Figure 3.1: Structures of glyceryl-substituted chloride derivatives. 3.1(a) [MIM_{1,g}][Cl]; (b) [DMI_{1,g}][Cl]; (c) [Pyrr_{1,g}][Cl]; (d) [Pip_{1,g}][Cl]; (e) [FHMPip_{1,g}][Cl] and (f) [Mor_{1,g}][Cl].

3.2.7 Preparation of *N*-methyl-*N*-glycerylpyrrolidinium dicyanamide ([Pyrr_{1,g}][N(CN)₂])

To a colorless solution of [Pyrr_{1,g}][N(CN)₂] (15.00 g, 0.07665 mol) in water (100 ml) 0.07818 mol of silver dicyanamide (white solid, freshly prepared from AgNO₃ and NaN(CN)₂ in water) was added. The mixture was stirred for 3 h at 40°C. After cooling at room temperature the precipitate was filtered off, washed with water (2×10 ml) and the resulting colorless aqueous solution (approximately 200 ml) was heated to 70°C under vacuum for 1 h to remove the water. The colorless liquid was dissolved in anhydrous acetone (Carlo Erba reagents, HPLC grade, 200 ml), and the solution was cooled at -20°C for 48 h. This was done to remove any silver salts if present. The silver salts were filtered on a glass filter (porosity 5) containing two different powdered layers of 1 cm each: - celite (lower layer) and decolorizing charcoal (upper layer). The solvent was removed under vacuum (2×10⁻³ mm Hg, 80°C, 6 h) to give the pure colorless IL. The product yield was 82%.

¹H NMR (250 MHz, D₂O) δ in ppm=2.23, 2.22 (m, 4H, -CH₂-CH₂-CH₂-CH₂-); 3.24 (s, 3H, CH₃-N⁺-CH₂-CH(OH)-CH₂(OH)); 3.38–3.63 (m, 8H, (CH₂)₂-N⁺-CH₂-CH(OH)-CH₂(OH)); 4.21 (m, 1H, CH₃-N⁺-CH₂-CH(OH)-CH₂(OH)).

¹³C NMR (63 MHz, D₂O): δ in ppm= 17.54, 18.38 (-CH₂-CH₂-N⁺-CH₂-CH₂-); 63.56 (CH₂-N⁺-CH₂); 62.84, 62.56 (CH₃-N⁺-CH₂-CH(OH)-CH₂(OH)); 60.60 (-CH₂-N⁺-CH₂-); 45.46 (CH₃-N⁺-CH₂-CH(OH)-CH₂(OH)); 63.72 (-CH₂-CH₂-N⁺-CH₂-CH(OH)-CH₂(OH)); 116.95 (N(CN)₂).

3.2.8 Preparation of 1-glyceryl-2,3-dimethylimidazolium dicyanamide [DMI_{1,g}][N(CN)₂]

To a colorless solution of [DMI_{1,g}][Cl] (15.00 g, 0.0726 mol) in water (100 ml) 0.07403 mol of silver dicyanamide (white solid, freshly prepared from AgNO₃ and NaN(CN)₂ in water) was added. The same procedure like the one of [Pyrr_{1,g}][N(CN)₂] was repeated. The product yield was 76%.

¹H NMR (250 MHz, D₂O) δ in ppm= 2.63 (s, 3H, ⁺N=C-CH₃); 3.65 (m, 2H, C-N-CH₂-CH(OH)-CH₂(OH)); 3.81 (s, 3H CH-N-CH₃); 4.04 (m, 1H, CH-N-CH₂-CH(OH)-CH-H(OH)); 4.12 (m, 1H, CH-N-CH₂-CH(OH)-CH-H(OH)); 4.34 (m, 1H, CH-N-CH₂-CH(OH)-CH₂(OH)); 7.39 (m, 2H, N-CH=CH-N).

¹³C NMR (63 MHz, D₂O): δ in ppm= 6.23 (CH₃-N⁺-C-CH₃); 31.80 (=C-N⁺-CH₂-CH(OH)-CH₂(OH)); 47.44 (N⁺-CH₃); 59.56 (=C-N⁺-CH₂-CH(OH)-CH₂(OH)); 67.21 (=C-N⁺-CH₂-CH(OH)-CH₂(OH)); 118.47, 119.37 (CH=CH); 118.13 (N(CN)₂).

3.2.9 Preparation of *N*-glyceryl-*N*-methylpiperidinium dicyanamide [Pip_{1,g}][N(CN)₂]

To a colorless solution of [Pip_{1,g}][Cl] (15.00 g, 0.07153 mol) in water (100 ml) 0.07296 mol of silver dicyanamide (white solid, freshly prepared from AgNO₃ and NaN(CN)₂ in water) was added. The same procedure like the one of [Pyrr_{1,g}][N(CN)₂] was repeated. The product yield was 87%.

¹H NMR (250 MHz, D₂O) δ in ppm=1.67–1.75 (p, *J*= Hz, 2H, -CH₂-CH₂-CH₂-N⁺-CH₂-CH(OH)-CH₂(OH)); 1.92–1.94 (m, 4H, CH₂-CH₂-N⁺-CH₂-CH₂); 3.19 (s, 3H, CH₃-N⁺-CH₂-CH(OH)-CH₂(OH)); 3.36–3.59 (m, 4H, CH₃-N⁺-CH₂-CH(OH)-CH₂(OH)); 3.36–3.59 (m, 4H, -CH₂-CH₂-N⁺-CH₂-CH₂-); 4.31 (p, 1H, -CH₂-CH₂-N⁺-CH₂-CH(OH)-CH₂(OH)).

¹³C NMR (63 MHz, D₂O): δ in ppm= 45.99 (-CH₂-N⁺-CH₃); 16.65 (CH₃-N⁺-CH₂-CH₂-CH₂-CH₂-); 63.63 (CH₃-N⁺-CH₂-CH₂-CH₂-); 64.91 (CH₃-N⁺-CH₂-CH₂-CH₂-); 65.63 (CH₃-N⁺-CH₂-CH(OH)-CH₂(OH)); 19.50 (CH₃-N⁺-CH₂-CH₂-CH₂-CH₂-); 62.02 (CH₃-N⁺-CH₂-CH(OH)-CH₂(OH)).

3.2.10 Preparation of *I*-glyceryl-*I*-methyl 4-hydroxypiperidinium dicyanamide [FHMPip_{1,g}][N(CN)₂]

To a colorless solution of [FHMPip_{1,g}][Cl] (20 g, 0.08861 mol) in water (100 ml) 0.09038 mol of silver dicyanamide (white solid, freshly prepared from AgNO₃ and NaN(CN)₂ in water) was added. The same procedure like the one of [Pyrr_{1,g}][N(CN)₂] was repeated. The product yield was 69%.

¹H NMR (250 MHz, D₂O) δ in ppm=1.91–1.98 (m, 2H, OH-CH-CH₂-CH₂-N⁺-CH₃); 2.14–2.21 (m, 2H, OH-CH-CH₂-CH₂-N⁺-CH₃); 3.24 (s, 3H, CH₃-N⁺-CH₂-CH(OH)-CH₂(OH)); 3.42–3.71 (m, 8H, (CH₂)₂-N⁺-CH₂-CH(OH)-CH₂(OH)); 4.05–4.09 (m, 1H, CH₃-N⁺-CH₂-CH(OH)-CH₂(OH)); 4.30–4.33 (m, 1H, CH₂-CH(OH)-CH₂-CH₂-).

¹³C NMR (63 MHz, D₂O): δ in ppm=24.16, 24.30 (-CH₂-CH(OH)-CH₂-); 45.76 (CH₃-N⁺-CH₂-CH(OH)-CH₂(OH)); 55.79, 55.80, 55.82 ((CH₂)₂-N⁺-CH₂-CH(OH)-CH₂(OH)); 59.27 (CH₃-N⁺-CH₂-CH(OH)-CH₂(OH)); 60.70 (CH₃-N⁺-CH₂-CH(OH)-CH₂(OH)); 62.91 ((-CH₂-CH(OH)-CH₂-); 116.91 (N(CN)₂).

3.2.11 Preparation of *N*-glyceryl-*N*-methylmorpholinium dicyanamide ([Mor_{1,g}][N(CN)₂])

To a colorless solution of [Mor_{1,g}][Br] (15.00 g, 0.07085 mol) in water (100 ml) 0.07228 mol of silver dicyanamide (white solid, freshly prepared from AgNO₃ and NaN(CN)₂ in water) was added. The same procedure like the one of [Pyrr_{1,g}][N(CN)₂] was repeated. The product yield was 83%.

¹H NMR (250 MHz, D₂O) δ in ppm=3.34 (s, 3H, CH₂-N⁺-CH₃); 4.31–4.40 (p, 1H, CH₃-N⁺-CH₂-CH(OH)-CH₂(OH)); 3.57–3.71 (m, 8H, (CH₂)₂-N⁺-CH₂-CH(OH)-CH₂(OH)); 4.08 (m, 4H, -CH₂-O-CH₂-).

¹³C NMR (63 MHz, D₂O): δ in ppm= 45.27 (-CH₂-N⁺-CH₃); 60.60 (-CH₂-O-CH₂-); 57.43 (CH₃-N⁺-CH₂-CH(OH)-CH₂(OH)); 57.65 (-CH₂-N⁺-CH₂); 58.05 (CH₃-N⁺-CH₂-CH(OH)-CH₂(OH)); 63.40 (CH₃-N⁺-CH₂-CH(OH)-CH₂(OH)); 116.97 (N(CN)₂).

3.2.12 Preparation of *I*-glyceryl-3- methylimidazolium dicyanamide [MIM_{1,g}][N(CN)₂]

To a colorless solution of [MIM_{1,g}][Cl] (15.00 g, 0.07787 mol) in water (100 ml) 0.07942 mol of silver dicyanamide (white solid, freshly prepared from AgNO₃ and NaN(CN)₂ in water) was

added. The same procedure like the one of $[\text{Pyrrr}_{1,g}][\text{N}(\text{CN})_2]$ was repeated. The product yield was 72%.

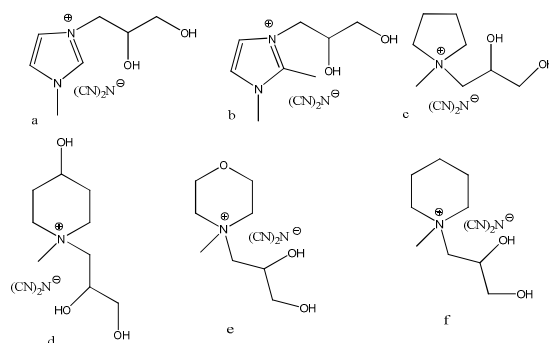


Figure 3.2: Structures of glyceryl-substituted $\text{N}(\text{CN})_2$ derivatives. 3.2(a) $[\text{MIM}_{1,g}][\text{N}(\text{CN})_2]$; (b) $[\text{DMI}_{1,g}][\text{N}(\text{CN})_2]$; (c) $[\text{Pyrrr}_{1,g}][\text{N}(\text{CN})_2]$; (d) $[\text{FHMPip}_{1,g}][\text{N}(\text{CN})_2]$; (e) $[\text{Mor}_{1,g}][\text{N}(\text{CN})_2]$ and (f) $[\text{Pip}_{1,g}][\text{N}(\text{CN})_2]$.

3.2.13 Preparation of *N*-methylpyrrolidinium bistriflimide ($[\text{Pyrrr}_{1,g}][\text{Tf}_2\text{N}]$)

To a colorless solution of $[\text{Pyrrr}_{1,g}][\text{Cl}]$ (15.00 g, 0.07665 mol) in water (100 ml) equimolar amount of LiTf_2N (io-li-tec) in 50 ml of water was added. The mixture was stirred for 3 h at 40°C . Immediately two separate layers were obtained. The product being more denser than water formed the lower layer. The product was not soluble in CH_2Cl_2 as well as acetone and three layers were formed when CH_2Cl_2 , water and IL was kept in the separating funnel as shown in Figure 3.4, below. The water was taken at each interval after a wash and AgNO_3 test was performed to check the presence of halide. The IL was washed 5 times to obtain a colourless transparent solution after AgNO_3 test. The pictures of the 5 washes are shown below in Figure 3.5. The lowest part i.e. the desired IL was collected. It was dried in rotary at 40°C under vacuum for 1 hr. The colourless liquid was dissolved in anhydrous acetonitrile (Carlo Erba reagents, HPLC grade, 200 ml), and the solution was cooled at -20°C for 48 h. This was done to remove any halide salt (LiCl), if present, and this made the IL completely pure. The lithium salts were filtered on a glass filter (porosity 5) containing two different powdered layers of 1 cm each: celite (lower layer) and decolourizing charcoal (upper layer). Charcoal was added only in case if the IL were brown or yellow coloured. The solvent was removed under vacuum (2×10^{-3} mm Hg, 80°C , 6h) to give the pure colourless IL. The product yield was 82%.

^1H NMR (250 MHz, CD_3CN) δ in ppm=4.22 (p, $J=5.71$ Hz, 1H, $\text{CH}_3\text{-N}^+\text{-CH}_2\text{-CH(OH)-CH}_2\text{(OH)}$); 3.29–3.58 (m, 4H, $\text{CH}_2\text{-N}^+\text{-CH}_2$); 3.17 (s, 3H, $\text{CH}_3\text{-N}^+\text{-CH}_2\text{-CH(OH)-CH}_2\text{(OH)}$); 3.29–3.58 (m, 4H, $\text{CH}_3\text{-N}^+\text{-CH}_2\text{-CH(OH)-CH}_2\text{(OH)}$); 2.28 (m, 4H, $\text{-CH}_2\text{-CH}_2\text{-N}^+\text{-CH}_2\text{-CH}_2\text{-}$).

^{13}C NMR (63 MHz, D_2O): δ in ppm= 20.48 ($\text{-CH}_2\text{-CH}_2\text{-N}^+\text{-CH}_2\text{-CH}_2\text{-}$); 21.31 ($\text{-CH}_2\text{-CH}_2\text{-N}^+\text{-CH}_2\text{-CH}_2\text{-}$); 63.56 ($\text{CH}_2\text{-N}^+\text{-CH}_2$); 65.51, 65.79 ($\text{CH}_3\text{-N}^+\text{-CH}_2\text{-CH(OH)-CH}_2\text{(OH)}$); 48.46 ($\text{CH}_3\text{-N}^+\text{-CH}_2\text{-CH(OH)-CH}_2\text{(OH)}$); 66.68 ($\text{-CH}_2\text{-CH}_2\text{-N}^+\text{-CH}_2\text{-CH(OH)-CH}_2\text{(OH)}$), 122 (Tf_2N).

3.2.14 Preparation of *l*-glycerol-2,3-dimethylimidazolium bistriflimide [$\text{DMI}_{1,\text{g}}$][Tf_2N]

To a colorless solution of [$\text{DMI}_{1,\text{g}}$][Cl] (10.00 g, 0.04816 mol) in water (100 ml) an equimolar amount of LiTf_2N (io-li-tec) in 50 ml of water was added. The same procedure like in case of [$\text{Pyrr}_{1,\text{g}}$][Tf_2N] was carried out. The product yield was 69%.

^1H NMR (250 MHz, D_2O) δ in ppm= 2.80 (s, 3H, $^+\text{N}=\text{C-CH}_3$); 3.84 (s, 2H, $\text{C-N-CH}_2\text{-CH(OH)-CH}_2\text{(OH)}$); 3.98 (s, 3H CH-N-CH_3); 4.29 (m, 1H, $\text{CH-N-CH}_2\text{-CH(OH)-CH-H(OH)}$); 4.35 (m, 1H, $\text{CH-N-CH}_2\text{-CH(OH)-CH-H(OH)}$); 4.46 (m, 1H, $\text{CH-N-CH}_2\text{-CH(OH)-CH}_2\text{(OH)}$); 7.55 (m, 2H, $\text{N-CH}=\text{CH-N}$).

^{13}C NMR (63 MHz, D_2O): δ in ppm= 6.23 ($\text{CH}_3\text{-N}^+\text{-C-CH}_3$); 31.80 ($=\text{C-N}^+\text{-CH}_2\text{-CH(OH)-CH}_2\text{(OH)}$); 47.44 ($\text{N}^+\text{-CH}_3$); 59.56 ($=\text{C-N}^+\text{-CH}_2\text{-CH(OH)-CH}_2\text{(OH)}$); 67.21 ($=\text{C-N}^+\text{-CH}_2\text{-CH(OH)-CH}_2\text{(OH)}$); 118.47, 119.37 ($\text{CH}=\text{CH}$); , 122 (Tf_2N).

3.2.15 Preparation of *N*-glyceryl-*N*-methylpiperidinium bistriflimide [$\text{Pip}_{1,\text{g}}$][Tf_2N]

To a colorless solution of [$\text{Pip}_{1,\text{g}}$][Cl] (15.00 g, 0.07665 mol) in water (100 ml) an equimolar amount of LiTf_2N (io-li-tec) in 50 ml of water was added. The same procedure like the one of [$\text{Pyrr}_{1,\text{g}}$][Tf_2N] was carried out. The product yield was 73%.

^1H NMR (250 MHz, D_2O) δ in ppm=1.67–1.75 (p, $J=$ Hz, 2H, $\text{-CH}_2\text{-CH}_2\text{-CH}_2\text{-N}^+\text{-CH}_2\text{-CH(OH)-CH}_2\text{(OH)}$); 1.92–1.94 (m, 4H, $\text{CH}_2\text{-CH}_2\text{-N}^+\text{-CH}_2\text{-CH}_2\text{-}$); 3.19 (s, 3H, $\text{CH}_3\text{-N}^+\text{-CH}_2\text{-CH(OH)-CH}_2\text{(OH)}$); 3.36–3.59 (m, 4H, $\text{CH}_3\text{-N}^+\text{-CH}_2\text{-CH(OH)-CH}_2\text{(OH)}$); 3.36–3.59 (m, 4H, $\text{-CH}_2\text{-CH}_2\text{-N}^+\text{-CH}_2\text{-CH}_2\text{-}$); 4.31 (p, 1H, $\text{-CH}_2\text{-CH}_2\text{-N}^+\text{-CH}_2\text{-CH(OH)-CH}_2\text{(OH)}$).

^{13}C NMR (63 MHz, D_2O): δ in ppm= 45.99 ($\text{-CH}_2\text{-N}^+\text{-CH}_3$); 16.65 ($\text{CH}_3\text{-N}^+\text{-CH}_2\text{-CH}_2\text{-CH}_2\text{-CH}_2\text{-}$); 63.63 ($\text{CH}_3\text{-N}^+\text{-CH}_2\text{-CH}_2\text{-CH}_2\text{-}$); 64.91 ($\text{CH}_3\text{-N}^+\text{-CH}_2\text{-CH}_2\text{-CH}_2\text{-}$); 65.63 ($\text{CH}_3\text{-N}^+\text{-CH}_2\text{-}$

CH(OH)-CH₂(OH)); 19.50 (CH₃-N⁺-CH₂-CH₂-CH₂-CH₂-CH₂-); 62.02 (CH₃-N⁺-CH₂-CH(OH)-CH₂(OH)), 122 (Tf₂N).

3.2.16 Preparation of *N*-glyceryl-*N*-methyl 4-hydroxypiperidinium bistriflimide [FHMPip_{1,g}][Tf₂N]

To a colorless solution of [FHMPip_{1,g}][Cl] (13.05 g, 0.0578 mol) in water (100 ml) an equimolar amount of LiTf₂N (io-li-tec) in 50 ml of water was added. The same procedure like the one of [Pyrr_{1,g}][Tf₂N] was carried out. The product yield was 55%. It was a hard sticky liquid.

3.2.17 Preparation of *N*-glyceryl-*N*-methylmorpholinium bistriflimide ([Mor_{1,g}][Tf₂N])

To a colourless solution of [Mor_{1,g}][Cl] (15.00 g, 0.0708 mol) in water (100 ml) an equimolar amount of LiTf₂N (io-li-tech) in 50 ml of water was added. The same procedure like the one of [Pyrr_{1,g}][Tf₂N] was carried out. The product yield was 82%.

¹H NMR (250 MHz, D₂O) δ in ppm=3.34 (s, 3H, CH₂-N⁺-CH₃); 4.31–4.40 (p, 1H, CH₃-N⁺-CH₂-CH(OH)-CH₂(OH)); 3.57–3.71 (m, 8H, (CH₂)₂-N⁺-CH₂-CH(OH)-CH₂(OH)); 4.08 (m, 4H, -CH₂-O-CH₂-).

¹³C NMR (63 MHz, D₂O): δ in ppm= 45.27 (-CH₂-N⁺-CH₃); 60.60 (-CH₂-O-CH₂-); 57.43 (CH₃-N⁺-CH₂-CH(OH)-CH₂(OH)); 57.65 (-CH₂-N⁺-CH₂); 58.05 (CH₃-N⁺-CH₂-CH(OH)-CH₂(OH)); 63.40 (CH₃-N⁺-CH₂-CH(OH)-CH₂(OH)); 122.4 (Tf₂N).

3.2.18 Synthesis of *N*-glyceryl-*N*-methylimidazolium Tf₂N⁻ ([MIM_{1,g}][Tf₂N])

To a colorless solution of [MIM_{1,g}][Cl] (15.00 g, 0.07786 mol) in water (100 ml) an equimolar amount of LiTf₂N (io-li-tec) in 50 ml of water was added. The same procedure like the one of [Pyrr_{1,g}][Tf₂N] was carried out. The product yield was 85%.

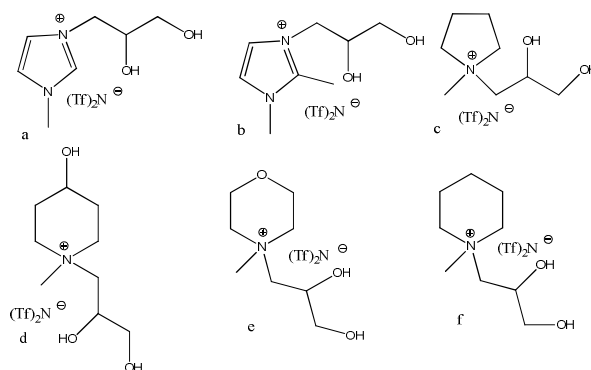


Figure 3.3: Structures of glyceryl-substituted Tf_2N derivatives. (a) $[\text{MIM}_{1,\text{g}}][\text{Tf}_2\text{N}]$; (b) $[\text{DMI}_{1,\text{g}}][\text{Tf}_2\text{N}]$; (c) $[\text{Pyrr}_{1,\text{g}}][\text{Tf}_2\text{N}]$; (d) $[\text{FHMPip}_{1,\text{g}}][\text{Tf}_2\text{N}]$; (e) $[\text{Mor}_{1,\text{g}}][\text{Tf}_2\text{N}]$ and (f) $[\text{Pip}_{1,\text{g}}][\text{Tf}_2\text{N}]$.

Commonly, all the $[\text{Tf}_2\text{N}]^-$ based ILs, having the glyceryl group on cation were not soluble in less quantity of water but were highly soluble when the amount of water was increased. Firstly, the Tf_2N was thought to be soluble in CH_2Cl_2 and hence we added CH_2Cl_2 to it as in less water the IL was not soluble. Thus, we obtained three separate layers as shown below in Figure 3.4. The lowest layer was the desired IL with Tf_2N anion and the middle layer was CH_2Cl_2 and the top most layer was water with all halides dissolved in it (it was assumed to have dissolved the maximum amount of halide in it). Hence, we can say that these type of ILs are very useful for extraction purposes in which the ILs are exceptionally forming different layers with organic solvent and water. Those these type of ILs were soluble in CH_3CN and all of them were washed in it to assume 100% removal of all halide salts.

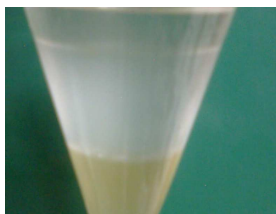


Figure 3.4: Separating funnel showing three different layers (a) IL (lowest layer); (b) CH_2Cl_2 (middle layer) and (c) H_2O (topmost layer).

The topmost layer (aqueous layer) was treated for AgNO_3 nitrate and when it was found positive, it was discarded and the entire system was washed again with fresh distilled water. The AgNO_3 tests were performed atleast 4 times, and more if required, unless the test was 100% negative.

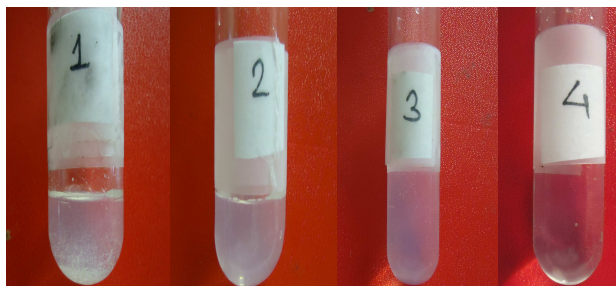


Figure 3.5: This figure represents various washings of AgNO_3 test from 1st to 4th. The precipitations decrease as we move from figures (1) to (4) (they are marked on the test-tubes).

3.2.19 Preparation of *N*-glyceryl-*N*-methylpyrrolidinium nitrate ([Pyrr_{1,g}][NO₃])

To a colorless solution of [Pyrr_{1,g}][Cl] (15.00 g, 0.0767 mol) in water (100 ml) an equimolar amount of NaNO_3 (RPE ACS) in 50 ml of water was added. The mixture was stirred for 24 h at 60°C. After stopping the reaction, the water was removed in the rotary at 60°C. Then acetonitrile was added to remove the NaCl salts (acetone was not used as IL was not soluble in acetone might be due to the glyceryl moiety). Then the solution was filtered in normal filter paper and then the entire solution was filtered on a glass filter (porosity 5) containing two different powdered layers of 1 cm each:- celite (lower layer) and decolorizing charcoal (upper layer). The charcoal was used in filter because the IL was yellowish-coloured. The solvent was removed under vacuum (2×10^{-3} mm Hg, 80°C, 6h) to give the pure colourless IL. The product yield was 79%.

Table 3.1a: Melting points of various glycerol chlorides

| Compounds | Melting points (°C) |
|------------------------------|-------------------------------|
| [Pyrr _{1,g}][Cl] | 100±2 |
| [Pip _{1,g}][Cl] | 115±2 |
| [DMI _{1,g}][Cl] | 115±2 |
| [Mor _{1,g}][Cl] | 137±2 |
| [FHMPip _{1,g}][Cl] | 110±2 |
| [MIM _{1,g}][Cl] | Viscous liquid which can flow |

3.3 Determination of some Physico-Chemical Parameters

Since the data on the purity of ILs are critical to the assessment of their physico-chemical properties and the polarity of ILs was reported to be water sensitive,²⁵ before every test of probe behavior the purity of ILs was first determined. To ensure that the water and other volatile solvents in ILs was reduced as low as possible, each IL was kept in a vacuum (pressure 10^{-3} mbar) with stirring at 80°C for at least 24 h prior to perform any measurement; contact with air was avoided during the measurements. The purity of each IL was first verified by NMR spectroscopy to check for residues of unreacted reactants or residual solvents.

Density was examined by the weight method at 25°C. Conductance measurements were performed using a CON 510 bench meter supplied with conductivity/TDS electrode. This electrode has a stainless steel ring and a cell constant of $K=1.0 \text{ cm}^{-1}$. It also has an inbuilt temperature sensor for automatic temperature compensation. Viscosity and rheological

measurements were conducted using a Brookfield DV-II + Pro concentric cylinder viscometer. Data were determined at shear rate ranging from 0 to 200 s^{-1} . All the data were measured near room temperature and are shown below in Table 3.1b.

Table 3.1b: Physical Properties of ILs

| Salt | C mol cm^{-3} | PM | κ S cm^{-1} (at 30°C) | Λ S cm^2 mol^{-1} | Vis (cP) at 30°C | Density (g/ml) |
|---|---------------------------|-------|---|--|------------------------|-------------------|
| [Pyrr _{1,g}][N(CN) ₂] | 0.0054 | 226.2 | 1.84×10^{-3} | 0.34 | 322.7 | 1.22 |
| [DMI _{1,g}][N(CN) ₂] | 0.0056 | 237.2 | 0.323×10^{-3} | 0.05 | 1141 | 1.32 |
| [Pip _{1,g}][N(CN) ₂] | 0.0049 | 240.3 | 0.272×10^{-3} | 0.05 | 970.3 | 1.18 |
| [FHMPip _{1,g}][N(CN) ₂] | 0.0057 | 256.3 | 0.232×10^{-3} | 0.04 | ND | 1.47 |
| [Mor _{1,g}][N(CN) ₂] | 0.0056 | 242.2 | 0.108×10^{-3} | 0.01 | 5367 | 1.37 |
| [MIM _{1,g}][N(CN) ₂] | 0.0059 | 223.2 | 0.440×10^{-3} | 0.07 | 932.4 | 1.31 |
| [Pyrr _{1,g}][Tf ₂ N] | 0.0035 | 440.4 | 0.643×10^{-3} | 0.18 | 322.7 | 1.55 |
| [DMI _{1,g}][Tf ₂ N] | 0.0036 | 451.4 | 0.095×10^{-3} | 0.02 | ND | 1.62 |
| [Pip _{1,g}][Tf ₂ N] | 0.0032 | 485.0 | 0.461×10^{-3} | 0.14 | 756.2 | 1.57 |
| [FHMPip _{1,g}][Tf ₂ N] | ----- | 470.5 | 0.00047×10^{-3} | ----- | ND | ND |
| [Mor _{1,g}][Tf ₂ N] | 0.0035 | 456.4 | 0.033×10^{-3} | 0.00 | ND | 1.61 |
| [MIM _{1,g}][Tf ₂ N] | 0.0037 | 437.4 | 0.360×10^{-3} | 0.09 | 766.5 | 1.61 |

^aC, molar concentration at 25°C for N(CN)₂ salts and at 35°C for Tf₂N salts; κ , ionic conductivity at 25°C; Λ , molar conductivity at 25°C. Vis=viscosity

3.4 Determination of $E_T(30)$ and Kamlet-Taft Parameters

UV-Vis absorption spectra of three solvatochromic dyes (Reichardt's betaine dye, *N,N*-diethyl-4-nitroaniline and 4-nitroaniline) dissolved in ILs were taken in a quartz cell with light path length of 1 mm on a Cary 2200 spectrophotometer (300–800 nm). Individual stock solutions of Reichardt's betaine dye, *N,N*-diethyl-4-nitroaniline and 4-nitroaniline were prepared in dichloromethane. In order to prepare a given dye/IL solution, the appropriate amount of the dye stock solution was micropipetted into a clean dry quartz cuvette. Residual dichloromethane was evaporated under gentle stream of argon gas. The IL was then added to the cuvette. The cuvette was then capped and sealed and the sample was mixed for an appropriate time before the experimental measurements.

3.5 Results and Discussions

3.5.1 Physico-Chemical Properties

For all synthesized glyceryl-substituted ILs the fundamental properties including density (ρ), viscosity (η) and conductivity (κ) were measured after accurate drying (see above) and the corresponding data are shown in Table 3.1b (above). The density (ρ) values lie in the range 1.62 to 1.18 g/ml. Thus, a moderate effect of cation structure on density and a more significant anion effect can be evidenced: i) dicyanamide salts have lower densities than the bistriflimide analogues; ii) the introduction of oxygen on cation core increases the density. Morpholinium salts have higher densities than piperidium, the introduction of an hydroxyl group on the piperidinium cation increases the density. Nevertheless, the cation and anion structure significantly affect viscosity (η). It is to note that in Table 3.1b, the viscosity values are reported at 30°C as some of these salts are extremely viscous liquids at lower temperatures. For the same reason all the conductivities are reported at 30°C.

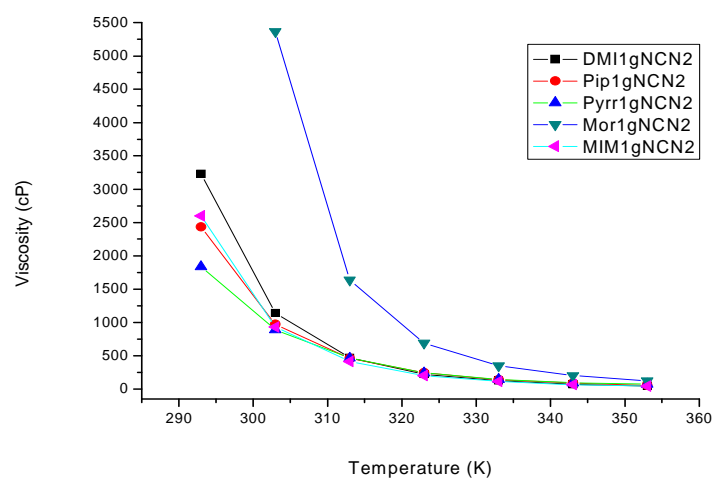
The temperature dependence of viscosity was investigated, with few exceptions, in the range 20 to 80°C. In the case of the dicyanamide salts, dynamic viscosity (Table 3.2) decreases on increasing the temperature: at lower temperatures, the viscosity decrease is significant whereas a more gentle descent behavior can be observed at higher temperatures (Figure 3.6).

Table 3.2: Viscosity values for six dicyanamide salts

| T (K) | [DMI _{1,g}] cP | [Pip _{1,g}] cP | [Pyrr _{1,g}] cP | [Mor _{1,g}] cP | [MIM _{1,g}] cP | [FHMPip _{1,g}] cP |
|-------|-----------------------------|-----------------------------|------------------------------|-----------------------------|-----------------------------|--------------------------------|
| 293 | 3227.5 | 2433 | 619.2 | ND ^a | 2599.5 | ND |
| 303 | 1141 | 970.3 | 322.7 | 5367 | 932.4 | ND |
| 313 | 470 | 461.4 | 179.6 | 1636 | 414.1 | 2007 |
| 323 | 221.5 | 243.5 | 104.9 | 691.3 | 201.6 | 798.7 |
| 333 | 126.5 | 140.1 | 53.7 | 349.5 | 114.2 | 414.0 |
| 343 | 72 | 88.9 | 45.0 | 201.7 | 66.9 | 226.7 |
| 353 | 46 | 56.9 | 35.1 | 122.8 | 43.1 | 125.3 |

^aND=
The
viscosi
ty

could not be determined as it was highly viscous.

**Figure 3.6:** Viscosity behavior of glyceryl N(CN)₂ compounds

The Arrhenius plots of viscosity according to eq (1) are shown in Figure 3.7.

$$\ln \eta = \ln A + E_{\eta}/RT \quad (1)$$

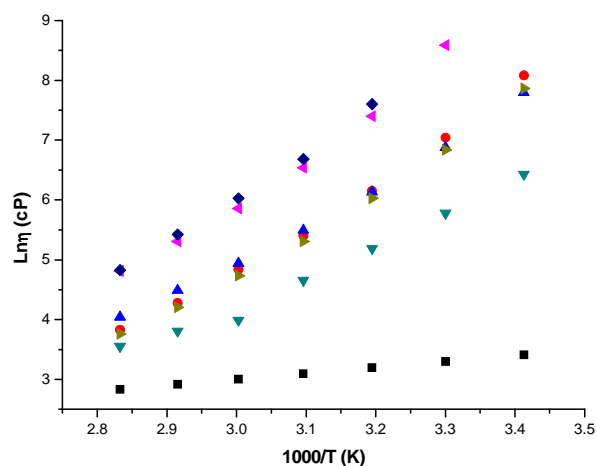


Figure 3.7: Arrhenius plots of viscosity for dicyanamide-based glyceryl ILs

These plots present a distinct curvature (see Appendix). However, the values of E_η , A and the linear fitting parameters (R^2) obtained are listed in Table 3.3. According to the values of R^2 , the five salts were approximately fit by the Arrhenius model in this temperature interval. It is however to note that all ILs exhibit high energy barriers, in agreement with the elevated viscosity values.

Table 3.3: Arrhenius Fitting parameters and Vogel-Tamman-Fulcher (VTF) parameters for viscosity behavior as a function of temperature ($N(CN)_2$)

| Compounds | E_η kJ mol ⁻¹ | A 10 ⁴ cP | R^2 | η_0 cP | B K | T_0 K | R^2 |
|--------------------------|----------------------------------|---------------------------|-------|----------------|------------|------------|--------|
| [Pyr _{1,g}] | 42.48 | 0.11 | 0.984 | 0.07 | 1125 (543) | 168 | 0.9990 |
| [DMI _{1,g}] | 59.86 | 0.0012 | 0.991 | 0.3 | 717 (168) | 215 | 0.9998 |
| [Pip _{1,g}] | 53.20 | 0.0068 | 0.993 | 0.5 | 691 (86) | 211 | 0.9999 |
| [Mor _{1,g}] | 66.01 | 0.00017 | 0.984 | 1.94 | 450 (23) | 246 | 0.9999 |
| [FHMPip _{1,g}] | 62.68 | 0.00068 | 0.995 | | | | |
| [MIM _{1,g}] | 57.05 | 0.0009 | 0.992 | 0.12 | 873 (60) | 205 | 0.9999 |

For these ILs, viscosity data have been also fitted to the VTF equation (2), the best fit lines are reported in Appendix 1.

$$\eta = \eta_0 \exp[B/(T-T_0)] \quad (2)$$

where η_0 (cP), B (K) and T_0 (K) are the fitting parameters. The best-fit parameters and the associated squared correlation coefficients R^2 are given in Table 3.3.

The effect of temperature on the viscosity was measured also in the case of bistriflimide salts. Analogously, dynamic viscosity (Table 3.4) decreases on increasing the temperature (Figure 3.8) and the Arrhenius plots are reported in Figure 3.9.

Table 3.4: Viscosity values for six bistriflimide salts

| T (K) | [DMI] _{1,g} cP | [Pip] _{1,g} cP | [Pyrr] _{1,g} cP | [Mor] _{1,g} cP | [MIM] _{1,g} cP |
|-------|----------------------------|----------------------------|-----------------------------|----------------------------|----------------------------|
| 293 | - | 2037 | 676 | - | 1259 |
| 303 | - | 756 | 321.3 | - | 766 |
| 313 | 1363 | 358 | 172.6 | 2619 | 361 |
| 323 | 524.5 | 188 | 100.4 | 1394 | 188 |
| 333 | 306.3 | 111 | 61.8 | 644 | 112 |
| 343 | 174.6 | 68 | 41.1 | 331 | 67 |
| 353 | 108.3 | 44 | 30.1 | 189 | 47 |

The IL [FHMPip]_{1,g}[Tf₂N] was a sticky jell and hence the viscosity is undeterminable for this kind of liquid.

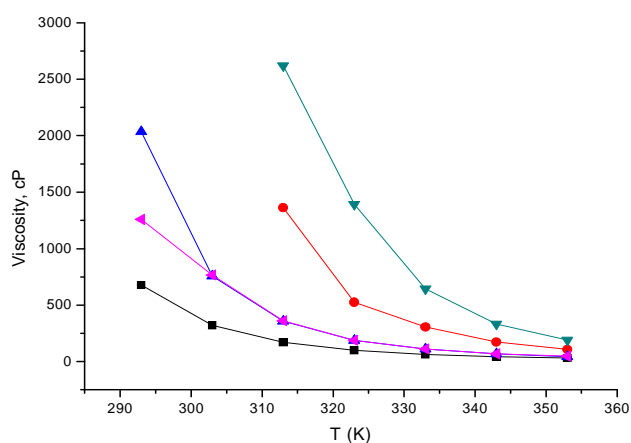


Figure 3.8: Behavior of viscosity with temperature for bistriflimide salts

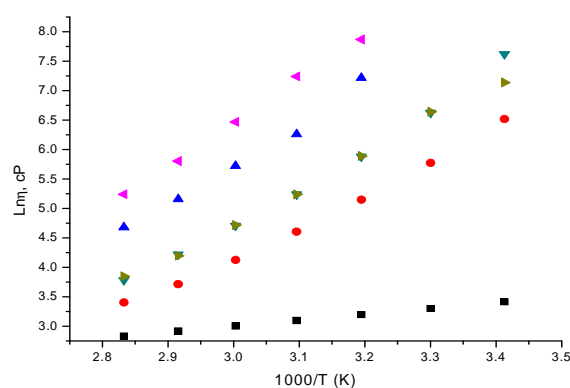


Figure 3.9: Arrhenius plot of viscosity for five bistriflimide-based glyceryl ILs

Table 3.5: Arrhenius Fitting parameters and VTF parameters for viscosity behavior as a function of temperature for Tf₂N ILs

| Compounds | E_{η} kJ mol ⁻¹ | A 10 ⁴ cP | R^2 | η_0 cP | B K | T_0 K | R^2 |
|------------------------|---------------------------------------|----------------------------|-------|----------------|--------|------------|---------|
| [Pyrr _{1,g}] | 44.72 | 0.067 | 0.994 | 0.09 | 979.5 | 193 | 0.99999 |
| [DMI _{1,g}] | 56.86 | 0.004 | 0.988 | 8.1 | 230 | 267 | 0.99991 |
| [Pip _{1,g}] | 54.04 | 0.004 | 0.991 | 0.47 | 628 | 217 | 0.99996 |
| [Mor _{1,g}] | 61.52 | 0.001 | 0.998 | ND | ND | - | - |
| [MIM _{1,g}] | 49.05 | 0.023 | 0.998 | ND | ND | - | - |

Generally, the bistriflimide ILs follow the Arrhenius behavior better than the dicyanamide salts; some ILs cannot be fitted to the VTF equation. Moreover, a similar trend in the activation barriers as defined by the E_{η} values can be observed for both series of ILs: for dicyanamide salts, [Pyrr_{1,g}] < [Pip_{1,g}] < [MIM_{1,g}] < [DMI_{1,g}] < [FHPip_{1,g}] < [Mor_{1,g}]; for bistriflimide salts, [Pyrr_{1,g}] < [MIM_{1,g}] < [DMI_{1,g}] < [FHPip_{1,g}] < [Mor_{1,g}]. It is noteworthy that when the B parameters are considered the activation energies appear to follow not exactly the same trend. In particular, for the dicyanamide salts the B parameter arising from the VTF analysis is completely in disagreement with the Arrhenius activation energy values for the [Pyrr_{1,g}] and [Mor_{1,g}]; the behavior of the two salts is inverted. A more deep analysis of the plots reported in the Appendix 1 shows that the behavior of pyrrolidinium is better described by the Arrhenius plot, the

moderate R^2 coefficient arises from the random scatter of some values and not from a not linear behavior. On the other hand, $[\text{Mor}_{1,g}][\text{N}(\text{CN})_2]$ is poorly described by equation 1.

Both, for dicyanamide and bistriflimide salts we have also investigated the behavior of conductivity with temperature, data are reported in Table 3.6 and Figure 3.10.

Table 3.6: Conductivity values for all dicyanamide and bistriflimide salts from 293 to 363 K in mS cm^{-1}

| Compounds | 293 | 303 | 313 | 323 | 343 | 353 | 363 |
|--|--------|--------|--------|--------|--------|-------|-------|
| $[\text{Pyr}_{1,g}][\text{N}(\text{CN})_2]$ | 1.191 | 1.84 | 2.54 | 3.41 | 4.35 | 5.39 | 6.52 |
| $[\text{DMI}_{1,g}][\text{N}(\text{CN})_2]$ | 0.147 | 0.323 | 0.610 | 1.024 | 1.598 | 2.36 | 3.21 |
| $[\text{Pip}_{1,g}][\text{N}(\text{CN})_2]$ | 0.140 | 0.272 | 0.498 | 0.821 | 1.254 | 1.677 | 2.28 |
| $[\text{Mor}_{1,g}][\text{N}(\text{CN})_2]$ | 0.052 | 0.109 | 0.212 | 0.389 | 0.614 | 0.910 | 1.332 |
| $[\text{FHMPip}_{1,g}][\text{N}(\text{CN})_2]$ | 0.120 | 0.232 | 0.387 | 0.759 | 1.235 | 1.508 | 1.92 |
| $[\text{MIM}_{1,g}][\text{N}(\text{CN})_2]$ | 0.210 | 0.440 | 0.832 | 1.325 | 1.980 | 2.81 | 3.77 |
| $[\text{Pyr}_{1,g}][\text{Tf}_2\text{N}]$ | 0.402 | 0.643 | 0.969 | 1.359 | 1.835 | 2.60 | 3.15 |
| $[\text{DMI}_{1,g}][\text{Tf}_2\text{N}]$ | 0.046 | 0.095 | 0.208 | 0.339 | 0.550 | 0.798 | 1.133 |
| $[\text{Pip}_{1,g}][\text{Tf}_2\text{N}]$ | 0.268 | 0.461 | 0.733 | 1.079 | 1.483 | 2.06 | 2.52 |
| $[\text{Mor}_{1,g}][\text{Tf}_2\text{N}]$ | 0.012 | 0.034 | 0.073 | 0.138 | 0.290 | 0.469 | 0.627 |
| $[\text{FHMPip}_{1,g}][\text{Tf}_2\text{N}]$ | 0.0001 | 0.0004 | 0.0014 | 0.0038 | 0.0096 | 0.021 | 0.045 |
| $[\text{MIM}_{1,g}][\text{Tf}_2\text{N}]$ | 0.197 | 0.360 | 0.591 | 0.938 | 1.494 | 1.92 | 2.48 |

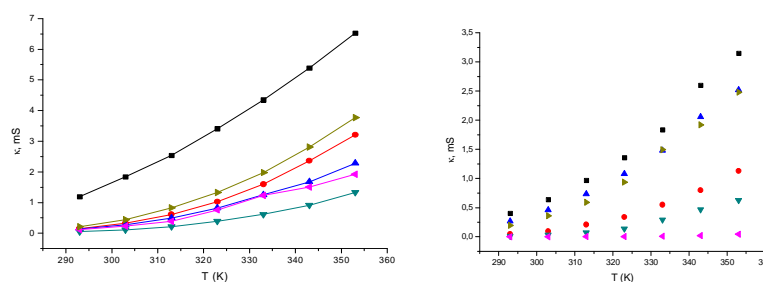


Figure 3.10: Behavior of conductivity of dicyanamide (left) and bistriflimides (right) salts with temperature

We have also reported the corresponding Arrhenius plots according to the equation 3 in Figures 3.11(a) and (b).

$$\ln \kappa = \ln A + (E_a/RT) \quad (3)$$

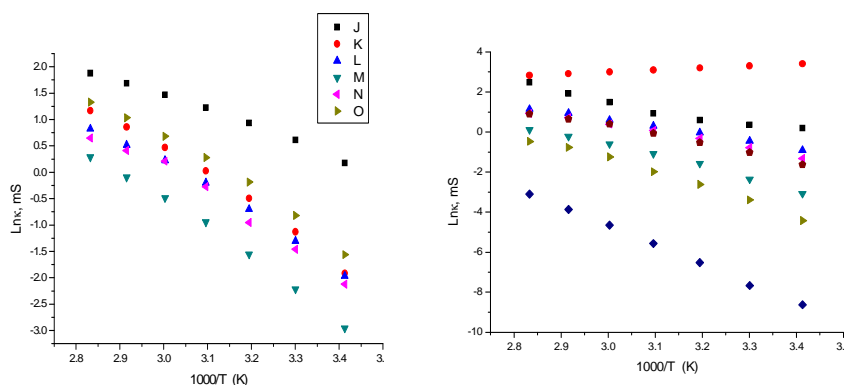


Figure 3.11: Arrhenius plots of conductivity for dicyanamides (left) and bistriflimides (right)

Since, as expected from viscosity results, at least in some cases conductivities exhibit some deviations from Arrhenius behavior (as shown in Figure 3.11 and plots in Appendix 1), also the VTF equation (4) was used to represent the temperature dependence of the conductivity:

$$\kappa = \kappa_{\infty} \exp[-B'/(T-T_0)] \quad (4)$$

The Arrhenius and VTF equation parameters as well as the related correlation coefficients are reported in Table 3.9. In agreement with the viscosity data, a similar trend in the activation barriers as defined by the E_{κ} values characterize the conductivities of dicyanamide and bistriflimide salts, $[\text{Pyrr}_{1,g}] < [\text{Pip}_{1,g}] < [\text{MIM}_{1,g}] < [\text{DMI}_{1,g}] < [\text{Mor}_{1,g}]$; the sole exception being represented by the position of $[\text{FHMPip}_{1,g}]^+$ based ILs. In particular, the E_{κ} value of $[\text{FHMPip}_{1,g}][\text{N}(\text{CN})_2]$ is quite low, at least in comparison with the analogous system. A more deep analysis of the data however shows that this IL gives a poor correlation using both the Arrhenius equation and the VTF equation: in this latter case it was impossible to fit all the data to equation 4 (see Appendix 1). $[\text{FHMPip}_{1,g}][\text{N}(\text{CN})_2]$ is really the sole IL based on a cation bearing three hydroxyl groups and a dicyanamide anion, therefore much more than all the other salts, absorbs water from the environment. Although manipulation of these ILs has been carried out with a particular attention to avoid the contact with air we cannot exclude that the presence of small amounts of water could affect some measurements.

On the other hand, $[\text{FHMPip}_{1,g}][\text{Tf}_2\text{N}]$ having as counteranion a hydrophobic species is almost a non-conducting system. The ability of the cation to give intra- and intermolecular H-bonding

increases dramatically the viscosity; this IL appears as a sticky jelly liquid, it is more or less a semi solid which turn to a viscous liquid at 90°C. Hence, the conductivity was also measured at this temperature, though we did not measure conductivities of any other ILs at this temperature. The conductivity of [FHMPip_{1,g}][Tf₂N] at 90°C was found to be 70.1 μ S.

Table 3.7: Arrhenius Fitting parameters and VTF parameters for viscosity behavior as a function of temperature

| Comp | E _κ kJ mol ⁻¹ | lnA mS | R ² | κ _∞ mS | B' | T ₀ K | R ² |
|---|---|-----------|----------------|----------------------|-----|---------------------|----------------|
| [Pyrr _{1,g}][N(CN) ₂] | 24.7 | 10.1 | 0.992 | 115 | 465 | 190 | 0.99994 |
| [DMI _{1,g}][N(CN) ₂] | 43.89 | 16.2 | 0.989 | 206 | 582 | 213 | 0.99989 |
| [Pip _{1,g}][N(CN) ₂] | 39.90 | 14.58 | 0.989 | 78 | 476 | 218 | 0.9994 |
| [Mor _{1,g}][N(CN) ₂] | 46.39 | 16.23 | 0.993 | 357 | 915 | 189 | 0.9997 |
| [FHMPip _{1,g}][N(CN) ₂] | 40.90 | 14.80 | 0.981 | | | | |
| [MIM _{1,g}][N(CN) ₂] | 40.99 | 15.42 | 0.987 | 174 | 539 | 212 | 0.99995 |
| [Pyrr _{1,g}][Tf ₂ N] | 29.64 | 11.32 | 0.996 | 191 | 724 | 176 | 0.9976 |
| [DMI _{1,g}][Tf ₂ N] | 45.72 | 15.89 | 0.989 | 109 | 664 | 207 | 0.9997 |
| [Pip _{1,g}][Tf ₂ N] | 32.17 | 12.00 | 0.992 | 65 | 470 | 208 | 0.9988 |
| [Mor _{1,g}][Tf ₂ N] | 57.20 | 19.26 | 0.988 | | | | ND |
| [FHMPip _{1,g}][Tf ₂ N] | 80.06 | 24.00 | 0.999 | | | | ND |
| [MIM _{1,g}][Tf ₂ N] | 36.58 | 13.50 | 0.991 | 47 | 367 | 227 | 0.9978 |

ND=not determined

It is noteworthy that the [Pyrr_{1,g}][N(CN)₂] has an extraordinarily high conductivity comparatively to all other ILs bearing the same dihydroxyl-substituted alkyl chain (glyceryl). Generally, pyrrolidinium-based ILs have higher conductivities and lower viscosity values than piperidinium ILs having the same counter anions and bearing the same substituent on nitrogen. In 2007, T. Yim et al.²⁶ evidenced this behavior investigating various allyl-substituted piperidinium- and pyrrolidinium-based ILs: among them, 1-allyl-1-methylpyrrolidinium bistriflimide [Pyrr_{1,a}][Tf₂N] showed the lowest viscosity (52 cP) and the highest conductivity (5.7 mS cm⁻¹). The lower viscosity of the pyrrolidinium ILs with respect to the piperidinium analogous was attributed to the lower number of carbon atom in the cation core. In general, larger cations make

ILs more viscous because of the increased intermolecular van der Waals interactions.^{27,28,29} However, ionic conductivity is proportional to the number of charge carrier ions and their mobility. That is, the bigger piperidinium cations reducing the rotational freedom of molecules lead to higher viscosities and lower ionic conductivities. The conformational bias of a six-membered ring to a rather stable chair-like conformation in the piperidinium structure seems also to contribute towards the higher viscosity of the piperidinium-based ILs. Both the lower energy barrier of a ring-flip and the smaller energy difference between the envelope and the half-chair conformations in a five-membered ring make a cyclopentane ring more flexible.

As expected, however, the presence of two hydroxyl groups reduces conductivity and increases viscosity. The conductivity values reported³⁰ for dialkyl substituted pyrrolidinium bistriflimide, [Pyrr_{1,n}][Tf₂N] (where, *n* = alkyl group), including branched alkyl chains and straight alkyl chains are generally higher than 10⁻³ S cm⁻¹ even at 12°C. On the other hand, when pyrrolidinium-based ILs bearing the same alkyl chains with different anions have been investigated³¹ a conductivity equivalent to 3.0 mS cm⁻¹ and viscosity equivalent to 164 cP have been reported for [Pyrr_{1,4}][NbF₆] at 328 K. Finally, when a series of ILs (including imidazolium, tetraalkyl ammonium, pyrrolidinium and piperidinium) based on (fluorosulfonyl) (pentafluoroethanesulfonyl)imide ([F(SO₂)(C₂F₅SO₂)N]⁻, FPFSI⁻) anion have been investigated³² it has been shown that the imidazolium salt, 1-methyl-3-ethylimidazolium fluorosulfonyl ([MIM_{1,2}][FPFSI]), had the least viscosity and the highest conductivity, although the pyrrolidinium IL, [Pyrr_{1,3}][FPFSI], compared to the analogous piperidinium salt, [Pip_{1,3}][FPFSI], had a lower viscosity and higher conductivity. It is to note that in our system, in the presence of a glyceryl group, pyrrolidinium-based ILs have the lowest viscosity and highest conductivity including the imidazolium salts.

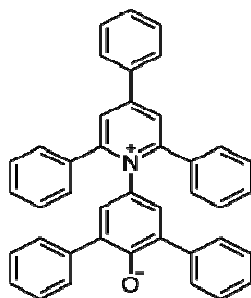
Since *N*-methyl-*N*-glycerylpyrrolidinium salts appeared to be inside this class of functionalized compounds the ILs having the best physico-chemical properties, we investigated also the behavior of conductivity of the corresponding nitrate salt, [Pyrr_{1,g}][NO₃]. In agreement with the higher ability of the relatively small nitrate anion to interact with the counteranion, conductivities significantly lower than those characterizing [Pyrr_{1,g}][Tf₂N] and [Pyrr_{1,g}][N(CN)₂] were found at all the investigated temperatures.

Table 3.8: Comparison of conductivities between three different ILs having various anions and common cation from 293 to 353 K

| Name of ILs | 293 | 303 | 313 | 323 | 333 | 343 | 353 |
|--|-------|-------|-------|-------|-------|-------|------|
| [Pyr _{1,g}][N(CN) ₂] | 1.191 | 1.84 | 2.54 | 3.41 | 4.35 | 5.39 | 6.52 |
| [Pyr _{1,g}][Tf ₂ N] | 0.402 | 0.643 | 0.969 | 1.359 | 1.835 | 2.60 | 3.15 |
| [Pyr _{1,g}][NO ₃] | 0.228 | 0.379 | 0.576 | 0.829 | 1.124 | 1.468 | 1.98 |

3.5.2 Solvatochromic Measurements and Polarity

So far, a large number of solvatochromic probes have been used to estimate the polarity of ILs. However, among them the Reichardt's dye 30 represents surely one of the most applied, probably due to fact that well-established empirical solvent polarity scales based on this probe are largely used also for molecular liquids.

**Figure 3.12:** Reichardt's dye

The polarity scale, $E_T(30)$, is defined as:

$$E_T(30) (\text{kcal mol}^{-1}) = 28\,591.5 / \lambda_{\text{max}} (\text{nm}) \quad (5)$$

where, λ_{max} is the wavelength maximum of the lowest energy band, intramolecular charge-transfer (CT) π - π^* absorption band of the zwitterionic phenolate molecule. Because of its zwitterionic structure, the solvatochromic property is strongly affected by the dipolarity, polarizability and hydrogen bond acidity of the solvent because they stabilize the dipolar ground

state more than the less dipolar Frank-Condon excited state. In Figure 3.13 it is reported the different solvation of ground and excited states on going from unpolar to polar solvents.

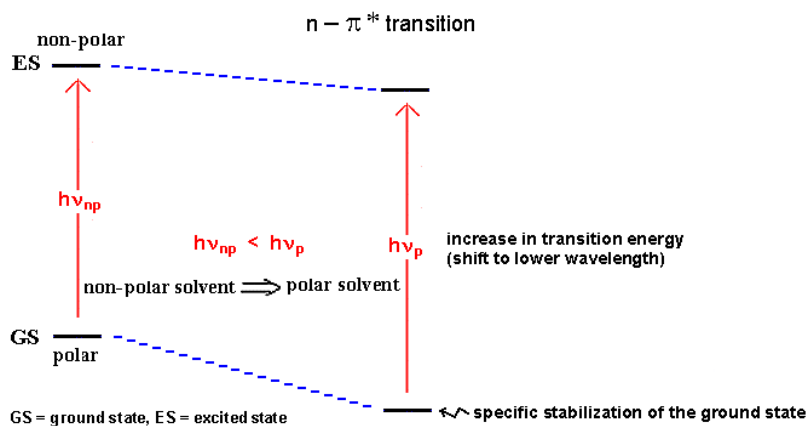


Figure 3.13: Different solvation of ground and excited states

Really, solvatochromism of 2,6-diphenyl-4-(2,4,6-triphenylpyridinio)-phenolate (Reichardt's dye or Betaine 30) results not only from a large reduction of dipole moment and hydrogen bonding on going from fundamental to excited state, but also from the modulation of the mesomeric effect.

When these spectroscopically derived empirical parameters are applied to the correlation analysis of solvent effects, it is tacitly assumed that the contribution of the various, nonspecific and specific, intermolecular forces to the overall interaction between solvatochromic probe and solvent molecules is the same as in the interaction between the solute and solvent of interest in the particular solvent-dependent process under investigation. The successful application of the $E_T(30)$ values in correlation analysis of a great variety of solvent-dependent processes demonstrates that this is often the case. However, according to the chemical structure of the solvatochromic probe molecule of 2,6-diphenyl-4-(2,4,6-triphenylpyridinio)-phenolate, this dye is not capable of interacting specifically and significantly with electron pair donor (EPD) solvents. That is, the Lewis basicity of solvents is not registered by this probe, whereas the solvent Lewis acidity is. This limit may have important consequences in the case of ILs bearing more or less basic anions.

Kamlet and Taft³³ have developed one of the most ambitious, and very successful, quantitative treatment of solvent effects which is able to consider also Lewis basicity, by means of a multiparameter equation that was introduced in 1976 and called linear solvation energy

relationship (LSER). Using three probes and defining these UV/Vis spectroscopically derived solvatochromic parameters, π^* , α and β , equation (6) was established:

$$XYZ = (XYZ)_o + s(\pi^* + d \delta) + a\alpha + b\beta + m\delta_H^2 \quad (6)$$

where $(XYZ)_o$, s , a , b and m are solvent-independent coefficients characteristic of the process under study and indicative of its susceptibility to the solvent properties π^* , α , β and δ_H^2 . In particular, π^* measures the exoergic effects of solute/solvent, dipole/dipole, and dipole/induced dipole interactions. That is, it measures the ability of a solvent to stabilize a neighboring charge or dipole by virtue of nonspecific dielectric interactions. In other words, these values represent a blend of dipolarity and polarizability of the solvent. For selected solvents, i.e. non-polychlorinated aliphatic solvents, with a single dominant bond dipole moment, π^* values are very nearly proportional to the solvent's molecular permanent dipole moment. The solvatochromic parameter α in equation 6 is a quantitative, empirical measure of the ability of a bulk solvent to act as an HBD toward a solute, whereas β is a quantitative, empirical measure of the ability of a bulk solvent to act as an HBA or an EPD toward a solute, forming a solute-to-solvent hydrogen bond or a solvent-to-solute coordinative bond, respectively. During the time, several sets of dyes have been used to derive the Kamlet-Taft parameters and many studies are quoted as an average of the values obtained for several of these dye sets. However, for ILs generally the Reichardt's dye, 4-nitroaniline and *N,N*-diethyl-4-nitroaniline are used. These dyes have been employed also in this thesis.

In particular, the solvent dipolarity/polarizability, π^* , which was initially normalized by taking dimethyl sulfoxide ($\pi^* = 1.00$) and cyclohexane ($\pi^* = 0.00$) as references, can be correlated to the wavelength maximum of the lowest energy band of *N,N*-diethyl-4-nitroaniline, a non-hydrogen bond donor solute.³⁴

$$\pi^* = (8.649 - 0.314 \times \nu_1) \quad (7)$$

The hydrogen bond donating acidity (HBD), α , is calculated using the $E_T(30)$ and π^* values

$$\alpha = 0.0649(E_T(30)) - 0.72\pi^* - 2.03 \quad (8)$$

Finally, the hydrogen bond accepting basicity (HBA), β , can be determined by using the following equation:

$$\beta = (1.035\nu_1 - \nu_2 + 2.64) / 2.80 \quad (9)$$

$$\nu_1 = 10^4 / \lambda_{4\text{Nitroaniline}} \quad \text{and} \quad \nu_2 = 10^4 / \lambda_{\text{NN-diethyl-4-nitroaniline}}$$

The Kamlet-Abboud-Taft parameters determined for the glyceryl-based ILs have been reported in Table 3.9 where also reference values of some molecular solvents and other ILs have been included.

Table 3.9: Solvatochromic parameters of ILs and molecular solvents

| Salt | $E_T(30)$ | E_T^N | π^* | α | β |
|--|---------------------|------------------|----------------|----------------|--------------|
| [bmim][N(CN) ₂] ^{a,b} | 51.4 | 0.639 (0.629) | 1.05 (1.13) | 0.51 (0.46) | Nd (0.70) |
| [emPyr][N(CN) ₂] ^a | 48.7 | 0.556 | 1.03 | 0.37 | Nd |
| [C ₅ dabco][N(CN) ₂] ^c | 48.4 | 0.546 | 1.11 | 0.31 | 0.55 |
| [Mor _{1,2}][N(CN) ₂] ^d | 50.3 | 0.605 | 1.12 | 0.43 | 0.5065 |
| [Mor _{1,4}][Tf ₂ N] | --- | --- | 1.00 | --- | 0.2048 |
| Water ^e | 53.7 ^{e,f} | 1.000 | 1.13 | 1.12 | 0.50 |
| Methanol ^e | 55.4 ^g | 0.760 | 0.73 | 1.05 | 0.61 |
| Acetone ^e | 42.2 ^{e,f} | 0.350 | 0.70 | 0.20 | 0.54 |
| Acetonitrile ^e | 45.6 ^g | 0.460 | 0.75 | 0.19 | 0.40 |
| [Pyr _{1,g}][N(CN) ₂] | 58.28 | 0.851 | 1.18 | 0.90 | 0.46 |
| [Pyr _{1,g}][Tf ₂ N] | 64.1 | 1.030 | 1.14 | 1.13 | 0.14 |
| [Pyr _{1,g}][NO ₃] | 57.86 | 0.838 | 1.19 | 0.87 | 0.53 |
| [Pip _{1,g}][N(CN) ₂] | 57.0 | 0.811 | 1.12 | 0.86 | 0.53 |
| [DMI _{1,g}][N(CN) ₂] | 57.0 | 0.813 | 1.15 | 0.84 | 0.46 |
| [Mor _{1,g}][N(CN) ₂] | 57.8 | 0.836 | 1.20 | 0.85 | 0.43 |
| [Pip _{1,g}][Tf ₂ N] | 62.8 | 0.991 | 1.13 | 1.23 | 0.11 |
| [FHMPip _{1,g}][N(CN) ₂] | 59.2 | 0.879 | 1.09 | 1.02 | 0.28 |
| [DMI _{1,g}][Tf ₂ N] | 61.2 | 0.941 | 1.14 | 0.93 | 0.11 |
| [Mor _{1,g}][Tf ₂ N] | 62.9 | 0.993 | 1.11 | 1.25 | 0.12 |
| [MIM _{1,g}][Cl] | 59.0 | 0.875 | 0.82 | 1.12 | 0.99 |
| [MIM _{1,g}][N(CN) ₂] | 57.6 | 0.831 | 1.17 | 0.87 | 0.47 |
| [MIM _{1,g}][Tf ₂ N] | 62.6 | 0.985 | 1.15 | 1.20 | 0.13 |
| [EMIM][Tf ₂ N] ^h | 52.0 | 0.657 | 0.90 | 0.76 | 0.28 |
| [EMIM][N(CN) ₂] ^h | 51.7 | 0.648 | 1.08 | 0.53 | 0.35 |
| [EMIM][NO ₃] ^h | 51.5 | 0.642 | 1.13 | 0.48 | 0.66 |
| [HOEMIM][Tf ₂ N] ^h | 60.8 | 0.929 | 1.03 | 1.17 | 0.34 |
| [HOEMIM][N(CN) ₂] ^h | --- | 0.784 | 1.11 | 0.80 | 0.51 |
| [HOEMIM][NO ₃] ^h | --- | 0.769 | 1.11 | 0.77 | 0.65 |

^aFrom reference 12. ^bFrom reference 35. ^cFrom reference 36. ^dFrom reference 37.

^eFrom reference 38. ^fFrom reference 39. ^gFrom reference 40. ^hShiguo et al. (2010).

Although non-hydroxyl ILs containing variable anions generally show comparable $E_T(30)$ values, in the range of 49.8–52.6 kcal/mol, irrespective of the nature of anion, this is not the same case for the corresponding hydroxyl⁴¹ and dihydroxyl ILs, which covered a rather wide

range of $E_T(30)$ values (51–64.1 kcal/mol), depending strongly on the nature of the anion. All ILs bearing one or two hydroxyl groups on the alkyl chain have higher π^* values (1.03–1.20) than molecular solvents, and in most cases slightly higher than non-hydroxyl ILs. However, little variation was observed on going from monohydroxyl to dihydroxyl derivatives, indicating the strong and comparable ability of the solvent dipolarity/polarizability of these functionalized ILs. The HBD ability, α value, is largely determined by the availability of HBD sites on the cation; as expected, the presence of hydroxyl groups on cation increases HBD ability. Nevertheless, it appears that more basic anions give much lower α values with a common cation in the hydroxyl ILs; for our ILs bearing two hydroxyl groups on the side alkyl chain α values range from 0.84 to 0.87 for the dicyanamide salts and from 0.93 to 1.23 for the bistriflimide-based IL. The introduction of another hydroxyl group on cation significantly increases H-bond acidity; the α value of [FHMPip_{1,g}][N(CN)₂] being 1.02 and that of [Pip_{1,g}][N(CN)₂] 0.86. On the other hand, the HBA parameter β , which is said to be controlled solely by the anions, increases in the order similar to the non-hydroxyl ILs, but of large magnitude; the β values of bistriflimides are around 0.11, those for dicyanamide-based ILs around 0.5 and a value of 0.99 was found for 1-methyl-3-glycerylimidazolium chloride, [MIM_{1,g}]Cl. The different HBA ability induced by the hydroxyl group could be indicative of the interaction between the anion and the hydrogen bond donor (OH). As previously observed, we confirm that the hydroxyl group is indispensable for the enhanced and expanded polarity, since the $E_T(30)$ scales for the 1/1 (molar ratio) binary mixtures of ethanol and the non-hydroxyl ILs were exclusively decreased as compared to each of the components.

Considering specifically the structure of Reichardt's dye, we can observe that this probe presents an easily accessible negative charge, at least when localized on oxygen, whereas the positive charge on the nitrogen is "buried" by its surrounding phenyl rings. Consequently, we can reasonably hypothesize that an unfunctionalized cation will be strongly localized and interact with the negative charge. This interaction can take advantage from some of the chemical features of the cation, such as the availability of the hydrogen on C(2)-H in 1,3-dialkyl substituted imidazolium ILs, although the charge–charge interaction should have a dominant effect. At variance, the anion interaction with the probe is less specific and strongly structure dependent. All IL anions are single-charged but they can show remarkable differences in shape and charge distribution. Small and linear ions, like dicyanamide, can approach closer to the positive charge of Reichardt's dye and specifically interact with it. For large spherical anions like BF₄[−] and PF₆[−],

steric hindrance results in a less close interaction. This reduces the strength of the specific Coulombic interaction according to the inverse distance law. In the absence of functional groups on cation or anion able to give specific interactions, short-range anionic or cationic-probe interactions can be disregarded. It is to note that in aprotic molecular solvents, probe solvation is only due to the ability of solvent molecules to align or anti-align their dipoles toward the positively- or negatively-charged centers; therefore, with respect to ILs, the interactions are weaker and always due to the same species. These considerations are pictorially illustrated in Figure 3.14.

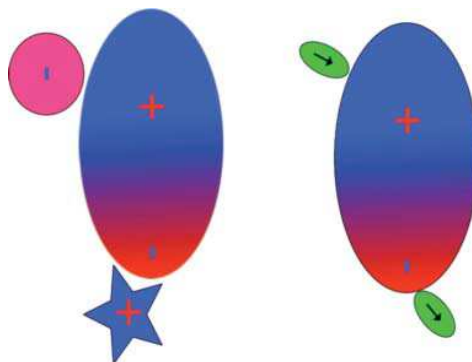


Figure 3.14: Illustration of interaction between the Reichardt's dye and the IL. The cation can get closer to the negative charge of Reichardt's dye (here represented as an ellipse) than the anion to the (delocalized and buried) positive charge. Molecular solvents align their dipoles with the electric field, but it is always the same molecule that interacts with the two charged centers.

In hydroxyl-functionalized ILs, practically the IL polarity becomes independent of the imidazolium moiety as well as the C(2)-H on imidazolium cation, since pyrrolidinium- and alkylammonium-based hydroxyl ILs also given high polarity. $ET_{(30)}$ of Reichardt's dye in mono-, di- and tri- hydroxyl-functionalized ILs is probably mainly influenced by the hydroxyl groups, which act as hydrogen bonds' donor modulated by the anion. Considering that Reichardt's dye is particularly sensitive to HBD solvents and dipolarity/polarizability effect, it can be conjectured that in hydroxyl ILs the phenolate oxygen on Reichardt's dye acting as a strong EPD or HBA center is suitable for ionic/charge–charge interactions with the cations of ILs and specific for hydrogen-bond interactions with HBD hydroxyl groups. The hydroxyl group on the piperidinium ring is probably more available to interact with the HBA center than the hydroxyl groups on the alkyl chain. However, considering the structure of the Reichardt's dye, as recently reported,³⁷ it is possible to hypothesize also the existence of interactions between the positive charge of the

pyridinium moiety and the anions of ILs, although, as explained above, the pyridinium ring does not act as a strong electron-pair acceptor (EPA) due to its delocalized and shielded positive charge by the three 2,4,6-phenyl groups. All of these solute–solvent interactions facilitate stabilization of the ground state of ionic probe, leading to increased and expanded polarity of hydroxyl ILs. In particular, in hydroxyl ILs having basic anions, such as $[\text{N}(\text{CN})_2]^-$, it has been reported³⁷ that the hydrogen atom of the hydroxyl group is fixed by a strong H-bonding between hydroxyl group and the coordinative and nucleophilic anions, giving to the OH group less freedom to interact with the phenolate part of the solvatochromic dye. These ILs present therefore a relatively low HBD ability. On the other hand, the formed strong hydrogen-bond in turn play as a bridge that bind the cation and anion, enhancing the rigidity of both the cation and anion and decreasing the magnitude of interaction with negatively charged phenolate oxygen and positively charged pyridinium moiety: this should determine a lower polarity than other hydroxyl ILs. In contrast, for the hydroxyl ILs bearing low coordinating anions, such as $[\text{Tf}_2\text{N}]^-$, the weak H-bonding between cations and anions, as well as the resulting high HBD ability of hydroxyl group induces efficient electrostatic and hydrogen-bond interactions between ILs and zwitterionic dye, thus stabilizing the ground state of ionic probe and giving “hyperpolarity”.

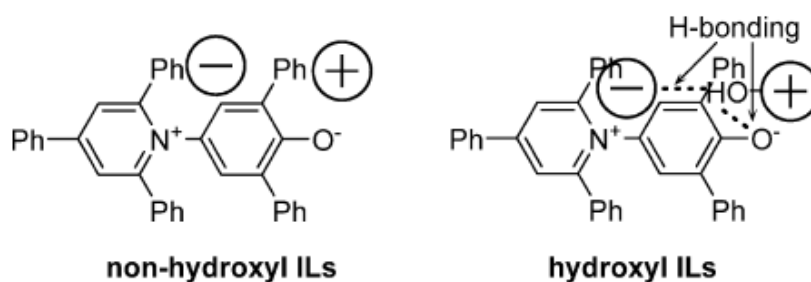
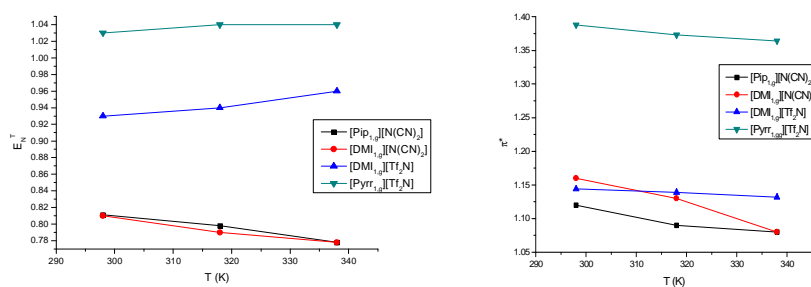


Figure 3.15: Cartoon illustrating a plausible mechanism between Reichardt’s dye and non-hydroxyl ILs (left) and with hydroxyl ILs (right)

Finally, since recently it has been shown that pyridinium-, pyrrolidinium- and phosphonium-based ILs present a substantial temperature dependence of polarity parameters, in this thesis the “thermosolvatochromism” of four glyceryl-substituted ILs, $[\text{Pip}_{1,g}][\text{N}(\text{CN})_2]$, $[\text{DMI}_{1,g}][\text{N}(\text{CN})_2]$, $[\text{DMI}_{1,g}][\text{Tf}_2\text{N}]$ and $[\text{Pyrr}_{1,g}][\text{Tf}_2\text{N}]$ was investigated determining the solvatochromic parameters by increasing the temperature from 25 to 45 and then to 65°C and immediately in the system the temperature was cooled from 65 to 45 and then to 25°C (see Appendix 2). Although the overall

changes in the polarity parameters increasing or decreasing the temperature in the interval 25–65°C (no significant differences were observed in function of the modality of change in this temperature range) was moderate a dependence on ILs structure was observed. In particular, the E_T^N values indicating dipolarity/polarizability and/or HBD acidity decrease linearly with increasing temperature in the case of the two dicyanamide-based ILs ([Pip_{1,g}][N(CN)₂] and [DMI_{1,g}][N(CN)₂]) but moderately increase with temperature for [DMI_{1,g}][Tf₂N], and practically remain constant for [Pyrr_{1,g}][Tf₂N]. Interestingly, also the Kamlet-Abboud-Taft are affected in different ways by temperature in the case of dicyanamide and bistriflimide salts. The polarizability parameter decreases on increasing the temperature for all the investigated ILs; however, this effect is more pronounced in the case of dicyanamides and associated to a decrease in HBD ability; for these salts, the α parameter decreases on increasing the temperature. At variance, an increase in H-bond ability can be observed for bistriflimides. On the other hand, the H-bond accepting (HBA) basicity (β) has always an opposite trend with respect H-bond donor acidity (α): i.e., decreases significantly in the case of bistriflimides and moderately increase for dicyanamides.



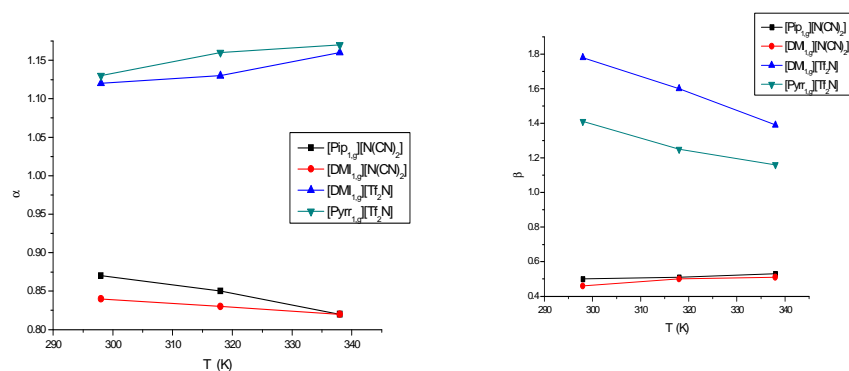


Figure 3.16: Variations of solvatochromic parameters with temperature. Top left— E_T^N variation for four ILs with temperature; top right— π^* variation for four ILs with temperature; bottom left— α variation for four ILs with temperature; and bottom right— β variation for four ILs with temperature.

The behavior of dicyanamide-based ILs is in agreement with that of a polar solvent; when the temperature is increased, in the case of betaine dye the ground state interactions are weakened, thus reducing the gap between the ground and excited state of the betaine dye. Contemporaneously, decreases also the H-bond donor acidity. The opposite effect of temperature in the case of bistriflimide-based ILs seems to be largely related to the decrease in H-bond accepting (HBA) basicity (β) of this anion on increasing temperature, which induces more efficient electrostatic and hydrogen-bond interactions between IL cation and the zwitterionic dye, determining an increase in H-bond donor acidity. However, a detailed discussion of the effect of the IL at molecular level in terms of these parameters is surely difficult being these properties determined by the combination of responses of two or more probes and the effects extremely moderate.

3.6 Conclusion

This investigation has evidenced the possibility to obtain hyper-polar ILs introducing a glyceryl moiety of the cation core. In particular, the cation *N*-methyl-*N*-glycerylpyrrolidinium [Pyrr_{1,g}]⁺ gives when associated to proper anions, such as dicyanamide and bistriflimide, ILs having not too high viscosities and moderate conductivities. [Pyrr_{1,g}][N(CN)₂] has the least viscosity and maximum conductivity among all the investigated glyceryl-substituted salts. The anionic nature, however, strongly affects also the

solvatochromic parameters: the lower coordinating ability of as $[\text{Tf}_2\text{N}]^-$ anion disfavoring the formation of H-bonding between IL cation and anion induces more efficient electrostatic and hydrogen-bond interactions between ILs and the zwitterionic dye (or, more in general, dissolved solutes), thus stabilizing the ground state of ionic probe and giving “hyperpolarity”.

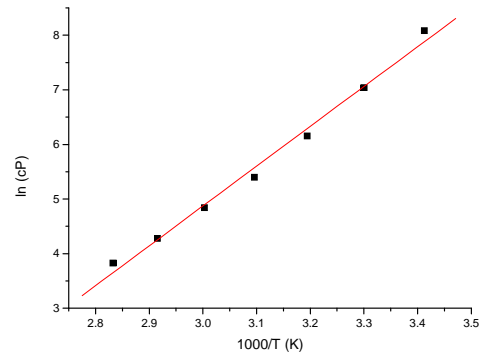
Chapter 3

Here, we report how the Fitting parameters are obtained using Origin8 software.

Appendix 1: Analysis of the behavior of viscosity values for [DMI_{1,g}][N(CN)₂], [Pip_{1,g}][N(CN)₂], [Pyr_{1,g}][N(CN)₂], [MIM_{1,g}][N(CN)₂], [FHMPip_{1,g}][N(CN)₂] with temperature.

Arrhenius Plots

$$\ln \eta = \ln \eta_0 + E/T$$



Linear Regression for Data:

$$Y = A + B * X$$

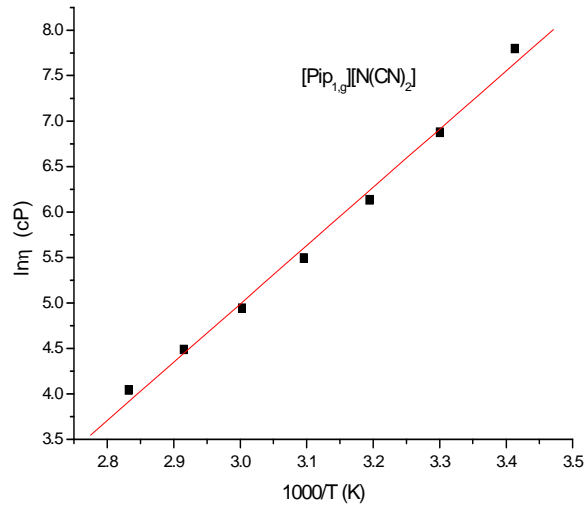
| Parameter | Value | Error | t-Value | Prob> t |
|-----------|-----------|---------|-----------|---------|
| A | -16.99294 | 0.95628 | -17.76989 | <0.0001 |
| B | 7.28837 | 0.30712 | 3.73316 | <0.0001 |

| R | R-Square(COD) | Adj. R-Square | Root-MSE(SD) | N |
|---------|---------------|---------------|--------------|---|
| 0.99559 | 0.9912 | 0.98944 | 0.15704 | 7 |

| Parameter | LCI | UCI |
|-----------|-----------|-----------|
| A | -19.45113 | -14.53476 |
| B | 6.49896 | 8.07779 |

ANOVA Table:

| Item | Degrees of Freedom | Sum of Squares | Mean Square | F Statistic |
|-------|--------------------|----------------|-------------|-------------|
| Model | 1 | 13.89054 | 13.89054 | 563.26307 |
| Error | 5 | 0.1233 | 0.02466 | |
| Total | 6 | 14.01385 | | |



$$Y = A + B * X$$

| Parameter | Value | Error | t-Value | Prob> t |
|-----------|----------|----------|----------|---------|
| A | -14.2237 | 60.73284 | -19.4091 | <0.0001 |
| B | 6.40484 | 0.23534 | 27.21496 | <0.0001 |

| R | R-Square(COD) | Adj. R-Square | Root-MSE(SD) | N |
|---------|---------------|---------------|--------------|---|
| 0.99664 | 0.99329 | 0.99195 | 0.12035 | 7 |

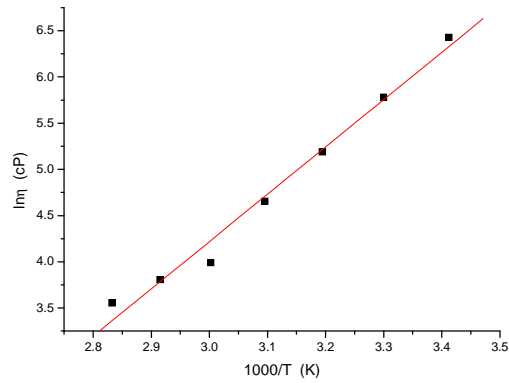
| Parameter | LCI | UCI |
|-----------|-----------|-----------|
| A | -16.10758 | -12.33994 |
| B | 5.79987 | 7.0098 |

ANOVA Table:

| Item | Degrees of Freedom | Sum of Squares | Mean Square | F Statistic |
|-------|--------------------|----------------|-------------|-------------|
| Model | 1 | 10.72689 | 10.72689 | 740.65419 |
| Error | 5 | 0.07241 | 0.01448 | |
| Total | 6 | 10.79931 | | |

Chapter 3

[Pyrr1,g][N(CN)2]



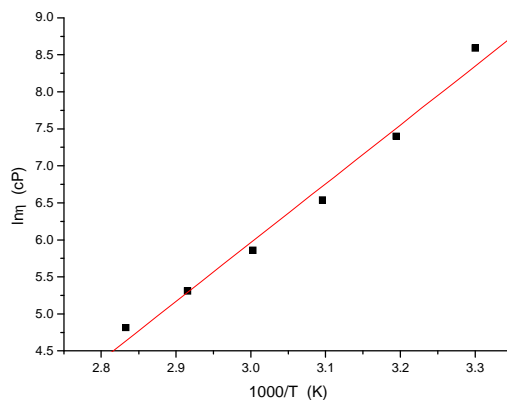
| Parameter | Value | Error | t-Value | Prob> t |
|-----------|-----------|---------|-----------|---------|
| A | -11.14128 | 0.90731 | -12.27949 | <0.0001 |
| B | 5.11995 | 0.29137 | 17.57195 | <0.0001 |

| R | R-Square(COD) | Adj. R-Square | Root-MSE(SD) | N |
|-------|---------------|---------------|--------------|---|
| 0.992 | 0.98406 | 0.98088 | 0.149 | 7 |

| Parameter | LCI | UCI |
|-----------|-----------|----------|
| A | -13.47359 | -8.80897 |
| B | 4.37096 | 5.86895 |

ANOVA Table:

| Item | Degrees of Freedom | Sum of Squares | Mean Square | F Statistic |
|-------|--------------------|----------------|-------------|-------------|
| Model | 1 | 6.85473 | 6.85473 | 308.77341 |
| Error | 5 | 0.111 | 0.0222 | |
| Total | 6 | 6.96573 | | |

[Mor_{1,g}][N(CN)₂]

$$Y = A + B * X$$

| Parameter | Value | Error | t-Value | Prob> t |
|-----------|-----------|---------|-----------|-----------|
| A | -17.88128 | 1.53402 | -11.65646 | 3.0965E-4 |
| B | 7.94817 | 0.50111 | 15.86113 | <0.0001 |

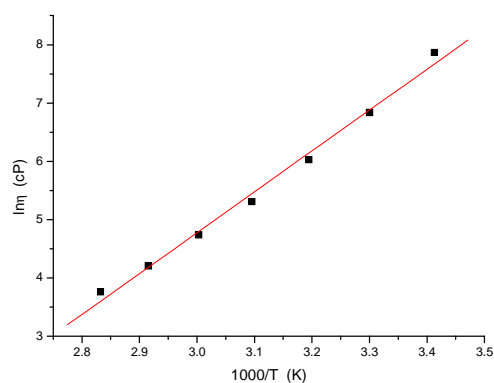
| R | R-Square(COD) | Adj. R-Square | Root-MSE(SD) | N |
|---------|---------------|---------------|--------------|---|
| 0.99214 | 0.98435 | 0.98044 | 0.19597 | 6 |

| Parameter | LCI | UCI |
|-----------|-----------|-----------|
| A | -22.14041 | -13.62216 |
| B | 6.55687 | 9.33947 |

ANOVA Table:

| Item | Degrees of Freedom | Sum of Squares | Mean Square | F Statistic |
|-------|--------------------|----------------|-------------|-------------|
| Model | 1 | 9.6612 | 9.6612 | 251.57546 |
| Error | 4 | 0.15361 | 0.0384 | |
| Total | 5 | 9.81481 | | |

[MIM_{1,g}][N(CN)₂]



$$Y = A + B * X$$

| Parameter | Value | Error | t-Value | Prob> t |
|-----------|-----------|---------|-----------|---------|
| A | -16.26218 | 0.86464 | -18.80811 | <0.0001 |
| B | 7.01302 | 0.27767 | 25.25693 | <0.0001 |

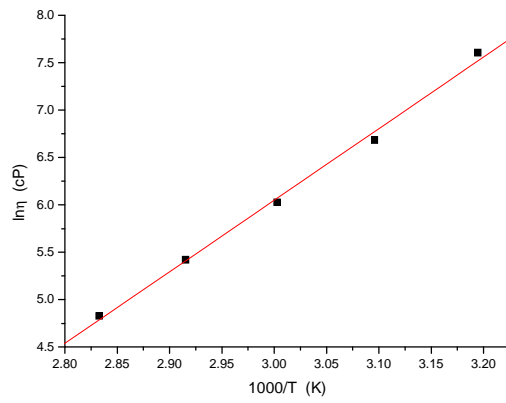
| R | R-Square(COD) | Adj. R-Square | Root-MSE(SD) | N |
|--------|---------------|---------------|--------------|---|
| 0.9961 | 0.99222 | 0.99067 | 0.14199 | 7 |

| Parameter | LCI | UCI |
|-----------|-----------|-----------|
| A | -18.48479 | -14.03956 |
| B | 6.29926 | 7.72679 |

ANOVA Table:

| Item | Degrees of Freedom | Sum of Squares | Mean Square | F Statistic |
|-------|--------------------|----------------|-------------|-------------|
| Model | 1 | 12.86082 | 12.86082 | 637.91255 |
| Error | 5 | 0.1008 | 0.02016 | |
| Total | 6 | 12.96162 | | |

[FHMPip_{1,g}][N(CN)₂]



| Parameter | Value | Error | t-Value | Prob> t |
|-----------|-----------|---------|-----------|------------|
| A | -16.59586 | 0.83926 | -19.77443 | 2.82602E-4 |
| B | 7.54823 | 0.27872 | 27.08212 | 1.10483E-4 |

| R | R-Square(COD) | Adj. R-Square | Root-MSE(SD) | N |
|---------|---------------|---------------|--------------|---|
| 0.99796 | 0.99593 | 0.99457 | 0.07978 | 5 |

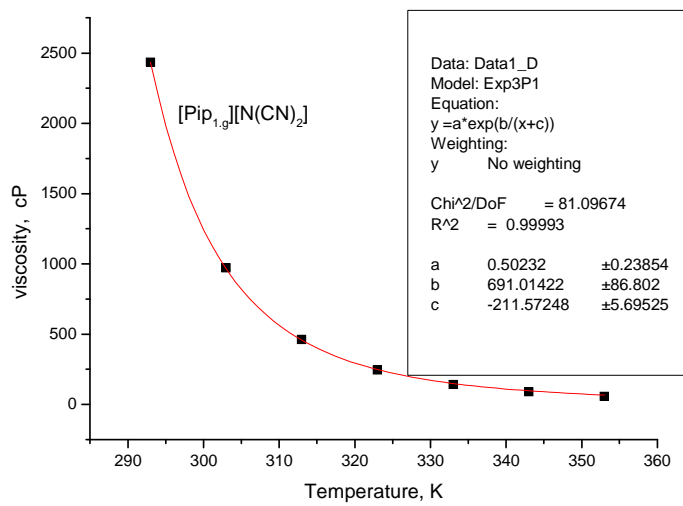
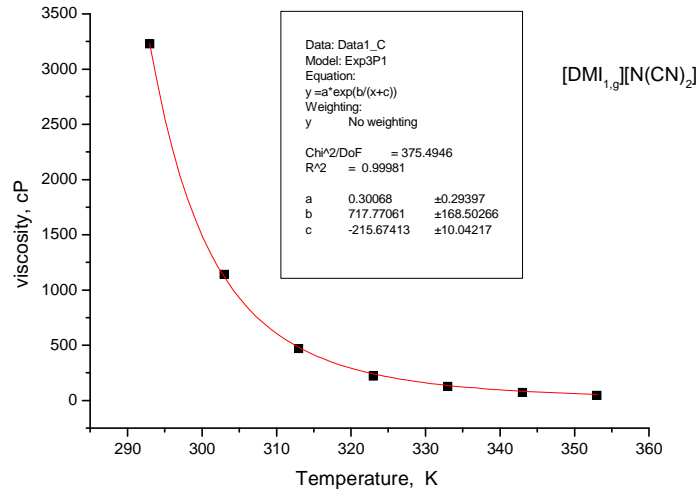
| Parameter | LCI | UCI |
|-----------|-----------|-----------|
| A | -19.26677 | -13.92495 |
| B | 6.66122 | 8.43523 |

ANOVA Table:

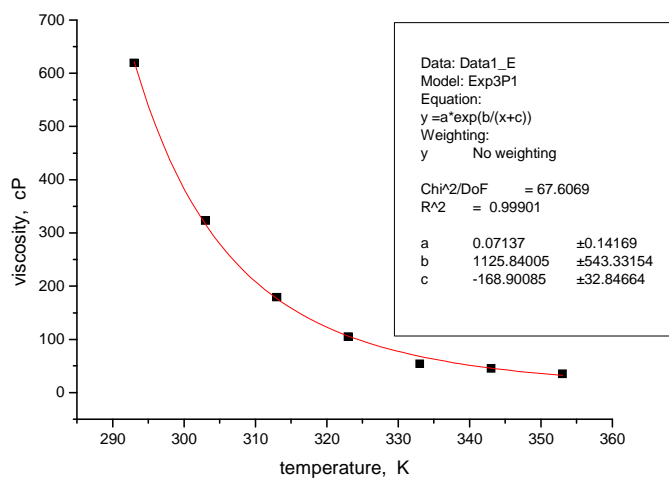
| Item | Degrees of Freedom | Sum of Squares | Mean Square | F Statistic |
|-------|--------------------|----------------|-------------|-------------|
| Model | 1 | 4.668 | 4.668 | 733.44137 |
| Error | 3 | 0.01909 | 0.00636 | |
| Total | 4 | 4.68709 | | |

FITTING to VTF Equation:

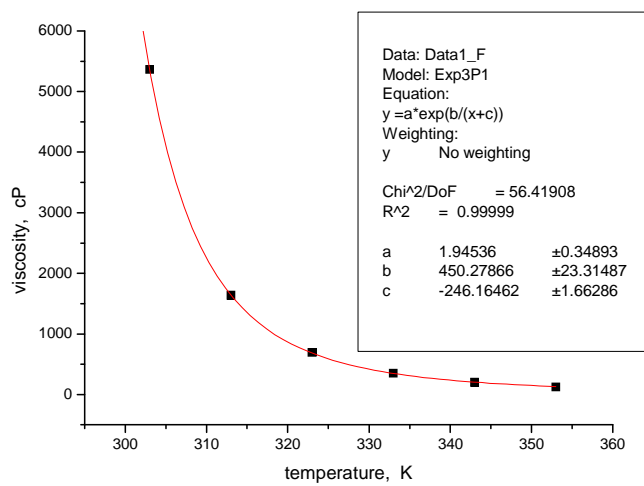
$$\eta = \eta_0 \exp[B/(T-T_0)]$$



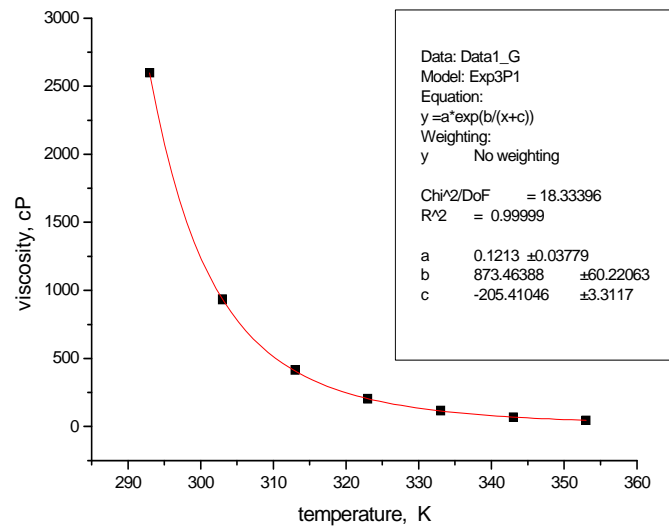
[Pyr_{1,9}][N(CN)₂]



$[\text{Mor}_{1,g}][\text{N}(\text{CN})_2]$



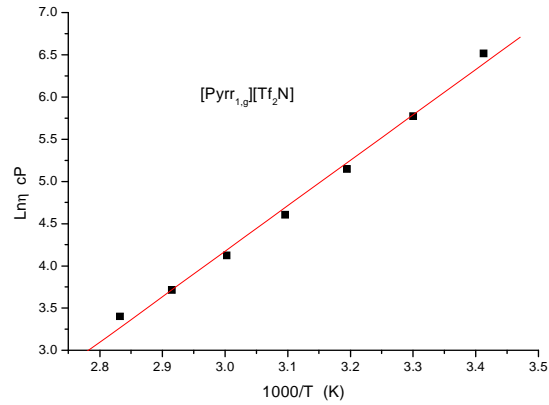
$[\text{MIM}_{1,g}][\text{N}(\text{CN})_2]$



Viscosity values for [DMI_{1,g}][Tf₂N], [Pip_{1,g}][Tf₂N], [Pyrr_{1,g}][Tf₂N], [MIM_{1,g}][Tf₂N] and [Mor_{1,g}][Tf₂N].

Arrhenius Plots

$$\ln \eta = \ln \eta_0 + E/T$$



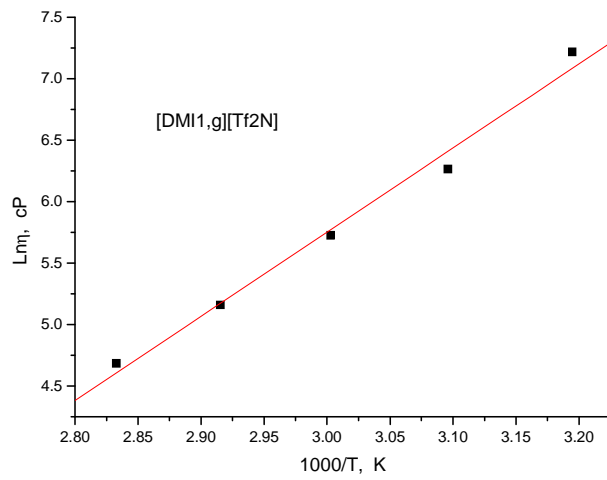
| Parameter | Value | Error | t-Value | Prob> t |
|-----------|-----------|---------|-----------|---------|
| A | -11.97782 | 0.5973 | -20.05225 | <0.0001 |
| B | 5.38364 | 0.19183 | 28.06534 | <0.0001 |

| R | R-Square(COD) | Adj. R-Square | Root-MSE(SD) | N |
|---------|---------------|---------------|--------------|---|
| 0.99684 | 0.99369 | 0.99243 | 0.09809 | 7 |

| Parameter | LCI | UCI |
|-----------|-----------|-----------|
| A | -13.51331 | -10.44234 |
| B | 4.89054 | 5.87675 |

ANOVA Table:

| Item | Degrees of Freedom | Sum of Squares | Mean Square | F Statistic |
|-------|--------------------|----------------|-------------|-------------|
| Model | 1 | 7.57898 | 7.57898 | 787.6635 |
| Error | 5 | 0.04811 | 0.00962 | |
| Total | 6 | 7.62709 | | |



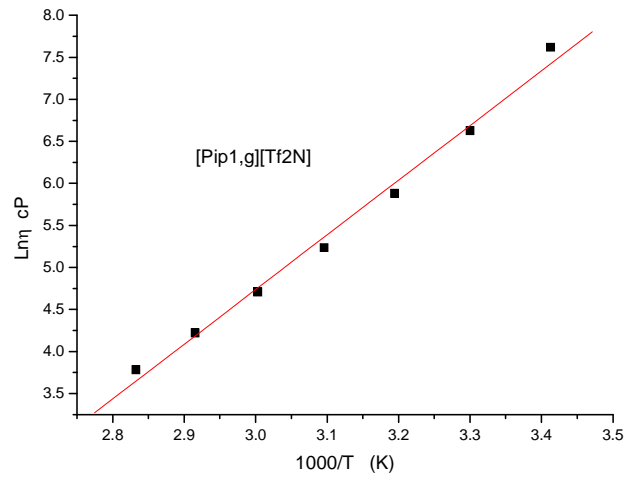
| Parameter | Value | Error | t-Value | Prob> t |
|-----------|-----------|---------|-----------|-----------|
| A | -14.79556 | 1.3106 | -11.28916 | 0.00149 |
| B | 6.84897 | 0.43525 | 15.73581 | 5.5786E-4 |

| R | R-Square(COD) | Adj. R-Square | Root-MSE(SD) | N |
|-------|---------------|---------------|--------------|---|
| 0.994 | 0.98803 | 0.98404 | 0.12458 | 5 |

| Parameter | LCI | UCI |
|-----------|-----------|-----------|
| A | -18.96649 | -10.62463 |
| B | 5.46381 | 8.23413 |

ANOVA Table:

| Item | Degrees of Freedom | Sum of Squares | Mean Square | F Statistic |
|-------|--------------------|----------------|-------------|-------------|
| Model | 1 | 3.84319 | 3.84319 | 247.61571 |
| Error | 3 | 0.04656 | 0.01552 | |
| Total | 4 | 3.88975 | | |



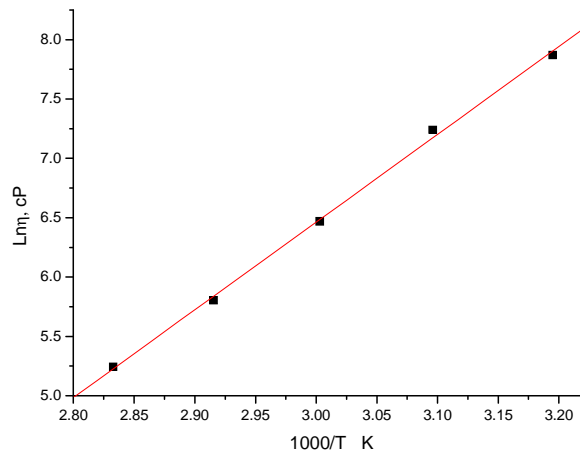
| Parameter | Value | Error | t-Value | Prob> t |
|-----------|----------|---------|-----------|---------|
| A | -14.7823 | 0.83895 | -17.61994 | <0.0001 |
| B | 6.50645 | 0.26942 | 24.14989 | <0.0001 |

| R | R-Square(COD) | Adj. R-Square | Root-MSE(SD) | N |
|---------|---------------|---------------|--------------|---|
| 0.99574 | 0.9915 | 0.9898 | 0.13777 | 7 |

| Parameter | LCI | UCI |
|-----------|----------|-----------|
| A | -16.9389 | -12.62571 |
| B | 5.81388 | 7.19901 |

ANOVA Table:

| Item | Degrees of Freedom | Sum of Squares | Mean Square | F Statistic |
|-------|--------------------|----------------|-------------|-------------|
| Model | 1 | 11.06995 | 11.06995 | 583.21705 |
| Error | 5 | 0.0949 | 0.01898 | |
| Total | 6 | 11.16486 | | |



| Parameter | Value | Error | t-Value | Prob> t |
|-----------|-----------|---------|-----------|---------|
| A | -15.73877 | 0.52372 | -30.05196 | <0.0001 |
| B | 7.40025 | 0.17393 | 42.54827 | <0.0001 |

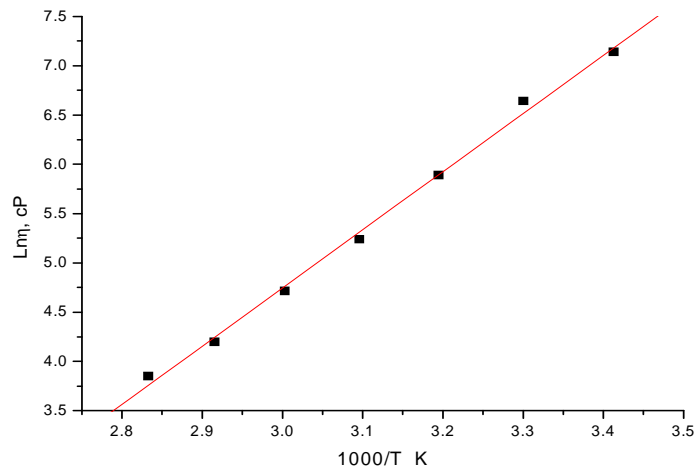
| R | R-Square(COD) | Adj. R-Square | Root-MSE(SD) | N |
|---------|---------------|---------------|--------------|---|
| 0.99917 | 0.99835 | 0.99779 | 0.04978 | 5 |

| Parameter | LCI | UCI |
|-----------|-----------|-----------|
| A | -17.40549 | -14.07206 |
| B | 6.84674 | 7.95376 |

ANOVA Table:

| Item | Degrees of Freedom | Sum of Squares | Mean Square | F Statistic |
|-------|--------------------|----------------|-------------|-------------|
| Model | 1 | 4.48677 | 4.48677 | 1810.35502 |
| Error | 3 | 0.00744 | 0.00248 | |
| Total | 4 | 4.49421 | | |

[MIM_{1,g}][Tf₂N]



$$Y = A + B * X$$

| Parameter | Value | Error | t-Value | Prob> t |
|-----------|-----------|---------|-----------|---------|
| A | -12.95642 | 0.51541 | -25.13828 | <0.0001 |
| B | 5.90028 | 0.16552 | 35.6477 | <0.0001 |

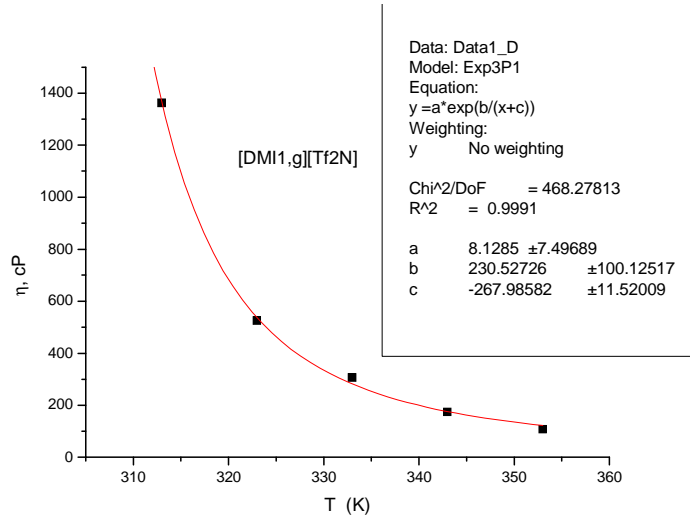
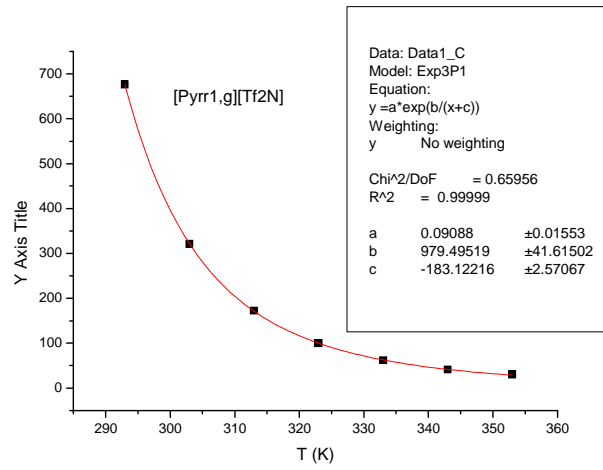
| R | R-Square(COD) | Adj. R-Square | Root-MSE(SD) | N |
|---------|---------------|---------------|--------------|---|
| 0.99804 | 0.99608 | 0.9953 | 0.08464 | 7 |

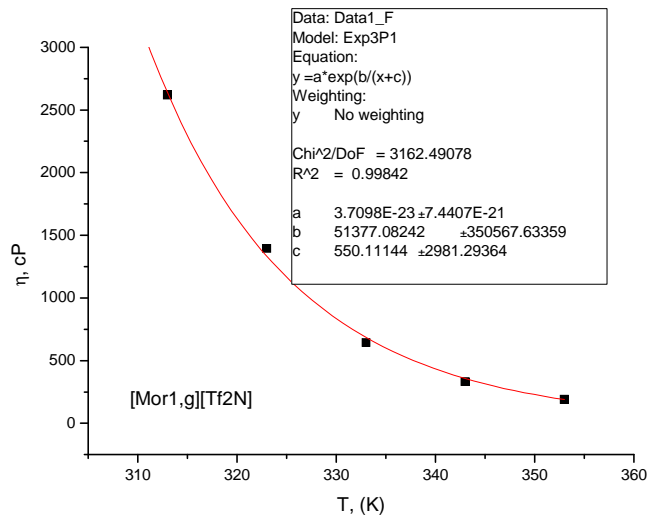
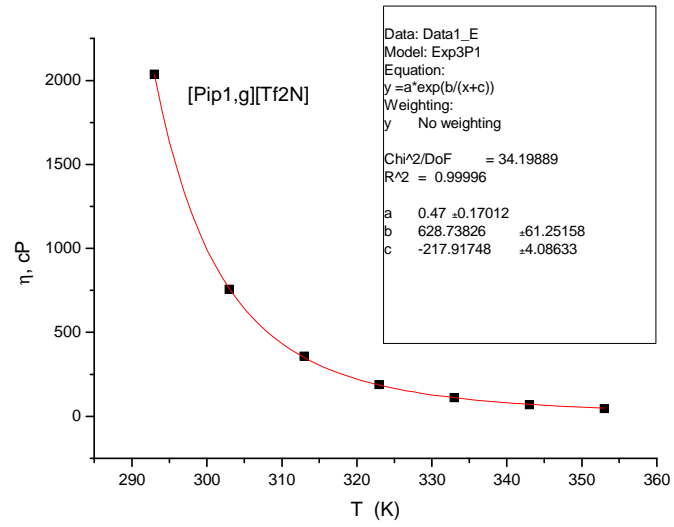
| Parameter | LCI | UCI |
|-----------|-----------|-----------|
| A | -14.28131 | -11.63153 |
| B | 5.4748 | 6.32575 |

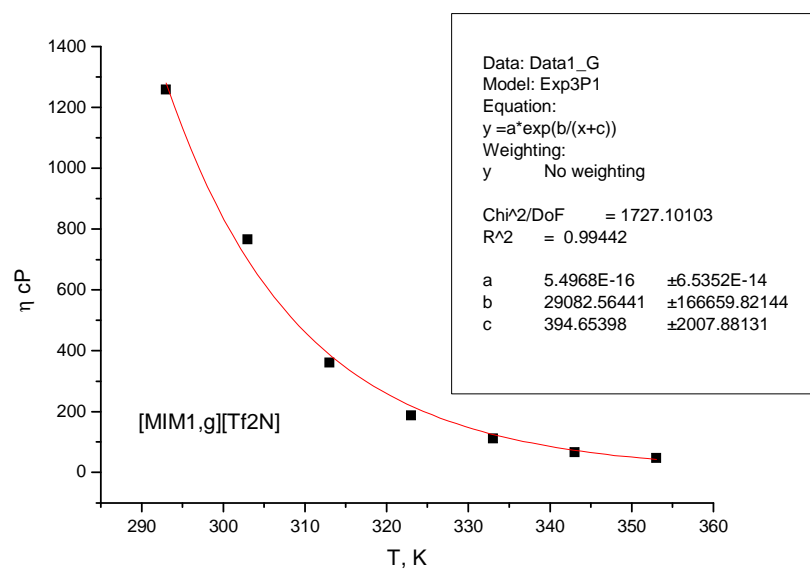
ANOVA Table:

| Item | Degrees of Freedom | Sum of Squares | Mean Square | F Statistic |
|-------|--------------------|----------------|-------------|-------------|
| Model | 1 | 9.10338 | 9.10338 | 1270.75857 |
| Error | 5 | 0.03582 | 0.00716 | |
| Total | 6 | 9.13919 | | |

VTF plots for all bistriflimide ILs:

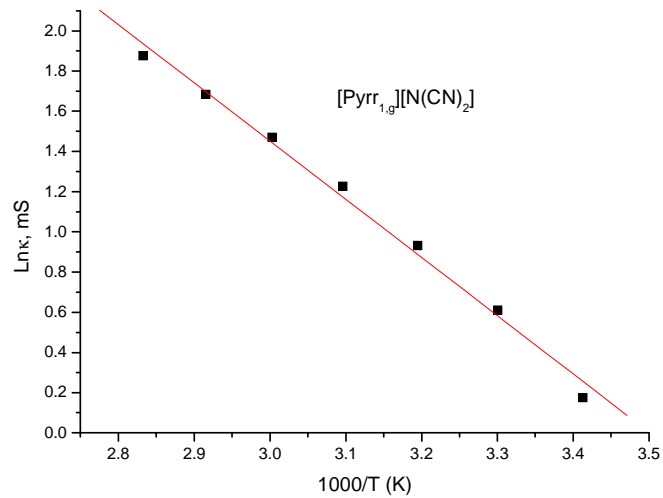






Conductivity

Arrhenius plots:



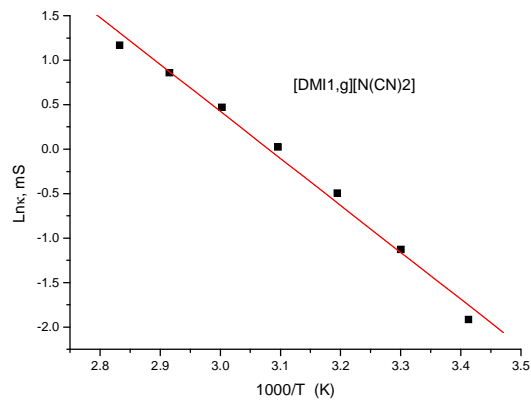
| Parameter | Value | Error | t-Value | Prob> t |
|-----------|----------|---------|-----------|---------|
| A | 10.14326 | 0.35029 | 28.95652 | <0.0001 |
| B | -2.89712 | 0.11249 | -25.75397 | <0.0001 |

| R | R-Square(COD) | Adj. R-Square | Root-MSE(SD) | N |
|----------|---------------|---------------|--------------|---|
| -0.99625 | 0.99252 | 0.99102 | 0.05752 | 7 |

| Parameter | LCI | UCI |
|-----------|----------|----------|
| A | 9.2428 | 11.04371 |
| B | -3.18629 | -2.60795 |

ANOVA Table:

| Item | Degrees of Freedom | Sum of Squares | Mean Square | F Statistic |
|-------|--------------------|----------------|-------------|-------------|
| Model | 1 | 2.19478 | 2.19478 | 663.26708 |
| Error | 5 | 0.01655 | 0.00331 | |
| Total | 6 | 2.21132 | | |



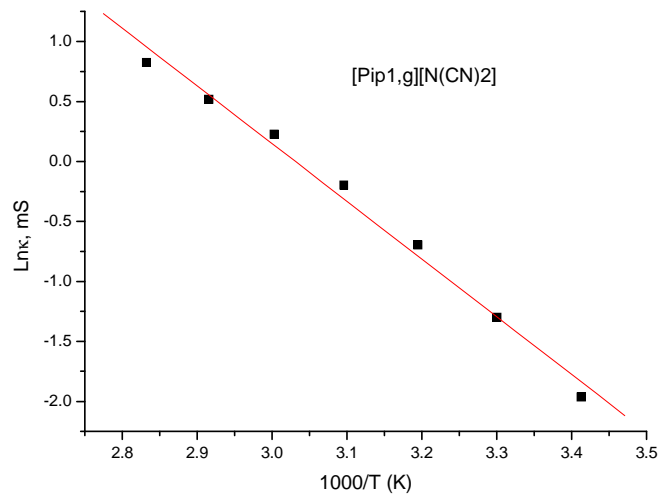
| Parameter | Value | Error | t-Value | Prob> t |
|-----------|----------|--------|-----------|---------|
| A | 16.26528 | 0.7405 | 21.96531 | <0.0001 |
| B | -5.28057 | 0.2378 | -22.20573 | <0.0001 |

| R | R-Square(COD) | Adj. R-Square | Root-MSE(SD) | N |
|----------|---------------|---------------|--------------|---|
| -0.99497 | 0.98996 | 0.98795 | 0.1216 | 7 |

| Parameter | LCI | UCI |
|-----------|----------|----------|
| A | 14.36177 | 18.16879 |
| B | -5.89186 | -4.66928 |

ANOVA Table:

| Item | Degrees of Freedom | Sum of Squares | Mean Square | F Statistic |
|-------|--------------------|----------------|-------------|-------------|
| Model | 1 | 7.29154 | 7.29154 | 493.09457 |
| Error | 5 | 0.07394 | 0.01479 | |
| Total | 6 | 7.36548 | | |



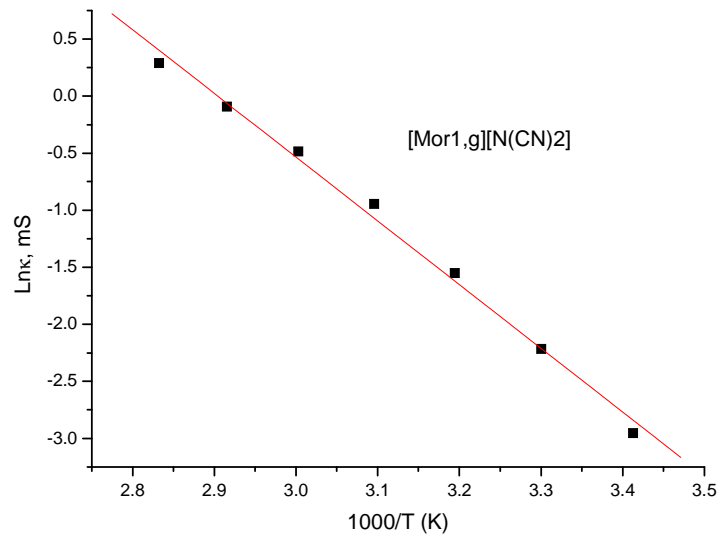
| Parameter | Value | Error | t-Value | Prob> t |
|-----------|----------|---------|-----------|---------|
| A | 14.58681 | 0.69299 | 21.04903 | <0.0001 |
| B | -4.8127 | 0.22255 | -21.62566 | <0.0001 |

| R | R-Square(COD) | Adj. R-Square | Root-MSE(SD) | N |
|---------|---------------|---------------|--------------|---|
| -0.9947 | 0.98942 | 0.98731 | 0.1138 | 7 |

| Parameter | LCI | UCI |
|-----------|----------|----------|
| A | 12.80542 | 16.3682 |
| B | -5.38477 | -4.24063 |

ANOVA Table:

| Item | Degrees of Freedom | Sum of Squares | Mean Square | F Statistic |
|-------|--------------------|----------------|-------------|-------------|
| Model | 1 | 6.05669 | 6.05669 | 467.66933 |
| Error | 5 | 0.06475 | 0.01295 | |
| Total | 6 | 6.12144 | | |



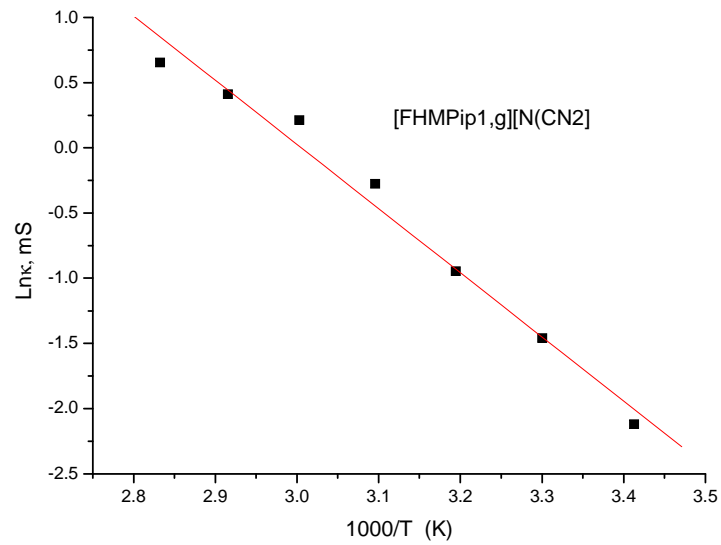
| Parameter | Value | Error | t-Value | Prob> t |
|-----------|----------|---------|-----------|---------|
| A | 16.2322 | 0.62194 | 26.09912 | <0.0001 |
| B | -5.58889 | 0.19973 | -27.98228 | <0.0001 |

| R | R-Square(COD) | Adj. R-Square | Root-MSE(SD) | N |
|----------|---------------|---------------|--------------|---|
| -0.99682 | 0.99365 | 0.99239 | 0.10213 | 7 |

| Parameter | LCI | UCI |
|-----------|----------|----------|
| A | 14.63344 | 17.83095 |
| B | -6.10231 | -5.07547 |

ANOVA Table:

| Item | Degrees of Freedom | Sum of Squares | Mean Square | F Statistic |
|-------|--------------------|----------------|-------------|-------------|
| Model | 1 | 8.16788 | 8.16788 | 783.00799 |
| Error | 5 | 0.05216 | 0.01043 | |
| Total | 6 | 8.22004 | | |



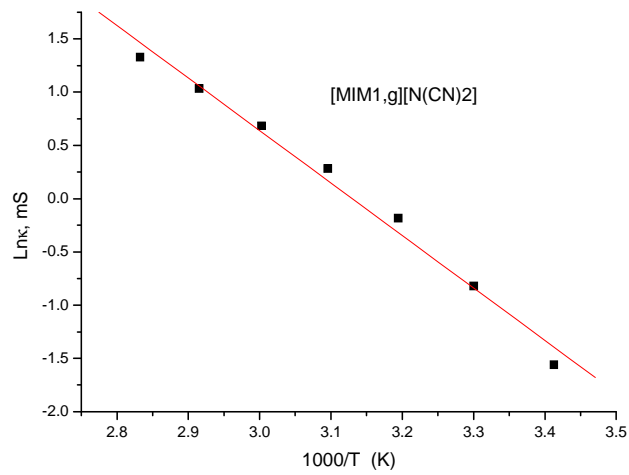
| Parameter | Value | Error | t-Value | Prob> t |
|-----------|----------|---------|-----------|---------|
| A | 14.80118 | 0.95055 | 15.57125 | <0.0001 |
| B | -4.92476 | 0.30526 | -16.13321 | <0.0001 |

| R | R-Square(COD) | Adj. R-Square | Root-MSE(SD) | N |
|----------|---------------|---------------|--------------|---|
| -0.99053 | 0.98115 | 0.97738 | 0.1561 | 7 |

| Parameter | LCI | UCI |
|-----------|----------|----------|
| A | 12.35773 | 17.24463 |
| B | -5.70944 | -4.14007 |

ANOVA Table:

| Item | Degrees of Freedom | Sum of Squares | Mean Square | F Statistic |
|-------|--------------------|----------------|-------------|-------------|
| Model | 1 | 6.34202 | 6.34202 | 260.2804 |
| Error | 5 | 0.12183 | 0.02437 | |
| Total | 6 | 6.46385 | | |



| Parameter | Value | Error | t-Value | Prob> t |
|-----------|----------|---------|-----------|---------|
| A | 15.42808 | 0.77999 | 19.77989 | <0.0001 |
| B | -4.92921 | 0.25048 | -19.67878 | <0.0001 |

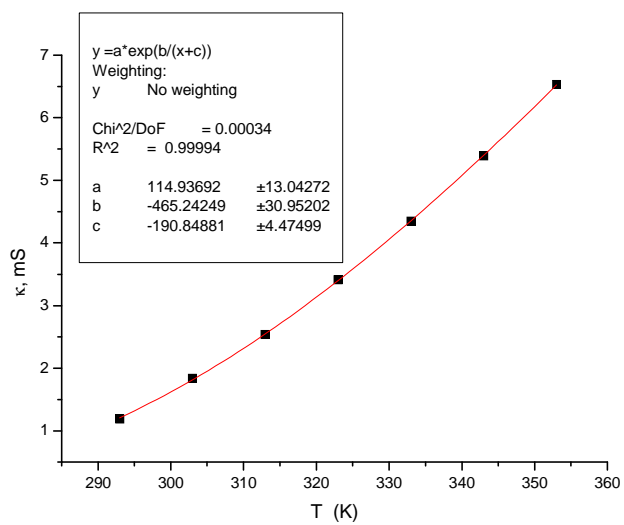
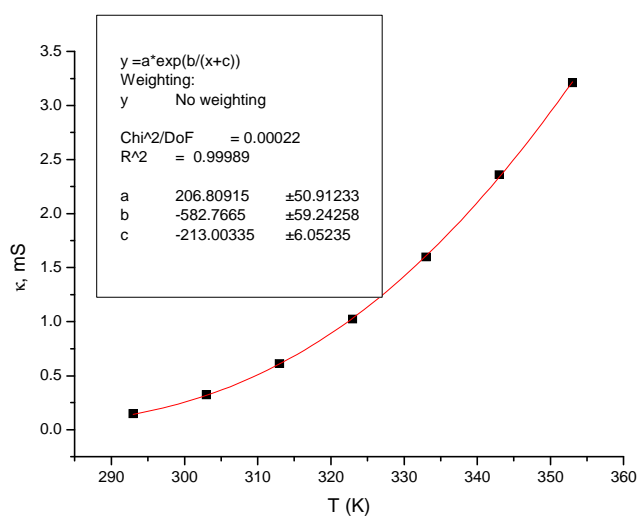
| R | R-Square(COD) | Adj. R-Square | Root-MSE(SD) | N |
|----------|---------------|---------------|--------------|---|
| -0.99361 | 0.98725 | 0.9847 | 0.12809 | 7 |

| Parameter | LCI | UCI |
|-----------|----------|----------|
| A | 13.42306 | 17.4331 |
| B | -5.5731 | -4.28532 |

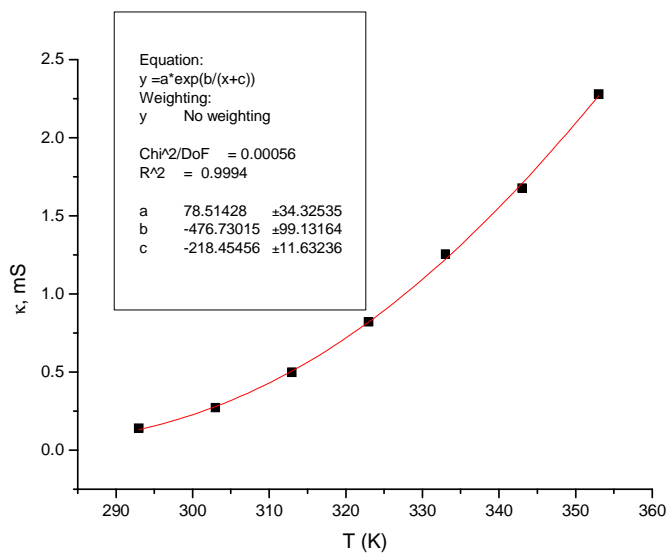
ANOVA Table:

| Item | Degrees of Freedom | Sum of Squares | Mean Square | F Statistic |
|-------|--------------------|----------------|-------------|-------------|
| Model | 1 | 6.35349 | 6.35349 | 387.25433 |
| Error | 5 | 0.08203 | 0.01641 | |
| Total | 6 | 6.43553 | | |

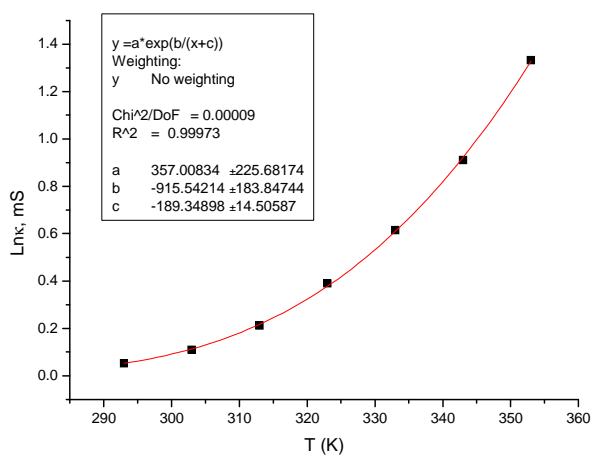
VTF plots for dicyanamide ILs:

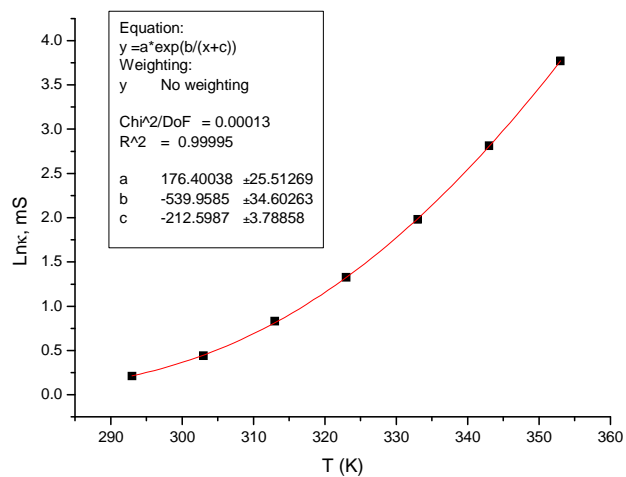
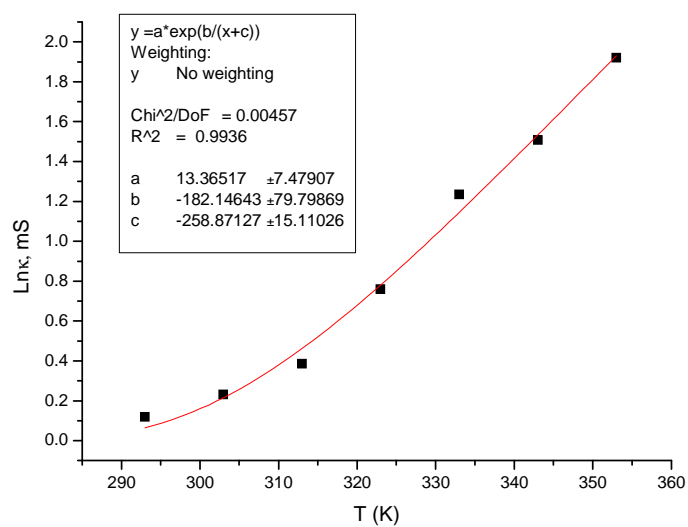
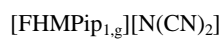
[Pyrr_{1,g}][N(CN)₂]**[DMI_{1,g}][N(CN)₂]**

[Pip_{1,g}][N(CN)₂]



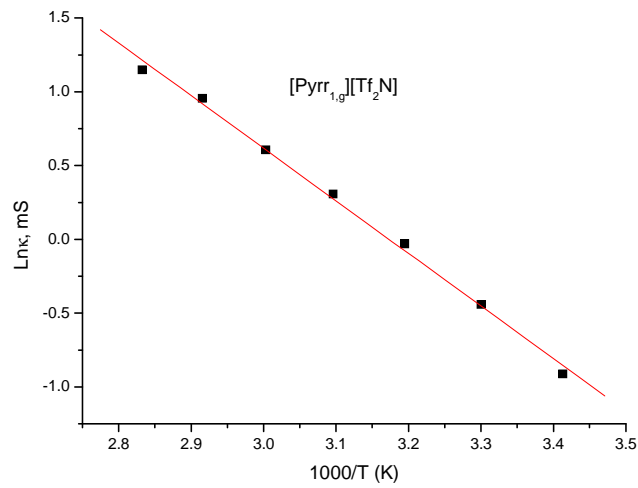
[Mor_{1,g}][N(CN)₂]





Bistriflimides

Arrhenius Plots

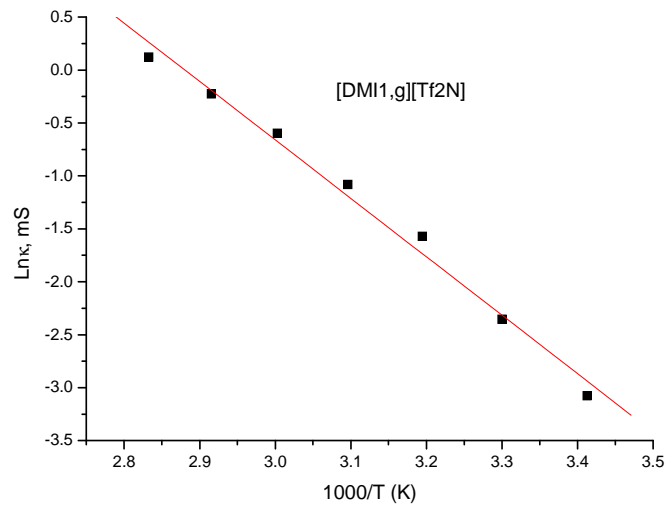


| Parameter | Value | Error | t-Value | Prob> t |
|-----------|---------------|---------------|--------------|---------|
| A | 11.31715 | 0.2996 | 37.77476 | <0.0001 |
| B | -3.56636 | 0.09621 | -37.06789 | <0.0001 |
| R | R-Square(COD) | Adj. R-Square | Root-MSE(SD) | N |
| -0.99819 | 0.99637 | 0.99565 | 0.0492 | 7 |

| Parameter | LCI | UCI |
|-----------|----------|----------|
| A | 10.54702 | 12.08729 |
| B | -3.81367 | -3.31904 |

ANOVA Table:

| Item | Degrees of Freedom | Sum of Squares | Mean Square | F Statistic |
|-------|--------------------|----------------|-------------|-------------|
| Model | 1 | 3.32588 | 3.32588 | 1374.02862 |
| Error | 5 | 0.0121 | 0.00242 | |
| Total | 6 | 3.33799 | | |



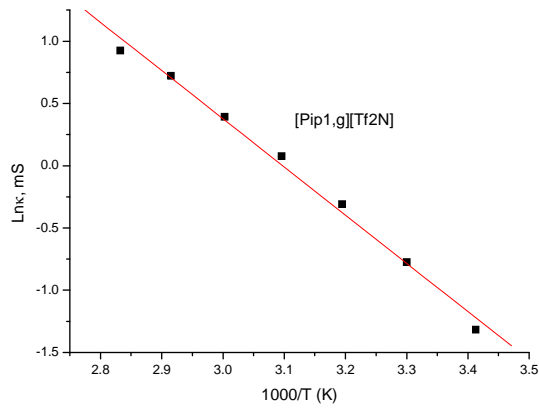
| Parameter | Value | Error | t-Value | Prob> t |
|-----------|----------|---------|-----------|---------|
| A | 15.89831 | 0.80234 | 19.81488 | <0.0001 |
| B | -5.51927 | 0.25766 | -21.42057 | <0.0001 |

| R | R-Square(COD) | Adj. R-Square | Root-MSE(SD) | N |
|---------|---------------|---------------|--------------|---|
| -0.9946 | 0.98922 | 0.98706 | 0.13176 | 7 |

| Parameter | LCI | UCI |
|-----------|----------|----------|
| A | 13.83583 | 17.9608 |
| B | -6.18161 | -4.85693 |

ANOVA Table:

| Item | Degrees of Freedom | Sum of Squares | Mean Square | F Statistic |
|-------|--------------------|----------------|-------------|-------------|
| Model | 1 | 7.96566 | 7.96566 | 458.84072 |
| Error | 5 | 0.0868 | 0.01736 | |
| Total | 6 | 8.05246 | | |



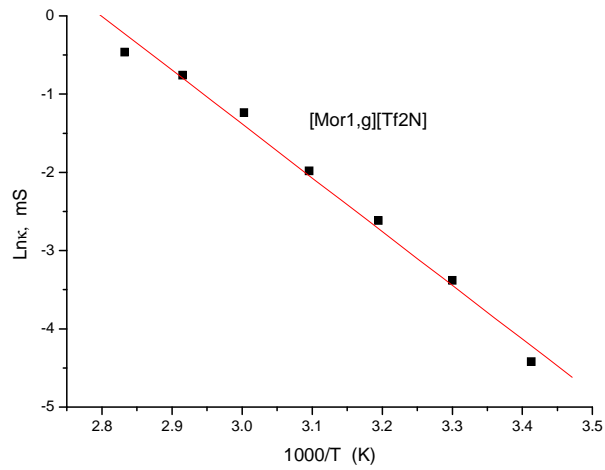
| Parameter | Value | Error | t-Value | Prob> t |
|-----------|----------|---------|-----------|---------|
| A | 12.00231 | 0.46955 | 25.56145 | <0.0001 |
| B | -3.87493 | 0.15079 | -25.69761 | <0.0001 |

| R | R-Square(COD) | Adj. R-Square | Root-MSE(SD) |
|----------|---------------|---------------|--------------|
| N | | | |
| -0.99624 | 0.99249 | 0.99098 | 0.07711 |

| Parameter | LCI | UCI |
|-----------|----------|----------|
| A | 10.7953 | 13.20932 |
| B | -4.26254 | -3.48731 |

ANOVA Table:

| Item | Degrees of Freedom | Sum of Squares | Mean Square | F |
|-----------|--------------------|----------------|-------------|---|
| Model | 1 | 3.92631 | 3.92631 | |
| 660.36697 | | | | |
| Error | 5 | 0.02973 | 0.00595 | |
| Total | 6 | 3.95604 | | |



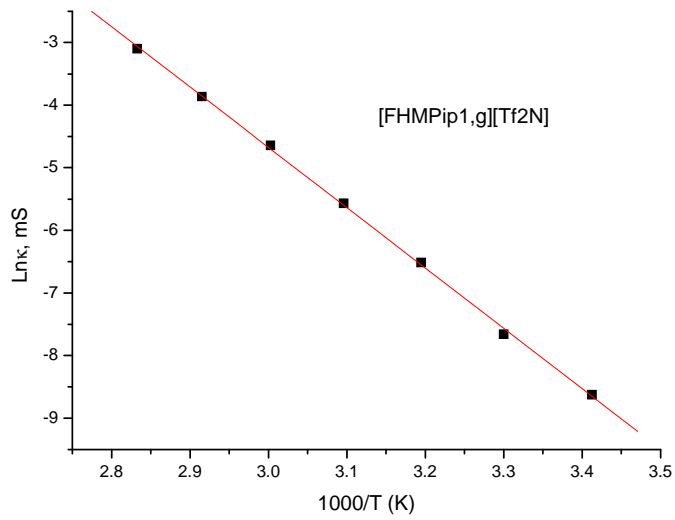
| Parameter | Value | Error | t-Value | Prob> t |
|-----------|----------|---------|-----------|---------|
| A | 19.26647 | 1.03119 | 18.68368 | <0.0001 |
| B | -6.88237 | 0.33115 | -20.78293 | <0.0001 |

| R | R-Square(COD) | Adj. R-Square | Root-MSE(SD) | N |
|---|---------------|---------------|--------------|---|
| - | 0.98856 | 0.98627 | 0.16934 | 7 |

| Parameter | LCI | UCI |
|-----------|----------|----------|
| A | 16.61571 | 21.91723 |
| B | -7.73363 | -6.03111 |

ANOVA Table:

| Item | Degrees of Freedom | Sum of Squares | Mean Square | F Statistic |
|-------|--------------------|----------------|-------------|-------------|
| Model | 1 | 12.38607 | 12.38607 | 431.93038 |
| Error | 5 | 0.14338 | 0.02868 | |
| Total | 6 | 12.52945 | | |



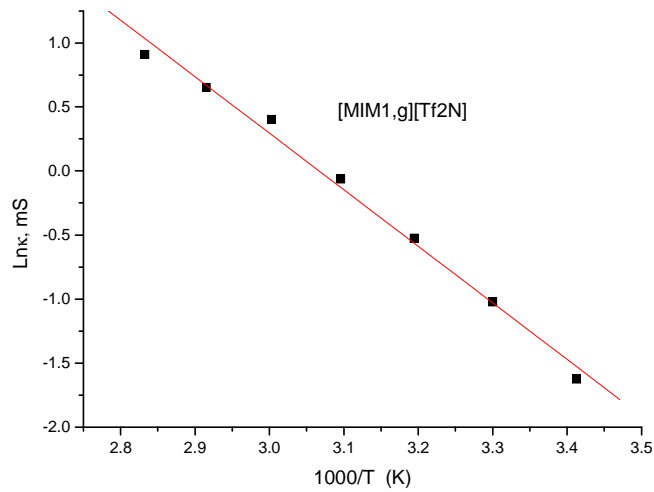
| Parameter | Value | Error | t-Value | Prob> t |
|-----------|----------|---------|-----------|---------|
| A | 24.2477 | 0.35351 | 68.59211 | <0.0001 |
| B | -9.63954 | 0.11352 | -84.91192 | <0.0001 |

| R | R-Square(COD) | Adj. R-Square | Root-MSE(SD) | N |
|----------|---------------|---------------|--------------|---|
| -0.99965 | 0.99931 | 0.99917 | 0.05805 | 7 |

| Parameter | LCI | UCI |
|-----------|----------|----------|
| A | 23.33898 | 25.15641 |
| B | -9.93136 | -9.34771 |

ANOVA Table:

| Item | Degrees of Freedom | Sum of Squares | Mean Square | F Statistic |
|-------|--------------------|----------------|-------------|-------------|
| Model | 1 | 24.29799 | 24.29799 | 7210.03402 |
| Error | 5 | 0.01685 | 0.00337 | |
| Total | 6 | 24.31484 | | |



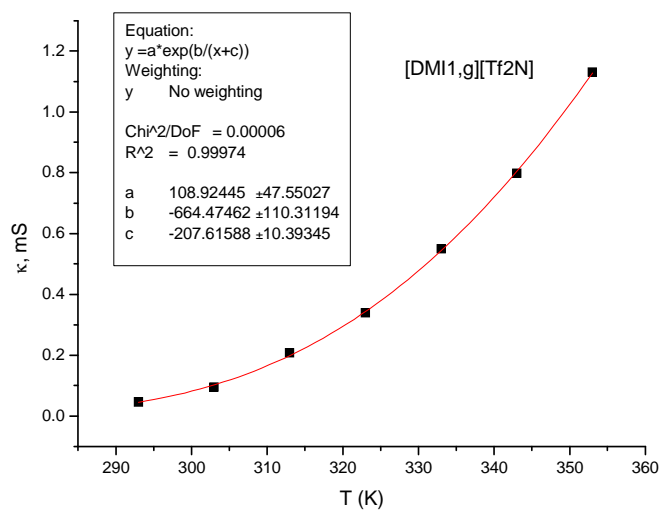
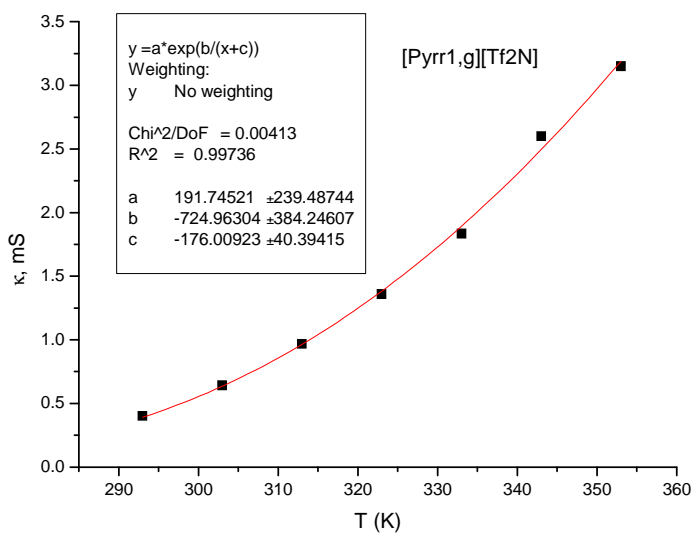
| Parameter | Value | Error | t-Value | Prob> t |
|-----------|----------|---------|-----------|---------|
| A | 13.54093 | 0.57919 | 23.37926 | <0.0001 |
| B | -4.41547 | 0.186 | -23.73929 | <0.0001 |

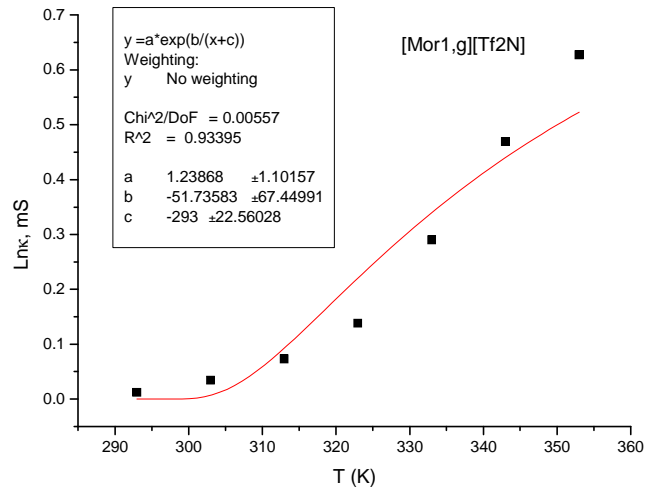
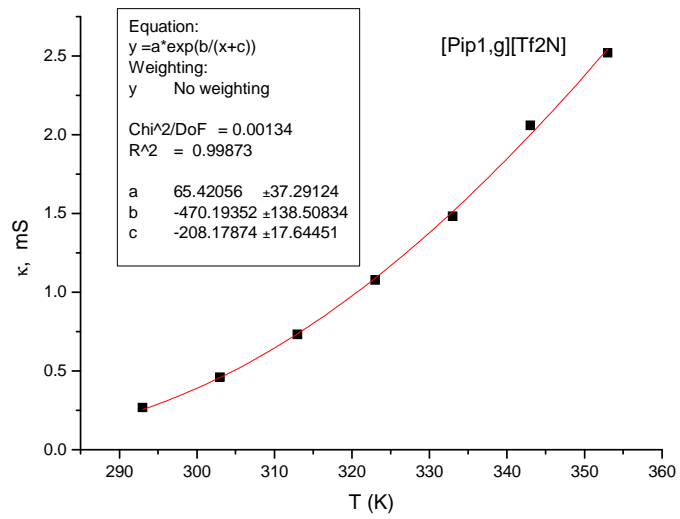
| R | R-Square(COD) | Adj. R-Square | Root-MSE(SD) | N |
|----------|---------------|---------------|--------------|---|
| -0.99559 | 0.99121 | 0.98945 | 0.09511 | 7 |

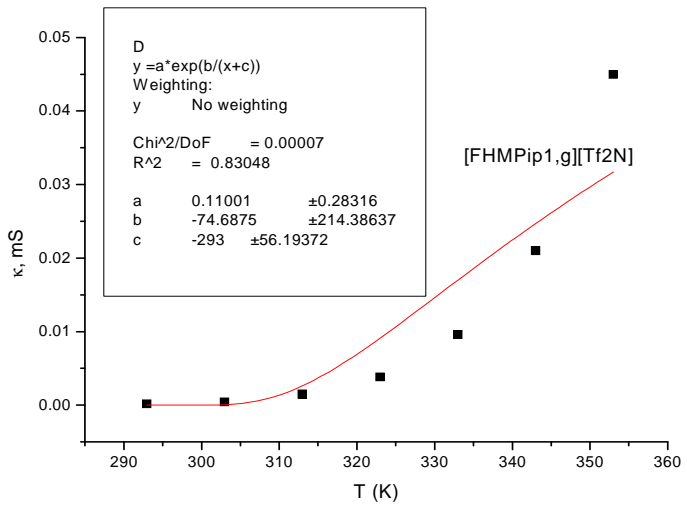
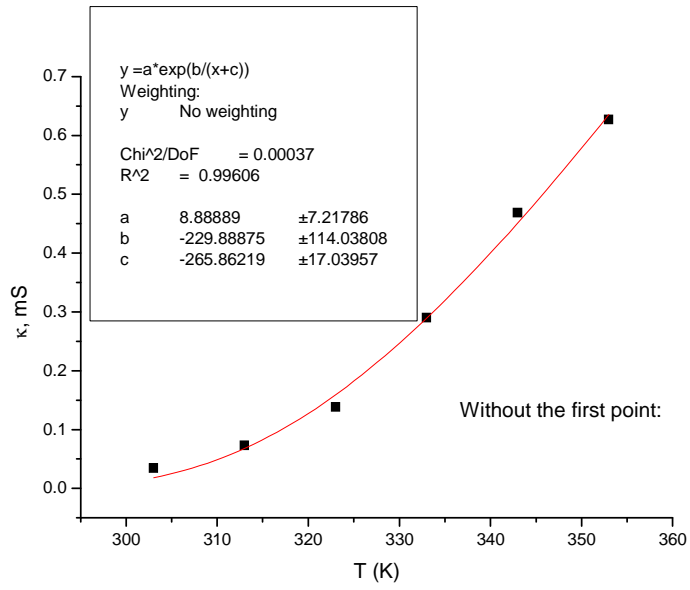
| Parameter | LCI | UCI |
|-----------|----------|----------|
| A | 12.05209 | 15.02978 |
| B | -4.89359 | -3.93735 |

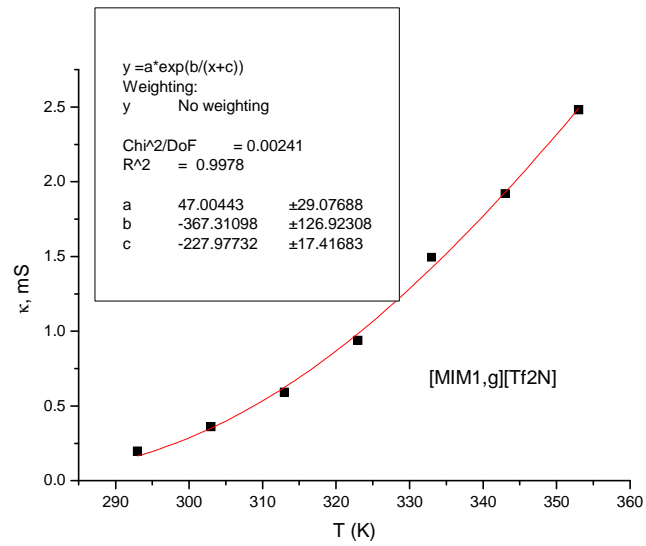
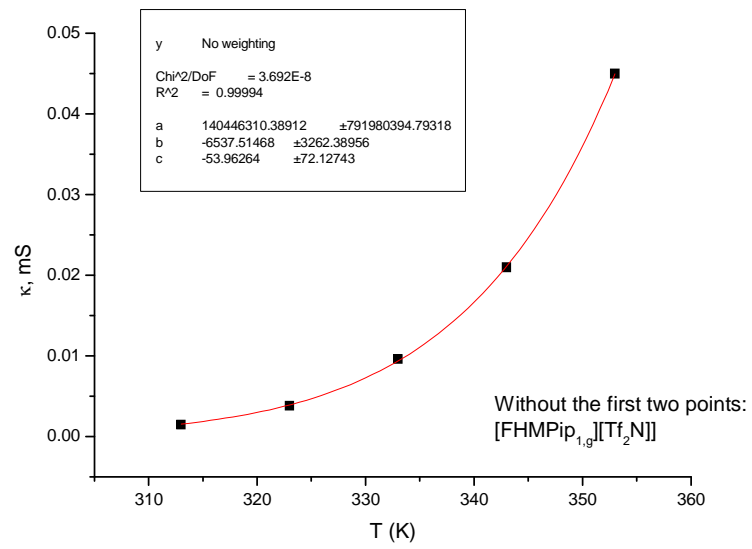
ANOVA Table:

| Item | Degrees of Freedom | Sum of Squares | Mean Square | F Statistic |
|-------|--------------------|----------------|-------------|-------------|
| Model | 1 | 5.09814 | 5.09814 | 563.55386 |
| Error | 5 | 0.04523 | 0.00905 | |
| Total | 6 | 5.14337 | | |









Evaluation of the sensitivity of the solvatochromic parameters to temperature**Table 3A1:** Changes in α , π^* , β and E_T^N , $E_{T(30)}$ at 25, 45, 65, 45 and 25°C ([Pip_{1,g}][N(CN)₂])

| Temperatures | $E_{T(30)}$ | E_T^N | α | β | π^* |
|--------------|-------------|---------|----------|---------|---------|
| 25 (going) | 56.99 | 0.811 | 0.87 | 0.50 | 1.12 |
| 45 (going) | 56.56 | 0.798 | 0.85 | 0.51 | 1.09 |
| 65 | 55.92 | 0.778 | 0.82 | 0.53 | 1.08 |
| 45 (return) | 56.41 | 0.794 | 0.85 | 0.51 | 1.10 |
| 25 (return) | 57.18 | 0.817 | 0.87 | 0.50 | 1.12 |

$E_{T(30)}$:- The %age increase of $E_{T(30)}$ on increasing the temperature from 25 to 45°C is 0.75 % and 45 to 65°C is 1.13% and on returning from 65 to 45°C is 0.87% and on returning from 45 to 25°C is 1.35%. The major difference is 1.88% that is when one moves from 25 to 65°C and back to 25 from 65°C is 2.20%. As we see the Table 3.8a we can say that $E_{T(30)}$ decreases linearly with the increase in the temperature and increases linearly with the decrease in temperature. This result also agrees with Shruti Trivedi et al.

E_T^N :- The %age increase of E_T^N on increasing the temperature from 25 to 45°C is 1.60% and 45 to 65°C is 2.51% and on returning from 65 to 45°C is 2.02% and on returning from 45 to 25°C is 2.82%. The major difference is 4.07% that is when one moves from 25 to 65°C and back to 25 from 65°C is 4.77%. This result also shows that the E_T^N value decrease linearly with the rise in temperature and the vice-versa. This result is in agreement with Shruti Trivedi et al.

α :- The %age increase of α on increasing the temperature from 25 to 45°C is 0.92% and 45 to 65°C is 4.32% and on returning from 65 to 45°C is 3.41% and on returning from 45 to 25°C is 2.30%. The major difference is 5.20% that is when one moves from 25 to 65°C and back to 25 from 65°C is 5.53%. This result also shows that the α value decrease linearly with the rise in temperature and the vice-versa. This result is in agreement with Shruti Trivedi et al.

β :- The %age increase of β on increasing the temperature from 25 to 45°C is 3.02% and 45 to 65°C is 2.38% and on returning from 65 to 45°C is 10.69% and on returning from 45 to 25°C is 4.83%. The difference from 25°C to 65°C is exceptionally low i.e. 0.57%. The percentage difference when one moves from 65°C to 25°C is 6.81%. The major difference is 10.69% that is when one moves from 65 to 45°C. Thus, one can say from these results that β is independent of temperature and the increase or decrease in β -values cannot be explained on basis of temperatures. This result is in agreement with Shruti Trivedi et al.

π^* :- The %age increase of π^* on increasing the temperature from 25 to 45°C is 2.33% and 45 to 65°C is 0.73% and on returning from 65 to 45°C is 2.43% and on returning from 45 to 25°C is 1.77%. When one moves from 25 to 65°C the difference is 3.05% and back to 25 from 65°C is 4.16%. This result also shows that the π^* value decrease linearly with the rise in temperature and the vice-versa. This result is in agreement with Shruti Trivedi et al.

Table 3A2: $\text{DMI}_{1,g} \text{N}(\text{CN})_2$ changes with temperature

| Temp | α | β | π^* | ET(30) | E_T^N |
|------|----------|---------|---------|--------|---------|
| 25 | 0.84 | 0.46 | 1.16 | 57.06 | 0.81 |
| 45 | 0.83 | 0.50 | 1.13 | 56.45 | 0.79 |
| 65 | 0.82 | 0.51 | 1.08 | 55.93 | 0.77 |
| 45 | 0.83 | 0.51 | 1.12 | 56.41 | 0.79 |
| 25 | 0.85 | 0.46 | 1.16 | 57.02 | 0.81 |

Table 3A3: $\text{DMI}_{1,g} \text{Tf}_2\text{N}$:- changes with temperature

| Temp | α | β | π^* | $E_T(30)$ | E_T^N |
|------|----------|---------|---------|-----------|---------|
| 25 | 1.12 | 0.178 | 1.144 | 61.2 | 0.93 |
| 45 | 1.13 | 0.160 | 1.139 | 61.4 | 0.94 |
| 65 | 1.16 | 0.139 | 1.132 | 61.8 | 0.96 |
| 45 | 1.13 | 0.164 | 1.137 | 61.5 | 0.94 |

| | | | | | |
|----|------|-------|-------|------|------|
| 25 | 1.10 | 0.178 | 1.143 | 61.0 | 0.93 |
|----|------|-------|-------|------|------|

Table 3A4: Pyrr_{1,g} Tf₂N:- changes with temperature

| Temp | α | β | π^* | $E_T(30)$ | E_T^N |
|------|----------|---------|---------|-----------|---------|
| 25 | 1.13 | 0.141 | 1.388 | 64.07 | 1.03 |
| 45 | 1.16 | 0.125 | 1.373 | 64.38 | 1.04 |
| 65 | 1.17 | 0.116 | 1.364 | 64.44 | 1.04 |
| 45 | 1.14 | 0.123 | 1.382 | 64.13 | 1.03 |
| 25 | 1.12 | 0.141 | 1.391 | 63.94 | 1.023 |

The above tables from 3.8 (a–d) show variations in various solvatochromic parameters with the rise in temperature and also decrease in temperature. E_T^N obtained from betaine dye 33, indicating dipolarity/polarizability and/or hydrogen bond donating (HBD) acidity, decreases linearly with increasing temperature within the two ILs. Changes in Kamlet–Taft parameters dipolarity/polarizability (π^*), HBD acidity (α), and HB accepting (HBA) basicity (β) with temperature show interesting trends. While π^* and α decrease linearly with increasing temperature within the two ILs, β appears to be independent of the temperature. Also, we can say that this kind of variations with temperatures from 25 to 65°C comes in an average of 0.7 to 4% which are not significantly important.

References

- ¹ (a) Rogers, R. D.; Seddon, K. R. *Ionic Liquids: Industrial Applications for Green Chemistry*, Eds.; ACS Symposium Series 818; American Chemical Society, Washington, DC, **2002**. (b) Seddon, K. R. *Green Chem.* **2002**, *4*, G25–G26. (c) Huddleston, J. G.; Visser, A. E.; Reichert, W. M.; Willauer, H. D.; Broken, G. A.; Rogers, R. D. *Green Chem.* **2001**, *3*, 156. (d) Cammarata, L.; Kazarian, S. G.; Salter, P. A.; Welton, T. *Phys. Chem. Chem. Phys.* **2001**, *3*, 5192. (e) Fletcher, K. A.; Pandey, S. *Appl. Spectrosc.* **2002**, *56*, 266. (f) Singh, T.; Kumar, A. *J. Phys. Chem. B* **2008**, *112*, 4079. (g) Scurto, A. M.; Aki, S. N. V. K.; Brennecke, J. F. *J. Am. Chem. Soc.* **2002**, *124*, 10276. (h) Pandey, S.; Fletcher, K. A.; Baker, S. N.; Baker, G. A. *Analyst* **2004**, *129*, 569. (i) Solinas, M.; Pfaltz, A.; Cozzi, P. G.; Leitner, W. *J. Am. Chem. Soc.* **2004**, *126*, 16142. (j) Pal, A.; Samanta, A. *J. Phys. Chem. B* **2007**, *111*, 4724. (k) Baker, S. N.; Baker, G. A.; Bright, F. V. *Green Chem.* **2002**, *4*, 165.
- ² (a) Freemantle, M. *Chem. Eng. News* **1998**, *30*, 32. (b) Newington, I.; Perez-Arlandis, J. M.; Welton, T. *Org. Lett.* **2007**, *9*, 5247. (c) Plechkova, N. V.; Seddon, K. R. *Methods and Reagents for Green Chemistry* **2007**, 105. (d) Rogers, R. D.; Visser, A. E.; Swatloski, R. P.; Reichert, W. *M. Abstracts of Papers, 220th ACS National Meeting*; American Chemical Society: Washington, DC, **2000**.
- ³ Karmakar, R.; Samanta, A. Dynamics of solvation of the fluorescent state of some electron donor-acceptor molecules in room temperature ionic liquids, [Bmim]⁺[(CF₃SO₂)₂N] and [Emim]⁺[(CF₃SO₂)₂N]. *J. Phys. Chem. A* **2003**, *107*, 7340–7346.
- ⁴ Reichardt, C. *Solvent Effects in Organic Chemistry*, 3rd ed.; Wiley-VCH: Weinheim, **2003**.
- ⁵ Bunce, E.; Stairs, R.; Wilson, H. *The Role of the Solvent in Chemical Reactions*; Oxford University Press: Oxford, **2003**.
- ⁶ Stobbe, H. *Liebigs Ann. Chem.* **1903**, *326*, 347–370.
- ⁷ Scheibe, G.; Felger, E.; Rossler, G. *Ber. Dtsch. Chem. Ges.* **1927**.
- ⁸ Sheppard, S. E. *Rev. Mod. Phys.* **1942**, *14*, 303–340.
- ⁹ (a) Frank, J. *Trans. Faraday Soc.* **1926**, *21*, 536–542. (b) Condon, C. U. *Phys. Rev.* **1928**, *32*, 858–872.
- ¹⁰ (a) Bowers, J.; Butts, C. P.; Martin, P. J.; Vergara-Gutierrez, M. C.; Heenan, R. K. *Langmuir* **2004**, *20*, 2191. (b) Miki, K.; Westh, P.; Nishikawa, K.; Koga, Y. *J. Phys. Chem. B* **2005**, *109*,

9014. (c) Katayanagi, H.; Nishikawa, K.; Shimozaki, H.; Miki, K.; Westh, P.; Koga, Y. *J. Phys. Chem. B* **2004**, *108*, 19451.

¹¹ Buckingham, A. D.; Fowler, P. W.; Hutson, J. M. *Chem. Rev.* **1988**, *83*, 963–988.

¹² Huyskens, P. L.; Luck, W. A. P.; Zeegers-Huyskens, T., Eds. *Intermolecular Forces*; Springer: Berlin, **1991**.

¹³ Israelachvili, J. N. *Intermolecular and Surface Forces*, 2nd ed.; **1992**.

¹⁴ (a) Reichardt, C. *Chem. Soc. Rev.* **1992**, *21*, 147. (b) Silva, P. L.; Bastos, E. L.; El Seoud, O. A. *J. Phys. Chem. B* **2007**, *111*, 6173. (c) Tada, E. B.; Silva, P. L.; El Seoud, O. A. *Phys. Chem. Chem. Phys.* **2003**, *5*, 5378. (d) Martins, C. T.; Lima, M. S.; Bastos, E. L.; El Seoud, O. A. *Eur. J. Org. Chem.* **2008**, 1165. (e) Martins, C. T.; Lima, M. S.; El Seoud, O. A. *J. Org. Chem.* **2006**, *71*, 9068. (f) Webb, M. A.; Morris, B. C.; Edwards, W. D.; Blumenfeld, A.; Zhao, X.; McHale, J. L. *J. Phys. Chem. A* **2004**, *108*, 1515. (g) Bastos, E. L.; Silva, P. L.; El Seoud, O. A. *J. Phys. Chem. A* **2006**, *110*, 10287. (h) Nicolet, P.; Laurence, C. *J. Chem. Soc., Perkin Trans.* **1986**, *2*, 1071. (i) Laurence, C.; Nicolet, P.; Helbert, M. *J. Chem. Soc., Perkin Trans.* **1986**, *2*, 1081. (j) Varadaraj, R.; Bock, J.; Valint, P., Jr.; Brons, N. *Langmuir* **1990**, *6*, 1377. (k) Nishida, S.; Morita, Y.; Fukui, K.; Sato, K.; Shiomi, D.; Takui, T.; Nakasuji, K. *Angew. Chem., Int. Ed.* **2005**, *44*, 7277. (l) Zhao, X.; Burt, J. A.; Knorr, F. J.; McHale, J. L. *J. Phys. Chem. A* **2001**, *105*, 11110. (m) Khupse, N. D.; Kumar, A. *J. Phys. Chem. B* **2010**, *114*, 376.

¹⁵ Sato, B. M.; de Oliveira, C. G.; Martins, C. T.; El Seoud, O. A. *Phys. Chem. Chem. Phys.*

2010, *12*, 1764.

¹⁶ Martins, C. T.; Sato, B. M.; El Seoud, O. A. *J. Phys. Chem. B* **2008**, *112*, 8330.

¹⁷ Wei, X.; Yu, L.; Wang, D.; Chen, G. Z. *Green Chem.* **2008**, *10*, 296.

¹⁸ Trivedi, S.; Malek, N. I.; Behera, K. and Pandey, S. *J. Phys. Chem. B* **2010**, *114*, 8118–8125.

¹⁹ Branco, L. C.; Rosa, J. N.; Ramos, J. J. M.; Afonso, C. A. M. *Chem. Eur. J.* **2002**, *8*, 3671–3677.

²⁰ Wallert, S.; Drauz, K.; Grayson, I.; Groger, H.; Maria, P. D. d.; Bolm, C. *Green Chem.* **2005**, *7*, 602–605.

²¹ Dzyuba, S. V.; Bartsch, R. A. *Tetrahedron Lett.* **2002**, *43*, 4657–4659.

²² (a) Ren, L.; Meng, L.; Lu, Q. *Chem. Lett.* **2008**, *37*, 106–107. (b) Recham, N.; Dupont, L.; Courty, M.; Djellab, K.; Larcher, D.; Armand, M.; Tarascon, J.-M. *Chem. Mater.*, in press. (c) Yang, X.; Yan, N.; Fei, Z. F.; Crespo-Quesada, R. M.; Laurency, G.; Kiwi-Minsker, L.; Kou, Y.; Li, Y. D.; Dyson, P. J. *Inorg. Chem.* **2008**, *47*, 7444–7446.

- ²³ (a) Wei, X.; Yu, L.; Wang, D.; Jin, X.; Chen, G. Z. *Green Chem.* **2008**, *10*, 296–305. (b) Wei, X.; Yu, L.; Jin, X.; Wang, D.; Chen, G. Z. *Adv. Mater.* **2009**, *21*, 776–780.
- ²⁴ Jin, H.; O'Hare, B.; Dong, J.; Arzhantsev, S.; Baker, G. A.; Wishart, J. F.; Benesi, A. J.; Maroncelli, M. *J. Phys. Chem. B.* **2008**, *112*, 81–92.
- ²⁵ Baker, S. N.; Baker, G. A.; Bright, F. V. *Green Chem.* **2002**, *4*, 165–169.
- ²⁶ Yim, T.; Lee, H. Y.; Kim, H.-J.; Mun, J.; Kim, S.; Oh, S. M. and Kim, Y. G. *Bull. Korean Chem Soc.* **2007**, *28*(9), 1567–1572.
- ²⁷ Bonhôte, P.; Dias, A.-P.; Armand, M.; Papageorgiou, N.; Kalyanasundaram, K.; Gratzel, M. *Inorg. Chem.* **1996**, *35*, 1168–1178.
- ²⁸ (a) Hagiwara, R.; Ito, Y. *J. Fluorine Chem.* **2000**, *105*, 221–227. (b) Nishida, T.; Tashiro, Y.; Yamamoto, M. *J. Fluorine Chem.* **2003**, *120*, 135–141. (c) Holbrey, J. D.; Seddon, K. R. *J. Chem. Soc., Dalton Trans.* **1999**, 2133–2139.
- ²⁹ (a) Buzzeo, M. C.; Evans, R. G.; Compton, R. G. *Chem. Phys. Chem.* **2004**, *5*, 1106–1120.
(b) Lee, J. S.; Bae, J. Y.; Lee, H.; Quan, N. D.; Kim, H. S.; Kim, H. J. *Ind. Eng. Chem.* **2004**, *10*, 1086–1089.
(c) Anthony, J. L.; Brennecke, J. F.; Holbrey, J. D.; Maginn, E. J.; Mantz, R. A.; Rogers, R. D.; Trulove, P. C.; Visser, A. E.; Welton, T. In *Ionic Liquids in Synthesis*; Wasserscheid, P.; Welton, T., Eds.; Wiley-VCH Verlag: Weinheim, **2003**; 41–126.
- ³⁰ Appetecchi, G. B.; Zane, M. M. D.; Carewska, M.; Alessandrini, F.; Passerini, S. *Electrochim. Acta.* **2009**, *54*, 1325–1332.
- ³¹ Kanatani, T.; Ueno, R.; Matsumoto, K.; Nohira, T.; Hagiwara, R. *J. Fluorine Chem.* **2009**, *130*, 979–984.
- ³² Liu, K.; Zhou, Y.-X.; Han, H.-B.; Zhou, S.-S.; Feng, W.-F.; Li, J. N. H., Huang, X.-J.; Armand, M.; Zhou, Z.-B. *Electrochim. Acta.* **2010**, *55*, 7145–7151.
- ³³ (a) Kamlet, M. J.; Taft, R. W. *J. Am. Chem. Soc.* **1976**, *98*, 283–377.
(b) Kamlet, M. J.; Carr, P. W.; Taft, R. W.; Abraham, M. H. *J. Am. Chem. Soc.* **1981**, *103*, 6062–6066.
(c) Taft, R. W.; Abboud, J.-L. M.; Kamlet, M. J.; Abraham, M. H. *J. Sol. Chem.* **1985**, *14*, 153–186.
(d) Abraham, M. H.; Kamlet, M. J.; Taft, R. W. *J. Am. Chem. Soc.* **1983**, *105*, 797–6801.
- ³⁴ (a) Marcus, Y. *Chem. Soc. Rev.* **1993**, *22*, 409–416. (b) Yoshida, Y.; Baba, O.; Saito, G. *J. Phys. Chem. B* **2007**, *111*, 4742–4749.

- ³⁵ Chiappe, C.; Pieraccini, D.; Zhao, D.; Fei, Z.; Dyson P. J. *Adv. Synt. Cat.* **2006**, *348*, 68.
- ³⁶ Persson, I. *Pure Appl. Chem.* **1986**, *58*, 1153.
- ³⁷ K. Dahl, G. M. Sando, D. M. Fox, T. E. Sutto, J. C. Owrutsky *J. Chem. Phys.* **2005**, *123*, 084504/1-11.
- ³⁸ Reichardt, C.; Harbusch-Gornert, E. *Liebigs Ann. Chem.* **1983**, 721–743.
- ³⁹ Laurence, C.; Nicolet, P.; Reichardt, C. *Bull. Soc. Chim. Fr.* **1987**, 125–130.
- ⁴⁰ (a) Dimroth, K.; Reichardt, C.; Siepmann, T.; Bohlmann, F. *Liebigs Ann. Chem.* **1963**, *661*, 1–37. (b) Dimroth, K.; Reichardt, C. *Liebigs Ann. Chem.* **1969**, *727*, 93–105. (c) Reichardt, C. *Liebigs Ann. Chem.* **1971**, *752*, 64–67.
- ⁴¹ Zhang, S.; Qi, X.; Ma, X.; Lu, L. and Deng, Y. *J. Phys. Chem. B* **2010**, *114*, 3912–3920.

Chapter 4

New class of ionic liquids containing seven-membered rings: their synthesis and properties and comparing them with other six-membered rings

Abstract

A series of functionalized and non-functionalized new ionic liquids (ILs) based on a cyclic seven-membered ring amine (hexamethylenimine, defined also as azepane) were prepared and their properties were compared with those of two other six-membered ring amines, i.e. a functionalized six-membered ring, namely morpholinium salts, and non-functionalized six-membered ring, namely piperidinium salts. The physico-chemical properties such as conductivity, viscosity and polarity were measured at different temperatures. A comparison between five-, six- and seven-membered ringed cations based ILs are reported here.

4.1 Introduction

Recently, Belhocine et al.¹ have reported the synthesis and some properties of a new class of ILs arising from azepane and have compared them with analogous ILs arising from 3-methylpiperidine, showing that both of these salts exhibited wide electrochemical windows. Nevertheless, the syntheses and the physical and electrochemical properties of ILs based on 1-alkyl-1-methylazepanium² were also reported in a recent patent application from INVISTA.³ Considering our interest in the development of new classes of ILs having improved properties, during the course of this PhD thesis, we have synthesized a series of hydroxyl-functionalized cyclic onium ILs based on six membered rings (morpholine and piperidine) and seven-membered rings (azepane). The physico-chemical properties as well as solvent properties were studied for all the above-mentioned ILs having $[N(CN)_2]^-$ as anion and were compared with those of analogously alkyl functionalized ILs.

4.2 Experimental section

In this section we have shown the synthesis of various ILs studied in this chapter. Also the schemes for each of the reactions are shown in this section.

4.2.1 Synthesis of all bromide, chloride and iodide salts

The various bromides, chlorides and iodides were prepared and are explained in this section.

4.2.1.1 Synthesis of [HME_{1,4}][I]

This synthesis involves 3 consecutive steps which are explained below.

N-butyl hexamethyleniminium bromide [HME_{H,4}][Br]

30.40 g (0.2218 mol) of bromobutane (Acros, 99%) was added dropwise over 1 h to a solution of 22 g (0.2218 mol) of hexamethylenimine (Aldrich 99%) in 100 ml of acetonitrile (J.T. Baker, Deventer, Holland) while stirring vigorously, and N₂ was bubbled through the solution. The mixture was refluxed for 8 h at 70°C. The molten salt was decanted, washed three times with 100 ml of CH₂Cl₂, and dried on a rotovapor for 1 h at 45°C, under low pressure. The product was dried in vacuum. If the product was found to have traces of brown or yellowish color, then it was washed with acetone and recrystallized in acetone. A crystalline white solid was obtained with a yield of 85%.

N-butyl hexamethylenimine [HME₄]

Equimolar amounts of Na₂CO₃·10H₂O and [HME_{H,4}][Br] were dissolved in pure distilled water. The organic base was then extracted in CH₂Cl₂ and after solvent removal the final product, a yellowish liquid, was analyzed by NMR. This product was completely insoluble in water. The weight of the product obtained was 9.16 g and the product yield was 69.73% .

N-butyl-N-methyl hexamethyleniminium iodide [HME_{1,4}][I]

7.919 g (0.0558 mol) of iodomethane (Acros, 99%) (2% molar excess of iodomethane was taken as it is highly volatile) was added dropwise to a solution of 8.49 g (0.0547 mol) of *N*-butyl hexamethylenimine in 40 ml of acetonitrile (J.T. Baker, Deventer, Holland) under vigorous stirring and N₂ was bubbled through the solution. The mixture was stirred at room temperature for 2 h as the reaction was exothermic. The formed molten salt was decanted, washed three times with 100 ml of CH₂Cl₂, and dried on a rotovapour for 30 mins at 45°C under low pressure. The product was dried in vacuum. If the product was found to have traces of brown or yellowish colour, then it was washed with acetone and recrystallized in acetone. A crystalline white solid was obtained and the weight of the product was 15.38 g and the product yield was 93.72%.

4.2.1.2 Synthesis of [HME_{1,e}][I]

This synthesis involves 3 consecutive steps as shown below.

N-ethanol hexamethyleniminium chloride [HME_{H,e}][Cl]

17.86 g (0.2218 mol) of 2-chloroethanol (Acros, 99%) was added dropwise over 1 h to a solution of 22 g (0.2218 mol) of hexamethylenimine (Aldrich 99%) in 100 ml of acetonitrile (J.T. Baker, Deventer, Holland) while stirring vigorously, and N₂ was bubbled through the solution. As the boiling point of bromoethane was quite low we took 2% more of it in the reflux. The mixture was refluxed for 12 h at 70°C. The molten salt was decanted, washed three times with 100 ml of CH₂Cl₂, and dried on a rotovapor for 1 h at 45°C, under low pressure. The product was dried in vacuum. If the product was found to have traces of brown or yellowish colour, then it was washed with acetone and recrystallized in acetone. A crystalline white solid was obtained with the product yield of 85%.

N-ethanol hexamethylenimine [HME_e]

Equimolar amounts of K₂CO₃ and [HME_{H,e}][Cl] were dissolved in pure distilled water. The organic base was then extracted using dichloromethane and after solvent removal the final product, a yellowish liquid, was analyzed by NMR. This product was completely insoluble in water. The weight of the product was 15.94 g and the product yield was 79.7%.

N-ethanol-N-methyl hexamethyleniminium iodide [HME_{1,e}][I]

15.80 g (0.11135 moles) of iodomethane (Acros, 99%) (2% molar excess of iodomethane was taken as it is highly volatile) was added dropwise to a solution of 15.94 g (0.11130 moles) of *N*-ethanol hexamethylenimine (prepared and approved by NMR) in 40 ml of acetonitrile (J.T. Baker, Deventer, Holland) while stirring vigorously, and N₂ was bubbled through the solution. This was stirred at room temperature for 2 h as the reaction was exothermic. The molten salt was decanted, washed three times with 100 ml of CH₂Cl₂, and dried on a rotovapor for 30 mins at 45°C under low pressure. The product was dried in vacuum. The product was washed with acetone and recrystallized in acetone. A crystalline white solid was obtained and the weight of the product 25 g and the product yield was 80.80%.

4.2.1.3 Synthesis of [HME_{1,g}][I]

This synthesis involves 3 consecutive steps which are shown below.

N-glyceryl hexamethyleniminium chloride [HME_{H,g}][Cl]

24.52 g (0.2218 mol) of 1,3-chloro propanediol (Acros, 99%) was added dropwise over 1 h to a solution of 22 g (0.2218 mol) of hexamethylenimine (Aldrich 99%) in 100 ml of acetonitrile (J.T. Baker, Deventer, Holland) while stirring vigorously, and N₂ was bubbled through the solution. The mixture was refluxed for 4.5 days at 70°C. The molten salt was decanted, washed three times with 100 ml of CH₂Cl₂, and dried on a rotovapor for 1 h at 45°C under low pressure. The product was dried in vacuum. If the product was found to have traces of brown or yellowish color, then it was washed with acetone and recrystallized in acetone. A crystalline white solid was obtained and the weight of the product was 40 g and the product yield was 86%.

N-glyceryl hexamethylenimine [HME_g]

Equimolar amounts of Na₂CO₃·10H₂O and [HME_{H,g}][Cl] were dissolved in pure distilled water. The final product was then extracted using dichloromethane and after solvent removal the purity of the collected product was estimated using NMR. The product yield was 72%.

N-glyceryl-N-methyl hexamethyleniminium iodide [HME_{1,g}][I]

0.0589 moles of iodomethane (Acros, 99%) (2% molar excess of iodomethane was taken as it is highly volatile) was added dropwise to a solution of 10 g (0.0577 moles) of *N*-glycerylhexamethylenimine (prepared and approved by NMR) in 40 ml of acetonitrile (J.T. Baker, Deventer, Holland) while stirring vigorously, and N₂ was bubbled through the solution. This was stirred at room temperature for 2 h as the reaction was exothermic. The molten salt was decanted, washed three times with 100 ml of CH₂Cl₂, and dried on a rotovapor for 30 mins at 45°C under low pressure. The product was dried in vacuum. If the product was found to have traces of brown or yellowish colour, then it was washed with acetone and recrystallized in acetone. A crystalline white solid was with 52% of product yield.

4.2.1.4 *N*-ethanol-*N*-methyl morpholinium chloride [Mor_{1,e}][Cl]

43.94 g (0.5457 mol) of 2-chloro ethanol (99%) was added dropwise over 1h to a solution of 55.2 g (0.5457 mol) of *N*-methylmorpholine (Acros, 99%) in 100 ml of acetonitrile (J.T. Baker, Deventer, Holland) while stirring vigorously, and N₂ was bubbled through the solution. As the

boiling point of bromoethane was very low we took 2% more of it in the reflux. The mixture was refluxed for 8h at 70°C. The molten salt was decanted, washed three times with 100 ml of CH₂Cl₂, and dried on a rotovapor for 1h at 45°C under low pressure. The product was dried in vacuum. If the product was found to have traces of brown or yellowish color, then it was washed with acetone and recrystallized in acetone. A crystalline white solid was obtained and the weight of the product was 46.21 g and the product yield was 46.61%.

4.2.1.5 *N*-ethanol-*N*-ethyl morpholinium chloride [Mor_{2,e}][Cl]

23.55 g (0.21609 moles) of 2-bromo ethanol (Aldrich, 98%) was added dropwise over 1 h to a solution of 27 g (0.2058 moles) of *N*-(2-hydroxylmorpholine) (Acros, 99%) in 100 ml of acetonitrile (J.T. Baker, Deventer, Holland) while stirring vigorously, and N₂ was bubbled through the solution. As the boiling point of bromoethane was very low we took 2% more of it in the reflux. The mixture was refluxed for 12 h at 70°C. The molten salt was decanted, washed three times with 100 ml of CH₂Cl₂, and dried on a rotovapor for 1 h at 45°C under low pressure. The product was dried in vacuum. If the product was found to have traces of brown or yellowish color, then it was washed with acetone and recrystallized in acetone. A crystalline white solid was obtained and the weight of the product was 41.77 g and the product yield was 82.63%.

4.2.1.6 *N*-ethanol-*N*-methyl piperidinium iodide [Pip_{1,e}][I]

26.64 g (0.1877 moles) of methyl iodide (Acros, 99%) was added dropwise over 1 h to a solution of 24.25 g (0.1877 moles) of *N*-ethanollpiperidine (Acros, 99%) in 100 ml of acetonitrile (J.T. Baker, Deventer, Holland) while stirring vigorously, and N₂ was bubbled through the solution. The mixture was refluxed for 4 h at 70°C. The molten salt was decanted, washed three times with 100 ml of CH₂Cl₂, and dried on a rotovapour for 1 h at 45°C under low pressure. The product was dried in vacuum. The product was washed with acetone and recrystallized in acetone. A brownish crystalline solid was obtained and the weight of the product was 39.11 g and the product yield was 76.85%.

4.2.1.7 *N*-ethanol-*N*-ethyl piperidinium iodide [Pip_{2,e}][I]

29.28 g (0.1877 moles) of 2-iodoethane (Aldrich, 99%) was added dropwise over 1 h to a solution of 24.25 g (0.1877 moles) of *N*-ethanollpiperidine (Aldrich 99%) in 100 ml of acetonitrile (J.T. Baker, Deventer, Holland) while stirring vigorously, and N₂ was bubbled through the solution. As the boiling point of iodoethane (bpt.=72 °C) was very low we took 2% more of it in the reflux. The mixture was refluxed for 4 h at 70°C. The molten salt was decanted,

washed three times with 100 ml of CH_2Cl_2 , and dried on a rotovapor for 1 h at 45°C under low pressure. The product was dried in vacuum. It was washed with acetone and recrystallized in acetone. A brownish-colored crystalline solid was obtained and the weight of the product was 45.14 g and the product yield was 84.33%.

$[\text{Mor}_{1,4}][\text{Br}]$ was prepared as reported in Chapter 2; whereas $[\text{Mor}_{1,g}][\text{Cl}]$ and $[\text{Pip}_{1,g}][\text{Cl}]$ were prepared as reported in Chapter 3.

4.2.2 Synthesis of dicyanamide salts

4.2.2.1 *N*-butyl-*N*-methyl hexamethyleniminium dicyanamide ($[\text{HME}_{1,4}][\text{N}(\text{CN})_2]$)

To a colorless solution of $[\text{HME}_{1,4}][\text{I}]$ (15 g, 0.0505 moles) in water (100 ml) 0.0515 moles (a little molar excess was taken assuming some silver dicyanamide will be lost during filtration process) of silver dicyanamide (white solid, freshly prepared from AgNO_3 and $\text{NaN}(\text{CN})_2$ in water) was added. The mixture was stirred for 3 h at 40°C . After cooling at room temperature the precipitate was filtered off, washed with water (2×10 ml) and the resulting colourless aqueous solution (approximately 200 ml) was heated to 70°C under vacuum for 1 h to remove the water. The colorless liquid was dissolved in anhydrous acetone (Carlo Erba reagents, HPLC grade, 200 ml), and the solution was cooled at -20°C for 48 h. Then, it was filtered on glass septa (porosity 4) containing two different powdered layers of 1 cm each:- celite (lower layer) and decolorizing carbon (upper layer). The solvent was removed under vacuum (2×10^{-3} mm Hg, 80°C , 6 h) to give the pure IL. The product yield was 82% after removal of silver by washing with acetone.

4.2.2.2 *N*-ethanol-*N*-methyl hexamethyleniminium dicyanamide ($[\text{HME}_{1,e}][\text{N}(\text{CN})_2]$)

To a colorless solution of $[\text{HME}_{1,e}][\text{I}]$ (10.55 g, 0.03700 moles) in water (100 ml) 0.03774 moles (a little molar excess was taken assuming some silver dicyanamide will be lost during filtration process) of silver dicyanamide (white solid, freshly prepared from AgNO_3 and $\text{NaN}(\text{CN})_2$ in water) was added. The mixture was stirred for 3 h at 40°C . After cooling at room temperature the precipitate was filtered off, washed with water (2×10 ml) and the resulting colourless aqueous solution (approximately 200 ml) was heated to 70°C under vacuum for 1 h to remove the water. The colorless liquid was dissolved in anhydrous acetone (Carlo Erba reagents, HPLC grade, 200 ml), and the solution was cooled at -20°C for 48 h. Then, it was filtered on glass septa (porosity 4) containing two different powdered layers of 1 cm each:- celite (lower layer) and decolorizing

carbon (upper layer). The solvent was removed under vacuum (2×10^{-3} mm Hg, 80°C , 6h) to give the pure IL. The product yield was 76% after removal of silver by washing with acetone.

4.2.2.3 *N*-glyceryl-*N*-methyl hexamethyleniminium dicyanamide ([HME_{1,g}][N(CN)₂])

To a colorless solution of [HME_{1,g}][I] (15 g, 0.04759 moles) in water (100 ml) 0.04854 moles (a little molar excess was taken assuming some silver dicyanamide will be lost during filtration process) of silver dicyanamide (white solid, freshly prepared from AgNO₃ and NaN(CN)₂ in water) was added. The mixture was stirred for 3 h at 40°C . After cooling at room temperature the precipitate was filtered off, washed with water (2×10 ml) and the resulting colorless aqueous solution (approximately 200 ml) was heated to 70°C under vacuum for 1 h to remove the water. The colorless liquid was dissolved in anhydrous acetone (Carlo Erba reagents, HPLC grade, 200 ml), and the solution was cooled at -20°C for 48 h. Then, it was filtered on glass septa (porosity 4) containing two different powdered layers of 1 cm each:- celite (lower layer) and decolorizing carbon (upper layer). The solvent was removed under vacuum (2×10^{-3} mm Hg, 80°C , 6 h) to give the pure IL. The product yield was 64% after the removal of silver by washing with acetone.

4.2.2.4 *N*-ethanol-*N*-methyl piperidinium dicyanamide ([Pip_{1,e}][N(CN)₂])

To a colorless solution of [Pip_{1,e}][I] (15 g, 0.08348 moles) in water (100 ml) 0.08514 moles (a little molar excess was taken assuming some silver dicyanamide will be lost during filtration process) of silver dicyanamide (white solid, freshly prepared from AgNO₃ and NaN(CN)₂ in water) was added. The mixture was stirred for 3 h at 40°C . After cooling at room temperature the precipitate was filtered off, washed with water (2×10 ml) and the resulting colorless aqueous solution (approximately 200 ml) was heated to 70°C under vacuum for 1 h to remove the water. The colourless liquid was dissolved in anhydrous acetone (Carlo Erba reagents, HPLC grade, 200 ml), and the solution was cooled at -20°C for 48 h. Then, it was filtered on glass septa (porosity 4) containing two different powdered layers of 1 cm each:- celite (lower layer) and decolorizing carbon (upper layer). The solvent was removed under vacuum (2×10^{-3} mm Hg, 80°C , 6 h) to give the pure IL. The product yield was 86% after the removal of silver by washing with acetone.

4.2.2.5 *N*-ethanol-*N*-methyl morpholinium dicyanamide ([Mor_{1,e}][N(CN)₂])

To a colorless solution of [Mor_{1,e}][Cl] (15 g) in water (100 ml) with 2% extra molar of silver dicyanamide (a little molar excess was taken assuming some silver dicyanamide will be lost

during filtration process) which is a white solid, freshly prepared from AgNO_3 and $\text{NaN}(\text{CN})_2$ in water was added. The mixture was stirred for 3 h at 40°C . After cooling at room temperature the precipitate was filtered off, washed with water (2×10 ml) and the resulting colourless aqueous solution (approximately 200 ml) was heated to 70°C under vacuum for 1 h to remove the water. The colorless liquid was dissolved in anhydrous acetone (Carlo Erba reagents, HPLC grade, 200 ml), and the solution was cooled at -20°C for 48 h. Then, it was filtered on glass septa (porosity 4) containing two different powdered layers of 1 cm each:- celite (lower layer) and decolorizing carbon (upper layer). The solvent was removed under vacuum (2×10^{-3} mm Hg, 80°C , 6 h) to give the pure IL. The product yield was 62% after the removal of silver by washing with acetone.

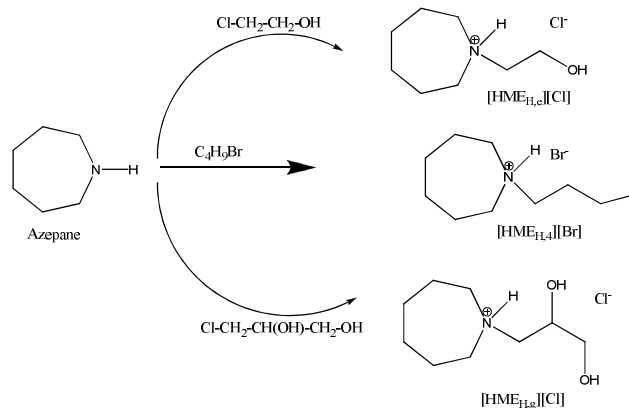
4.2.2.6 *N*-ethanol-*N*-ethyl morpholinium dicyanamide ([Mor_{2,e}][N(CN)₂])

To a colorless solution of [Mor_{2,e}][Br] (15 g, 0.06246 moles) in water (100 ml) 0.06371 moles (a little molar excess was taken assuming some silver dicyanamide will be lost during filtration process) of silver dicyanamide (white solid, freshly prepared from AgNO_3 and $\text{NaN}(\text{CN})_2$ in water) was added. The mixture was stirred for 3 h at 40°C . After cooling at room temperature the precipitate was filtered off, washed with water (2×10 ml) and the resulting colourless aqueous solution (approximately 200 ml) was heated to 70°C under vacuum for 1 h to remove the water. The colorless liquid was dissolved in anhydrous acetone (Carlo Erba reagents, HPLC grade, 200 ml), and the solution was cooled at -20°C for 48 h. Then, it was filtered on glass septa (porosity 4) containing two different powdered layers of 1 cm each:- celite (lower layer) and decolorizing carbon (upper layer). The solvent was removed under vacuum (2×10^{-3} mm Hg, 80°C , 6 h) to give the pure IL. The product yield was 68% after the removal of silver by washing with acetone.

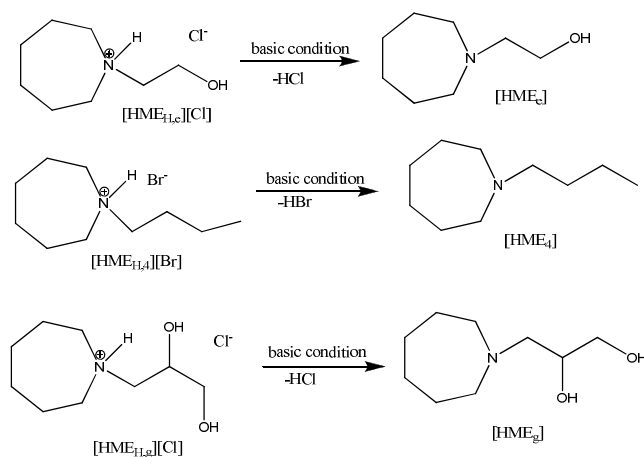
4.2.2.7 *N*-ethanol-*N*-ethyl piperidinium dicyanamide ([Pip_{2,e}][N(CN)₂])

To a colorless solution of [Pip_{2,e}][I] (15 g, 0.0526 moles) in water (100 ml) 0.0537 moles (a little molar excess was taken assuming some silver dicyanamide will be lost during filtration process) of silver dicyanamide (white solid, freshly prepared from AgNO_3 and $\text{NaN}(\text{CN})_2$ in water) was added. The mixture was stirred for 3 h at 40°C . After cooling at room temperature the precipitate was filtered off, washed with water (2×10 ml) and the resulting colourless aqueous solution (approximately 200 ml) was heated to 70°C under vacuum for 1 h to remove the water. The colourless liquid was dissolved in anhydrous acetone (Carlo Erba reagents, HPLC grade, 200 ml), and the solution was cooled at -20°C for 48 h. Then, it was filtered on glass septa (porosity 4) containing two different powdered layers of 1 cm each:- celite (lower layer) and decolorizing

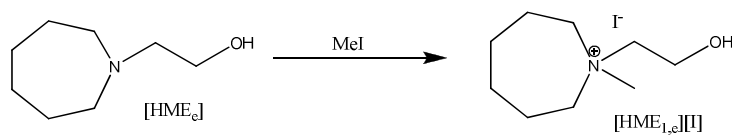
carbon (upper layer). The solvent was removed under vacuum (2×10^{-3} mm Hg, 80°C , 6 h) to give the pure IL. The product yield was 78% after removal of silver by washing with acetone.

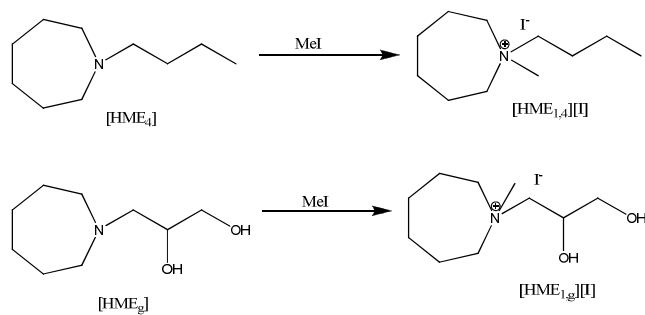


Scheme 4.1: Synthesis of bromide and chloride derivatives of hexamethylenimine

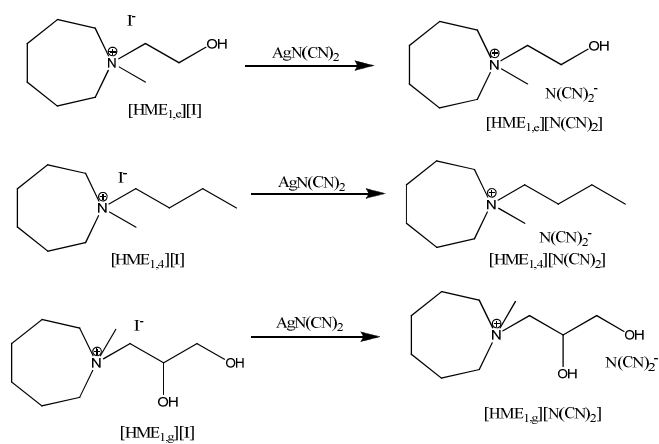


Scheme 4.2: Removal of the hydrogen chloride/bromide under basic condition

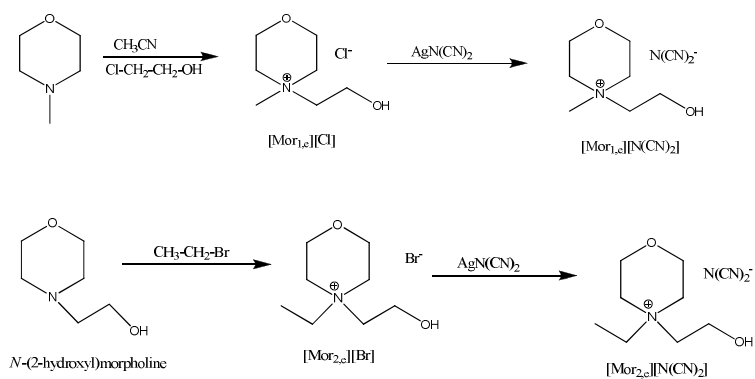


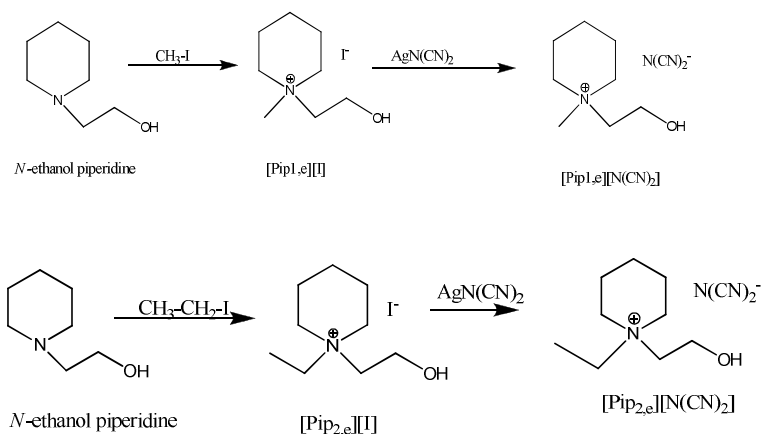


Scheme 4.3: Synthesis of the respective iodide derivatives of azepane



Scheme 4.4: Synthesis of dicyanamide derivatives of azepane





Scheme 4.5: Synthesis of functionalized piperidinium and morpholinium ILs

4.3 Results and Discussion

4.3.1 Physico-chemical properties

For all synthesized ILs the fundamental properties including density (ρ), viscosity (η) and conductivity (κ) were measured after accurate drying (see chapter 3) and the corresponding data are shown in Table 4.1. The density (ρ) values lie in the range 1.37 to 1.15 g/ml. Thus, a moderate effect of cation structure on density and a more significant anion effect can be evidenced: i) the dicyanamide salt has a lower density than the bistriflimide analogues; ii) the introduction of oxygen on cation core increases density. Generally, morpholinium salts have higher densities than piperidinium and the introduction of an hydroxyl group on the alkyl chain increases density; iii) passing from piperidinium to azepanium cation increases density. Nevertheless, the cation structure significantly affect viscosity (η). Generally, viscosity increases in the order $[\text{Pip}]^+ < [\text{HmE}]^+ \leq [\text{Mor}]^+$; however, the presence of hydroxyl groups on cation determines a more drastic increase in the viscosities of morpholinium-based ILs with respect to the others. It is noteworthy that in Table 4.1. the viscosity values are reported at 30°C being the viscosities of some salts extremely high. The temperature dependence of viscosity was investigated, with few exceptions, in the range 20 to 80 °C. In all cases, dynamic viscosity (Table 4.2a and b) decreases on increasing temperature: at lower temperatures, the viscosity decrease is significant whereas a more gentle descent behaviour can be observed at higher temperatures.

Table 4.1: Temperature-dependent physico-chemical properties

| Salt | C <i>mol cm³</i> | PM | κ S cm ⁻¹ (at 30°C) | Λ S cm ² mol ⁻¹ | Viscosity y (cP) at 30°C | d (g/ml) |
|------------------------------------|--------------------------------|--------|---|---|-----------------------------------|-----------------|
| [HME _{1,4}] | 0.0054 | 236.36 | 2.10×10^{-3} | 0.389 | 297 | 1.27 |
| [Mor _{1,4}] ^a | 0.0050 | 224 | 1.76×10^{-3} | 0.352 | 280 | 1.12 |
| [HME _{1,g}] | 0.0054 | 254.33 | 0.20×10^{-3} | 0.037 | 1105 | 1.37 |
| [Mor _{1,g}] ^b | 0.0056 | 242.28 | 0.10×10^{-3} | 0.018 | 5367 | 1.37 |
| [Pip _{1,g}] ^b | 0.0049 | 240.30 | 0.27×10^{-3} | 0.055 | 970 | 1.18 |
| [HME _{1,e}] | 0.0057 | 224.31 | 1.79×10^{-3} | 0.314 | 221 | 1.28 |
| [Mor _{1,e}] | 0.0058 | 212.25 | 1.55×10^{-3} | 0.267 | 332 | 1.24 |
| [Pip _{1,e}] | 0.0074 | 210.28 | 2.03×10^{-3} | 0.274 | 196 | - |
| [HME _{1,4}] ^c | 0.0030 | 481.54 | 0.66×10^{-3} | 0.222 | 273 | 1.43 |
| [Mor _{2,e}] | 0.0053 | 226.27 | 1.13×10^{-3} | 0.213 | 538.9 | 1.19 |
| [Pip _{2,e}] | 0.0052 | 224.30 | 1.58×10^{-3} | 0.304 | 135.1 | 1.16 |

^aData taken from chapter 2. ^bData taken from chapter 3. ^cThis IL is [HME_{1,4}][Tf₂N] and the values agree with reference 3.

The Arrhenius plots of viscosity according to equation (1):

$$\ln \eta = \ln A + E_{\eta}/RT \quad (1)$$

present a distinct curvature (see Appendix). However, the values of E_{η} , A, and the linear fitting parameters (R^2) obtained are listed in Table 4.3a. According to the values of R^2 , the five salts were approximately fit by the Arrhenius model in this temperature interval. It is however to note that all ILs exhibit high energy barriers, in agreement with the elevated viscosity values; the higher value characterizing the *N*-glyceryl-*N*-methylmorpholinium cation. It is to note that the E_{η} values for the dialkyl and methyl-glyceryl substituted [HME]⁺ cation are lower than those characterizing the corresponding piperidinium-based ILs.

Table 4.2a: Viscosity values from 20–80°C for six N(CN)₂ ILs

| T(K) | HME _{1,4} | Mor _{1,4} ^a | Pip _{1,4} | Pip _{1,g} ^b | HME _{1,g} | Mor _{1,g} ^b |
|------|--------------------|---------------------------------|--------------------|---------------------------------|--------------------|---------------------------------|
| 293 | 623 | 589 | 429 | 2433 | 2969 | ND |
| 303 | 297 | 280 | 212 | 970 | 1105 | 5367 |
| 313 | 153 | 156 | 106 | 461 | 987 | 1636 |

| | | | | | | |
|-----|----|----|----|-----|-----|-----|
| 323 | 96 | 94 | 83 | 243 | 556 | 691 |
| 333 | 59 | 55 | 52 | 140 | 308 | 349 |
| 343 | 39 | 38 | 23 | 89 | 180 | 202 |
| 353 | 29 | 29 | 15 | 57 | 89 | 123 |

^aThese values are taken from Chapter 2 for comparison. ^bThese values are taken from Chapter 3 for comparison.

Table 4.2b: Viscosity values from 20–80°C for five N(CN)₂ and one Tf₂N ILs

| T(K) | Mor _{1,e} | Pip _{1,e} | HME _{1,e} | HME _{1,4} Tf ₂ N ^c | Mor _{2,e} | Pip _{2,e} |
|------|--------------------|--------------------|--------------------|--|--------------------|--------------------|
| 293 | 685 | 292 | 483 | 550.3 | 1195 | 225 |
| 303 | 332 | 196 | 221 | 273 | 539 | 135 |
| 313 | 156 | 93 | 146 | 144 | 280 | 84 |
| 323 | 113 | 79 | 98 | 81 | 155 | 53 |
| 333 | 74 | 58 | 65 | 51 | 99 | 37 |
| 343 | 46 | 40 | 34 | 38 | 64 | 28 |
| 353 | 36 | 23 | 28 | 27 | 44 | 21 |

^cThese values are in agreement with reference 3.

For these ILs, viscosity data have been also fitted to the Vogel-Tamman-Fulcher (VTF) equation (2), the best fit lines are reported in Appendix.

$$\eta = \eta_0 \exp[B/(T-T_0)] \quad (2)$$

where η_0 (cP), B (K) and T_0 (K) are fitting parameters. The best-fit parameters and the associated squared correlation coefficients R^2 are given in Tables 4.3a and b.

In Table 4.4. is reported the behavior of conductivity with temperature whereas figure 4.1 reports the corresponding Arrhenius plots according to equation (3):

$$\ln \kappa = \ln A + (E_a/RT) \quad (3)$$

Table 4.3a: Arrhenius Fitting parameters for viscosity behavior as a function of temperature

| ILs | E_η (kJ mol ⁻¹) | LnA cP | R |
|-----------------------|--|-----------|-------|
| [HME _{1,4}] | 43.77 | -11.67 | 0.996 |
| [Mor _{1,4}] | 43.69 | -11.67 | 0.996 |
| [Pip _{1,4}] | 46.63 | -13.12 | 0.993 |
| [Pip _{1,g}] | 53.27 | -14.23 | 0.997 |
| [HME _{1,g}] | 46.88 | -11.29 | 0.988 |
| [Mor _{1,g}] | 66.11 | -17.89 | 0.992 |

| | | | |
|--|-------|--------|-------|
| [Mor1,e] | 41.86 | -10.81 | 0.993 |
| [Pip1,e] | 34.78 | -8.61 | 0.990 |
| [HME1,e] | 40.20 | -10.42 | 0.995 |
| [HME _{1,4}][Tf ₂ N] | 43.45 | -11.65 | 0.995 |
| [Mor2,e] | 47.07 | -12.37 | 0.997 |
| [Pip2,e] | 34.21 | -8.69 | 0.997 |

Table 4.3b: Vogel-Tamman-Fulcher (VTF) parameters for viscosity behavior as a function of temperature

| ILs | η_0 cP | B K | T ₀ K | R ² |
|--|----------------|---------|---------------------|----------------|
| [HME _{1,4}] | 0.159 | 829.71 | 192 | 0.9998 |
| [Mor1,4] | 0.167 | 826.03 | 191 | 0.9998 |
| [Pip1,4] | 0.100 | 903.42 | 185 | 0.9966 |
| [Pip1,g] | 0.181 | 890.58 | 199 | 0.9999 |
| [HME1,g] | 24.84 | 230.02 | 245 | 0.9776 |
| [Mor1,g] | 1.948 | 450.15 | 246 | 0.9999 |
| [Mor1,e] | 0.495 | 621.31 | 207 | 0.9983 |
| [Pip1,e] | 0.003 | 2559.93 | 70 | 0.9860 |
| [HME1,e] | 2.161 | 350.44 | 228 | 0.9960 |
| [HME _{1,4}][Tf ₂ N] | 0.026 | 1285.18 | 164 | 0.9998 |
| [Mor2,e] | 0.164 | 905.47 | 191 | 0.9999 |
| [Pip2,e] | 0.025 | 1499 | 128 | 0.9997 |

Since, as expected from viscosity results, at least in some cases conductivities exhibit relevant deviations from Arrhenius behavior, also the Vogel-Tamman-Fulcher (VTF) equation (4) was used to represent the temperature dependence of the conductivity:

$$\kappa = \kappa_{\infty} \exp[-B'/(T-T_0)] \quad (4)$$

The Arrhenius and VTF equation parameters as well as the related correlation coefficients are reported in Table 4.5.

Table 4.4a: Conductivity values from 20 to 80° C for six N(CN)₂ ILs

| Temp (K) | HME _{1,4} | Mor _{1,4} ^a | Pip _{1,4} | Pip _{1,g} ^b | HME _{1,g} | Mor _{1,g} ^b |
|----------|--------------------|---------------------------------|--------------------|---------------------------------|--------------------|---------------------------------|
| 293 | 1.35 | 1.11 | 2.21 | 0.14 | 0.12 | 0.05 |
| 303 | 2.10 | 1.76 | 2.94 | 0.27 | 0.20 | 0.10 |
| 313 | 2.92 | 2.52 | 3.62 | 0.49 | 0.39 | 0.21 |
| 323 | 3.91 | 3.40 | 4.49 | 0.82 | 0.69 | 0.38 |
| 333 | 4.98 | 4.38 | 7.21 | 1.25 | 0.97 | 0.61 |
| 343 | 6.15 | 5.46 | 9.18 | 1.67 | 1.59 | 0.91 |
| 353 | 7.50 | 6.60 | 10.5 | 2.28 | 1.98 | 1.33 |

^aThese values are taken from Chapter 2 for comparison. ^bThese values are taken from Chapter 3 for comparison.

Table 4.4b: Conductivity values from 20 to 80° C for five N(CN)₂ and one Tf₂N ILs

| Temp (K) | Mor _{1,e} | Pip _{1,e} | HME _{1,e} | HME Tf ₂ N ^c | Mor _{2,e} | Pip _{2,e} |
|----------|--------------------|--------------------|--------------------|------------------------------------|--------------------|--------------------|
| 293 | 1.02 | 1.49 | 1.21 | 0.42 | 0.71 | 1.16 |
| 303 | 1.55 | 2.03 | 1.79 | 0.66 | 1.13 | 1.58 |
| 313 | 2.31 | 3.36 | 2.87 | 0.99 | 1.72 | 2.12 |
| 323 | 3.19 | 4.18 | 3.67 | 1.40 | 2.56 | 2.67 |
| 333 | 4.14 | 5.49 | 4.8 | 1.92 | 3.47 | 3.30 |
| 343 | 5.26 | 6.10 | 5.68 | 2.47 | 4.45 | 3.97 |
| 353 | 6.36 | 7.29 | 6.86 | 3.01 | 5.57 | 4.63 |

^cThese values are in agreement with reference 3.

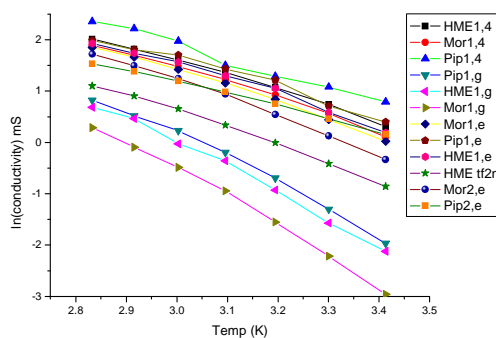
**Figure 4.1:** Conductivity behavior with temperature

Table 4.5: Arrhenius Fitting parameters and Vogel-Tamman-Fulcher (VTF) parameters for conductivity behavior as a function of temperature

| ILs | E_{κ} (kJ mol ⁻¹) | Ln A mS | R | κ mS | B' (K) | T ₀ (K) | R ² |
|------------------------------------|---|------------|-------|----------------|-----------|-----------------------|----------------|
| [HME _{1,4}] ^a | 24.17 | 10.3 | 0.996 | 134.40 | 470.05 | 190 | 0.999 |
| [Mor _{1,4}] | 25.25 | 10.5 | 0.990 | 91.87 | 393.01 | 204 | 0.999 |
| [Pip _{1,4}] | 23.47 | 10.3 | 0.982 | 2043.8 | 1274.7 | 109 | 0.981 |
| [Pip _{1,g}] | 40.01 | 14.5 | 0.989 | 78.51 | 476.73 | 218 | 0.999 |
| [HME _{1,g}] | 41.32 | 14.9 | 0.992 | 69.44 | 454.68 | 224 | 0.994 |
| [Mor _{1,g}] | 46.47 | 16.2 | 0.993 | 357.01 | 915.54 | 189 | 0.999 |
| [Mor _{1,e}] | 26.30 | 10.8 | 0.992 | 101.91 | 414.41 | 203 | 0.999 |
| [Pip _{1,e}] | 23.11 | 9.96 | 0.973 | 31.58 | 166.51 | 239 | 0.994 |
| [HME _{1,e}] | 24.87 | 10.4 | 0.982 | 48.01 | 246.53 | 226 | 0.998 |
| [HME _{1,4}] ^b | 28.36 | 10.8 | 0.994 | 60.73 | 446.61 | 204 | 0.999 |
| [Mor _{2,e}] | 29.63 | 11.8 | 0.993 | 122.98 | 458.03 | 205 | 0.999 |
| [Pip _{2,e}] | 19.84 | 8.34 | 0.995 | 61.07 | 440.69 | 18 | 0.999 |

^aThis symbol represents dicyanamide is the counter anion and ^bthis symbol represents the counter anion is Tf₂N

Generally, piperidinium-based ILs have higher conductivities and lower viscosity values than azepanium-based ILs with the corresponding counteranion as well substituents on the nitrogen. Also in this case, the lower number of carbon atoms in the cation core reduces viscosity and increases conductivity. As more times observed, larger cations make ILs more viscous because of the increased intermolecular van der Waals interactions.^{4,5,6} Ionic conductivity is proportional however not only to the number of charge carrier ions but also to their mobility; the different mobility of the six- and seven-membered rings of piperidinium and azepanium cation may affect the values characterizing both classes of ILs. Finally, it is to note that although the presence of two hydroxyl groups reduces significantly conductivity and increases viscosity a sole hydroxyl group has a not so drastic effect, in particular in the case of the azepanium-based ILs.

4.3.2 Solvent properties

In Table 4.6 are reported the polarity parameters of the investigated ILs determined spectrophotometrically at 25°C using three solvatochromic dyes (Reichardt's dye, 4-nitroaniline, and *N,N*-diethylaniline) on the basis of the equations reported in chapter 3. In agreement with the behavior observed for other classes of ILs and extensively discussed in chapter 3, the solvent properties of piperidinium-, morpholinium- and azepanium-based ILs are affected by the cationic

structure; generally, the presence of an hydroxyl group significantly increases the ability of the solvent to act as a hydrogen bonding donator. Monohydroxyl- or dihydroxyl-functionalized ILs are characterized by high α values. It is however noteworthy that also the non-functionalized [HME_{1,4}][Tf₂N] and [HME_{1,4}][N(CN)₂] are characterized by high α values (0.88 and 0.69, respectively), significantly higher than the corresponding piperidinium (0.31), morpholinium (0.38) salts and pyrrolidinium (0.37) (reported in Table 4.6) below; suggesting possible conformational effects on the ability of IL cation to interact with the Reichardt's dye. Nevertheless, the values here reported confirm that with the similar cation more basic anions give significantly lower α values; the anion–cation interactions are in the three-dimensional network characterizing ILs and this mutually affect the properties of the constituents of IL.

Table 4.6. Polarity parameters of ILs and organic solvents at 25°C

| Salt | $E_T(30)$ | E_T^N | π^* | α | β |
|--|---------------------|------------------|----------------|----------------|--------------|
| [bmim][N(CN) ₂] ^{a,b} | 51.4 | 0.639 (0.629) | 1.05 (1.13) | 0.51 (0.46) | Nd (0.70) |
| [emPyr][N(CN) ₂] ^a | 48.7 | 0.556 | 1.03 | 0.37 | Nd |
| [C ₅ dabco][N(CN) ₂] ^c | 48.4 | 0.546 | 1.11 | 0.31 | 0.55 |
| [Mor _{1,2}][N(CN) ₂] ^d | 50.3 | 0.605 | 1.12 | 0.43 | 0.506 |
| [Mor _{1,4}][Tf ₂ N] | --- | --- | 1.00 | --- | 0.205 |
| Water ^e | 53.7 ^{e,f} | 1.000 | 1.13 | 1.12 | 0.50 |
| Methanol ^e | 55.4 ^g | 0.760 | 0.73 | 1.05 | 0.61 |
| Acetone ^e | 42.2 ^{e,f} | 0.350 | 0.70 | 0.20 | 0.54 |
| Acetonitrile ^e | 45.6 ^g | 0.460 | 0.75 | 0.19 | 0.40 |
| [Pip _{1,g}][N(CN) ₂] ^h | 57.0 | 0.811 | 1.12 | 0.86 | 0.53 |
| [Mor _{1,g}][N(CN) ₂] ^h | 57.8 | 0.836 | 1.20 | 0.85 | 0.43 |
| [MIM _{1,g}][N(CN) ₂] ^h | 57.6 | 0.831 | 1.17 | 0.87 | 0.47 |
| [HME _{1,e}][N(CN) ₂] | 57.44 | 0.825 | 1.12 | 0.89 | 0.52 |
| [HME _{1,4}][Tf ₂ N] | 55.76 | 0.773 | 0.98 | 0.88 | 0.28 |
| [Mor _{1,e}][N(CN) ₂] | 55.80 | 0.775 | 1.13 | 0.78 | 0.49 |
| [Pip _{1,e}][N(CN) ₂] | 55.65 | 0.77 | 1.11 | 0.78 | 0.51 |
| [HME _{1,4}][N(CN) ₂] | 54.52 | 0.735 | 1.14 | 0.69 | 0.47 |
| [Mor _{1,4}][N(CN) ₂] ⁱ | 49.48 | 0.5796 | 1.12 | 0.38 | 0.53 |
| [Pip _{1,4}][N(CN) ₂] | 48.6 | 0.552 | 1.13 | 0.31 | 0.49 |
| [EMIM][Tf ₂ N] ^j | 52.0 | 0.657 | 0.90 | 0.76 | 0.28 |
| [EMIM][N(CN) ₂] ^j | 51.7 | 0.648 | 1.08 | 0.53 | 0.35 |
| [EMIM][NO ₃] ^j | 51.5 | 0.642 | 1.13 | 0.48 | 0.66 |
| [HOEMIM][Tf ₂ N] ^j | 60.8 | 0.929 | 1.03 | 1.17 | 0.34 |
| [HOEMIM][N(CN) ₂] ^j | --- | 0.784 | 1.11 | 0.80 | 0.51 |
| [HOEMIM][NO ₃] ^j | --- | 0.769 | 1.11 | 0.77 | 0.65 |

^aFrom reference 12. ^bFrom reference 7. ^cFrom reference 8. ^dFrom reference 9.

^eFrom reference 10. ^fFrom reference 11. ^gFrom reference 12. ^hValues obtained from chapter 3.

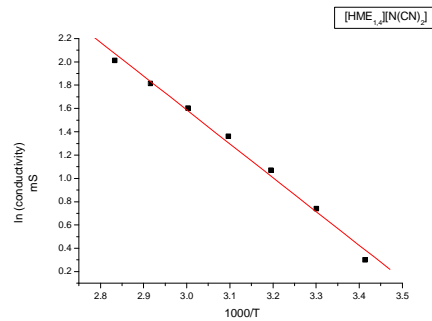
ⁱValues obtained from chapter 2. ^jShiguo et al. (2010).

4.4 Conclusion

Azepanium-based ILs represent an interesting class of ILs characterized by high polarity, in particular, a high hydrogen-bond acidity even in the case of *N,N*-dialkyl substituted salts. Nevertheless, although they have a lower conductivity and high viscosity with respect to the analogous piperidinium-based ILs differences are not dramatic. Finally, the introduction of an unique hydroxyl group on the alkyl chain on cation has only a moderate effect on the physico-chemical properties of azepanium and piperidinium salts whereas two hydroxyl groups are able to significantly affect conductivity and viscosity.

Appendix:3

Analysis of the behavior of conductivity values for [HME_{1,4}][N(CN)₂], [Mor_{1,4}][N(CN)₂], [Pip_{1,4}][N(CN)₂], [HME_{1,g}][N(CN)₂], [Mor_{1,g}][N(CN)₂], [Pip_{1,g}][N(CN)₂], [HME_{1,e}][N(CN)₂], [Mor_{1,e}][N(CN)₂], [Pip_{1,e}][N(CN)₂], [Mor_{2,e}][N(CN)₂], [Pip_{2,e}][N(CN)₂] and [HME_{1,4}][Tf₂N].



Linear Regression for [HME_{1,4}][N(CN)₂]:

$$Y = A + B * X$$

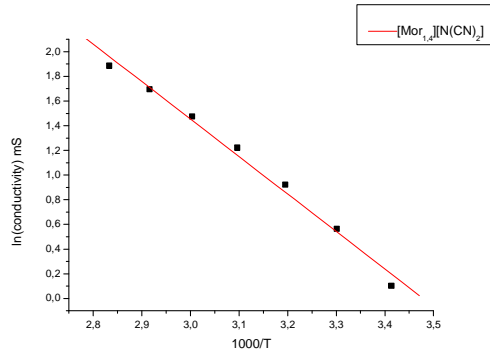
| Parameter | Value | Error | t-Value | Prob> t |
|-----------|----------|---------|-----------|---------|
| A | 10.3091 | 0.36339 | 28.36923 | <0.0001 |
| B | -2.90717 | 0.1167 | -24.91183 | <0.0001 |

| R | R-Square(COD) | Adj. R-Square | Root-MSE(SD) | N |
|--------|---------------|---------------|--------------|---|
| -0.996 | 0.99201 | 0.99041 | 0.05968 | 7 |

| Parameter | LCI | UCI |
|-----------|----------|----------|
| A | 9.37498 | 11.24323 |
| B | -3.20715 | -2.60719 |

ANOVA Table:

| Item | Degrees of Freedom | Sum of Squares | Mean Square | F Statistic |
|-------|--------------------|----------------|-------------|-------------|
| Model | 1 | 2.21003 | 2.21003 | 620.59903 |
| Error | 5 | 0.01781 | 0.00356 | |
| Total | 6 | 2.22784 | | |



Linear Regression for [Mor_{1,4}][N(CN)₂]:

$$Y = A + B * X$$

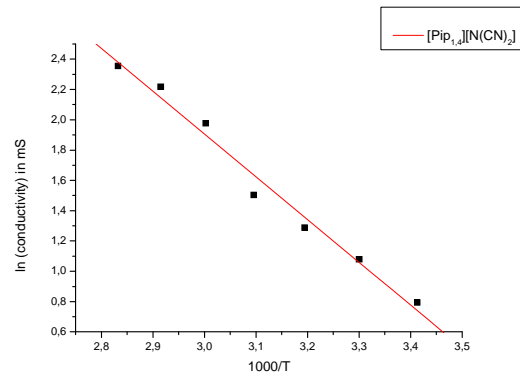
| Parameter | Value | Error | t-Value | Prob> t |
|-----------|----------|---------|-----------|---------|
| A | 10.563 | 0.42096 | 25.09287 | <0.0001 |
| B | -3.03649 | 0.13518 | -22.46174 | <0.0001 |

| R | R-Square(COD) | Adj. R-Square | Root-MSE(SD) | N |
|----------|---------------|---------------|--------------|---|
| -0.99508 | 0.99019 | 0.98822 | 0.06913 | 7 |

| Parameter | LCI | UCI |
|-----------|----------|----------|
| A | 9.4809 | 11.6451 |
| B | -3.38399 | -2.68899 |

ANOVA Table:

| Item | Degrees of Freedom | Sum of Squares | Mean Square | F Statistic |
|-------|--------------------|----------------|-------------|-------------|
| Model | 1 | 2.41102 | 2.41102 | 504.52992 |
| Error | 5 | 0.02389 | 0.00478 | |
| Total | 6 | 2.43492 | | |



Linear Regression for $[Pip_{1,4}][N(CN)_2]$:

$$Y = A + B * X$$

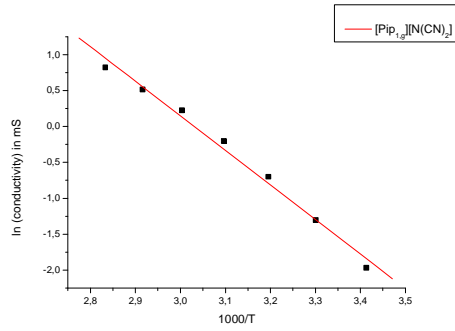
| Parameter | Value | Error | t-Value | Prob> t |
|-----------|----------|---------|-----------|---------|
| A | 10.37516 | 0.5282 | 19.6425 | <0.0001 |
| B | -2.82318 | 0.16962 | -16.64369 | <0.0001 |

| R | R-Square(COD) | Adj. R-Square | Root-MSE(SD) | N |
|---------|---------------|---------------|--------------|---|
| -0.9911 | 0.98227 | 0.97872 | 0.08674 | 7 |

| Parameter | LCI | UCI |
|-----------|----------|----------|
| A | 9.01739 | 11.73294 |
| B | -3.25922 | -2.38715 |

ANOVA Table:

| Item | Degrees of Freedom | Sum of Squares | Mean Square | F Statistic |
|-------|--------------------|----------------|-------------|-------------|
| Model | 1 | 2.08418 | 2.08418 | 277.01228 |
| Error | 5 | 0.03762 | 0.00752 | |
| Total | 6 | 2.1218 | | |



Linear Regression for [Pip_{1,g}][N(CN)₂]:

$$Y = A + B * X$$

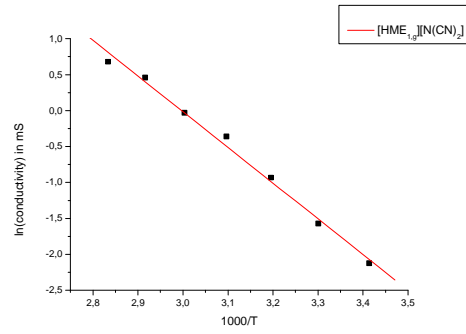
| Parameter | Value | Error | t-Value | Prob> t |
|-----------|----------|---------|-----------|---------|
| A | 14.58681 | 0.69299 | 21.04903 | <0.0001 |
| B | -4.8127 | 0.22255 | -21.62566 | <0.0001 |

| R | R-Square(COD) | Adj. R-Square | Root-MSE(SD) | N |
|---------|---------------|---------------|--------------|---|
| -0.9947 | 0.98942 | 0.98731 | 0.1138 | 7 |

| Parameter | LCI | UCI |
|-----------|----------|----------|
| A | 12.80542 | 16.3682 |
| B | -5.38477 | -4.24063 |

ANOVA Table:

| Item | Degrees of Freedom | Sum of Squares | Mean Square | F Statistic |
|-------|--------------------|----------------|-------------|-------------|
| Model | 1 | 6.05669 | 6.05669 | 467.66933 |
| Error | 5 | 0.06475 | 0.01295 | |
| Total | 6 | 6.12144 | | |



Linear Regression for $[\text{Mor}_{1,g}][\text{N}(\text{CN})_2]$:

$$Y = A + B * X$$

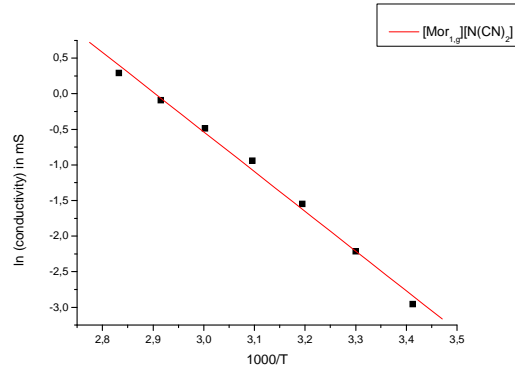
| Parameter | Value | Error | t-Value | Prob> t |
|-----------|----------|---------|-----------|---------|
| A | 14.89548 | 0.59823 | 24.89924 | <0.0001 |
| B | -4.97014 | 0.19211 | -25.87076 | <0.0001 |

| R | R-Square(COD) | Adj. R-Square | Root-MSE(SD) | N |
|----------|---------------|---------------|--------------|---|
| -0.99629 | 0.99258 | 0.9911 | 0.09824 | 7 |

| Parameter | LCI | UCI |
|-----------|----------|----------|
| A | 13.35768 | 16.43328 |
| B | -5.46399 | -4.4763 |

ANOVA Table:

| Item | Degrees of Freedom | Sum of Squares | Mean Square | F Statistic |
|-------|--------------------|----------------|-------------|-------------|
| Model | 1 | 6.45945 | 6.45945 | 669.296 |
| Error | 5 | 0.04826 | 0.00965 | |
| Total | 6 | 6.5077 | | |



Linear Regression for Data1_T:

$$Y = A + B * X$$

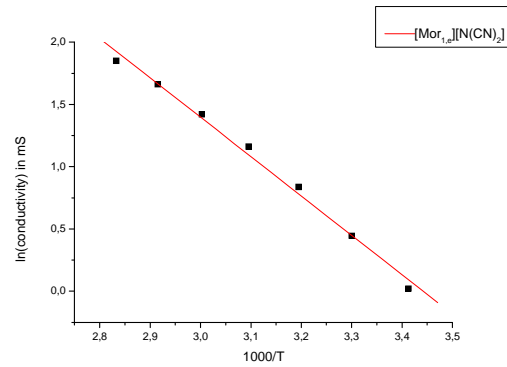
| Parameter | Value | Error | t-Value | Prob> t |
|-----------|----------|---------|-----------|---------|
| A | 16.2322 | 0.62194 | 26.09912 | <0.0001 |
| B | -5.58889 | 0.19973 | -27.98228 | <0.0001 |

| R | R-Square(COD) | Adj. R-Square | Root-MSE(SD) | N |
|----------|---------------|---------------|--------------|---|
| -0.99682 | 0.99365 | 0.99239 | 0.10213 | 7 |

| Parameter | LCI | UCI |
|-----------|----------|----------|
| A | 14.63344 | 17.83095 |
| B | -6.10231 | -5.07547 |

ANOVA Table:

| Item | Degrees of Freedom | Sum of Squares | Mean Square | F Statistic |
|-------|--------------------|----------------|-------------|-------------|
| Model | 1 | 8.16788 | 8.16788 | 783.00799 |
| Error | 5 | 0.05216 | 0.01043 | |
| Total | 6 | 8.22004 | | |



Linear Regression for $[\text{Mor}_{1,e}][\text{N}(\text{CN})_2]$:

$$Y = A + B * X$$

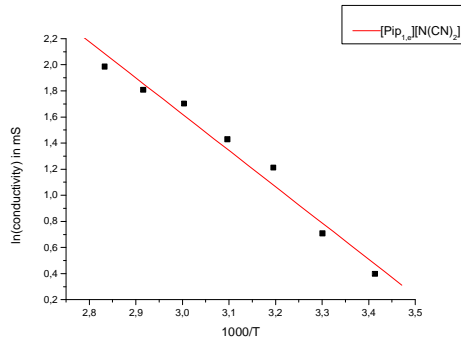
| Parameter | Value | Error | t-Value | Prob> t |
|-----------|----------|---------|-----------|---------|
| A | 10.88576 | 0.38061 | 28.60097 | <0.0001 |
| B | -3.16281 | 0.12223 | -25.87636 | <0.0001 |

| R | R-Square(COD) | Adj. R-Square | Root-MSE(SD) | N |
|----------|---------------|---------------|--------------|---|
| -0.99629 | 0.99259 | 0.99111 | 0.0625 | 7 |

| Parameter | LCI | UCI |
|-----------|---------|----------|
| A | 9.90738 | 11.86415 |
| B | -3.477 | -2.84861 |

ANOVA Table:

| Item | Degrees of Freedom | Sum of Squares | Mean Square | F Statistic |
|-------|--------------------|----------------|-------------|-------------|
| Model | 1 | 2.61579 | 2.61579 | 669.58618 |
| Error | 5 | 0.01953 | 0.00391 | |
| Total | 6 | 2.63533 | | |



Linear Regression for $[Pip_{1,e}][N(CN)_2]$:

$$Y = A + B * X$$

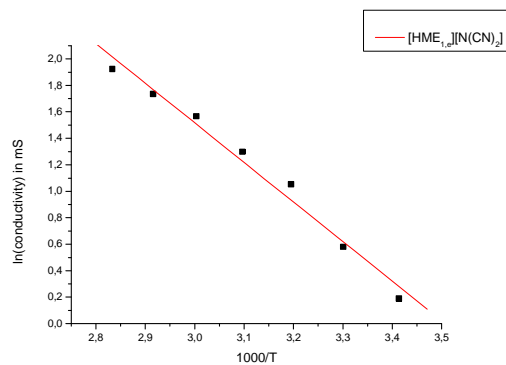
| Parameter | Value | Error | t-Value | Prob> t |
|-----------|----------|---------|-----------|---------|
| A | 9.96122 | 0.6402 | 15.55955 | <0.0001 |
| B | -2.78007 | 0.20559 | -13.52226 | <0.0001 |

| R | R-Square(COD) | Adj. R-Square | Root-MSE(SD) | N |
|---------|---------------|---------------|--------------|---|
| -0.9866 | 0.97338 | 0.96806 | 0.10513 | 7 |

| Parameter | LCI | UCI |
|-----------|----------|----------|
| A | 8.31554 | 11.60691 |
| B | -3.30856 | -2.25158 |

ANOVA Table:

| Item | Degrees of Freedom | Sum of Squares | Mean Square | F Statistic |
|-------|--------------------|----------------|-------------|-------------|
| Model | 1 | 2.02102 | 2.02102 | 182.8514 |
| Error | 5 | 0.05526 | 0.01105 | |
| Total | 6 | 2.07628 | | |



Linear Regression for $[HME_{1,e}][N(CN)_2]$:

$$Y = A + B * X$$

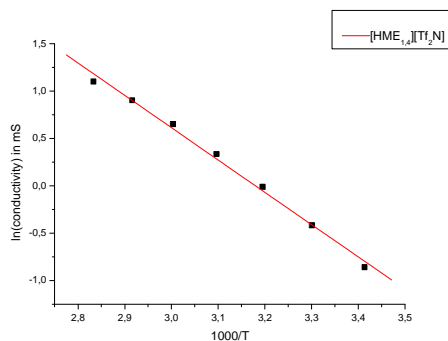
| Parameter | Value | Error | t-Value | Prob> t |
|-----------|----------|---------|-----------|---------|
| A | 10.49174 | 0.55885 | 18.77388 | <0.0001 |
| B | -2.9916 | 0.17947 | -16.66933 | <0.0001 |

| R | R-Square(COD) | Adj. R-Square | Root-MSE(SD) | N |
|----------|---------------|---------------|--------------|---|
| -0.99112 | 0.98232 | 0.97879 | 0.09177 | 7 |

| Parameter | LCI | UCI |
|-----------|----------|----------|
| A | 9.05518 | 11.92831 |
| B | -3.45293 | -2.53026 |

ANOVA Table:

| Item | Degrees of Freedom | Sum of Squares | Mean Square | F Statistic |
|-------|--------------------|----------------|-------------|-------------|
| Model | 1 | 2.34026 | 2.34026 | 277.86651 |
| Error | 5 | 0.04211 | 0.00842 | |
| Total | 6 | 2.38237 | | |



Linear Regression for [HME_{1,4}][Tf₂N]:

$$Y = A + B * X$$

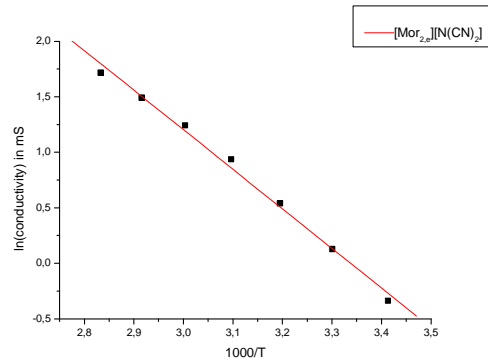
| Parameter | Value | Error | t-Value | Prob> t |
|-----------|----------|---------|----------|---------|
| A | 10.84726 | 0.35894 | 30.22046 | <0.0001 |
| B | -3.41148 | 0.11527 | -29.596 | <0.0001 |

| R | R-Square(COD) | Adj. R-Square | Root-MSE(SD) | N |
|----------|---------------|---------------|--------------|---|
| -0.99716 | 0.99432 | 0.99319 | 0.05894 | 7 |

| Parameter | LCI | UCI |
|-----------|----------|----------|
| A | 9.92458 | 11.76994 |
| B | -3.70779 | -3.11518 |

ANOVA Table:

| Item | Degrees of Freedom | Sum of Squares | Mean Square | F Statistic |
|-------|--------------------|----------------|-------------|-------------|
| Model | 1 | 3.0433 | 3.0433 | 875.92319 |
| Error | 5 | 0.01737 | 0.00347 | |
| Total | 6 | 3.06067- | | |



Linear Regression for $[\text{Mor}_{2,e}][\text{N}(\text{CN})_2]$:

$$Y = A + B * X$$

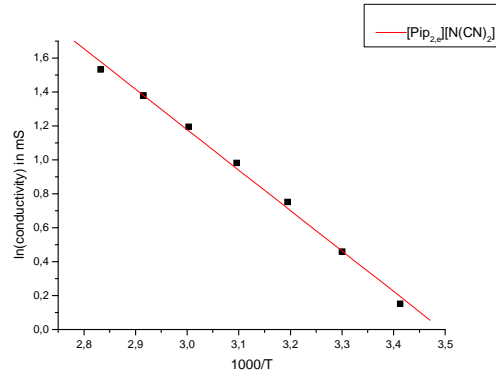
| Parameter | Value | Error | t-Value | Prob> t |
|-----------|----------|---------|-----------|---------|
| A | 11.89358 | 0.39727 | 29.93812 | <0.0001 |
| B | -3.56345 | 0.12758 | -27.93128 | <0.0001 |

| R | R-Square(COD) | Adj. R-Square | Root-MSE(SD) | N |
|----------|---------------|---------------|--------------|---|
| -0.99681 | 0.99363 | 0.99236 | 0.06524 | 7 |

| Parameter | LCI | UCI |
|-----------|----------|----------|
| A | 10.87236 | 12.9148 |
| B | -3.8914 | -3.23549 |

ANOVA Table:

| Item | Degrees of Freedom | Sum of Squares | Mean Square | F Statistic |
|-------|--------------------|----------------|-------------|-------------|
| Model | 1 | 3.32046 | 3.32046 | 780.1565 |
| Error | 5 | 0.02128 | 0.00426 | |
| Total | 6 | 3.34174 | | |



Linear Regression for [Pip_{2,e}][N(CN)₂]:

$$Y = A + B * X$$

| Parameter | Value | Error | t-Value | Prob> t |
|-----------|----------|---------|-----------|---------|
| A | 8.33791 | 0.22337 | 37.32842 | <0.0001 |
| B | -2.38635 | 0.07173 | -33.26782 | <0.0001 |

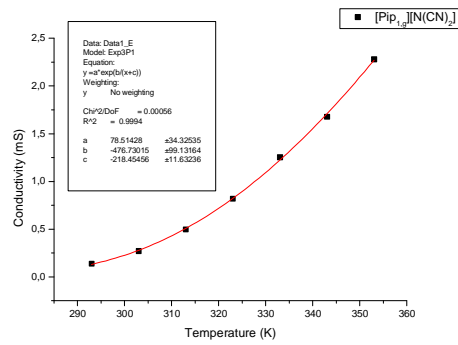
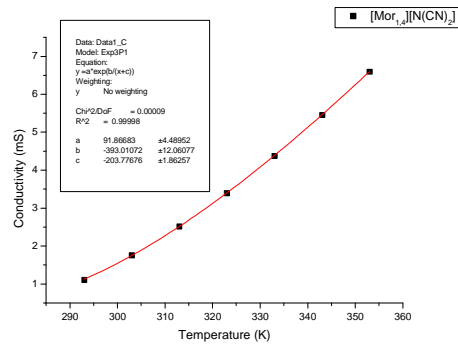
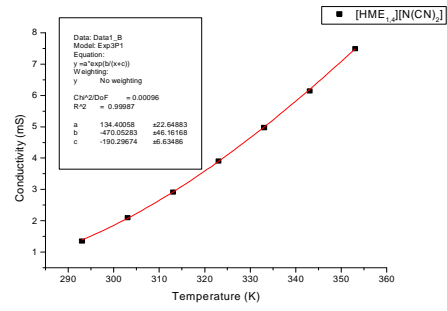
| R | R-Square(COD) | Adj. R-Square | Root-MSE(SD) | N |
|----------|---------------|---------------|--------------|---|
| -0.99775 | 0.9955 | 0.9946 | 0.03668 | 7 |

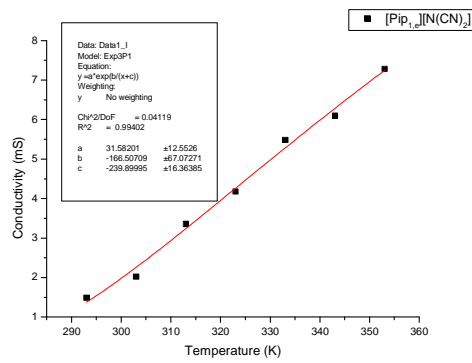
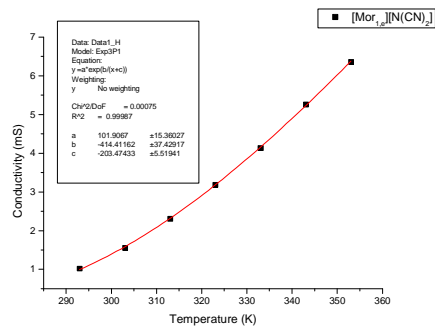
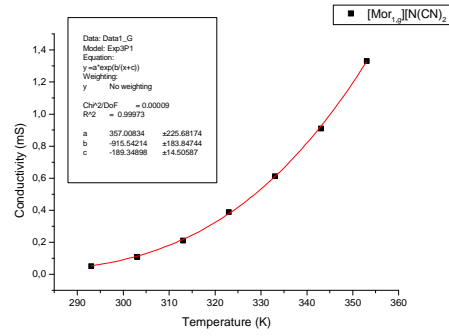
| Parameter | LCI | UCI |
|-----------|----------|----------|
| A | 7.76373 | 8.91209 |
| B | -2.57074 | -2.20195 |

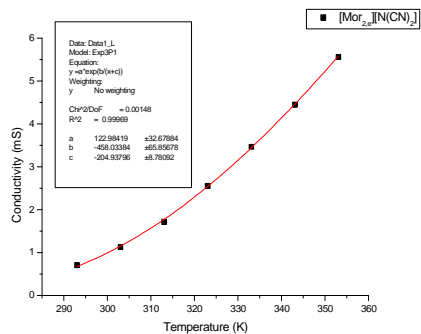
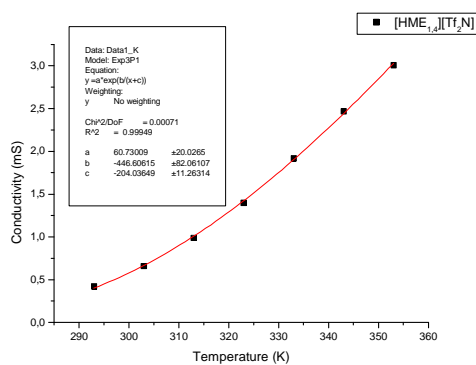
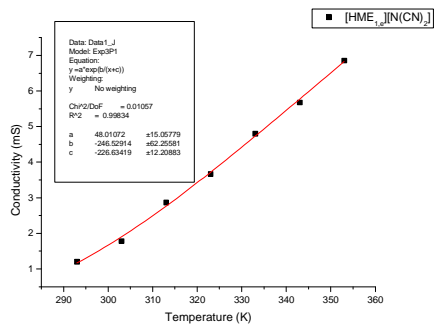
ANOVA Table:

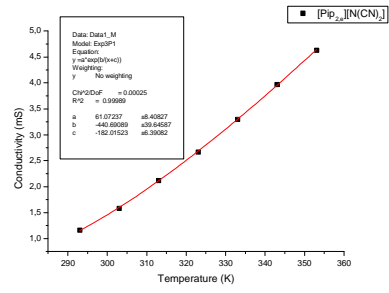
| Item | Degrees of Freedom | Sum of Squares | Mean Square | F Statistic |
|-------|--------------------|----------------|-------------|-------------|
| Model | 1 | 1.4891 | 1.4891 | 1106.74818 |
| Error | 5 | 0.00673 | 0.00135 | |
| Total | 6 | 1.49583 | | |

VTF plots:

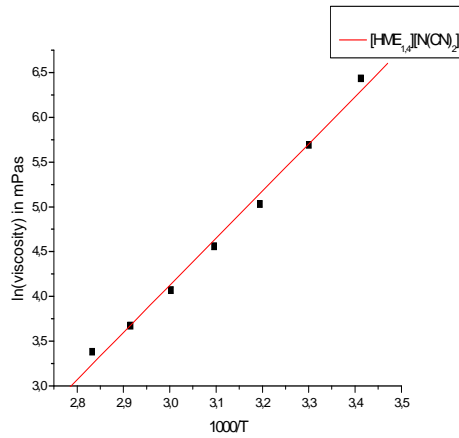








Appendix 4: Appendix for Arrhenius values for viscosity:



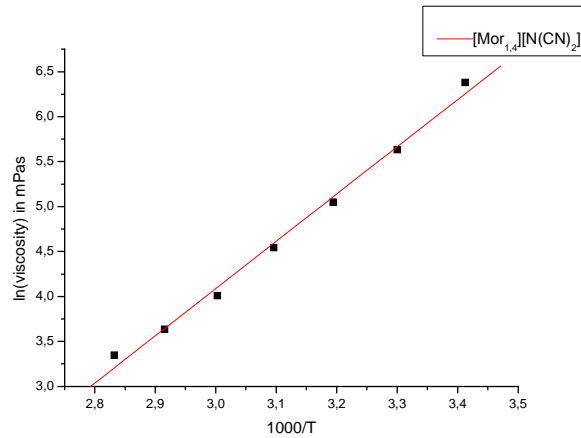
| Parameter | Value | Error | t-Value | Prob> t |
|-----------|-----------|---------|-----------|---------|
| A | -11.67187 | 0.67374 | -17.32396 | <0.0001 |
| B | 5.26504 | 0.21636 | 24.33419 | <0.0001 |

| R | R-Square(COD) | Adj. R-Square | Root-MSE(SD) | N |
|--------|---------------|---------------|--------------|---|
| 0.9958 | 0.99163 | 0.98995 | 0.11064 | 7 |

| Parameter | LCI | UCI |
|-----------|-----------|----------|
| A | -13.40378 | -9.93997 |
| B | 4.70886 | 5.82122 |

ANOVA Table:

| Item | Degrees of Freedom | Sum of Squares | Mean Square | F Statistic |
|-------|--------------------|----------------|-------------|-------------|
| Model | 1 | 7.24871 | 7.24871 | 592.15262 |
| Error | 5 | 0.06121 | 0.01224 | |
| Total | 6 | 7.30992 | | |



Linear Regression for [Mor_{1,4}][N(CN)₂]:

$$Y = A + B * X$$

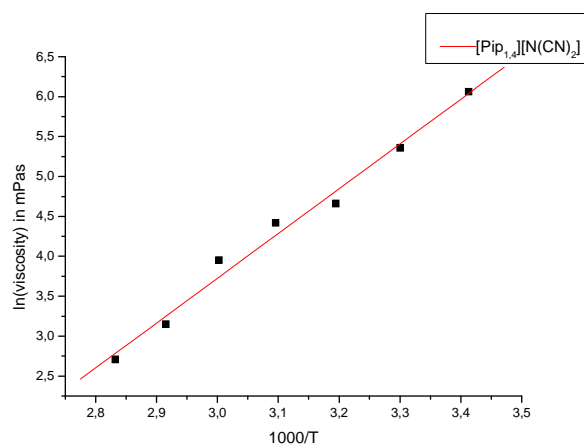
| Parameter | Value | Error | t-Value | Prob> t |
|-----------|----------|---------|----------|---------|
| A | -11.6754 | 0.60696 | -19.2358 | <0.0001 |
| B | 5.25449 | 0.19492 | 26.95737 | <0.0001 |

| R | R-Square(COD) | Adj. R-Square | Root-MSE(SD) | N |
|---------|---------------|---------------|--------------|---|
| 0.99658 | 0.99317 | 0.9918 | 0.09967 | 7 |

| Parameter | LCI | UCI |
|-----------|-----------|-----------|
| A | -13.23564 | -10.11516 |
| B | 4.75343 | 5.75554 |

ANOVA Table:

| Item | Degrees of Freedom | Sum of Squares | Mean Square | F Statistic |
|-------|--------------------|----------------|-------------|-------------|
| Model | 1 | 7.21969 | 7.21969 | 726.70006 |
| Error | 5 | 0.04967 | 0.00993 | |
| Total | 6 | 7.26937 | | |



Linear Regression for [Pip_{1,4}][N(CN)₂]:

$$Y = A + B * X$$

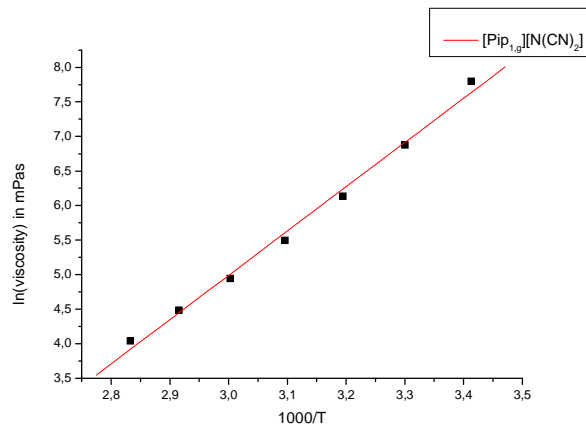
| Parameter | Value | Error | t-Value | Prob> t |
|-----------|-----------|---------|-----------|---------|
| A | -13.10266 | 0.91477 | -14.32342 | <0.0001 |
| B | 5.60888 | 0.29377 | 19.09291 | <0.0001 |

| R | R-Square(COD) | Adj. R-Square | Root-MSE(SD) | N |
|---------|---------------|---------------|--------------|---|
| 0.99321 | 0.98647 | 0.98376 | 0.15022 | 7 |

| Parameter | LCI | UCI |
|-----------|-----------|-----------|
| A | -15.45416 | -10.75117 |
| B | 4.85373 | 6.36403 |

ANOVA Table:

| Item | Degrees of Freedom | Sum of Squares | Mean Square | F Statistic |
|-------|--------------------|----------------|-------------|-------------|
| Model | 1 | 8.22641 | 8.22641 | 364.53926 |
| Error | 5 | 0.11283 | 0.02257 | |
| Total | 6 | 8.33924 | | |



Linear Regression for Data1_R:

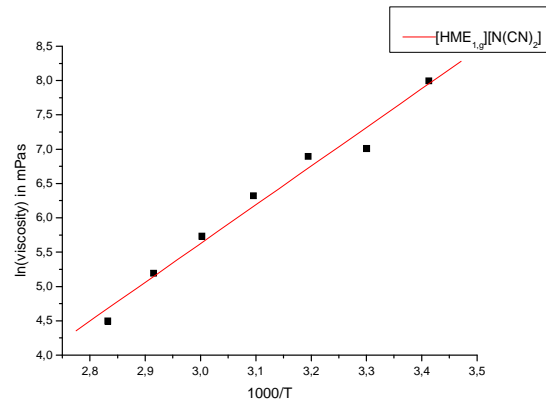
$$Y = A + B * X$$

| Parameter | Value | Error | t-Value | Prob> t |
|-----------|---------------|---------------|--------------|---------|
| A | -14.23234 | 0.72635 | -19.59446 | <0.0001 |
| B | 6.40765 | 0.23326 | 27.47035 | <0.0001 |
| R | R-Square(COD) | Adj. R-Square | Root-MSE(SD) | N |
| 0.9967 | 0.99342 | 0.9921 | 0.11928 | 7 |

| Parameter | LCI | UCI |
|-----------|-----------|-----------|
| A | -16.09947 | -12.36521 |
| B | 5.80804 | 7.00725 |

ANOVA Table:

| Item | Degrees of Freedom | Sum of Squares | Mean Square | F Statistic |
|-------|--------------------|----------------|-------------|-------------|
| Model | 1 | 10.73631 | 10.73631 | 754.62013 |
| Error | 5 | 0.07114 | 0.01423 | |
| Total | 6 | 10.80745 | | |



Linear Regression for [HME_{1,g}][N(CN)₂]:

$$Y = A + B * X$$

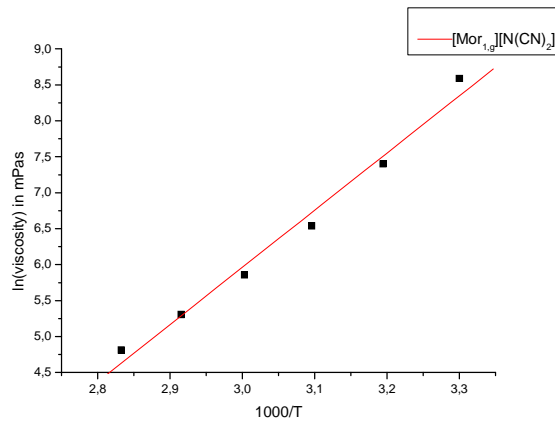
| Parameter | Value | Error | t-Value | Prob> t |
|-----------|-----------|---------|----------|------------|
| A | -11.29169 | 1.20666 | -9.35781 | 2.34807E-4 |
| B | 5.63895 | 0.3875 | 14.552 | <0.0001 |

| R | R-Square(COD) | Adj. R-Square | Root-MSE(SD) | N |
|--------|---------------|---------------|--------------|---|
| 0.9884 | 0.97693 | 0.97232 | 0.19815 | 7 |

| Parameter | LCI | UCI |
|-----------|----------|----------|
| A | -14.3935 | -8.18988 |
| B | 4.64284 | 6.63506 |

ANOVA Table:

| Item | Degrees of Freedom | Sum of Squares | Mean Square | F Statistic |
|-------|--------------------|----------------|-------------|-------------|
| Model | 1 | 8.31486 | 8.31486 | 211.76077 |
| Error | 5 | 0.19633 | 0.03927 | |
| Total | 6 | 8.51119 | | |



Linear Regression for [Mor_{1,e}][N(CN)₂]:

$$Y = A + B * X$$

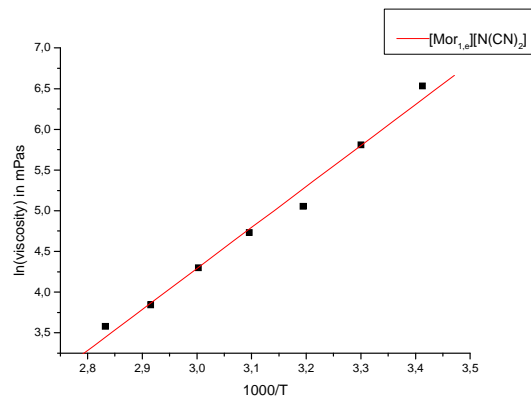
| Parameter | Value | Error | t-Value | Prob> t |
|-----------|-----------|---------|-----------|------------|
| A | -17.89178 | 1.5282 | -11.70775 | 3.04386E-4 |
| B | 7.95154 | 0.49921 | 15.92832 | <0.0001 |

| R | R-Square(COD) | Adj. R-Square | Root-MSE(SD) | N |
|---------|---------------|---------------|--------------|---|
| 0.99221 | 0.98448 | 0.9806 | 0.19522 | 6 |

| Parameter | LCI | UCI |
|-----------|-----------|-----------|
| A | -22.13474 | -13.64883 |
| B | 6.56552 | 9.33756 |

ANOVA Table:

| Item | Degrees of Freedom | Sum of Squares | Mean Square | F Statistic |
|-------|--------------------|----------------|-------------|-------------|
| Model | 1 | 9.66939 | 9.66939 | 253.7113 |
| Error | 4 | 0.15245 | 0.03811 | |
| Total | 5 | 9.82183 | | |



Linear Regression for [Mor_{1,e}][N(CN)₂]:

$$Y = A + B * X$$

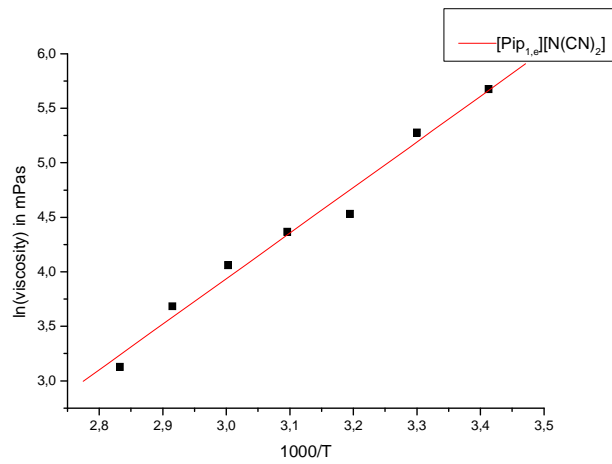
| Parameter | Value | Error | t-Value | Prob> t |
|-----------|-----------|---------|-----------|---------|
| A | -10.81502 | 0.83295 | -12.98395 | <0.0001 |
| B | 5.03518 | 0.26749 | 18.82363 | <0.0001 |

| R | R-Square(COD) | Adj. R-Square | Root-MSE(SD) | N |
|---------|---------------|---------------|--------------|---|
| 0.99302 | 0.98609 | 0.9833 | 0.13679 | 7 |

| Parameter | LCI | UCI |
|-----------|-----------|----------|
| A | -12.95619 | -8.67385 |
| B | 4.34757 | 5.72279 |

ANOVA Table:

| Item | Degrees of Freedom | Sum of Squares | Mean Square | F Statistic |
|-------|--------------------|----------------|-------------|-------------|
| Model | 1 | 6.62961 | 6.62961 | 354.32907 |
| Error | 5 | 0.09355 | 0.01871 | |
| Total | | 6 | 6.72316 | |



Linear Regression for [PiP_{1,e}][N(CN)₂]:

$$Y = A + B * X$$

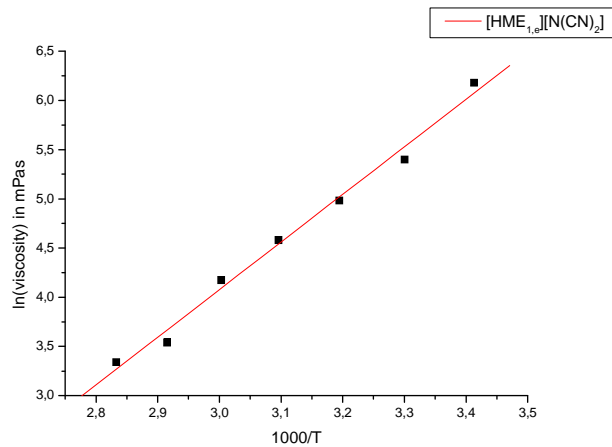
| Parameter | Value | Error | t-Value | Prob> t |
|-----------|----------|---------|-----------|------------|
| A | -8.61399 | 0.82178 | -10.48209 | 1.36339E-4 |
| B | 4.18387 | 0.26391 | 15.8537 | <0.0001 |

| R | R-Square(COD) | Adj. R-Square | Root-MSE(SD) | N |
|--------|---------------|---------------|--------------|---|
| 0.9902 | 0.98049 | 0.97659 | 0.13495 | 7 |

| Parameter | LCI | UCI |
|-----------|-----------|----------|
| A | -10.72644 | -6.50153 |
| B | 3.50548 | 4.86226 |

ANOVA Table:

| Item | Degrees of Freedom | Sum of Squares | Mean Square | F Statistic |
|-------|--------------------|----------------|-------------|-------------|
| Model | 1 | 4.57735 | 4.57735 | 251.33969 |
| Error | 5 | 0.09106 | 0.01821 | |
| Total | 6 | 4.66841 | | |



Linear Regression for $[\text{HME}_{1,e}][\text{N}(\text{CN})_2]$:

$$Y = A + B * X$$

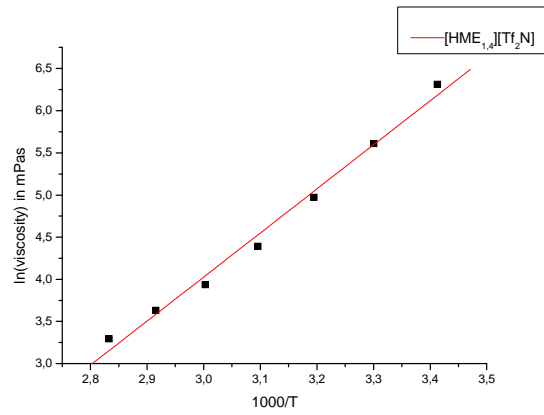
| Parameter | Value | Error | t-Value | Prob> t |
|-----------|-----------|---------|----------|---------|
| A | -10.42817 | 0.66329 | -15.7219 | <0.0001 |
| B | 4.83531 | 0.21301 | 22.70023 | <0.0001 |

| R | R-Square(COD) | Adj. R-Square | Root-MSE(SD) | N |
|---------|---------------|---------------|--------------|---|
| 0.99518 | 0.99039 | 0.98847 | 0.10892 | 7 |

| Parameter | LCI | UCI |
|-----------|----------|----------|
| A | -12.1332 | -8.72313 |
| B | 4.28776 | 5.38286 |

ANOVA Table:

| Item | Degrees of Freedom | Sum of Squares | Mean Square | F Statistic |
|-------|--------------------|----------------|-------------|-------------|
| Model | 1 | 6.11374 | 6.11374 | 515.30064 |
| Error | 5 | 0.05932 | 0.01186 | |
| Total | 6 | 6.17306 | | |



Linear Regression for [HME_{1,4}][Tf₂N]:

$$Y = A + B * X$$

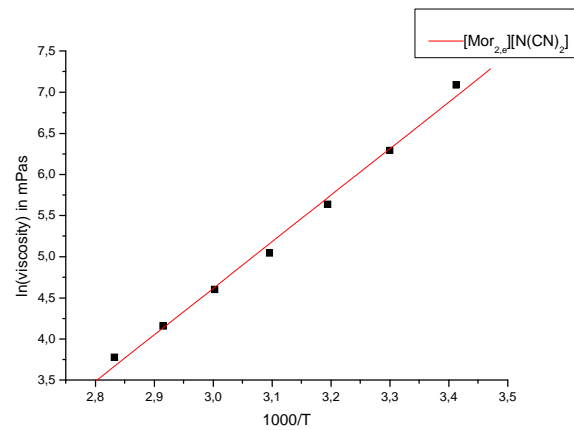
| Parameter | Value | Error | t-Value | Prob> t |
|-----------|-----------|---------|-----------|---------|
| A | -11.65207 | 0.73978 | -15.75081 | <0.0001 |
| B | 5.22645 | 0.23757 | 21.99964 | <0.0001 |

| R | R-Square(COD) | Adj. R-Square | Root-MSE(SD) | N |
|---------|---------------|---------------|--------------|---|
| 0.99487 | 0.98977 | 0.98773 | 0.12148 | 7 |

| Parameter | LCI | UCI |
|-----------|-----------|----------|
| A | -13.55372 | -9.75042 |
| B | 4.61576 | 5.83715 |

ANOVA Table:

| Item | Degrees of Freedom | Sum of Squares | Mean Square | F Statistic |
|-------|--------------------|----------------|-------------|-------------|
| Model | 1 | 7.14286 | 7.14286 | 483.98435 |
| Error | 5 | 0.07379 | 0.01476 | |
| Total | 6 | 7.21665 | | |



Linear Regression for Data1_Y:

$$Y = A + B * X$$

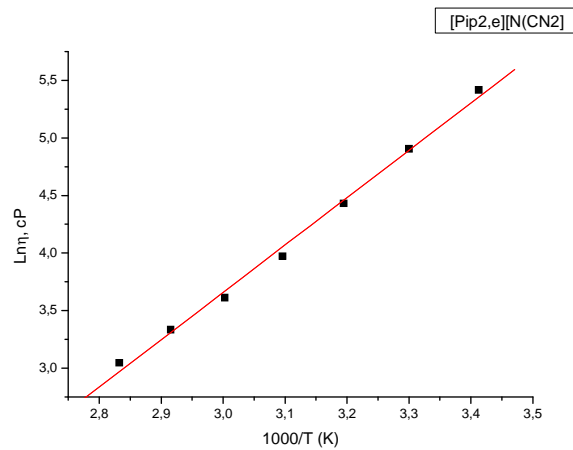
| Parameter | Value | Error | t-Value | Prob> t |
|-----------|-----------|---------|-----------|---------|
| A | -12.36863 | 0.61735 | -20.03498 | <0.0001 |
| B | 5.66129 | 0.19825 | 28.55558 | <0.0001 |

| R | R-Square(COD) | Adj. R-Square | Root-MSE(SD) | N |
|---------|---------------|---------------|--------------|---|
| 0.99695 | 0.99391 | 0.99269 | 0.10138 | 7 |

| Parameter | LCI | UCI |
|-----------|-----------|-----------|
| A | -13.95558 | -10.78168 |
| B | 5.15166 | 6.17092 |

ANOVA Table:

| Item | Degrees of Freedom | Sum of Squares | Mean Square | F Statistic |
|-------|--------------------|----------------|-------------|-------------|
| Model | 1 | 8.38085 | 8.38085 | 815.42099 |
| Error | 5 | 0.05139 | 0.01028 | |
| Total | 6 | 8.43224 | | |



Linear Regression for Data1_Z:

$$Y = A + B * X$$

| Parameter | Value | Error | t-Value | Prob> t |
|-----------|----------|---------|-----------|---------|
| A | -8.68894 | 0.39275 | -22.12322 | <0.0001 |
| B | 4.11541 | 0.12613 | 32.62898 | <0.0001 |

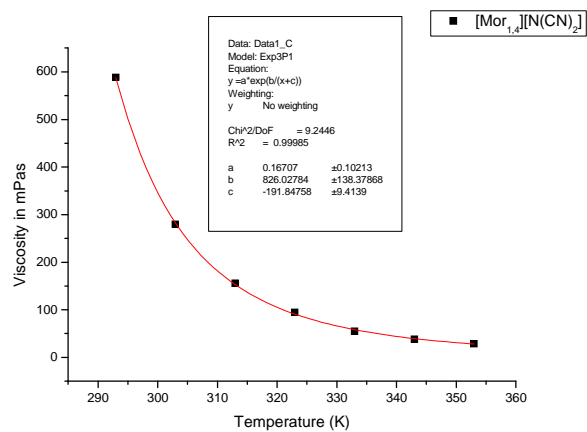
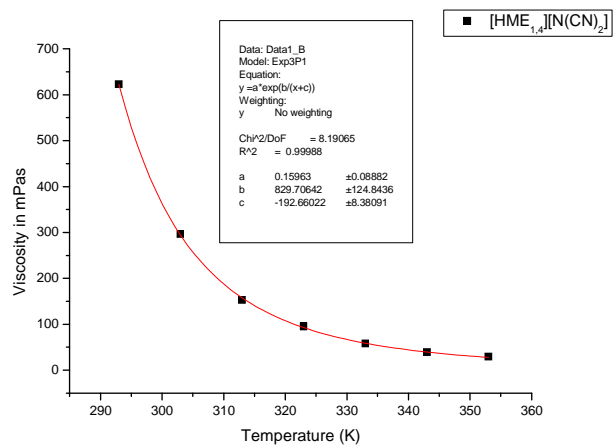
| R | R-Square(COD) | Adj. R-Square | Root-MSE(SD) | N |
|---------|---------------|---------------|--------------|---|
| 0.99766 | 0.99533 | 0.99439 | 0.0645 | 7 |

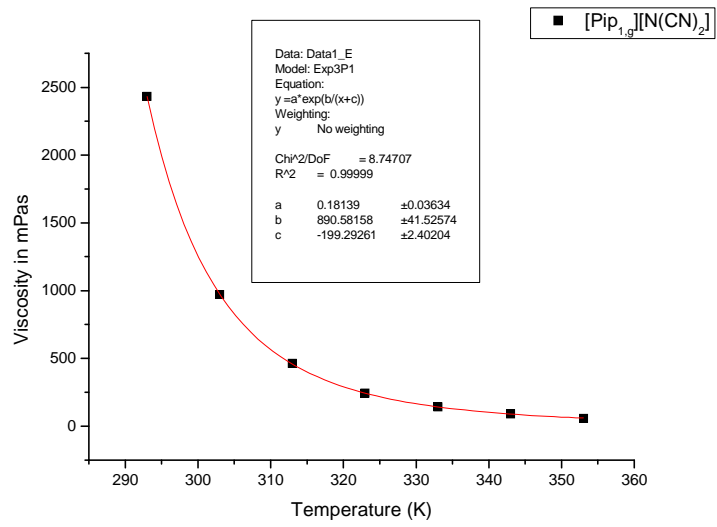
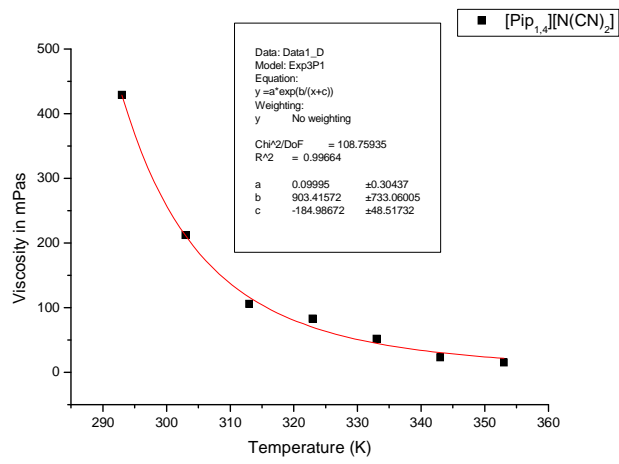
| Parameter | LCI | UCI |
|-----------|----------|----------|
| A | -9.69854 | -7.67934 |
| B | 3.79119 | 4.43963 |

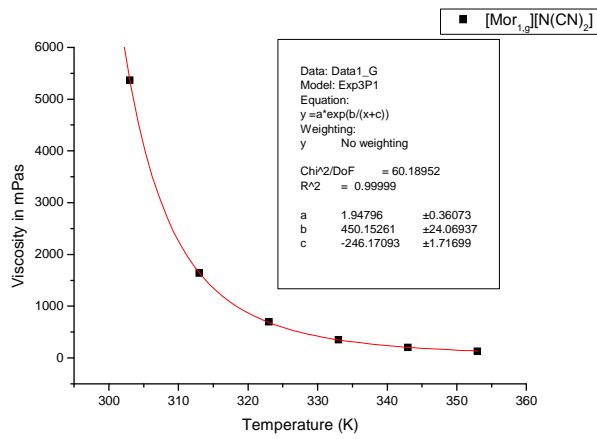
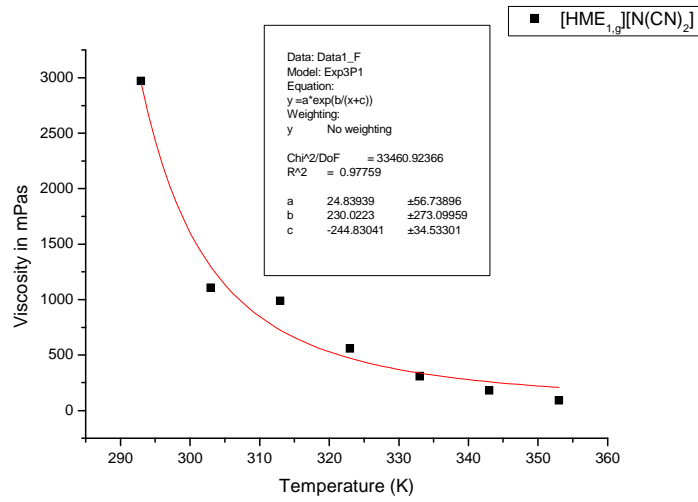
ANOVA Table:

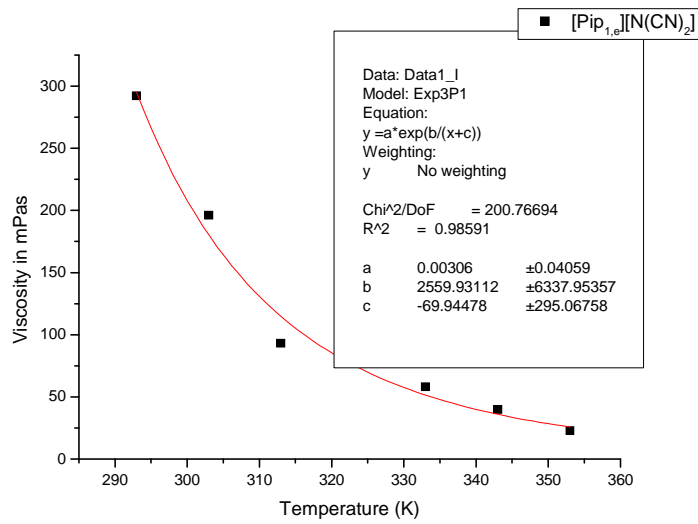
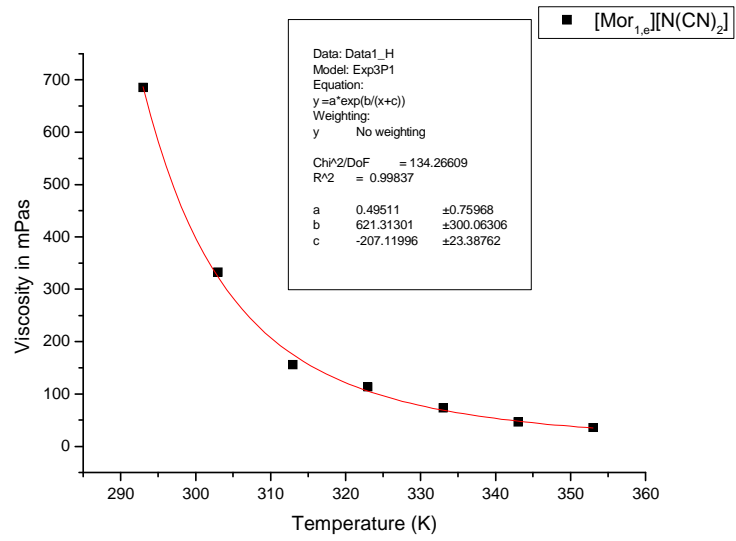
| Item | Degrees of Freedom | Sum of Squares | Mean Square | F Statistic |
|-------|--------------------|----------------|-------------|-------------|
| Model | 1 | 4.42878 | 4.42878 | 1064.65008 |
| Error | 5 | 0.0208 | 0.00416 | |
| Total | 6 | 4.44958 | | |

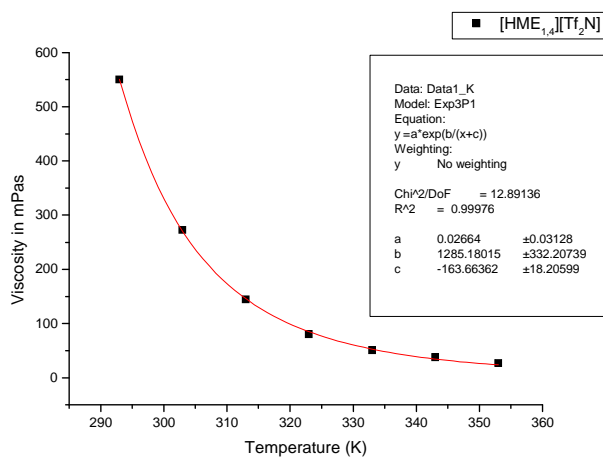
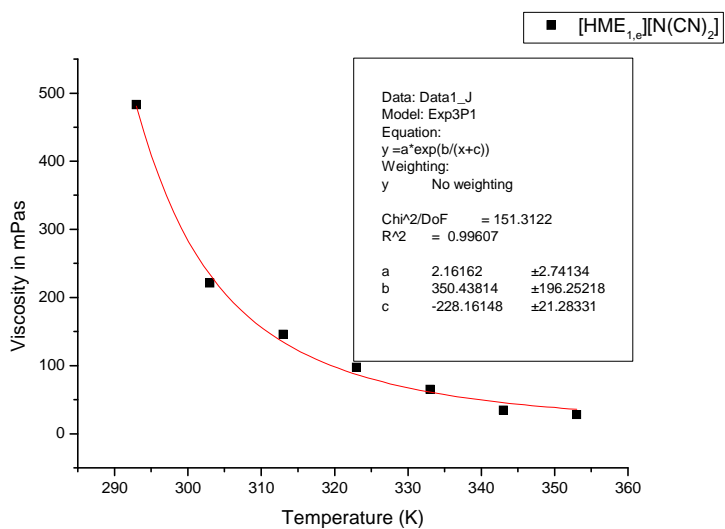
VTF plots for viscosity

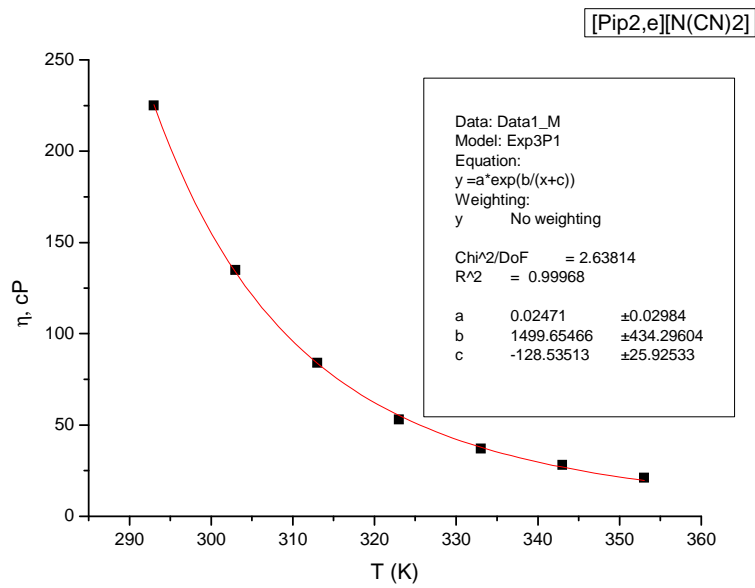
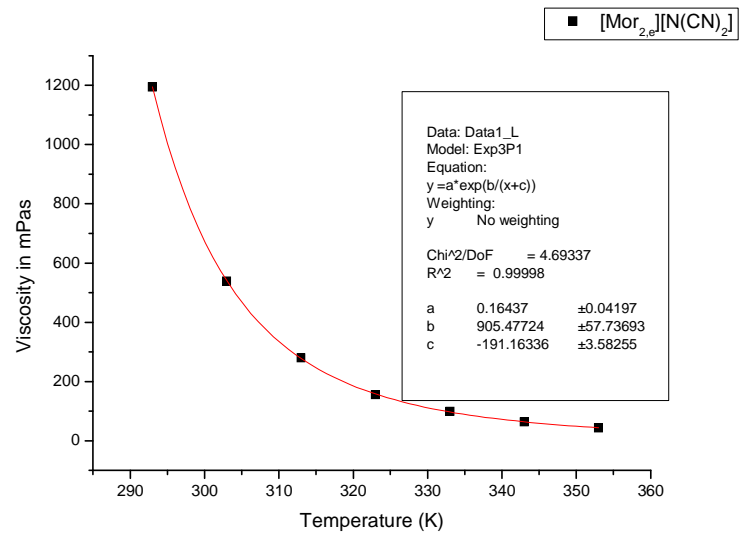












References

- ¹ CCDC reference number 792935. For crystallographic data in CIF or other electronic format see DOI: 10.1039/c0gc00534g
- ² INVISTATM, 'DYTEKR_HMI', Technical Information, 2008; <http://dytek.invista.com/>.
- ³ Belhocine, T.; Forsyth, S. A.; Gunaratne, H. Q. N.; Nieuwenhuyzen, M.; Puga, A. V.; Seddon, K. R.; Srinivasan, G. and Whiston, K. *Green Chem.* **2010**, DOI: 10.1039/c0gc00534g.
- ⁴ Bonhôte, P.; Dias, A.-P.; Armand, M.; Papageorgiou, N.; Kalyanasundaram, K.; Gratzel, M. *Inorg. Chem.* **1996**, *35*, 1168–1178.
- ⁵ (a) Hagiwara, R.; Ito, Y. *J. Fluorine Chem.* **2000**, *105*, 221–227. (b) Nishida, T.; Tashiro, Y.; Yamamoto, M. *J. Fluorine Chem.* **2003**, *120*, 135–141. (c) Holbrey, J. D.; Seddon, K. R. *J. Chem. Soc., Dalton Trans.* **1999**, 2133–2139.
- ⁶ (a) Buzzeo, M. C.; Evans, R. G.; Compton, R. G. *ChemPhysChem* **2004**, *5*, 1106–1120.
(b) Lee, J. S.; Bae, J. Y.; Lee, H.; Quan, N. D.; Kim, H. S.; Kim, H. J. *Ind. Eng. Chem.* **2004**, *10*, 1086–1089.
(c) Anthony, J. L.; Brennecke, J. F.; Holbrey, J. D.; Maginn, E. J.; Mantz, R. A.; Rogers, R. D.; Trulove, P. C.; Visser, A. E.; Welton, T. In *Ionic Liquids in Synthesis*; Wasserscheid, P.; Welton, T., Eds.; Wiley-VCH Verlag: Weinheim, **2003**; pp 41–126.
- ⁷ Chiappe, C.; Pieraccini, D.; Zhao, D.; Fei, Z.; Dyson P. J. *Adv. Synt. Cat.* **2006**, *348*, 68.
- ⁸ Persson, I. *Pure Appl. Chem.* **1986**, *58*, 1153.
- ⁹ Dahl, K. G.; Sando, M.; Fox, D. M.; Sutto, T. E.; Owrutsky, J. C. *J. Chem. Phys.* **2005**, *123*, 084504/1-11.
- ¹⁰ Reichardt, C.; Harbusch-Gornert, E. *Liebigs Ann. Chem.* **1983**, 721–743.
- ¹¹ Laurence, C.; Nicolet, P.; Reichardt, C. *Bull. Soc. Chim. Fr.* **1987**, 125–130.
- ¹² (a) Dimroth, K.; Reichardt, C.; Siepmann, T.; Bohlmann, F. *Liebigs Ann. Chem.* **1963**, *661*, 1–37.
(b) Dimroth, K.; Reichardt, C. *Liebigs Ann. Chem.* **1969**, *727*, 93–105.
(c) Reichardt, C. *Liebigs Ann. Chem.* **1971**, *752*, 64–67.
- ¹³ Shiguo, Z.; Qi, X.; Ma, X.; Lu, L. and Deng, Y. *J. Phys. Chem. B* **2010**, *114*, 3912–3920.

Chapter 5

Applications of Brønsted acidic ILs in esterifications and transesterifications

Abstract

This chapter shows that Brønsted acidic ionic liquids (ILs) can be used as solvents and catalysts in esterification reactions as well as in transesterification reactions. In both the cases, ILs bearing Brønsted acidic cations associated with the “acidic” $[\text{HSO}_4]^-$ anion gave the best yields. In the case of esterification of acetic acid with octanol a high conversion was also obtained using a functionalized acidic IL bearing a $-\text{COOH}$ group attached on the alkyl chain, Bet.HCl. Finally, acetylation of β -methyl-D-glucopyranoside in Brønsted acidic ILs occurred with a complete regioselectivity toward the primary hydroxyl group on C(6); after 4 h at 60°C in $[\text{HMIM}][\text{HSO}_4]$ a conversion around 70% was obtained.

5.1 Introduction

Esterification of carboxylic acids with alcohols is a reaction of industrial importance.¹ Several bulk and fine chemicals are produced in this manner in chemical, petrochemical and pharmaceutical industries. The Fischer esterification is a reversible reaction which requires an acid catalyst. The equilibrium is pushed to the product side by taking excess of a reactant and/or by continuously removing the water formed in the reaction. Sometimes it is necessary to employ an additional solvent to carry over the water in the form of azeotrope. Such operations require large energy input to recycle the solvents and the excess reactants. The loss of volatile organic solvents to the atmosphere results into increase in the cost of production and also damage to the environment.²

The majority of the ILs reported for esterification are imidazole^{3,4,5,6,7,8,9,10,11} and pyridine^{7,8,12} derivatives although

Pralhad et al.² used simple triethylammonium salts ($[(\text{C}_2\text{H}_5)_3\text{NH}][\text{HSO}_4]$, $[(\text{C}_2\text{H}_5)_3\text{NH}][\text{H}_2\text{PO}_4]$ and $[(\text{C}_2\text{H}_5)_3\text{NH}][\text{BF}_4]$) as Brønsted acidic catalysts and media for esterification of carboxylic acids with primary alcohols. These ILs were conveniently prepared in one step using inexpensive and easily available materials. Also in this case hydrogen sulfate as the anionic part gave the best yield.

Several transesterifications reactions, including enzyme-catalyzed reactions, are already reported using ILs. Laszlo and Compton in the year 2002¹³ reported chymotrypsin-catalyzed transesterification in ILs and IL/supercritical carbon dioxide. They used the ILs 1-butyl-3-methylimidazolium hexafluorophosphate ($[\text{Bmim}][\text{PF}_6]$) and 1-octyl-3-methylimidazolium hexafluorophosphate ($[\text{Omim}][\text{PF}_6]$). The yields obtained in these cases were found to be

consistent with those observed in conventional organic solvents. Nara et al.¹⁴ reported lipase-catalyzed transesterifications of 2-hydroxymethyl-1,4-benzodioxane in two different ILs, [Bmim][PF₆] and [Bmim][BF₄]. The hydrophobic and hydrophilic properties of ILs and organic solvents did influence the lipase activity of this reaction. Himmer et al.¹⁵ reported transesterification of methylsulfate and ethylsulfate ILs. This was an environmentally benign way to synthesize long-chain and functionalized alkylsulfate ILs. Similarly, many other transesterifications were carried out in various Brønsted acidic ILs.

In this chapter, we report a series of acidic ILs which were prepared using various *N*-bases like morpholine, imidazole, pyrrolidine, piperidine and betaine. These *N*-bases were treated with equimolar quantities of strong inorganic acids, like HCl, H₂SO₄, HNO₃, CF₃COOH and H₃PO₄. All the synthesized acidic ILs were applied in esterification of acetic acid with octanol, 1,2-propanediol and methyl- β -D-glucopyranoside. In all the investigated reactions, [HPyrr][HSO₄] and [HMIM][HSO₄] was found to be the best acid catalyst. The same acidic ILs were also tested in the transesterification of ethyl-trans cinnamate with methanol and octanol. Transesterification of ethyl trans-cinnamate with methanol in presence of [HPyrr][HSO₄] gave the best results among all.

5.2 Materials and Methods

5.2.1 Synthesis of *N*-methylimidazolium hydrogen sulphate ([HMIM][HSO₄])

25.63 g (0.251 moles) of sulfuric acid (96%) was added dropwise to 20.6 g (0.251 moles) of *N*-methylimidazole. The dropwise addition was made slowly to avoid the exothermic fuming reaction. The contents were finally stirred for 4 to 5 h at 60°C to ensure that all of the *N*-methylimidazole are reacted. Then, the mixture was kept in the rotary for 1 h at 65°C to ensure all the water contents were lost to obtain a colorless viscous liquid.

5.2.2 Synthesis of *N*-methylimidazolium sulfate ([HMIM]₂[SO₄]²⁻)

12.82 g (0.1255 moles) of sulfuric acid (96%) was added dropwise to 20.6 g (0.251 moles) of *N*-methylimidazole. The dropwise addition was made slower to avoid the exothermic fuming reaction. The contents were finally stirred for 4 to 5 h at 60°C to ensure that all of the *N*-methylimidazole are reacted. Then, the mixture was kept in the rotary for 1 h at 65°C to ensure all the water contents were lost to obtain a colourless white solid with melting point of 66±2°C. It was highly hygroscopic and hence highly soluble in water.

5.2.3 Synthesis of *N*-methylimidazolium dihydrogen phosphate ([HMIM][H₂PO₄])

28.94 g (0.251 moles) of phosphoric acid (85%) was added dropwise to 20.6 g (0.251 moles) of *N*-methylimidazole. The dropwise addition was made slower to avoid the exothermic fuming reaction. The contents were finally stirred for 4 to 5 h at 60°C to ensure that all of the *N*-methylimidazole are reacted. Then, the mixture was kept in the rotary for 1 h at 65°C to ensure all the water contents were lost to obtain a colorless solid. Its melting point was 90°C, comparatively higher than other imidazolium Brønsted acidic ILs. This ILs was less hygroscopic than the imidazolium sulphate and hydrogen sulfate ILs reported above.

5.2.4 Synthesis of *N*-methylimidazolium trifluoroacetate ([HMIM][CF₃COO])

29.21 g (0.251 moles) of trifluoroacetic acid (98%) was added dropwise to 20.6 g (0.251 moles) of *N*-methylimidazole. The dropwise addition was made slower to avoid the exothermic fuming reaction. The contents were finally stirred for 4 to 5 h at 60°C to ensure that all of the *N*-methylimidazole are reacted. Then, the mixture was kept in the rotary for 1 h at 65°C to ensure all the water contents were lost to obtain a very hygroscopic solid. Its melting point was equal to 55±2°C.

5.2.5 Synthesis of *N*-methylimidazolium nitrate ([HMIM][NO₃])

24.33 g (0.251 moles) of nitric acid (65%) was added dropwise to 20.6 g (0.251 moles) of *N*-methylimidazole. The dropwise addition was made slower to avoid the exothermic fuming reaction. The contents were finally stirred for 4 to 5 h at 60°C to ensure that all of the *N*-methylimidazole are reacted. Then the mixture was kept in the rotary for 1 h at 65°C to ensure all the water contents were lost to obtain a very hygroscopic solid. Its melting point was equal to 45±2°C.

5.2.6 Synthesis of *N*-methylimidazolium chloride ([HMIM][Cl])

24.73 g (0.251 moles) of hydrochloric acid (37%) was added dropwise to 20.6 g (0.251 moles) of *N*-methylimidazole. The dropwise addition was made slower to avoid the exothermic fuming reaction. The contents were finally stirred for 4 to 5 h at 60°C to ensure that all of the *N*-methylimidazole are reacted. Then, the mixture was kept in the rotary for 1 h at 65°C to ensure all the water contents were lost to obtain a colorless solid.

5.2.7 Synthesis of *N*-methylmorpholinium hydrogen sulphate ([HMor][HSO₄])

18.4 g (0.1819 moles) of sulfuric acid (96%) was added dropwise to 18.58 g (0.1819 moles) of *N*-methylmorpholine. The dropwise addition was made slower to avoid the exothermic fuming reaction. The contents were finally stirred for 4 to 5 h at 60°C to ensure that all of the *N*-methylmorpholine are reacted. Then, the mixture was kept in the rotary for 1 h at 65°C to ensure all the water contents were lost to obtain a brown-colored viscous liquid.

5.2.8 Synthesis of *N*-methylmorpholinium sulfate ([HMor]₂[SO₄]²⁻)

18.4 g (0.1819 moles) of sulfuric acid (96%) was added dropwise to 9.29 g (0.09095 moles) of *N*-methylmorpholine. The dropwise addition was made slower to avoid the exothermic fuming reaction. The contents were finally stirred for 4 to 5 h at 60°C to ensure that all of the *N*-methylmorpholine are reacted. Then, the mixture was kept in the rotary for 1 h at 65°C to ensure all the water contents were lost to obtain a brown-colored semi-liquid compound.

5.2.9 Synthesis of *N*-methylmorpholinium chloride ([HMor][Cl])

18.4 g (0.1819 moles) of hydrochloric acid (37%) was added dropwise to 17.93 g (0.1819 moles) of *N*-methylmorpholine. The dropwise addition was made slower to avoid the exothermic fuming reaction. The contents were finally stirred for 4 to 5 h at 60°C to ensure that all of the *N*-methylmorpholine are reacted. Then, the mixture was kept in the rotary for 1 h at 65°C to ensure all the water contents were lost to obtain a solid.

5.2.10 Synthesis of *N*-methylmorpholinium nitrate ([HMor][NO₃])

18.4 g (0.1819 moles) of nitric acid (65%) was added dropwise to 17.63 g (0.1819 moles) of *N*-methylmorpholine. The dropwise addition was made slower to avoid the exothermic fuming reaction. The contents were finally stirred for 4 to 5 h at 60°C to ensure that all of the *N*-methylmorpholine are reacted. Then, the mixture was kept in the rotary for 1 h at 65°C to ensure all the water contents were lost to obtain a solid.

5.2.11 Synthesis of *N*-methylpiperidinium hydrogen sulfate ([HPip][HSO₄])

16.32 g (0.1646 moles) of sulfuric acid (96%) was added dropwise to 16.81 g (0.1646 moles) of *N*-methylpiperidine. The dropwise addition was made slower to avoid the exothermic fuming reaction. The contents were finally stirred for 4 to 5 h at 60°C to ensure that all of the *N*-

methylpiperidine are reacted. Then, the mixture was kept in the rotary for 1 h at 65°C to ensure all the water contents were lost to obtain a viscous liquid.

5.2.12 Synthesis of *N*-methylpiperidinium sulfate ([HPip]₂[SO₄]²⁻)

16.32 g (0.1646 moles) of sulfuric acid (96%) was added dropwise to 8.405 g (0.0823 moles) of *N*-methylpiperidine. The dropwise addition was made slower to avoid the exothermic fuming reaction. The contents were finally stirred for 4 to 5 h at 60°C to ensure that all of the *N*-methylpiperidine are reacted. Then, the mixture was kept in the rotary for 1 h at 65°C to ensure all the water contents were lost to obtain a brown-colored viscous liquid.

5.2.13 Synthesis of *N*-methylpiperidinium nitrate ([HPip][NO₃])

16.32 g (0.1646 moles) of nitric acid (65%) was added dropwise to 15.96 g (0.1646 moles) of *N*-methylpiperidine. The dropwise addition was made slower to avoid the exothermic fuming reaction. The contents were finally stirred for 4 to 5 h at 60°C to ensure that all of the *N*-methylpiperidine are reacted. Then, the mixture was kept in the rotary for 1 h at 65°C to ensure all the water contents were lost to obtain a yellow-colored solid.

5.2.14 Synthesis of *N*-methylpyrrolidinium hydrogen sulfate ([HPyrr][HSO₄])

16.38 g (0.1924 moles) of sulfuric acid (96%) was added dropwise to 19.65 g (0.1924 moles) of *N*-methylpyrrolidine. The dropwise addition was made slower to avoid the exothermic fuming reaction. The contents were finally stirred for 4 to 5 h at 60°C to ensure that all of the *N*-methylpyrrolidine are reacted. Then, the mixture was kept in the rotary for 1 h at 65°C to ensure all the water contents were lost to obtain a brown-colored viscous liquid.

5.2.15 Synthesis of *N*-methylpyrrolidinium chloride ([HPyrr][Cl])

16.38 g (0.1924 moles) of hydrochloric acid (37%) was added dropwise to 18.96 g (0.1924 moles) of *N*-methylpyrrolidine. The dropwise addition was made slower to avoid the exothermic fuming reaction. The contents were finally stirred for 4 to 5 h at 60°C to ensure that all of the *N*-methylpyrrolidine are reacted. Then, the mixture was kept in the rotary for 1 h at 65°C to ensure all the water contents were lost to obtain a colorless viscous liquid.

5.2.16 Synthesis of betaine hydrogen chloride (Bet.HCl)

4.21 g (0.0427 moles) of hydrochloric acid (37%) was added dropwise to 5 g (0.0427 moles) of betaine. The dropwise addition was made slower to avoid the exothermic fuming reaction. The contents were finally stirred for 4 to 5 h at 60°C to ensure that all of the betaine are reacted. Then, the mixture was kept in the rotary for 1 h at 65°C to ensure all the water contents were lost to obtain a solid. The mpt was 252°C.

5.3 Experimental Section

5.3.1 Procedure for esterification of acetic acid with octanol

To 1 ml of the selected Brønsted acidic IL, 2 ml (0.0127 moles) of octanol and 1 equivalent mole of acetic acid (Carlo Erba, 99.9%) were added. The reaction was heated for 4 h at 110°C. Then, products were separated, as reported below. The crude reaction mixtures were analyzed by NMR. All the conversions and yields are reported in Table 5.1.

5.3.2 Procedure for esterification of acetic acid with 1,2-propanediol

To 1 ml of the selected Brønsted acidic IL ([HMIM][Cl] or [HMIM][NO₃] or [HMIM][HSO₄] or [HMIM][H₂PO₄]) 0.518 g (0.0068 moles) of 1,2-propanediol (Fluka, 99.5%) and 1.1 equivalent mole of acetic acid (Carlo Erba, 99.9%) were added. The reaction was heated for 4 h at 60°C. Then, products were extracted with ethyl ether and, after solvent evaporation at reduced pressure, the crude reaction mixtures were analyzed by NMR and GC-MS. Results are reported in Table 5.3.

5.3.3 Procedure for esterification of acetic acid with β -methyl-D-glucopyranoside

To 1.5 ml of the selected Brønsted acidic ILs ([HMIM][Cl] or [HMIM][NO₃] or [HMIM][HSO₄] or [HMIM][H₂PO₄]) 0.5 g (0.00258 moles) of β -methyl-D-glucopyranoside and 1.1 equivalent mole of acetic acid (Carlo Erba, 99.9%) were added. The reaction was heated for 4 h at 60°C. Then, products were extracted with ethyl ether and, after solvent evaporation at reduced pressure, the crude reaction mixtures were analyzed by NMR. Results are reported in Tables 5.4 and 5.5.

5.3.4 Procedure for transesterification of trans-ethyl cinnamate

5.3.4.1 Transesterification using methanol

To 1 g (0.00567 moles) of *trans*-ethyl cinnamate 3 equivalents of methanol and an equimolar amount of the selected Brønsted acidic IL ([HPyrr][HSO₄], [HMIM][HSO₄](1:1), [HMIM][HSO₄](1:1.1), [Bet][H₂SO₄], [HMor][Cl] and [HPip][HSO₄]) were added and the reaction mixture was heated at 90°C for 30 h into a reactor fitted with a reflux condenser. After stopping, the products were extracted with ethyl ether and, after solvent evaporation at reduced pressure, the crude reaction mixtures were analyzed by NMR. Results are reported in Tables 5.6 and 5.7.

5.3.4.2 Transesterification using octanol

To 1 g (0.00567 moles) of *trans*-ethyl cinnamate equimolar amounts of octanol as well as equimolar amounts of the selected Brønsted acidic ILs ([HMIM][HSO₄](1:1) and [HMIM][HSO₄](1:1.1)) were added. After stopping the reaction, products were extracted with ethyl ether and, after solvent evaporation at reduced pressure, the crude reaction mixtures were analyzed by NMR. Results are reported in Table 5.8.

5.4 Results and Discussions

These Brønsted acidic ILs (not all of them were used in every reactions) were used as solvents and acid catalysts in three esterification reactions and one transesterification reaction. The preparations and few properties were already mentioned in the Materials and Methods section and the structures are shown below in Figure 5.1.

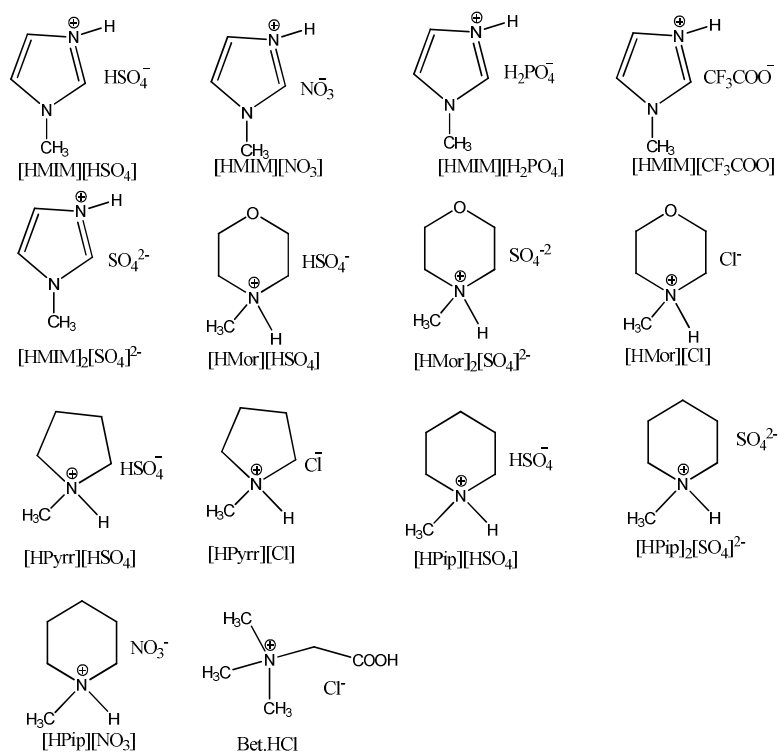
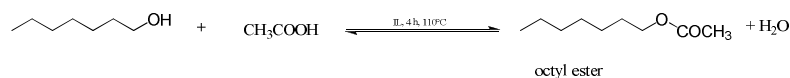


Figure 5.1: Brønsted acidic ILs used in this chapter

The Brønsted acidic IL giving the higher conversions was subjected to recycling experiments.

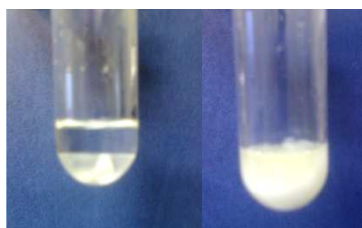
5.4.1. Esterification between octanol and acetic acid

Various ILs prepared in this section were used as solvents and acid catalysts for the esterification of acetic acid with octanol. The reactions were carried out at 110°C, by working with a 1:1 molar ratio of octanol w.r.t. acetic acid (Scheme 5.1) (reagent concentration around 12 M). To evaluate the catalytic ability of the different ILs, reactions were stopped after 4 h and the conversions were evaluated by NMR. Data are reported in Table 5.1.



Scheme 5.1: Esterification of octanol with acetic acid using Brønsted acidic ILs

It is noteworthy that for all ILs having HSO_4^- , SO_4^{2-} , NO_3^- and H_2PO_4^- as counteranion, after the stopping the reactions, when the temperature was brought to room conditions, two phases were formed; the lower phase constituted by the IL and water and an upper layer due to the formed ester and unreacted alcohol. This latter could be easily separated from the IL by simply decanting into another flask. The decanted liquid was dried under reduced pressure to remove unreacted acetic acid and any water, if present. The recovered organic phase ranged from 30 to 82%. The IL (lower layer), when recycled, was dried under reduced pressure to remove water formed during the esterification process. The picture of two different layers is shown below. In the case of [HDabco][Cl] and [HPyrr][Cl], since at room temperature the reaction mixture was practically an unique solid phase, ethyl ether was used to recover the product. [HMor][Cl] gave another situation, at room temperature the IL solidified and formed the lower layer whereas the ester constituted the upper layer. Hence, the separation was also solvent-free in this case.



Figures 5.2(a) and (b)

Figure 5.2 Figures showing stage after the reaction. **(a):** Two different layers are formed. Top layer (ester + unreacted alcohol) lower layer (IL + water formed during the reaction). The same situation was for all ILs having HSO_4^- , SO_4^{2-} , NO_3^- and H_2PO_4^- as counteranion. **Figure 5.2 (b):** case of [HDabco]Cl in which just one solid layer was formed and ether was used for extraction of the product.

Table 5.1: Esterification of acetic acid with octanol (T=110 °C), time =4 h

| Entry | IL | Ester : alcohol ^a | Yield% |
|-------|--|------------------------------|--------|
| 1 | [HMIM][HSO ₄] ^b | 76 : 24 | 75 |
| 2 | [HMIM][HSO ₄] ^c | 82 : 18 | 46 |
| 3 | [HMor][HSO ₄] | 80 : 20 | 67 |
| 4 | [HPyrr][HSO ₄] | 92 : 8 | 80 |
| 5 | [HPip][HSO ₄] | 88 : 12 | 77 |
| 6 | [HPip] ₂ [SO ₄] ²⁻ | 55 : 45 | 53 |
| 7 | [HMor] ₂ [SO ₄] ⁻² | 41 : 59 | 50 |

| | | | |
|----|--|---------|----|
| 8 | [HMIM] ₂ [SO ₄] ²⁻ | 20 : 80 | 48 |
| 9 | [HMIM][H ₂ PO ₄] | 21 : 79 | 73 |
| 10 | [HMIM][NO ₃] | 61 : 38 | 52 |
| 11 | [HPip][NO ₃] | 0 : 100 | 0 |
| 12 | [HPyrr][Cl] | 24 : 76 | 71 |
| 13 | [HDabco][Cl] | 20 : 80 | 50 |
| 14 | [HMor][Cl] | 34 : 66 | 30 |
| 15 | [HMIM][CF ₃ COO] | 43 : 57 | 72 |
| 16 | [Bet][HCl] | 85 : 15 | 76 |

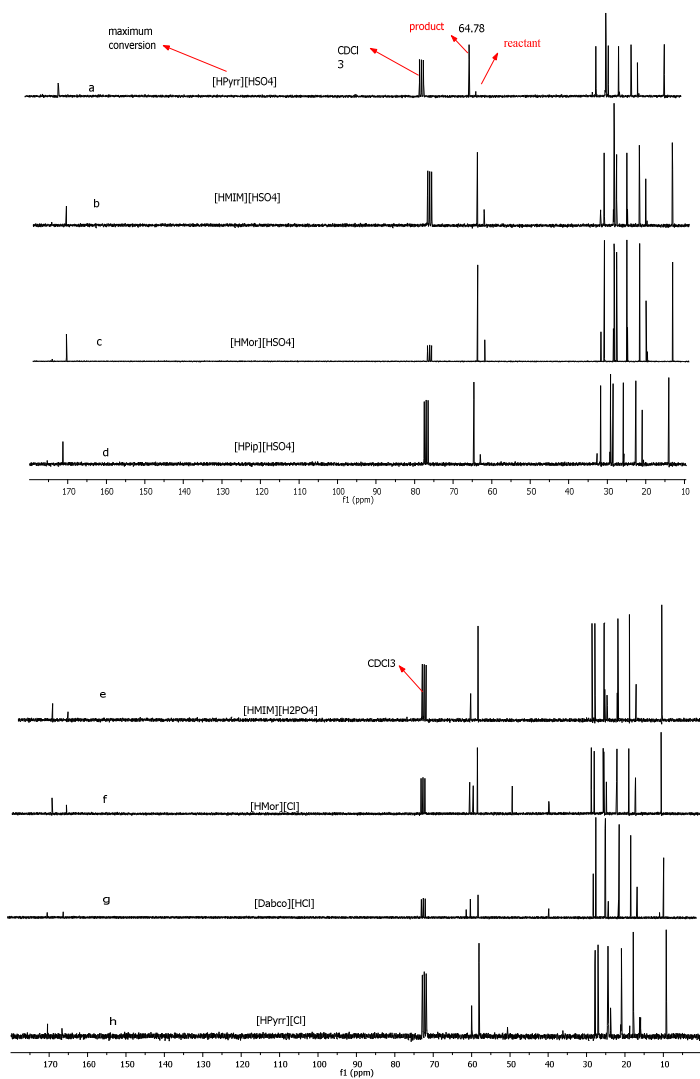
^aThis ratio refers to the ratio between the yield of product (ester) to the yield of the unreacted alcohol, determined on the basis of the NMR spectra. ^bThis refers that the reaction was carried out at a low temperature i.e. 75–80°C. ^cThis refers that the reaction was carried out in a long closed test-tube.

All the above reactions were in which the molar ratio of the reactants were 1:1. The decreasing catalytic activity for the various above-mentioned Brønsted acidic ILs is as follows:- [HPyrr][HSO₄] > [HPip][HSO₄] > [Bet][HCl] > [HMIM][HSO₄] (temp=110°C) > [HMor][HSO₄] > [HMIM][HSO₄] (temp=75–80°C) > [HMIM][NO₃] > [HPip]₂[SO₄]²⁻ > [HMIM][CF₃COO] > [HMor]₂[SO₄]²⁻ > [HMor][Cl] > [HPyrr]Cl > [HMIM][H₂PO₄] > [HMIM]₂[SO₄]²⁻ = [HDabco]Cl. Thus, we can conclude that the Brønsted acidic ILs with hydrogen sulfate as the counter anion gave the best results: in particular, [HPyrr][HSO₄] gave up to 92% of conversion. On the other hand, Brønsted acidic ILs having the unprotonated sulfate as anion gave significantly lower conversions. Though the cationic order was same, i.e. [HPip][HSO₄] > [HMIM][HSO₄] > [HPip]₂[SO₄]²⁻ > [HMIM]₂[SO₄]²⁻. Therefore, the presence of a sufficient acidic proton in the anionic part appears to play an important role in the activation of the reaction. About this, it is noteworthy that when [HMIM][H₂PO₄] was used as catalyst and solvent only very low conversions were obtained (21%) showing that the acidity of the protons present on this anion is not sufficient to play a catalytic role. In the case of nitrate-based ILs (entries 10 and 11), [HMIM][NO₃] gave a conversion yield of 61% whereas [HPip][NO₃] degraded at the reaction temperature and the reaction failed.

Finally, Brønsted acids having Cl⁻ as counteranion did not give high conversion yields like the hydrogen sulfates; conversions ranged from 20 to 34%, depending on IL cation. Analogously, a moderate conversion characterized also when the reaction was carried out in [HMIM][CF₃COO]; the conversion yield was 43%.

In Table 5.1, a data related to the use of a task-specific ammonium-based IL, Bet.HCl, bearing an acidic group on the alkyl chain is also reported. Although, as previously discussed, chloride-

based ILs gave yields significantly lower than $[\text{HSO}_4^-]$ based ILs, in case of Bet.HCl, the presence of an acidic functional group ($-\text{COOH}$) on the alkyl chain allows to obtain conversions comparable to the best ILs. Nevertheless, since this IL is solid at room temperature and the product is not soluble in this medium it was possible to recover the formed ester by simple decanting procedure. Below, are reported the C-NMR spectra for various entries mentioned Above.



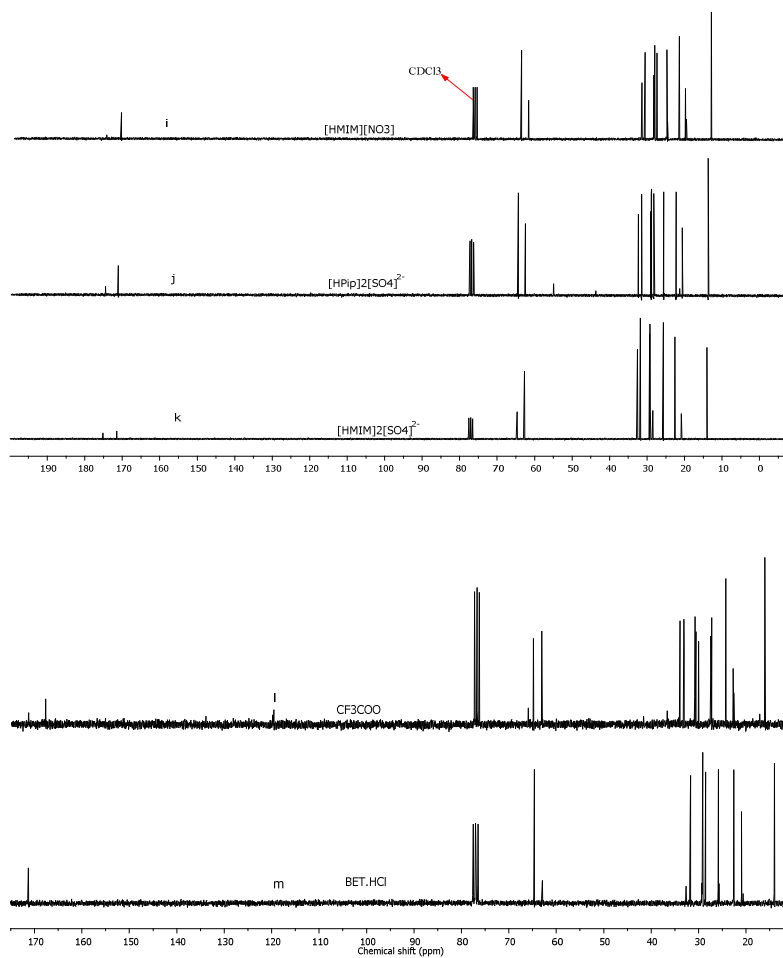


Figure 5.3: C-NMR showing comparison between various acidic ILs used

Since the best results/yields were obtained using [HPyrr][HSO₄], this IL has been selected for recycling experiments. Data reported in Table 2 show that at least three recycles can be performed without significant decrease in reactivity although the recovery of the product by simple decantation of the upper phase becomes less efficient.

Table 5.2: Recycling of [HPyrr][HSO₄]

| No. of recycle | Conversion % | Yield% |
|----------------|--------------|--------|
| Fresh | 92 | 80 |
| 1 | 92 | 78 |
| 2 | 85 | 60 |
| 3 | 82 | 56 |

The C-NMR for the 3 cycles are compared with the fresh one and are shown below in Figure 5.4.

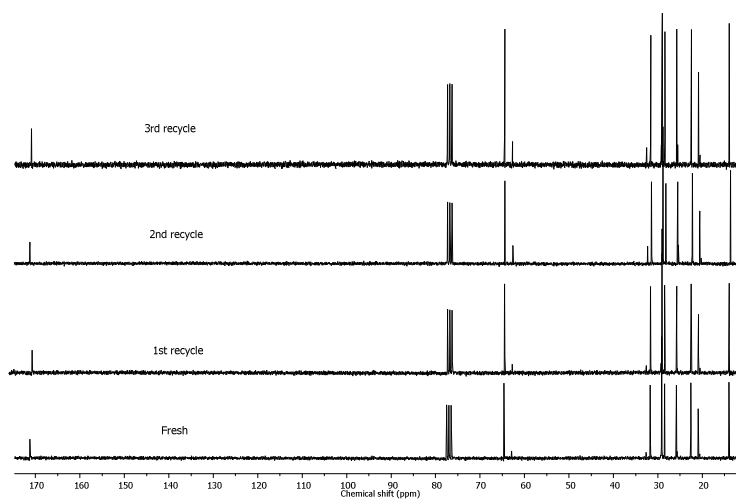
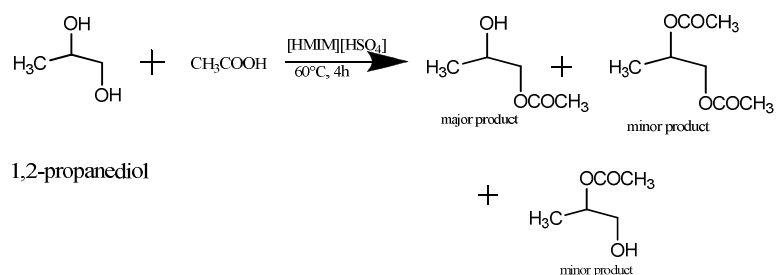


Figure 5.4: C-NMR comparing between fresh, 1st, 2nd and 3rd recycle of [HPyrr][HSO₄]

5.4.2 Esterification between 1,2-propanediol and acetic acid

In order to evaluate the selectivity of the esterification process in Brønsted acidic ILs, the reaction of acetic acid with 1,2-propanediol was investigated in different Brønsted acidic ILs having the same cation and four different anions ([HMIM]Cl, [HMIM][NO₃], [HMIM][HSO₄] and [HMIM][H₂PO₄]). Reactions were carried at 60°C, using 1.1:1 molar ratio of acetic acid w.r.t. 1,2-propanediol, reagent concentration around 7 M. After 4 h products were extracted using dichloromethane as solvent. The reaction mixtures were analyzed by GC-MS and NMR.



Scheme 5.2: Esterification of 1,2-propanediol using acetic acid in Brønsted acidic ILs

The presence of two different hydroxyl groups in the employed alcohol increases the number of possible products: in particular, it is possible the formation of two monoacetyl derivatives (arising from the esterification of the primary or secondary hydroxyl group, respectively) and one diacetyl derivative. GC-MS analysis evidenced the formation of all three products, the main product being the expected monoacetyl derivative arising from esterification of the primary alcohol. Product recovery depended on the time of IL used and the data are reported in Table 5.3.

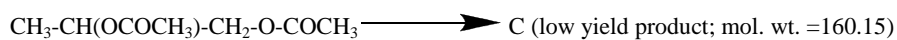
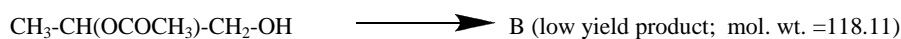
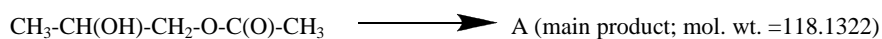


Table 5.3: Product recovered using four Brønsted acidic ILs

| ILs | Product recovered |
|---|-------------------|
| [HMIM][Cl] | 20% |
| [HMIM][NO ₃] | NR |
| [HMIM][HSO ₄] | 67% |
| [HMIM][H ₂ PO ₄] | 45% |

From the above Table 5.3, we can see that, in analogy with the behavior observed in esterification of acetic acid with octanol, [HMIM][HSO₄] gave the highest recovery of the reaction product. Unfortunately, the reaction occurs with a low regioselectivity; NMR analysis

indicated the formation of all three products in a ratio ranging around 1:1:1; a product distribution which was confirmed also by the GC-MS analysis. The H-NMR and C-NMR for the best results of the above reaction is shown below in Figure 5.5.

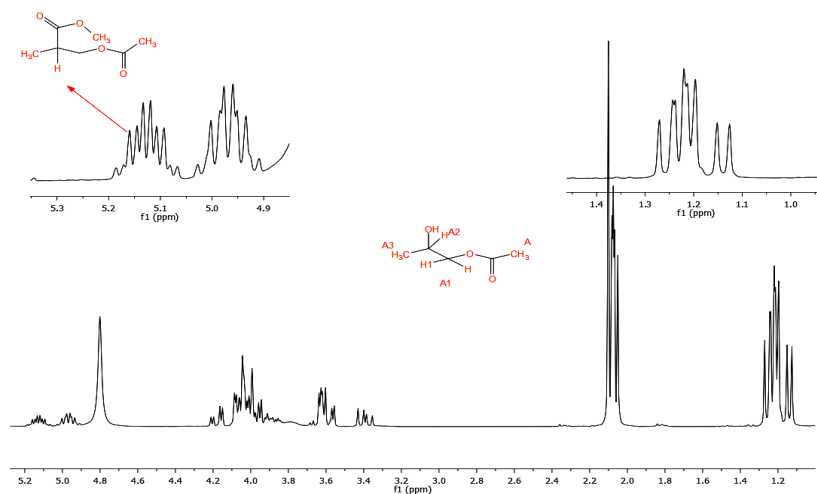
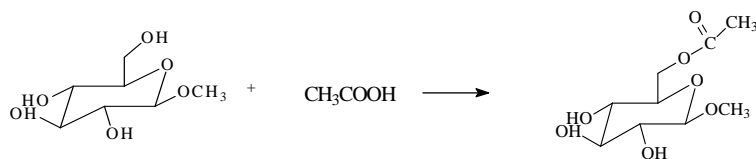


Figure 5.5: H-NMR and C-NMR for esterification of glycerol with acetic acid using [HMIM][HSO₄]

5.4.3 Esterification between β -methyl-D-glucopyranoside with acetic acid



Scheme 5.3: Esterification between β -methyl-D-glucopyranoside with acetic acid

The selectivity of the esterification reaction was also checked using β -methyl-D-glucopyranoside as substrate. Reactions were conducted at a lower reagent concentration (around 1.5 M) to facilitate the sugar dissolution. The behavior of the reaction was checked stopping the esterification after 1, 2 and 4 h and longer; if needed. The reaction mixtures were extracted with ethyl ether and product distribution was checked by NMR. In this case, the reaction occurred with a high regioselectivity: only the acetyl derivative arising from esterification of primary

hydroxyl group on C(6) was detected besides the unreacted product, conversions at different reaction times are reported in Table 5.4.

Table 5.4: Product conversion using four Bronsted acidic ILs

| ILs | 1 h | 2 h | 4 h |
|---|-------|-----|-----|
| [HMIM][Cl] | NR | NR | NR |
| [HMIM][NO ₃] | 36% | 50% | 30% |
| [HMIM][HSO ₄] | ----- | 60% | 70% |
| [HMIM][H ₂ PO ₄] | ----- | 40% | 50% |

Table 5.5: Showing yields of the recovered products

| ILs | Yield |
|---|-------|
| [HMIM][Cl] | 0% |
| [HMIM][NO ₃] | 40% |
| [HMIM][HSO ₄] | 70% |
| [HMIM][H ₂ PO ₄] | 50% |

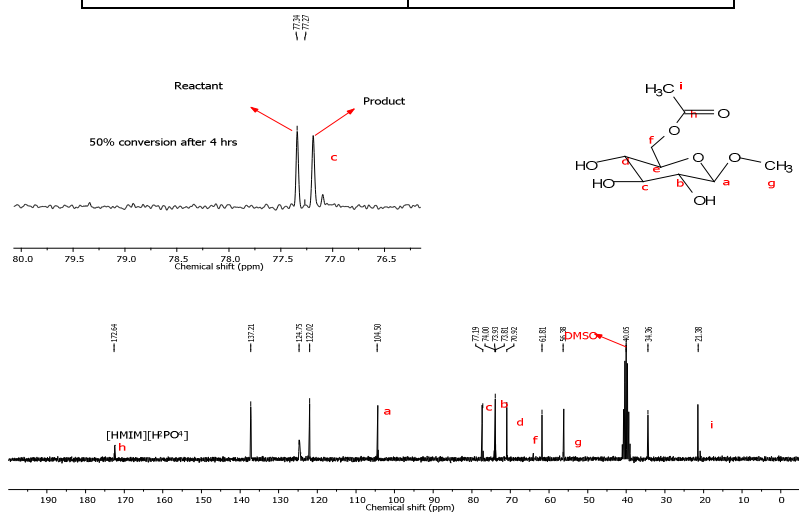


Figure 5.6: C-NMR evidencing the acetylation at C6-position of sugar

Below, we can see the changes in the reactants and products ratio after 1, 2 and 4 h of reaction using [HMIM][NO₃]. It is to note the decreased conversion on increasing the reaction time from

2 to 4 h. Probably, this peculiar behavior has to be attributed to the nature of [HMIM][NO₃] which, less than [HMIM][HSO₄], is able to “capture” the produced water. The presence of increasing amounts of free-water, after that limit value of the coordinating ability typical of the nitrate anion, may favor the hydrolysis process shifting the equilibrium position towards reagents.

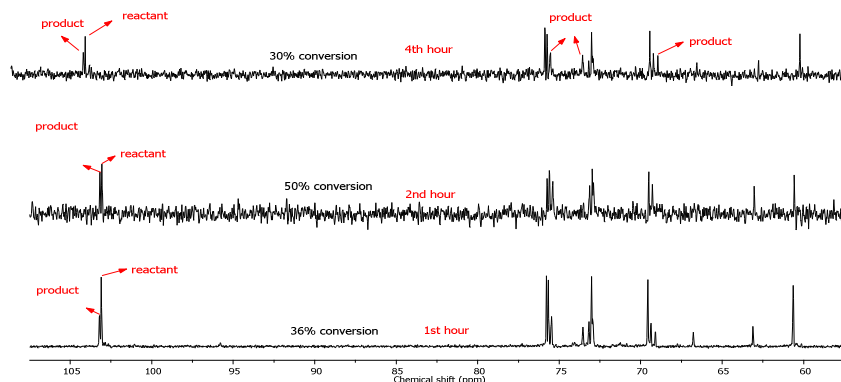
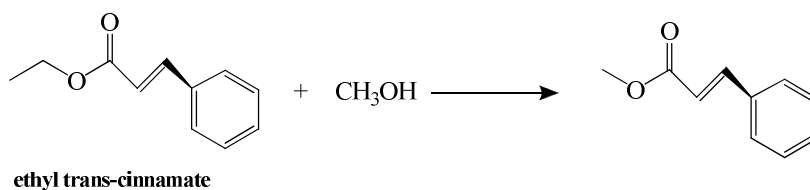


Figure 5.7: C-NMR at 1st, 2nd and 4th hour showing reversibility reactions in case of [HMIM][NO₃]

Also in this reaction, therefore, the higher conversion was obtained in the IL having hydrogensulfate as counteranion, [HMIM][HSO₄]. Attempts to increase the conversion prolonging the reaction beyond 4 h failed; i.e., multi acetates started forming. Hence, it was advisable to stop the reaction at 4 h.

5.4.4 Transesterification of *trans*-ethyl cinnamate using alcohols

The possibility to use Brønsted acidic ILs in transesterification processes was checked investigating the reaction of ethyl *trans*-cinnamate with a small alkyl-chained alcohol, such as methanol, and with a longer alkyl-chained alcohol such as octanol. Initially, the reaction with methanol was investigated in [Hpip][HSO₄] and temperature and reaction time were varied to find the best conditions. The results are shown in Table 5.6. The scheme is shown in the next page. (Scheme 5.4).

**Scheme 5.4:** Esterification of ethyl-trans cinnamate**Table 5.6:** Transesterification of ethyl *trans*-cinnamate in [HPip][HSO₄] using CH₃OH

| Entries | Time (h) | Temp (°C) | Conversion % | Yield% ^a |
|-----------------|----------|-----------|--------------|---------------------|
| 1 | 5 | Rt | NR | 0 |
| 2 | 24 | Rt | NR | 0 |
| 3 | 5 | 40 | NR | 0 |
| 4 | 5 | 50 | NR | 0 |
| 5 | 5 | 60 | NR | 0 |
| 6 | 12 | 60 | NR | 0 |
| 7 | 17 | 60 | NR | 0 |
| 8 | 24 | 60 | NR | 0 |
| 9 | 28 | 60 | NR | 0 |
| 10 | 28 | 70 | NR | 0 |
| 11 | 28 | 80 | NR | 0 |
| 12 | 28 | 90 | 52 | 48% |
| 13 ^b | 28 | 90 | 73 | 66% |

^aYields were determined after product extraction with ethyl ether.^bThe molar ratio of the ester and alcohol is 1:3 in this case.

Rt=Room temperature; NR=no reaction.

From data reported in Table 5.6, we can state that in entry 13 are reported the conditions giving the best result. In particular, practically no conversion was observed until the temperature was raised to 90°C (a reactor fitted with a reflux condenser was used to avoid methanol evaporation); at this temperature, using an equimolar amount of CH₃OH, a conversion around 50% was obtained (see entry 12) whereas in the presence of an excess of alcohol (3 equivalents) conversion increased at 73%. These latter conditions were used to test the efficiency of other ILs. Results are reported in Table 5.7.

Table 5.7: Transesterification of ethyl trans cinnamate using CH₃OH in various ILs

| Entries | IL | Conversion % | Yield% |
|-----------------|--|--------------|--------|
| 14 ^a | [HMor][Cl] | NR | 0 |
| 15 ^b | [HMor][Cl] | NR | 0 |
| 18 ^a | Bet.H ₂ SO ₄ | NR | 0 |
| 19 ^b | [HPyrr][HSO ₄] | 95 | 95% |
| 20 ^a | [HMIM][HSO ₄] | 37 | 87% |
| 21 ^a | [HMIM][HSO ₄] ^c | 75 | 92% |

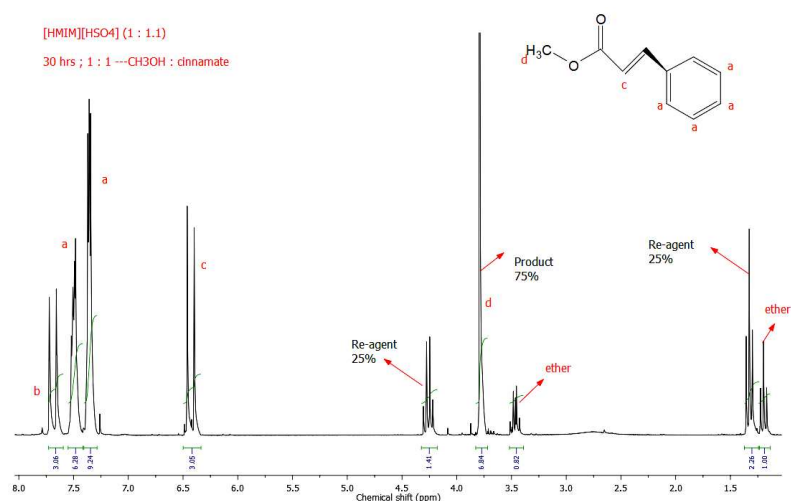
^aThis symbol denotes the molar ratio between the ester and the alcohol is 1:1.

^bThis symbol denotes the molar ratio between the ester and the alcohol is 1:3.

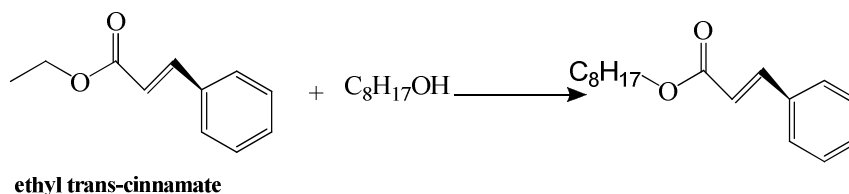
^cThis symbol refers that acid is 1.1 equivalent with respect to the nitrogen base.

All the reactions are carried out at 90°C for 28 h.

It is to note that whereas no conversion was obtained in chloride based ILs also working with an excess of alcohol, conversions ranging from 40 to 95 % characterized reactions performed in hydrogensulfate-based ILs. The best results were obtained in the case of In particular, in [HMIM][HSO₄] a significant increase in conversion was obtained working in the presence of an excess of acid H₂SO₄, probably as a consequence of the superacidic behavior of species of the type, A---H-A⁻, which should be present in the reaction mixture.

**Figure 5.8:** H-NMR showing methyl-trans cinnamate product using [HMIM][HSO₄]

When the transesterification process of ethyl *trans*-cinnamate in [HMIM][HSO₄] was carried out using octanol lower conversions were obtained under comparable conditions, however, also in this case, the presence of a small excess of inorganic acid (H₂SO₄) significantly increased conversions (Table 5.7). In this case, all reactions were performed maintaining the ratio between ester and the alcohol equal to 1; the high boiling point of octanol assured that the reagent was not lost during the reaction. The scheme is shown below.



Scheme 5.5: Esterification of octanol and ethyl-*trans* cinnamate

Table 5.8: Transesterification of *trans*-ethyl cinnamate and octanol in various Brønsted acidic ILs

| Entries | Time (h) | Temp. (°C) | IL used | Conversion % | Yield% |
|---------|----------|------------|--|--------------|--------|
| 1 | 5 | 80–90 | [HMIM][HSO ₄] | NR | 0 |
| 2 | 38 | 75 | [HMIM][HSO ₄] | 35 | 70% |
| 3 | 30 | 90 | [HMIM][HSO ₄] | 25 | 25% |
| 4 | 30 | 90 | [HMIM][HSO ₄] ^a | 52 | 78% |

^aThis symbol refers that acid is 1.1 equivalent more than the nitrogen base.
The molar ratio between the alcohol and the ester in all the cases were 1:1.

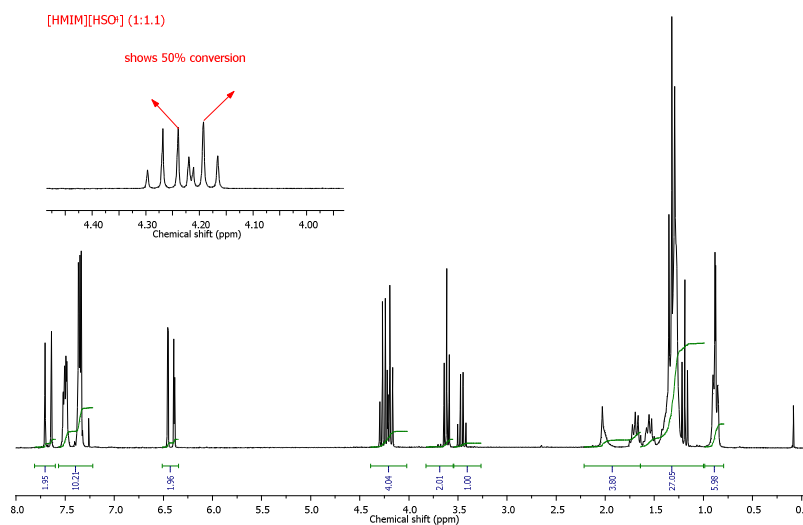


Figure 5.9: HNMR showing transesterification of ethyl trans cinnamate using octanol

5.5 Conclusion

These data show that Brønsted acidic ILs can be used as solvents and catalysts in esterification and transesterification reactions. In both cases, ILs bearing Brønsted acidic onium (pyrrolidinium) or imidazolium cations, associated with the “acidic” $[\text{HSO}_4]^-$ anion, gave the best yields. In the case of esterification of acetic acid with octanol a high conversion was also obtained using a task-specific ammonium-based IL, Bet.HCl, bearing an acidic group ($-\text{COOH}$) on the alkyl chain. Finally, acetylation of β -methyl-D-glucopyranoside in Brønsted acidic ILs occurred with high regioselectivity: only the acetyl derivative arising from esterification of the primary hydroxyl group on C(6) was detected, beside the unreacted product (30%), when the reaction was performed in $[\text{HMIM}][\text{HSO}_4]$.

References

- ¹ Larock, R. C. *Comprehensive Organic Transformations*, VCH: New York, **1999**.
- ² Ganeshpure, P.A.; George, G. and Das, J. *ARKIVOC*. **2007**, 273–278.
- ³ Cole, A. C.; Jensen, J. L.; Ntai, I.; Tran, K. L. T.; Weaver, K. J.; Forbes, D. C.; Davis Jr., J. *H. J. Am. Chem. Soc.* **2002**, *124*, 5962.
- ⁴ Fraga-Dubreuil, J.; Bourahla, K.; Rahmouni, M.; Bazureau, J. P.; Hamelin, J. *Catal. Commun.* **2002**, *3*, 185.
- ⁵ Zhu, H. P.; Yang, F.; Tang, J.; He, M. Y. *Green Chem.* **2003**, *5*, 38.
- ⁶ Nguyen, H. P.; Znifeche, S.; Baboulene, M. *Synth. Commun.* **2004**, *34*, 2085.
- ⁷ Arfan A.; Bazureau, J. P. *Org. Proc. Res. Dev.* **2005**, *9*, 743.
- ⁸ Xing, H.; Wang, T.; Zhou, Z.; Dai, Y. *Ind. Eng. Chem. Res.* **2005**, *44*, 4147.
- ⁹ Joseph, T.; Sahoo, S.; Halligudi, S. B. *J. Mol. Catal. A: Chemical* **2005**, *234*, 107.
- ¹⁰ Siddiqui, S. A. *Synlett* **2006**, 155.
- ¹¹ Zhang, Z.; Wu, W.; Han, B.; Jiang, T.; Wang, B.; Liu, Z. *J. Phys. Chem. B* **2005**, *109*, 16176.
- ¹² Gui, J.; Cong, X.; Liu, D.; Zhang, X.; Hu, Z.; Sun, Z. *Catal. Commun.* **2004**, *5*, 473.
- ¹³ Joseph A. Laszlo and , David L. Compton. *Ionic Liquids*, **2002**, Chapter 30, pp 387–398. *ACS Symposium Series*, Vol. 818.
- ¹⁴ S.J. Nara, J.R. Harjani and M.M. Salunkhe *Tetrahedron Lett.*, **2002**, 2979–2982.
- ¹⁵ S. Himmler, S. Hörmann, R. van Hal, P.S. Schulz and P. Wasserscheid. *Green Chem.*, **2006**, *8*, 887–894.

Chapter 6

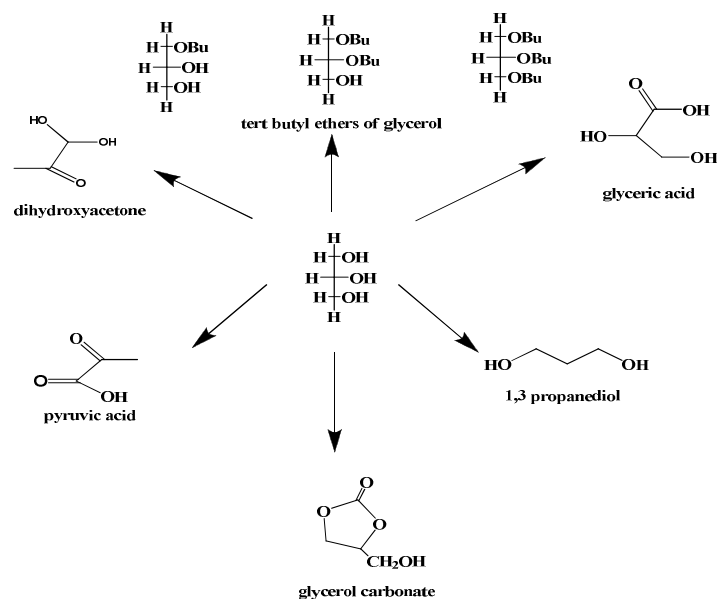
Preparation and Characterization of Glycerol Carbonate using Basic ILs

Abstract

In this chapter, glycerol carbonate is prepared using glycerol and dimethyl carbonate (DMC) i.e., two cheap compounds are used to prepare an important compound (glycerol carbonate) which is used as a solvent, additive and as a chemical intermediate. The basic ILs specially the ones possessing the $\text{N}(\text{CN})_2^-$ as the counter anion, gave the best results: in $[\text{Mor}_{1,4}][\text{N}(\text{CN})_2]$ at 120°C it is possible to obtain the complete conversion of glycerol into the corresponding glycerol carbonate in 13 h.

6.1 Introduction

The Biodiesel, whose production keeps on going day by day, is conveniently manufactured from vegetable oils by transesterification of triglycerides with methanol. This process gives glycerol (1,2,3-trihydroxypropane, central compound in Scheme 6.1) as a byproduct; glycerol production in the United States already averages more than 350,000 tons per year while in Europe the production has tripled within the last 10 years. Glycerol is therefore the byproduct with the largest economic impact in the modern oleochemical industry,¹ being formed in different processes such as glycerides transesterification, alcoholysis, hydrolytic cleavage under pressure and saponification with alkalis.^{2,3} It is also produced by dedicated processes such as the synthesis from propene⁴ or the fermentation of simple sugars.⁵ The production of biofuels and biolubricants from biomass is much expanding (and will continue to grow) so that the production of bio-glycerol, in the past considered of great value for a successful closing of the economic balance of the lipid-utilization process, is now exceeding the request. The risk that large amounts of glycerol are produced and will accumulate as a waste has speed-up the industry and academia research towards the identification of new opportunities for using such byproduct either directly (as fuel even in the same biodiesel production plants⁶), or by converting it into useful derivatives. A lot of interesting products are obtainable from glycerol. Some of these are shown in Scheme 6.1.



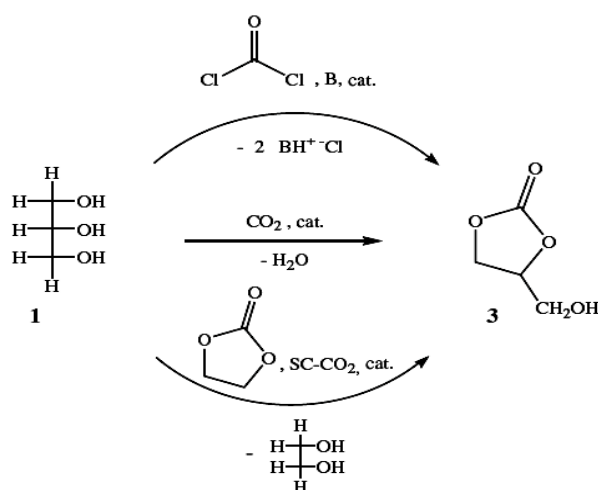
Scheme 6.1: Various products obtainable from glycerol

From glycerol it is possible to obtain new intermediates to use in the production of fine chemicals (e.g. dihydroxyacetone, glyceric acid, pyruvic acid and 1,3-propanediol) either by fermentation^{7,8,9} or using chemical routes¹⁰ (Scheme 6.1).

Glycerol carbonate, a stable colorless liquid, represents an important derivative of glycerol that shows low toxicity, good biodegradability and high boiling point. For its properties it finds several applications in different industrial sectors, especially as a polar high boiling solvent or intermediate in organic syntheses (i.e., monomer in the synthesis of polycarbonates and other polymeric materials in the plastic field¹¹ as well as in the synthesis of very valuable intermediates such as glycidol,¹² which is employed in textile, plastics, pharmaceutical and cosmetics industries), as a precursor in biomedical applications and as a protection group in the carbohydrates chemistry. It is also used as a component in membranes for gas separation instead of ethylene and propylene carbonates,¹³ in the synthesis of polyurethanes¹⁴ and in the production of surfactants.¹⁵ As a chemical intermediate it reacts readily with alcohols, phenols and carboxylic acids with loss of CO₂ as well as with aliphatic amine with carbon dioxide recovery. Finally, glycerol carbonate and its derivatives can be used as electrolytes and solvents in lithium ion batteries and it is considered a green substitute for important petro-derivative compounds as ethylene carbonate or propylene carbonate.¹⁶

Development of successful routes to produce glycerol carbonate from renewable raw materials will be an important issue for different industrial sectors, since a valuable product could be obtained at high volumes and low prices, competitive to compounds derived from petroleum. The new economical and environmental tendencies support this approach and promote the interest in the development of new innovative processes for the manufacture of chemical products that will efficiently cover market needs under a sustainable conception of industrial production.¹⁷

The main methods for the preparation of glycerol carbonate are based on the reaction of glycerol with (a) a carbonate source (phosgene, a dialkyl carbonate or an alkylene carbonate), (b) urea, and (c) carbon monoxide and oxygen. Traditionally, cyclic carbonates have been prepared by reaction of glycols with phosgene,^{18,19} but due to the high toxicity and corrosive nature of phosgene alternative routes such as transesterification reaction²⁰ of dialkyl or alkylene carbonates to obtain cyclic carbonates have been explored (Scheme 2).



Scheme 6.2: Synthesis of glycerol carbonate by phosgenation (upper part). Direct carboxylation (middle part) or transesterification of glycerol (lower part)

For instance, ethylene carbonate, a commercial product with interesting physical properties (low toxicity, low evaporation rate, biodegradability, high solvency, etc.) has been widely used as carbonate source for preparing glycerol carbonate.²¹ The transesterification between glycerol and ethylene carbonate is generally performed with an alkaline base.²² For instance, using sodium bicarbonate, at 130°C, the yield of glycerol carbonate reached 81% after 30 mins. However, the main problem associated with these catalysts is the requirement of a final

neutralization step. For doing this, at the end of the reaction, a mineral acid (phosphoric acid, sulphuric acid, benzenesulphonic acid, etc.) is added to the system to neutralize the catalysts, followed by distillation under reduced pressure for the recovery of glycerol carbonate from the reaction mixture, which contains reactants, salts and products. Despite the fact that heterogeneous base catalysts should allow easy separation and recycling of the catalyst by filtration avoiding the neutralization step and reducing waste formation, there are few examples for the synthesis of glycerol carbonate by transesterification of ethylene carbonate and glycerol in the presence of solid catalysts. Thus, Sugita et al. have performed²³ the transesterification reaction in the presence of aluminium oxide as catalyst. When the reaction was carried out at 135–140 °C under reduced pressure with progressive removal of ethylene glycol, glycerol carbonate was obtained with 99% yield.

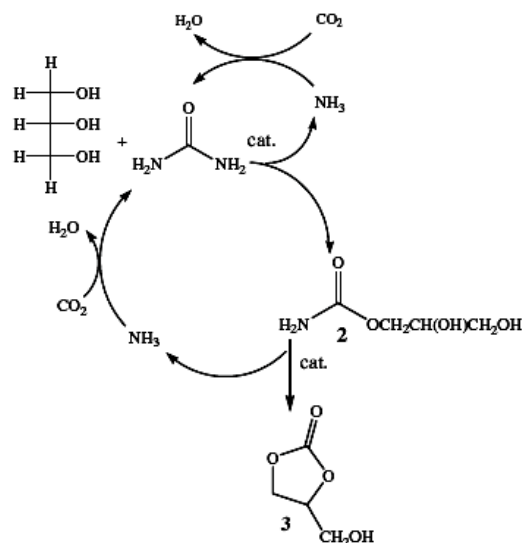
One alternative approach that avoid the formation of the highly boiling ethylene glycol is the use of dimethyl carbonate (DMC) as a carbonate source. DMC can be manufactured by environmental safe industrial methods and potentially from CO₂ and renewable sources.²⁴

Likewise, glycerol carbonate has been also obtained from glycerol and DMC by a transesterification catalyzed by lipases. Kim et al.²⁵ in the year 2007 demonstrated *Candida Antarctica* (CALB, Novozym 435) lipase as the first enzymatic example for the synthesis of glycerol carbonate. He suggested addition of molecular sieves to scavenge the methanol which is generated during the reaction to promote the reaction towards the product side, i.e., in other words the reaction was accelerated. There were drawbacks with this kind of reaction using lipase as it was cost-effective and by high temperature the lipase was deactivated and it was not environmentally friendly since it involved usage of THF. However, one can know from this literature that the molar ratio between glycerol and DMC taken into account plays an important role in the product formation. Also variation of reaction temperature had a considerable affect on the synthesis of the product.

Recently, Kyung Hwa Lee et al.²⁶ suggested a solvent-free reaction in which DMC was used as the substrate as well as the solvent. But glycerol is not miscible in DMC; hence, silica-gel was used as solid support to glycerol. When glycerol-coated silica gel was supplied, the transesterification rate by immobilized lipase was more than tenfold increased than that of free glycerol. The optimum conditions were determined as follows: molar ratio of DMC to glycerol was 10 and the reaction temperature was 70°C in the presence of glycerol-coated silica gel with a 1:1 ratio. The Novozyme 435 biocatalyst and silica gel could be reused by the repeated batch operation. Glycerol carbonate was successfully synthesized with the conversion of more than 90% for 48 h in the solvent-free transesterification system.

But, also other catalysts, like CaO, K₂CO₃ and imidazolium-2-carboxylate, have been used under different reaction conditions to produce glycerol carbonate. Rokicki et al.²⁷ used K₂CO₃ as an efficient catalyst to produce glycerol carbonate from glycerol and DMC at 75°C obtaining a quantitative amount of the expected product. Analogously, Ochoa-Gómez et al. in 2009 reported the preparation of glycerol carbonate using CaO as the catalyst. The calcination of CaO increased dramatically its activity due to the removal of hydroxide from its surface. But at high temperatures the recycled CaO was deactivated from time to time. In 2003, Holbrey et al. reported²⁸ the synthesis of a compound named, imidazolium-2-carboxylate, which has been used²⁹ recently by Prashant et al. as a catalyst to produce glycerol carbonate. It is noteworthy that high conversions and yields have obtained only under basic conditions and, generally, catalytic activity increases with catalyst basic strength.

Nevertheless, among the alternative pathways to produce glycerol carbonate have to be mentioned also the direct reaction of glycerol with CO₂ or carbon monoxide and oxygen, in the presence of Cu(I) as catalyst,³⁰ the reaction of glycerol and ethylene carbonate in supercritical CO₂, in the presence of zeolites³¹ and use of urea as source of the carbonate group, a process this latter patented^{32,33} in 2002. More recently, the glycerolysis of urea (Scheme 6.3) has been performed³⁴ by Aresta et al. under catalytic conditions. In particular, *c*-zirconium phosphate has shown a good activity as catalyst affording 80% of conversion of glycerol under mild reaction conditions; 3 h at 418 K, using equimolar amounts of the two reagents (glycerol and urea) with a catalyst load of 0.6–1.5% w/w with respect to glycerol. The catalyst could easily recovered and reused in subsequent cycles of reaction.



Scheme 6.3: Synthesis of glycerol carbonate by glycerolysis of urea

Since, despite the intense activity in IL chemistry no data have been reported related to the use of ILs as solvents and /or catalysts in synthesis of glycerol carbonate by reaction of glycerol with DMC, during the course of this thesis attempts have been carried out to use ILs as catalysts in this process. To this aim, several neutral or basic ILs, synthesized in this thesis, have been tested ($[\text{Mor}_{1,4}][\text{N}(\text{CN})_2]$, $[\text{Mor}_{1,g}][\text{N}(\text{CN})_2]$, $[\text{HME}_{1,4}][\text{N}(\text{CN})_2]$, $[\text{HME}_{1,4}][\text{Tf}_2\text{N}]$, $[\text{Mor}_{1,2}][\text{Tf}_2\text{N}]$, $[\text{MIM}_{1,e}][\text{N}(\text{CN})_2]$) and their activity has been compared with that of tradition ILs ($[\text{BMIM}][\text{Tf}_2\text{N}]$, $[\text{BMIM}][\text{PF}_6]$).

6.2 Results and Discussions

To test the ability of ILs to act as catalysts in the transesterification of DMC with glycerol, preliminary experiments were carried out at 120°C using $[\text{Mor}_{1,4}][\text{N}(\text{CN})_2]$ as solvent and performing the reactions under different conditions, Table 6.1. On the basis of the data reported in Table 6.1., it was possible to establish that the reaction performed using 0.5 of IL and 3 eq mol of DMC gave the highest conversion. Since, we cannot exclude that similar results could be obtained at lower temperatures the same reaction was carried out at 40, 60, 80, 120 and 140°C (Table 6.2). At 140°C (bath temperature), the rapid darkening of the reaction mixture evidenced a degradation process, therefore subsequent investigations were performed at temperatures not higher than 120°C. Nevertheless, considering that DMC has a boiling point of 90°C to avoid the

progressive depletion of this reagent, the reactions performed at temperatures above 80°C were carried out in double-reflux holding flasks.

Table 6.1: Different conditions using [Mor_{1,4}][N(CN)₂] at 120°C for 13h

| Amt of IL (g) | Some additional conditions | Conversion % |
|--|--|--------------|
| 0.5 | Glycerol-coated with silica gel ^a | NR |
| 5 mol% of [Mor _{1,4}][N(CN) ₂] | 3.2 equivalents of DMC | NR |
| 0.5 | 1 equivalent of DMC | 20% |
| 0.5 | 3 equivalents of DMC ^b | 92% |

^aSilica-gel was used because DMC as well as glycerol are not miscible.

^b3.2 equivalents of DMC is preferred because bpt. of DMC is 90°C and the reaction temperature is 120°C.

Table 6.2: Different reaction temperature

| Time (h) | 40°C | 60°C | 80°C | 120°C | 140°C |
|----------|------|------|------|-------|----------|
| 3 | NR | NR | NR | 60% | Degraded |
| 6 | NR | NR | 10% | 75% | Degraded |
| 9 | NR | NR | ~20% | 90% | Degraded |
| 13 | NR | NR | 60% | 99% | Degraded |

NR=no reaction. The numbers denoted in % ages are product conversion percentages.

Finally, the progress of the reaction performed at 120°C (bath temperature) was evaluated stopping the process at different times (Table 6.3 and Figure 6.2.).

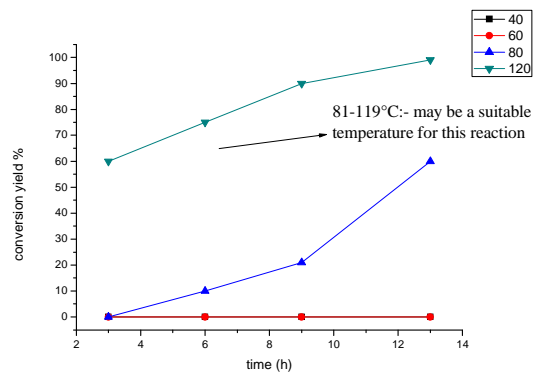


Figure 6.1: A plot showing conversion yields at various temperatures

Table 6.3: Different time of reaction with the same IL: $[\text{Mor}_{1,4}][\text{N}(\text{CN})_2]$ at 120°C

| Time of the reaction (h) | Amount of IL (g) | Conversion ratio | Conversion % |
|--------------------------|------------------|------------------|--------------|
| 7.5 | 0.5 | 4.5 : 4.3 | 60 |
| 10 | 0.5 | 12.1 : 7.5 | 75 |
| 13 | 0.5 | 12 : 0.8 | 92 |
| 24 | 0.5 | 12 : 0.6 | 99 |

In Figure 6.3 are reported the ^{13}C NMR spectra registered after 7.5, 10, 13 and 24 h.

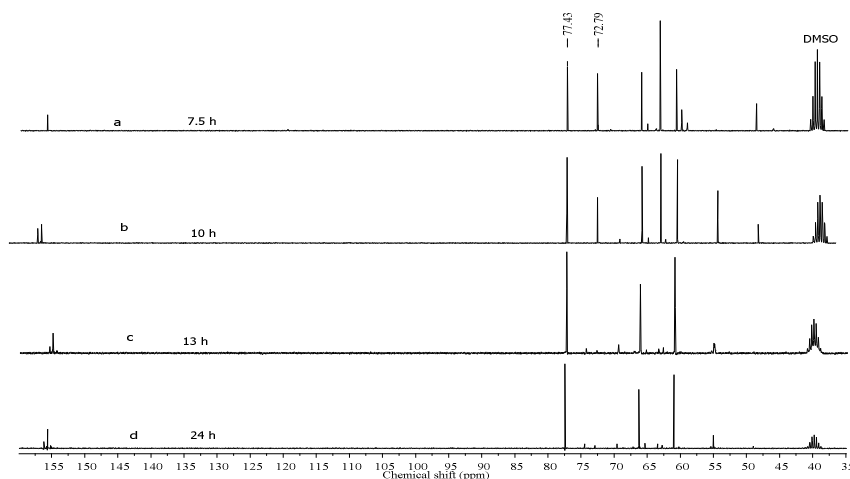
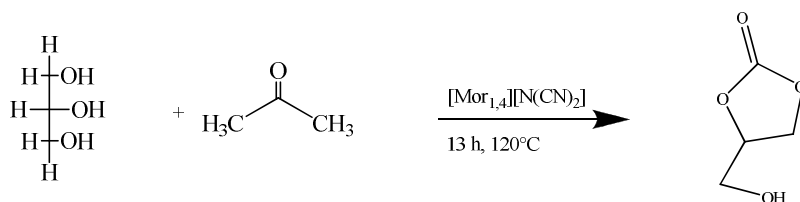


Figure 6.2: C-NMR of glycerol carbonate at 7.5, 10, 13 and 24 h when $[\text{Mor}_{1,4}][\text{N}(\text{CN})_2]$ is catalyst. (a) reaction between glycerol and DMC for 7.5 h at 120°C ; (b) reaction between glycerol and DMC for 10 h at 120°C ; (c) reaction between glycerol and DMC for 13 h at 120°C and (d) reaction between glycerol and DMC for 24 h at 120°C .

The peak 77.43 is related to the CH carbon of the product, whereas that 72.79 corresponds to the reagent CH carbon. With the increase in time interval from 7.5 to 13 h we can observe a drastic increase in the product signals (77, 66.4 and 61.6 ppm) and a simultaneous decrease in the reactant peaks (72 and 62.5). It is to note that the increase in time interval from 13 to 24 h does not give any significant increase in the product level. Hence, we decided to carry out all the remaining reactions for 13 h only.



Scheme 6.4: Formation of glycerol carbonate using ILs

Subsequently, the catalytic ability of this IL was compared with that of other ILs performing a series of reactions under identical conditions (reagent concentrations, temperature, time) using a parallel reactor system. Data are reported in Table 6.4.

Table 6.4: Various catalysts showing their respective conversions at 120°C

| ILs | Ratio Product: Reagent | yield % |
|--|---------------------------|---------------|
| [Mor _{1,4}][N(CN) ₂] | 9.5 : 0.5 | 92 |
| [Mor _{1,g}][N(CN) ₂] | 4.7 : 0.5 | 90 |
| [Mor _{1,2}][Tf ₂ N] | NR | NR |
| [HME _{1,4}][N(CN) ₂] | 0.5 : 0.6 | Less than 50% |
| [HME _{1,4}][Tf ₂ N] | NR | NR |
| [mim _{1,e}][N(CN) ₂] | 8.5 : 0.4 | 95% |
| [bmim][Tf ₂ N] | NR | NR |
| [bmim][PF ₆] | NR | NR |

NR= no reaction. All the reactions were carried out for 13h.

[Mor_{1,4}][N(CN)₂] and [mim_{1,e}][N(CN)₂] appeared to be the best ILs. The decreasing catalytic activity order is as follows: [mim_{1,e}][N(CN)₂] > [Mor_{1,4}][N(CN)₂] > [Mor_{1,g}][N(CN)₂] > [HME_{1,4}][N(CN)₂].

To the basic nature of the dicyanamide-based ILs we attribute the catalytic effect of these ILs. However, we cannot exclude that the no reactivity observed in bistriflimide- and hexafluorophosphate-based ILs can contribute the no-solubility of glycerol in these media.

In Figure 6.3, are reported the NMR spectra of the reactions performed in [Mor_{1,4}][N(CN)₂], [Mor_{1,g}][N(CN)₂] and [mim_{1,e}][N(CN)₂].

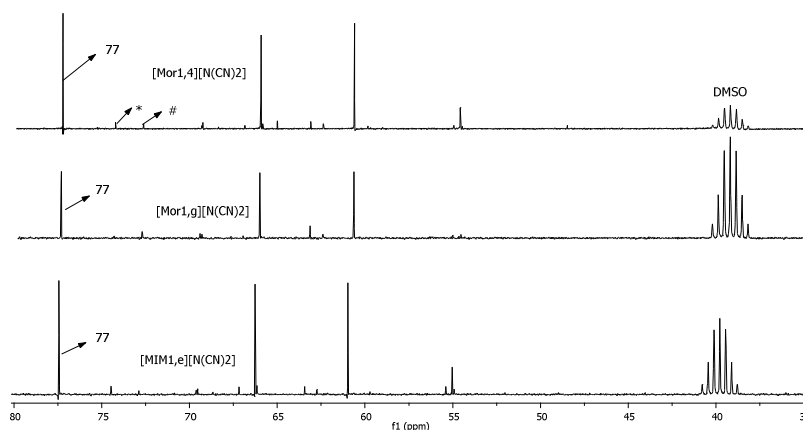


Figure 6.3: Comparison of various ILs in the product formation. (*) is byproduct at 74 and (#) is unreacted glycerol

By comparison in Figure 6.5 is reported the NMR spectrum of glycerol carbonate recently published by Arresta et al.

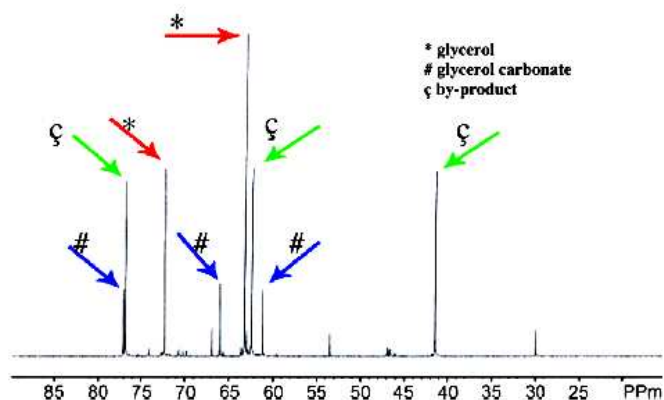


Figure 6.4: CNMR suggested by Arresta et al. ^{13}C NMR (100 MHz, in CD_3OD) spectrum of the reaction solution after the 5th cycle and extraction of the formed carbonate: the mixture is essentially formed by three species, i.e. glycerol (*), residual glycerol carbonate (#) and the byproduct (ζ).

Considering the conversions obtained in the investigated dicyanamide-based ILs and the specific properties of these media (including toxicity data), $[\text{Mor}_{1,4}][\text{N}(\text{CN})_2]$ was used to test the recyclability of the systems; product was extracted with ethyl ether (or distilled under reduced pressure) and the IL was reused. At least 4 recycles could be performed without significant reduction of the conversion (Table 6.5 and Figure 6.6).

Table 6.5: Recycle of IL $[\text{Mor}_{1,4}][\text{N}(\text{CN})_2]$ at 120°C for 13h

| No. of the cycle | Ratio of the reactant to the product formed | Conversion % |
|-----------------------|---|----------------|
| 1 st Cycle | 9.5 : 0.5 | More than 90 % |
| 2 nd Cycle | 9.4 : 0.6 | More than 90 % |
| 3 rd Cycle | 5.9 : 0.2 | More than 90 % |
| 4 th Cycle | 9.4 : 1 | More than 90 % |

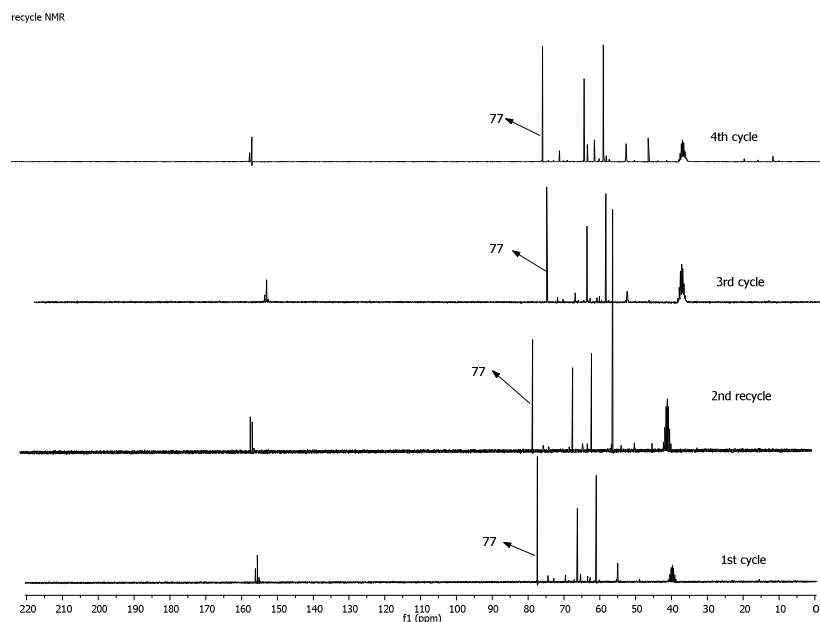


Figure 6.5: C-NMR is shown for various recycles of $[\text{Mor}_{1,4}][\text{N}(\text{CN})_2]$ in the glycerol carbonate formation. One can observe that there is no drastic change from 1st cycle to 4th cycle. Hence, one can say $[\text{Mor}_{1,4}][\text{N}(\text{CN})_2]$ is a suitable solvent/catalyst for such reactions.

6.3 Experimental Section

6.3.1 Materials and Methods

Glycerol was obtained from Sigma-Aldrich. DMC was also obtained from Sigma-Aldrich and were used as present. The ILs like $[\text{Mor}_{1,4}][\text{N}(\text{CN})_2]$, $[\text{bmim}][\text{Tf}_2\text{N}]$, $[\text{bmim}][\text{PF}_6]$, $[\text{Mor}_{1,2}][\text{Tf}_2\text{N}]$, $[\text{Mor}_{1,g}][\text{N}(\text{CN})_2]$, $[\text{HME}_{1,4}][\text{N}(\text{CN})_2]$, $[\text{HME}_{1,4}][\text{Tf}_2\text{N}]$ and $[\text{mim}_{1,e}][\text{N}(\text{CN})_2]$ were used. The synthesis of $[\text{Mor}_{1,4}][\text{N}(\text{CN})_2]$ is explained in chapter 2, whereas the synthesis of $[\text{Mor}_{1,g}][\text{N}(\text{CN})_2]$ is explained in chapter 3 and the synthesis of $[\text{HME}_{1,4}][\text{N}(\text{CN})_2]$ and $[\text{HME}_{1,4}][\text{Tf}_2\text{N}]$ are explained in chapter 2,3 and 4.

6.3.2 Synthesis of glycerol carbonate

In a 100 cm³ flask equipped with a magnetic stirrer, condenser and thermometer, glycerol (12.61 g, 0.1369 mol), DMC (12.33 g, 0.4107 mol) and the selected IL (1 g or 0.5 g, depending on the conditions of the reactions) were placed. The transesterification reaction progress was monitored by collecting samples of the reaction mixture and observing the changes of the signal derived from the cyclic carbonate carbonyl group (1796 cm⁻¹) by means of NMR. At the start of the

reaction there were two separate layers but at the end of the reaction we can see just layer. The formation of a sole phase can be taken as the end point of reaction. In cases of $[\text{Tf}_2\text{N}]^-$ and $[\text{PF}_6]^-$ based ILs there were two separate layers at the start as well as at the end of the reaction. The product was extracted using diethyl ether though through this procedure we could extract less than 50% of the formed product. A significant amount of product remained in the IL. Better recovery could be obtained by distillation of the product at 137°C (0.5 mm of Hg).

^1H NMR (400 MHz, DMSO- d_6): δ (ppm) 5.29 (t, 1H, OH), 4.81–4.76 (m, 1H, CH), 4.48 (dd, 1H, OCH_2), 4.28 (dd, 1H, OCH_2CH), 3.65 (ddd, 1H, CH_2OH), 3.50 (ddd, 1H, CH_2OH).

^{13}C NMR (CDCl $_3$, 75 MHz): 156.7, 77.8, 66.6, 61.6 (for glycerol carbonate).

Below we can see the FTIR spectrum for glycerol carbonate in $[\text{Mor}_{1,4}][\text{N}(\text{CN})_2]$.

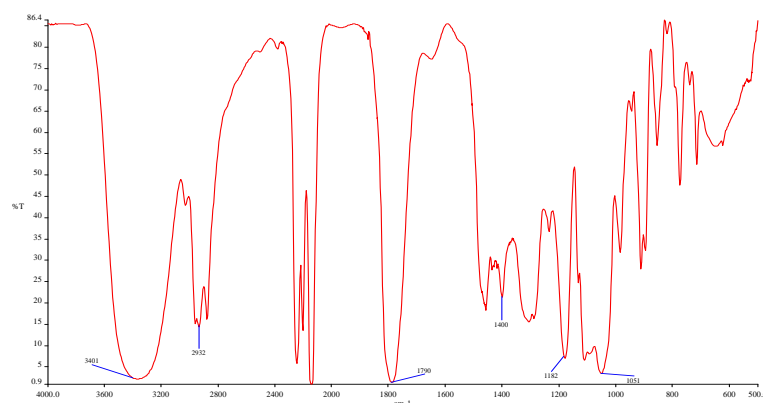


Figure 6.6: FT-IR spectrum of glycerol carbonate

FT-IR (film): 3401 (s. OH), 2931 (n. CH $_2$), 1796 (n. OC(O)O), 1403 (s. CH $_2$), 1181 (s. CH), 1054 cm^{-1} (s. OH).

6.4 Conclusions

From the above results, one can state that the basic dicyanamide-based ILs are able to act as solvent–catalyst in glycerol carbonate synthesis by reaction of glycerol with DMC. In $[\text{Mor}_{1,4}][\text{N}(\text{CN})_2]$, it is possible to obtain a practically complete conversion in 13 h. Under comparable conditions no reaction was observed in $[\text{bmim}][\text{Tf}_2\text{N}]$ and $[\text{bmim}][\text{PF}_6]$. Moreover, $[\text{Mor}_{1,4}][\text{N}(\text{CN})_2]$ was recycled 4 times without any change in its catalytic conversion activity.

References

- ¹ Zheng, Y.; Chen, X.; Shen, Y. *Chem. Rev.* **2008**, *108*, 5253.
- ² Kim, M.; Salley, S.O.; Ng, K.Y.S. *Energy Fuels* **2008**, *22* (6), 3594.
- ³ Czauderna, M.; Kowalczyk, J. *J. Chrom. B* **2007**, *858*, 8.
- ⁴ Farben, I.G. Oppau and Hydebreck, **1943**.
- ⁵ Wang, Z.-X.; Zhuge, J.; Fang, H.; Prior, B.A. *Biotechnol. Adv.* **2001**, *19*, 201.
- ⁶ Bondioli, D.; *La Chim. e l'Industria* **2004**, 46.
- ⁷ Aresta, M.; Dibenedetto, A.; in: Barbaro, P.; Bianchini, C. (Eds.), *Catalysts for sustainable energy production*, **2009**, 444 pp.
- ⁸ Gätgens, C.; Degner, U.; Bringer-Meyer, S.; Herrmann, U. *Appl. Microbiol. Biotechnol.* **2007**, *76*, 553.
- ⁹ Brian, C. *US Patent* 4900668, **1990**.
- ¹⁰ Ketchie, W.C.; Murayama, M.; Davis, R.J. *J. Catal.* **2007**, *250*, 264.
- ¹¹ Plasman, V.; Caulier, T.; Boulos, N. *Plast. Addit. Compd.* **2005**, *7* (2), 30.
- ¹² Yoo, J.; Mouloungui, Z.; Gaset, A. U.S. Patent 6,316,641 (**2001**).
- ¹³ Kovvali, A.S.; Sirkar, K.K. *Ind. Eng. Chem. Res.* **2002**, *41*, 2287–2295.
- ¹⁴ Randall, D.; Vos, R. De; European Patent, EP 419114, **1991** to Imperial Chemical Industries PLC, UK.
- ¹⁵ Weuthen, M.; Hees, U. Germany Patent, DE 4335947, **1995** to Henkel, Germany.
- ¹⁶ Shieh, W.; Dell, S.; Repic, O. *J. Org. Chem.* **2002**, *67*, 2188–2191.
- ¹⁷ Soares, R.; Simonetti, D.A.; Dumesic, J.A. *Angew. Chem. Int. Ed.* **2006**, *45*, 3982–3985.
- ¹⁸ McKetta, J.J. (Executive Ed.), Cunningham, W.A. (Associate Ed.), *Encyclopedia of Chemical Processing and Design*, vol. 20, Marcel Decker, New York, **1984**, p. 177.
- ¹⁹ Strain, F. U.S. Patent 2,446,145, **1948**.
- ²⁰ (a) Vieville, C.; Yoo, J.W.; Pelet, S.; Mouloungui, Z. *Catal. Lett.* **1998**, *56*, 245.
(b) Patel, Y.; George, J.; Pillai, S.M.; Munshi, P. *Green Chem.* **2009**, *11*, 1056.
- ²¹ Mouloungui, Z.; Yoo, J.W.; Gachen, C.; Gaset, A.; Vermeersch, G. EP 0,739,888 (**1996**).
- ²² Bell, J. B.; Currier, V. A. and Malkemus, J. D. US Pat. 2 915 529, **1959**.
- ²³ Sugita, A.; Sone, Y.; Kaeryama, M. JP06329663, **1994**.
- ²⁴ Won La, K.; Chul, J.; Jung, H.; Kim, I.; Baeck, S.-H.; Song, K. *J. Mol. Catal. A.:Chem.* **2007**, *269*, 41–45.
- ²⁵ Kim, S.C.; Kim, Y.H.; Lee, H.; Yoon, D.Y.; Song, B.K. *J. Mol. Catal. B: Enzymatic* **2007**, *49*, 75–78.

-
- ²⁶ Lee, K.H. et al. *Bioprocess Biosyst Eng.* (2010) DOI 10.1007/s00449-010-0431-9
- ²⁷ Rokicki, G.; Rakoczy, P.; Parzuchowski, P.; Sobiecki, M. *Green Chem.* **2005**, *7*, 529–539.
- ²⁸ Holbrey, J. D.; Reichert, W. M.; Tkatchenko, I.; Bouajila, E.; Walter, O.; Tommasi, I.; Rogers, R. D. *Chem. Commun.* **2003**.
- ²⁹ Naik, P. U.; Petitjean, L.; Refes, K.; Picquet, M.; Plasserauda, L. *Adv. Synth. Catal.* **2009**, *351*, 1753–1756.
- ³⁰ (a) Teles, J. H.; Rieber, N.; Harder, W. German Patent DE4225870, **1992**.
(b) Teles, J. H.; Rieber, N.; Harder, W. European Patent EP 0582201, **1993**.
(c) Teles, J. H.; Rieber, N.; Harder, W. U.S. Patent 5,359,094, **1994**.
- ³¹ Vieville, C.; Yoo, J. W.; Pelet, S. and Mouloungui, Z. *Catal. Lett.*, **1998**, *56*, 245.
- ³² Okutsu, M. and Kitsuki, T. US Patent 6 495 703, **2002**.
- ³³ Claude, S.; Mouloungui, Z.; Yoo, J.-W. and Gaset, A. US Patent 6 025 504, **2000**.
- ³⁴ Aresta, M.; Dibenedetto, A.; Nocito, F.; Ferragina, C. *J. Cat.* **2009**, *268*, 106–114.